Durability of Reinforced Concrete Members Strengthened with CFRP Plates and Subjected to Moisture and Salts

Dissertation

submitted to, and approved by,

the Department of Architecture, Civil Engineering and Environmental Sciences of the Technische Universität Carolo - Wilhelmina zu Braunschweig

in candidacy for the degree of a
Doktor-Ingenieur (Dr.-Ing.)

By
Eng. Amal Alfar, MSc.
from Amman, Jordan

Submitted on 2 June 2006
Oral Examination on 23 October 2006

Professoral advisor Prof. Dr.-Ing. H. Budelmann
Prof. Dr.-Ing. L. Franke

(2006)

Dauerhaftigkeit von mit Kohlenfaserverbundwerkstoffen verstärkten Stahlbetonbauteilen bei Einwirkung von Wasser und Salzen

Von der
Fakultät für Architektur, Bauingenieurwesen und Umweltwissenschaften
der Technischen Universität Carolo-Wilhelmina
zu Braunschweig

Zur Erlangung des Grades eines
Doktor-Ingenieurs (Dr.-Ing.)
eingereichte

Dissertation

von
Eng. Amal Alfar, MSc.
aus Amman, Jordan

Eingereicht am 2. Jun. 2006
Mündliche Prüfung am 23. Okt. 2006

Berichterstatter Prof. Dr.-Ing. H. Budelmann
Prof. Dr.-Ing. L. Franke

(2006)

Zusammenfassung

Der weltweite und stetige Verfall der Infrastrukturbauwerke macht auf die Notwendigkeit von wirksamen Gegenmaßnahmen aufmerksam und stellt für all jene, die sich mit Stahlbetonkonstruktionen befassen, eine große Herausforderung dar. Extern angeklebte Platten und Gewebe aus Kohlefaserverbundwerkstoff (CFRP) zur Verstärkung oder Ertüchtigung verfügen über eine hervorragende Effizienz. Eindrucksvolle und weltweite Anwendungen stellen dies unter Beweis. Der Einsatz von CFRP ist durch eine Reihe von Leistungsmerkmalen bedingt wie z.B. durch eine hohe Dehnsteifigkeit, ein hohes Verhältnis von Festigkeit zu Masse, die einfache Ausführung wegen ihres geringen Gewichts und vor allem wegen ihrer vorzüglichen Dauerhaftigkeit unter vielen Umgebungsbedingungen.

Aber trotz all dieser guten Attribute werden auch Bedenken geäußert. Diese zielen insbesondere auf das Langzeitverhalten unter sehr aggressiven Umgebungsbedingungen ab. In solchen Fällen können die mit CFRP verstärkten Konstruktionsbauteile wässrigen Lösungen von Salzen und Alkalien, unmittelbarer UV- Strahlung und hohen Temperaturen ausgesetzt sein, sehr oft in kombinierter, auch sich verstärkender Form des Angriffs. Als Folge davon ist nicht nur mit der Korrosion der Innenbewehrung und mit Betonangriff zu rechnen, sondern auch mit der Degradation des Klebverbundes. Tritt letzterer ein, dann ist die Verstärkungswirkung überhaupt in Frage gestellt. Man hat davon auszugehen, dass ein geschädigter und damit unzureichender Klebverbund zu plötzlichem Versagen der Gesamtkonstruktion führen kann.

In vergangenen Jahrzehnt sind umfangreiche Forschungsergebnisse berichtet worden. Meist haben sich diese mit dem mechanischen Verhalten und den Versagensarten von mit CFRP verstärkten Stahlbeton- und Spannbetonbauteilen befasst, wobei eine etwaige Vorschädigung der beschriebenen Art nicht untersucht worden ist. Der hohe Kenntnis- und Entwicklungsstand ist in zahlreiche nationale und internationale Regelwerke eingeflossen. Andererseits herrscht ein deutlicher Mangel an aktuellen Daten zum Verhalten verstärkter Bauteile unter realer Nutzung. Hierfür mag es viele Gründe geben. In jedem Fall behindert der Mangel an Daten zum Praxisverhalten verstärkter Bauteile die breitere Anwendung der CFRP Verstärkung. Es wird in der Zukunft dringend erforderlich, der Dauerhaftigkeit nicht nur der einzelnen Werkstoffe sondern auch des Verbundes im realen Praxiseinsatz zu beschreiben und Brauchbarkeitskriterien hinsichtlich der Dauerhaftigkeit unter extremen Umweltbedingungen zu erarbeiten.

In der hier vorgelegten Arbeit werden folgende Ziele verfolgt. Zum einen soll die Dauerhaftigkeit des Klebverbundes unter die Schädigung beschleunigenden Laborbedingungen untersucht werden. Dabei werden die Schädigungsparameter in Anlehnung an die realen Umweltbedingungen so eingestellt, dass sie für den Nahen Osten insbesondere für Jordanien repräsentativ sind. Zum anderen wird die Dauerhaftigkeit des Klebverbunds an Bauteilen studiert, die über eine gewisse Zeitdauer am Toten Meer und bei Aqaba ausgelagert worden waren.

Die experimentellen Arbeiten sind an zwei Orten, nämlich in den Laboratorien des Instituts für Baustoffe, Massivbau und Brandschutz (IBMB) der TU Braunschweig und des Building Research Center(BRC) der Royal Scientific Society ((RSS) in Amman, Jordanien durchgeführt worden. Die Versuche gliederten sich in 3 Blöcke:

1. Werkstoffuntersuchungen an CFRP- Lamellen und Klebharzen

2. Langzeituntersuchungen an durch CFRP- Lamellen verstärkten Stahlbetonplatten unter Dauerbiegelast und bei gleichzeitiger Beaufschlagung durch wässrige Salzlösung hoher Konzentration

3. Verbundversuche an Betonprismen mit CFRP Lamellen (Haftscherversuche)

Vor Versuchsbeginn sind die Klimadaten von Amman und anderer Regionen in Jordanien zusammen gestellt worden, um die Höchsttemperatur und relative Luftfeuchtigkeit in den Versuchen einstellen zu können. Des weiteren wurden die in Jordanien gemessenen Werte der Oberflächentemperatur und die Chlorideindringprofile von bewitterten Betonbauteilen ausgewertet. Für die Versuche wurden die CFRP-Lamellen eines Herstellers gewählt. Die Klebstoffe (kalthärtende, zweikomponentige Epoxydharze) dreier Hersteller wurden untersucht. Die thermischen und mechanischen Eigenschaften dieser Werkstoffe sind bei den Temperaturen 23° und 50° C und nach Lagerung (Vorkonditionierung) in Luft 65 % r. F., Wasser, Salzlösung und nach UV- Bestrahlung geprüft worden.

Das Verbundverhalten der CFRP- Lamellen auf Beton ist an 30 Stahlbetonbiegeplatten und an 66 Haftscherkörpern untersucht worden. 12 Platten und 21 Haftscherkörper sind am IBMB hergestellt und geprüft worden. Am RSS sind 18 Platten und 45 Haftscherkörper hergestellt und geprüft worden.

Die Stahlbetonplatten wurden vor CFRP- Verstärkung durch Biegung belastet und in der Zugzone vorgerissen (symmetrische 3- Punktbelastung). Daran anschließend lagerten sie bei konstanter Biegebelastung unter den jeweiligen Umgebungsbedingungen über eine Dauer von rd. 4 Monaten. Die Umgebungsbedingen sind bereits oben beschrieben worden. Nach dieser ersten Belastungsdauer sind die Platten entlastet worden, und es erfolgte die Verstärkung. Daran anschließend wurden die verstärkten Platten wieder durch Biegung über rd. 1 Jahr belastet und den o.g. Umgebungsbedingungen ausgesetzt. Die verstärkten und die unverstärkten Vergleichsplatten wurden dann bis zum Versagen geprüft. Entsprechendes erfolgte für die Haftscherkörper.

Die Untersuchung der Probekörper unter den realen Einwirkungen in Jordanien und unter den Laboreinwirkungen ermöglichten die vergleichende Bewertung der Dauerhaftigkeit und des Verbundverhaltens.

Die Eigenschaften der Werkstoffe selbst zeigten ein beträchtliche Schädigung bei Einwirkung von wässrigen Lösungen und hoher Temperatur. Diese Aussage gilt in erster Linie für die Kleber, während die CFRP- Lamelle i.W. unbeeinflusst blieb. Eine messbare Schädigung der Kleber im verstärkten Zustand war nicht festzustellen. Die Biegeplatten versagten alle bei in etwa gleichen Bruchlasten ungeachtet der Lagerungsbedingungen. Die Bruchart war einheitlich und zeigte sich als progressives und spontanes Abschälen, das am Punkt mit max M und max Q einsetzte und in Richtung Endauflager propagierte. Während blieben Platten, die bei Raumluft gelagert worden waren, ein Verbundbruch im Betonuntergrund auftrat, versagte der Verbund der Platten in aggressiver Umgebung stets durch ein Versagen der Adhäsion zwischen Kleber und Beton. Zur Klärung dieser überraschenden Ergebnisse sind weitere Untersuchungen notwendig. Für die praktische Anwendung kann man aber folgern, dass die CFRP- Verstärkung unter den Umweltbedingungen von Jordanien vertretbar ist, sofern die Kleber eine ausreichend hohe Glasübergangstemperatur aufweisen und die Verstärkung gegen hohe Temperaturen, das Eindringen von Wasser bzw. wässrige Salzlösung und direkte UV- Bestrahlung wirksam geschützt wird.

Abstract

The continual degradation of infrastructures worldwide has prompted the need for effective solutions, posing major challenges to those involved with reinforced concrete structures. Externally bonded carbon fiber reinforced polymer (CFRP) composite plates in lieu of bonded steel plates showed a great potential in the area of structural rehabilitation, and impressive applications have been reported in the literature. Their use in these applications is predicated on performance attributes linked to their high stiffness and strength-to-weight ratios, ease of installation, potential lower systems level cost, and potentially high durability.

However, there are heightened concerns related to the overall durability of these materials and retrofitted structures, especially as related to their capacity for sustained performance under harsh environmental conditions. In aggressive environments, CFRP retrofitted systems are subjected to moisture, salts, alkalines, ultraviolet radiations and high temperatures, which not only causing steel to corrode and concrete to deteriorate, but it may degraded the adhesive bond, hence limiting the strength of the retrofitted system. This is evident, since, at best, an insufficient bond renders the external reinforcement as ineffective as it is the main to transfer stresses between the adherents, thus defeating any contribution to have been gained by the placement of fibers there in the first place, and, at worst, may potentially results in a catastrophic failure of the retrofitted element.

Considerable research has been reported in the last decade or so on the mechanical behaviour and failure modes of the CFRP strengthened RC elements. The level of understanding of structural behaviour has reached a stage where several design guidelines have been issued and developed around the world. On the other hand, actual data and case histories on durability are sparse, not sufficiently documented or not easily accessible to the engineering community. Such limitation in knowledge is restricting the wide scale use of CFRP composites in rehabilitation works. Ways of assessing durability issues are urgently needed, and considerable work needs to be carried out to develop the acceptance criteria of employing CFRP composites in retrofitting deteriorated and substandard structures located at severe environments.

Consequently, this study intends to examine the durability of the adhesive bond under accelerated laboratory conditions that mimic harsh environmental conditions, and under severe real-life environments that are prevalent at the Middle East countries, particularly at the Dead Sea and Aqaba regions of Jordan. Dead Sea region is considered one of the most corrosive environments throughout the world.

The aim of the study is to enlighten the consequences of the severe environments on the CFRP retrofitted systems in order to evaluate the feasibility of retrofitting Jordanian deteriorated and sub-standard industrial and engineering structures that are located in very severe environments.

To achieve the main objective of this research project, an intensive experimental work was conducted at two international organizations; the Institute for Building Materials, Concrete Structures & Fire Protection (iBMB) at the Carolo-Wilhelmina Technical University of Germany, and the Building Research Center (BRC) at the Royal Scientific Society (RSS) of Jordan.

The accomplished experimental work was divided into three main work packages as illustrated hereunder:

1. Examinations on single materials, epoxies and CFRP plates;
2. Examination of the long term behaviour of slabs with high salt concentrations and CFRP externally bonded reinforcement under bending stress; and

3. Examinations on composite specimens, CFRP plates, epoxy adhesive and concrete.

Before testing started certain procedures have been carried out, such as collecting environmental data, i.e. ambient maximum and minimum temperatures and humidity prevailing at Amman, Dead Sea and Aqaba regions, in addition to some measurements to quantify the concrete surface temperatures and chloride contents for some reinforced concrete structures located at the three considered sites mentioned above.

The mechanical properties of three selected structural adhesives and one selected type of CFRP plates were evaluated after conditioning in different environments, i.e. humidity, water, salt solutions, alkaline solutions, and ultra violet radiations. All associated with two different temperatures, ambient temperature of 23 ºC and hot temperature of 50 ºC.

The behaviour of the bond between concrete and CFRP plates was studied and evaluated by testing thirty RC slab specimens and sixty six concrete prism specimens, of which twelve slabs and twenty one prisms were manufactured at iBMB laboratories and the rest at RSS laboratories.

Slab specimens were cracked to simulate deteriorated structures at site, and then were exposed to several environments, i.e. normal laboratory conditions, salt solutions, Amman environment, Dead Sea and Aqaba regions for almost 4 months, while under sustained loading. Loaded specimens were retrofitted with CFRP plates using the three selected types of adhesives. Specimens were conditioned again for almost one year at the corresponding respective environments, before testing under three-point loading.

Also, prism specimens were exposed to normal laboratory conditions, salt solutions, 50 ºC high temperature and 50 % humidity, Amman environment, and Dead Sea and Aqaba environments for almost four months before the application of the CFRP plates, and went into another conditioning period of almost one year at the same respective environments, before testing in pure shear.

Testing of similar specimens under-real life exposure conditions and simulated laboratory conditions allowed for a detailed evaluation of the durability and the behaviour of the bond between the CFRP plates and concrete in terms of bond strength, failure modes and strength gain.

Results of testing single materials demonstrated severe degradation for all adhesive types when exposed to solutions, particularly if associated with high temperatures. The degree of degradation was deferent between the tested types depending on the chemical composition of each type. On the contrary, CFRP plates retained most of their mechanical properties after exposure.

The severity of degradation of the adhesive materials was not reflected in the obtained results from the conducted pull-off and flexural tests. Specimens failed by CFRP debonding with comparable failure loads to each other and to the reference specimens. Peeling failures had limited the capacity of slab specimens to about 70 % of their expected capacity. The only difference was the location of the failure planes; delamination at the top of the concrete layer for specimens exposed to normal conditions insuring very strong bond, and separation at the adhesive/concrete interface for specimens exposed to severe environment. In view of that, there was no firm conclusion regarding the consequences from the severe environments on the retrofitted systems. But, according to the results obtained so far, it seems that, CFRP composites could be used to retrofit substandard structures at Jordan, taking into consideration the selected composite and adhesive types to have high glass transition temperatures. Additionally, the retrofitted system should be protected as much as possible from direct contact with solutions and high temperatures.

Acknowledgement

I am having a hard time believing that I have actually completed this work. It sure took a lot of sleepless nights to get to this point. There might be only my name on the cover of this dissertation but this was team work more than anything else. Everybody who believed in me, who supported me, who helped me at every stage of the work, I thank you all from the bottom of my heart.

I would like to express my sincere gratitude and appreciation to the members of my committee for their willing participation to accommodate me amidst their busy schedules.

It was a tremendous experience to work under the guidance of Prof. Dr.-Ing. Harald Budelmann, whose valuable advice and encouragement were very important for the completion of this research. I would like to thank him for his endless guidance, friendship, patience and support during the course of this research.

I would like to express my sincere gratitude and indebtedness for Prof. Dr.-Ing. Ferdinand Rostásy. Thank you a million times for your guidance, your patience, for every word you said to get me in line and make me finish this work. Also, I would like to acknowledge his contribution on translating my abstract into the German language, the experimental work, the technical contents in this dissertation and editing my publication. I feel really lucky to have the opportunity to learn from him in person.

I cannot think of words to express my deepest appreciation and truthful feelings to Dr. Tareq Al-Hadid for his unconditional love, encouragement and endless support during my years of working journey with him. I'm particularly obliged to him for providing me with the opportunity to work on this research project. Without his dedication willingness, this opportunity would not have been possible. I'm really deeply honoured to have him to serve on my committee.

I wish to acknowledge and thank Dr. Frank Schmidt Doehl and Dr. Matthias Wobst for their friendship, support and help during the research work. Gratitude is extended to Dr. Matthias for devoting his time for helping in solving many barriers that I encountered during my stay at Germany.

A big "Thank you!" goes to Mr. Rolf Epperlein for his friendship and working along with me during numerous tests at both Germany and Jordan. Thanks are due to Mr. Oliver Dienelt for his help in obtaining the needed papers, books, etc., from different sources.

My gratitude also extends to all my friends and colleagues for all the discussions, cooperation and for the wonderful time we have shared.

I would like to acknowledge and express particular thanks to the organizations that provided financial support for the research project and without which any of this work would have been possible, namely Federal Ministry for Economic Cooperation and Development (BMZ), and the German Research Foundation (DFG) that made this project possible.

Finally, I will always have my cordial appreciation and love to my father, brothers and sisters for their love, understanding and moral support throughout this time. Thank you all for telling me a thousand times "You can do it!" every time I called crying. I love you all and what would I do without you?

This dissertation is dedicated to my mother's soul that is a never-ending source of love, pride and inspiration to me; and to every one who had helping and supporting me during my hard time as a diminutive way of saying, *Thank You*.

Table of Contents

Notations

Notations and abbreviations are explained in the main text when they first appear. A list of symbols is presented hereunder with the corresponding SI-units in brackets, in addition to the nomenclature.

Roman Letters

A_c	Cross sectional area of concrete (mm^2)
A_f	Cross sectional area of FRP external reinforcement (mm^2)
A_s	Cross sectional area of internal steel reinforcement in tension (mm^2)
E_a	Modulus of elasticity of adhesive layer (MPa)
E_c	Modulus of elasticity of concrete (MPa)
E_f	Modulus of elasticity of external FRP reinforcement (MPa)
E_s	Modulus of elasticity of steel (MPa)
G_a	Shear modulus of adhesive layer (MPa)
G_f	Interfacial fracture energy (Nmm)
I_c	Second moment of inertia of the concrete cross-section (mm^4)
I_f	Second moment of inertia of the external FRP strip cross-section (mm^4)
$I_{tr,f}$	Second moment of inertia of the strengthened section transformed to FRP strip (mm^4)
$M(x)$	Bending moment acting on the x coordinate (Nmm)
M_{cr}	Crack moment (kNm)
M_n	Nominal moment strength (Nmm)
M_u	Ultimate bending moment of the strengthened section
N_c	Axial force acting on the concrete section (N)
$V(x)$	Shear force acting at the x coordinate (N)
a	Un plated length between the support and the FRP strip end
b	Concrete section width (mm)
b_f	FRP strip width (mm)
c	Distance from extreme compression fiber to the neutral axis (mm)
d	Effective depth of the concrete section
dx	Differential length (mm)
f'_c	Compressive strength of concrete (MPa)
f_{ctm}	Mean value of axial tensile strength in concrete (MPa)
f_f	Strength of FRP external reinforcement (MPa)
f_s	Strength of internal reinforcing steel (MPa)
f_y	Yield strength of internal reinforcing steel (MPa)
h	Over all depth of concrete section (mm)
k_e	Empirical constant in the width influence factor

k_b	Width influence factor
k_c	Concrete surface influence factor
k_n	Environmental factor
t_a	Thickness of adhesive layer (mm)
t_f	Thickness of FRP external reinforcing (mm)
T_g	Glass transition temperature (ºC)
x	Neutral axis depth (mm)

Greek Letters

Ω^*	Constant defined in the simplified linear approach to solve the differential equation governing the FRP strip tensile stresses in Zone I of the bond-slip relationship (1/mm)
α	Factor defined as the first static moment of the plate divided by both the plate width and the homogenous moment of inertia of the section (1/ mm^2)
β_1	Ratio of the depth of the equivalent rectangular stress block to the depth of the neutral axis
ε_c	Strain level in concrete (mm/mm)
ε_{cu}	Concrete ultimate strain (mm/mm)
ε_f	Strain level in FRP strip (mm/mm)
ε_{fu}	Design rupture strain of FRP reinforcement (mm)
ε_s	Strain level in internal reinforcing steel (mm/mm)
ε_y	Strain corresponding to the yield strength of internal reinforcing steel (mm/mm)
γ	Multiplier on f'_c to determine the intensity of an equivalent rectangular stress distribution
ρ_f	Externally FRP bonded reinforcement ratio
ρ_s	Longitudinal internal reinforcing steel ratio in tension
σ	Normal stress (MPa)
σ_c	Concrete stress on the longitudinal direction (MPa)
$\sigma_{c,b}$	Concrete tensile stress on the bottom fiber of the section (MPa)
τ_x	Interfacial shear stress (MPa)

Nomenclature

G	Specimens prepared and tested at iBMB laboratories at Germany
J	Specimens prepared and tested at RSS laboratories at Jordan
E1	Epoxy Type 1
E1M	Epoxy Type 1 Modified
E2	Epoxy Type 2
N	Normal laboratory conditions
S	Salt solution exposure
A	Real life environment prevailing at Amman city - Jordan
Q	Real life environment prevailing at Aqaba region - Jordan
D	Real life environment prevailing at Dead Sea region - Jordan

1. Introduction

1.1. Motivation

Many countries around the world have tremendous needs to repair and strengthen their civil infrastructure, and Jordan is no exception. Existing reinforced concrete (RC) structures may for a variety of reasons be found to perform unsatisfactorily under service conditions. This could be attributed to ageing, poor initial design/or construction, lack of maintenance, increased load demand, and environmentally induced degradation, FIB [1]. Another important aspect is that a large number of existing structures in earthquake-prone areas all over the world need strengthening and upgrading for both seismic pre-earthquake and post-earthquake upgrading/repair due to various reasons, such as code changes or earthquake damage.

Corrosion of reinforcing steel embedded in concrete is considered to be the major cause of deterioration in civil infrastructure facilities. RC structures in close vicinity to marine environments, industrial environments, and those subjected to the effects of road salt usage, are particularly prone to premature deterioration.

Concrete is a highly alkaline material with a pH value of about 13, resulting in the formation of a passive layer that protects the steel from undergoing corrosion. This protective layer can be destroyed if the pH value reduces below 11.5 or if chloride ions penetrate into the concrete. The high concentration of chloride ions in aggressive environments, e.g., sea water combined with conditions of high temperature and humidity and exposure to tidal cycles make it possible for chloride ions to reach the reinforcement even for high quality concrete. Corrosion initiated when chloride ion concentration reaches a critical threshold value of 0.4 % by weight of cement. Corrosion products forming on the reinforcing bar can take up a volume as much as six times that of the original iron, Mehta [2]. This expansive process induces internal stresses in concrete and eventually can lead to cracking, spalling or delamination of the concrete around reinforcing steel. Furthermore, the cross sectional area of the reinforcing bar can be significantly reduced. Such unpleasant results can severely reduce the strength of the structure and the service life.

Corrosion has been witnessed as a problem in Jordan during the past few years, particularly in coastal and industrial belts as well as in other aggressive environments. Figure 1.1 illustrates forms of deterioration of reinforced concrete structures in Jordan.

Marine construction and industrial plants located at the shores of the Dead Sea and the Red Sea of Aqaba region are subjected to very severe environmental conditions. Dead Sea is one of the most severe corrosive environments in the world. It is characterized by high temperature and humidity, in addition, to the severe ground and ambient salinity with high levels of chlorides in soil and ground water. Severe environmental conditions are sometimes aggravated by chemical seepage, abrasion, and vibration during operation of the structure. As a result, severe deterioration and damage to structural elements have occurred, which may jeopardize the safety and/or disrupt the continuity of production.

Various repair solutions have been tried in the past, but none of the measures have provided long-term solutions. Repetitive repairs are being carried out frequently every two years for the deteriorated structural elements. This could eventually lead to very serious consequences in terms of increase of maintenance cost, reduction of productivity and a complete halt to production operations due to

shutdowns necessary for maintenance. Such an unpleasant outcome could have serious consequences on the national economy, and present an urgent need for retrofitting with alternative materials to steel, that do not corrode.

Nowadays advanced composite materials, fiber reinforced polymer (FRP) composites, in the form of plates or laminates in lieu of bonded steel plates showed a great potential in the area of structural rehabilitation. Composites offer many advantages in structural uses, such as higher strengths and lighter weights, and the most important they are corrosion resistant materials.

Albeit, impressive applications of FRP materials have been reported in the literature, there are still worries and concerns regarding the durability performance of these materials under severe environmental conditions. Of particular concern is the bond between the FRP and the surface of the concrete substrate. Thus, it is essential to investigate the performance of the bond, and the response of the overall structural elements strengthened with FRP strips under different environmental conditions, before adopting them to repair and strengthen deteriorated structures exposed to adverse environments in general and in Jordan in particular.

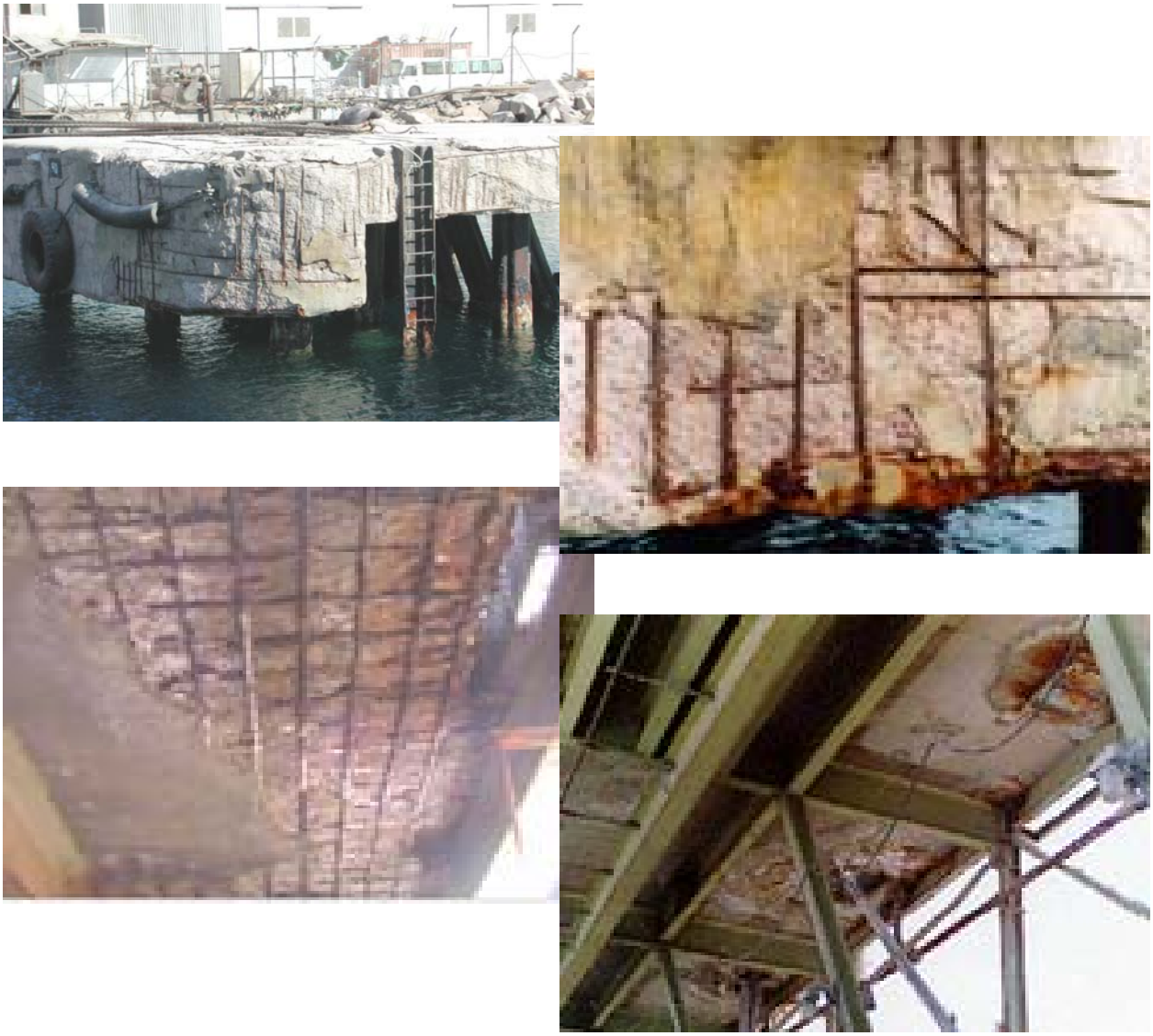

Figure 1.1: Deterioration of RC structures at Jordan, Al Far and Kahhaleh [3]

1.2. Background

With limited available funds and an increasing number of deteriorated structures, economical retrofitting techniques appear to be one of the most viable choices. Typical traditional retrofitting techniques involve the use of steel or reinforced concrete jackets, post-tensioning, installation of additional supports or bearing members, or by epoxy bonding of reinforcing plates to the tension face of structural members.

For the past thirty years, the technique for externally strengthening existing RC structures by bonding steel plates has been developed and widely used all over the world. Many experiments and applications show that this technique is simple, economic and efficient, Ranisch [4], Ranisch and Rostásy [5], Holzenkämpfer [6], and Brosens [7]. Notwithstanding the advantages of such a scheme for strengthening, there are disadvantages associated with the use of steel plates, including (1) heavy weight and difficulty in handling and installation; (2) susceptibility to corrosion particularly at the steel plate-epoxy interface that may cause loss in bond strength; (3) limited delivery lengths and increased number of joints, Meier [8], and Karbhari and Engineer [9].

The corrosion problem has limited the use of externally bonded reinforcement technique for outdoor applications, and the technical problems have limited the use for confined spaces and long span applications. These difficulties and limitations were potentially conquered through the use of FRP composites. Resistance to corrosion, high strength and stiffness-to-weight ratio, and versatility of fabrication have made FRP materials an alternative solution to steel plates in retrofitting applications, FIB [1], Rostásy [10], Nanni and Dolan[11], Rostásy et al. [12], and ACI [13].

In reviewing the literature concerned with the selection of composite materials for external strengthening applications, a range of materials were cited. Current commercially available FRP composites are aramid (AFRP), carbon (CFRP) and glass (GFRP). The FRP materials consist of continuous fibers embedded within adhesive matrix. The adhesive is required to bond the fibers together, transmit loads between them, and protect them from environmental attack. FRP composites in the form of sheets or plates are bonded to a concrete substrate with a structural adhesive in a similar manner for bonding steel plates; mostly used adhesives are epoxies.

Among different types of FRP composites, CFRP composites appear to be the most applicable and effective for external strengthening of RC structures, Rahimi [14]. They have the highest elastic modulus when compared to other FRP composites. Their tensile strength is normally at least twice as high as steel (related to cross section) but can be over by 10 times (related to weight), while their weight is only about 20 % of that of steel. This property leads to the speed and ease of handling and site installation, less labour, lower shut-down costs, and almost free of site constraints and interruptions to existing services, which typically offset the high initial cost of the materials, making them very competitive with other traditional strengthening techniques. Additionally, they are appropriate for outdoor applications as they are corrosion resistant, Darby [15], Meier and Kaiser [16], Rostásy [17], Neubauer [18], and Nanni [19].

Strengthening with externally bonded CFRP plates has been shown to be applicable to many types of RC structural elements. They may be bonded to the tension side of structural members (e.g., slabs or beams) to provide additional flexural strength. They may be bonded to web sides of joists and beams or wrapped around columns to provide additional shear strength. They may be wrapped around columns to increase concrete confinement and thus increasing strength and ductility. Among many other applications, CFRP plates may be used to strengthen concrete and masonry walls to better resist lateral loads, as well as

circular structures, i.e., tanks, silos, and pipelines, to resist internal pressure and reduce corrosion, Rostásy and Neubauer [20], Alkhrdaji et al., [21], and Tommaso et al. [22].

Despite the advantages that CFRP plates provide for enhancing structural strength, there are a number of issues and concerns associated with the durability and long-term performance of the retrofitted system. Issues include but are not limited to the composite material and the integrity of the adhesive bonded joints, assuming the durability of reinforcing steel and concrete is well known and documented. Composites are the reinforcing materials for upgrading and strengthening substandard structures, while, the bond is the means for the transfer of forces between the concrete and the reinforcing plate in order to develop a composite action and enhancing the load-carrying capacity of the structure.

Concerns arise in view of the fact that adhesives may deteriorate if exposed to moisture, salts, alkalines, ultraviolet radiation and high temperatures. There are threats regarding the overall functionality and durability for civil structures operating under severe environments. Concrete may deteriorate and spall, steel corrodes, composites may damage, and the adhesive bond may be degraded and falls causing premature debonding of the reinforcing plate at an even earlier stage, thus nullifying the benefits obtained by adding external reinforcement, Mays and Hutchison [23], Karbhari et al. [24], and Teng et al. [25]. Therefore, there is an urgent need to investigate the effects of long-term degradation on the FRP-concrete interface in various representative environments, and to select the appropriate type of adhesive and composite material for a specified environment.

Considerable research has been reported in the last decade or so on the mechanical behaviour and failure modes of the CFRP strengthened RC elements. The level of understanding of structural behaviour has reached a stage where several design guidelines have been issued and developed around the world, FIB [1], ACI [13], CSTR [26], ISIS [27], JSCE [28], and JCI [29]. On the other hand, limited research on durability issues has resulted in limited design guidance with the most comprehensive treatment given by ACI [13].

Furthermore, case histories on durability issues are not sufficiently documented or not easily accessible to the engineering community. Such limitation in knowledge is restricting the wide scale use of FRP composites in rehabilitation works. Ways of assessing durability issues are urgently needed, and considerable work needs to be carried out to develop the acceptance criteria of employing FRP in retrofitting substandard structures at severe environments, Karbhari et al. [24].

The research done to date on durability of externally bonded FRP reinforcements for RC elements has been mainly performed on un-cracked concrete elements and seldom included sustained loads during conditioning. This study intends to examine the durability performance of the bond between CFRP plates and pre cracked concrete slabs under accelerated laboratory conditions that mimic harsh environmental conditions, and under real-life severe environments that are prevalent at the Middle-East countries, particularly at the Dead Sea and Aqaba regions of Jordan.

It is anticipated that this research study will provide an experimental evidence and insight of the effect that moisture, chlorides and high temperatures will have on the strength of the interfacial CFRP-concrete bond. Additionally, reduction factors, if any, related to various environmental conditions will be precisely determined to allow the design of safely strengthened concrete structures under severe environmental conditions.

1.3. Project Significance

The Civil Engineering Research Foundation (CERF) and the Market Development Alliance (MDA) recently completed a durability gap study that highlighted key durability areas that are still needed to address durability concerns of FRP materials. In their report, CERF [30], the authors summarized the following top research needs related to the use of FRP in civil infrastructure that are addressed in one or more forms in this research effort:

1. "Testing under combined conditions (stress, moisture, solution, temperature, and/or other regimes) at both the material and structural levels is critical".
2. "Development of standardized solutions and conditions for laboratory studies that closely simulate actual field conditions".

Available data regarding the durability performance of the interfacial bond between the composite materials and the concrete substrate have been primarily based on laboratory environmental testing conditions, which may not realistically reflect the true degradation process. The research presented herein provides information for examining the consequences of real-life aggressive environments on the effectiveness of the CFRP retrofitting scheme. Testing of similar specimens under several different environmental conditions, e.g., Germany and Jordan, particularly in very severe environmental conditions, allowed a detailed evaluation of the behaviour of the interfacial CFRP-concrete bond in terms of strength and failure modes.

Furthermore, this research intends to increase the existing database for one-way RC slabs strengthened with bonded CFRP composites. Limited amount of information is available on RC one and two-way slabs, albeit the problem of their upgrade both in buildings and bridges is quite common. In practice, the needs for strengthening of slabs either for purpose of load capacity increase, material deterioration, or due to structural modifications of slabs are widespread. The simple and direct extrapolation of results obtained from beams to design of strengthening measures for slabs is inappropriate due to their lack of shear reinforcement that may lead to earlier premature brittle failure in shear due to increased moment capacity.

1.4. Research Objectives

Although many studies have shown the promise of CFRP plates for retrofitting, the most significant technical obstacle hindering the extended use of these materials in civil applications are the lack of knowledge of long-term performance and of durability data particularly under severe environmental conditions.

This research seeks to fill gaps of knowledge by evaluating the durability of the interfacial CFRP plates-concrete bond, and to understand the bond behaviour under real-life aggressive environmental conditions, such as those prevalent at the Dead Sea and Aqaba regions.

To study the long-term performance and durability issues related to strengthening with CFRP plates, an experimental investigation was carried out with the following main objectives:

1. To select one type of CFRP plates and three types of adhesives with high glass transition temperature, T_g, from the most efficient and reputable commercially available materials.

2. To examine and compare the chemical and mechanical properties of the selected CFRP plates and adhesives under different environments, such as normal laboratory conditions, high temperatures, humidity, salt solutions, alkaline solutions, and ultra violet radiations.
3. To investigate and compare the response of precracked RC slabs strengthened with CFRP plates after one year of exposure to different environments, such as real-life environments prevailing at Amman, Dead Sea region and Aqaba region of Jordan, and simulated laboratory severe environments at iBMB's laboratories of Germany.
4. To perform shear tests on plain concrete specimens that were strengthened with CFRP plates, after one year of exposure to different environments, such as real-life environments prevailing at Amman, Dead Sea region and Aqaba region of Jordan, and simulated laboratory severe environments at iBMB's laboratories of Germany.
5. To identify the different failure modes of reinforced concrete slabs strengthened with CFRP plates, and to relate them with various types of environmental exposures by developing a mathematical model which could predict bond strengths under different environments.
6. To assess possible degradation of bond strength and the rate of degradation due to indoor and outdoor severe environmental exposures.
7. To evaluate the feasibility of using CFRP plates to retrofit deteriorated and substandard structures in Jordan, particularly those located at the Dead Sea and Aqaba regions.

1.5. Outline of Dissertation

This dissertation is divided into six chapters, in addition to appendices that summarize the test results. Furthermore, the dissertation includes an abstract in German language.

Chapter 1 addresses the motivation and background, and provides the significance and objectives of the research project.

Chapter 2 reviews comprehensively the state-of-the-art knowledge regarding durability issues and strengthening behaviour. Failure modes, debonding and bond strength models are also laid out.

Chapter 3 describes the experimental program. It includes the testing of three types of adhesives and one type of CFRP plates, in addition to the preparations and testing of RC slabs and concrete prisms. The experimental work was divided into three main work packages, namely: (1) Examinations on single materials, epoxies and CFRP plates; (2) Examinations of the long term behaviour of slabs with high salt concentrations and externally bonded CFRP reinforcement in bending; and (3) Examinations on composite specimens, CFRP plates, epoxy, and concrete.

Chapter 4 presents the test results and discussions.

Chapter 5 is devoted for the analysis of the test results and the outcome of the study. Additionally, it proposes an analytical model to predict bond strength for retrofitted structures in severe environments. Durability and service life estimation of CFRP retrofitted systems are also included.

Chapter 6 summarizes the dissertation and lists observations, conclusions and general remarks on the recommendations for future research.

2. Literature Review-State of the Art

2.1. General

With more and more attention being paid to the strengthening of RC structures with FRP composites, an exponential growth of research has resulted in a vast amount of published literature. The aim of this chapter is to provide a state-of-the art review of the current progress of research studies related to the object of this research study.

To provide a broadly based understanding of the subject, the major environmental conditions that affect composites durability are reviewed. The strengthening behaviour and failure modes are discussed and outlined, with more concentration on the adhesive bond.

2.2. Durability

It is envisaged that many applications of CFRP strengthening would be for outdoor structures. Hence the durability of the strengthened system under all kinds of environments has to be known. Herein, durability can be described as "the ability of a structural system to maintain its initial properties over time, under appropriate loading and specified environmental conditions", Karbhari et al. [24].

In the case of strengthening an RC element with composites, the main regions of durability consideration are the composite material itself, the concrete substrate and the adhesive interfacial bond.

FRP composites can be affected by a variety of factors, including those related to the service environment or damage to the composite. Carbon fibers are very durable materials, but the matrix that bounded the fibers together may be susceptible to environmental conditions. Generally, durability of adhesives is dependent on several factors including the adhesive components and proportion, as well as curing time and exposure conditions.

Properly designed, well compacted and cured concrete can be expected to show good durability and should remain maintenance free for many years under normal service conditions. The durability of RC concrete is possibly one of the most well studied subjects in civil engineering because of its importance. Therefore, concrete durability will not be discussed herein. Nevertheless, it should be stated that the concrete cover is likely to represent the weakest component in the strengthened zone. Concrete surface must be of good sound condition. Corroded steel if any should be cleaned thoroughly from rust, inspected with respect to its residual load bearing capacity, and missing steel should be compensated with new steel. Spalled and chloride contaminated areas of concrete should be well repaired by conventional patching or repair materials. Concrete surface must be roughened to a coarse sandpaper texture and must be cleaned of all dirt and debris. Also, it should be free from all apparent moisture. Surface preparation is a key step in the process of bonding two materials since the success of the plate bonding technique depends primarily on the degree of composite action, which can be achieved between the external plate and concrete

In the durability study, the main separate environmental conditions include moisture, alkali, high temperature, freeze-thaw cycles, ultraviolet radiation and fire. Only the effects of the environmental conditions encountered in this research are comprehensively detailed hereunder.

2.2.1. Dry Heat

CFRP composites are exposed to thermal effects both during their fabrication and service life when strengthening concrete structures. The response of the CFRP strengthened structures is mainly the matrix of the composite and the adhesive joint. Temperature elevation can affect the mechanical properties of the CFRP system in a variety of ways.

Normal ambient temperatures are not considered detrimental as long as the composite system is properly selected and fabricated so that the glass transition temperature (T_g) is always higher than the service temperature of the structure by about 30 °C, Karbhari et al. [24]. T_g is defined as the midpoint of the temperature range over which the polymeric material changes from relatively hard, elastic, glass-like substance to a relatively viscous rubbery material. T_g is a special characteristic for each adhesive, and its value depends on the type of adhesive used and its constituents. Typical values for glass transition temperatures for adhesives are in the range of (40 - 60) °C, Karbhari et al. [24].

A slight increase in the surrounding temperature can result in a beneficial post-cure of the composite material. But an increase in surrounding temperatures could also negatively affect the overall composite behaviour by increasing the residual stresses due to different thermal expansion rates between the fibers and the matrix. The residual stresses may lead to microcracking and damage of the matrix.

Beyond the T_g, the matrix looses its mechanical characteristics and its ability to transfer stresses between the fibers, thus the tensile properties of the overall composite is reduced, Hollaway and Leeming [31].

The bond between the concrete and the epoxy, as well as the bond between the epoxy and the FRP plate, could also be affected by different thermal expansion properties. Microcracks within the bond could form and eventually propagate and lead to premature debonding failure.

Furthermore, the coefficient of thermal expansion for the adhesive joints is in the range of (40 to 90) x 10^{-6}/K, which is about (3 to 10) times that of plain concrete being ≈ (10 x 10)$^{-6}$/K. The differential coefficient of thermal expansions between concrete and adhesive creates tangential stresses which, at varying temperatures, cause cracking in the concrete that may lead to the breaking of the bond between concrete substrate and FRP plate, Bisby [32].

Carbon fibers that exhibit better thermal properties than the matrix can continue to support some load in the fiber direction until the temperature threshold of the fibers is reached. This can occur at very high temperatures; higher than 275 °C, Green [33].

Kumhara et al. [34] concluded from his study that for temperatures higher than the adhesive T_g, the tensile strength of CFRP materials is reduced in excess of 20 %.

2.2.2. Moisture

The effect of humid air or water on CFRP retrofitted systems may lead to the degradation of the matrix and the adhesive bonded joint. Carbon fibers are not affected by water, Hollaway and Leeming [31].

Most adhesives can absorb moisture by instantaneous surface absorption and diffusion. Usually the moisture concentration increases initially with time until reaching saturation after several days of exposure to humid atmosphere. Moisture uptake depends on several factors including thickness of material, void content, polymer type, temperature and presence of microcracks. The degree of moisture

absorption is aggravated when adhesives are exposed to temperatures above T_g values, i.e., adhesives in the rubbery form tend to absorb more water than in the rigid form.

Water may plasticize, induce relaxation and swell the adhesives causing degradation in the mechanical properties. The elastic moduli and strengths are significantly reduced by water-induced plasticization, Mays and Hutchinson, [23]. Also, water may lead to unwanted chemical reactions in the polymers causing depress their glass transition temperatures, Hollaway and Leeming [31]. Drying can reverse the process but may not result in complete attainment of original mechanical properties.

It was concluded from several research studies that the exposure to aqueous solutions had a significant detrimental effect on the retrofitted systems, with most degradation at the level of the adhesive layer between the composite and the concrete, Karbhari and Engineer [9], Karbhari et al. [24], Leung et al. [35], David and Neuner [36], Zheng and Morgan [37], and Woo and Piggot [38].

2.2.3. Alkaline Solutions

Alkaline chemicals, contaminated soil and concrete are typical sources for alkaline, which may have detrimental effects on the retrofitted systems. Concrete pore solution is our primary concern as the CFRP composites may be in direct contact with. Normally, the pH level of the concrete pore solution is in the range of (12.5~13.5).

Resins in composites can protect the fibers from the alkaline attack, but not for long periods of time. Alkaline solution can accelerate the degradation of some types of resins and also the adhesive bonded joint between the concrete and the composite materials. The degree of degradation in adhesive mechanical properties is aggravated if alkalines are in conjunction with high temperatures. Whereas, Carbon fibers are considered resistant to alkali environments, FIB [1], Karbhari et al. [24], Chin et al. [39] and Rahman [40].

2.2.4. Salt Solutions

Many of the civil engineering infrastructures are in close proximity to the sea and subjected to salt effects in addition to high humidity. Others such as bridges are exposed to salts in winter time for ice removal. Several researchers studied the effect of salt solution on the FRP composites to determine the level of degradation related to that particular condition. They reported a significant deterioration in the tensile strength of the composite matrix and the adhesives when exposed to salt solution, in particular if it is associated with high temperature. Carbon fibers are not affected with salts, Karbhari and Engineer [9], and Sonawala and Spontak, [41].

2.2.5. Ultra Violet Radiation

The effect of ultraviolet light on polymeric compounds is well known. On prolonged exposure to sunlight the matrix may harden and discolour.

Although the portion of the top surface that is affected may only be a few microns deep, the damaged area may contain high stress concentrations and consequently fracture the material at lower overall stress levels, CERF [30]. Protective resins are commonly used to help protect this top surface, but prolonged exposure can wear down that coating.

2.3. Strengthening Behaviour

A large number of experiments on the FRP strengthening of RC structural members, particularly beams, have been carried out, Neubauer [18], Rostásy and Neubauer [20], Swamy [42], Ritchie et al., [43], Quantrill et al. [44], Quantrill et al. [45], Arduini and Nanni [46], Arduini et al. [47], Garden et al. [48], Garden and Hollaway [49], Spadea et al. [50], Maalej and Bian [51], Nguyen et al. [52], Rahimi and Hutchinson [53], Fanning and Kelly [54], White et al. [55], Pham and Al-Mahaidi [56], and Brena et al. [57]. No matter whatever researchers used large or small-scale specimens in their investigations, the FRP external reinforcements increased the load-carrying capacity as well as the stiffness. On the other hand, external strengthening reduced the deflection capacities as compared to the non-retrofitted reference specimens.

Furthermore, many parameters that contribute to the overall strength and stiffness of the flexural members were specifically studied. The studies concluded that the load capacity of the strengthened member depends upon several parameters that can be summarized as follows: (a) the geometry of the beam and FRP strip; (b) the bond at the interface between concrete and FRP strip; (c) the mechanical properties of concrete, FRP strip and adhesive; (d) surface preparation procedures; (e) type of steel reinforcement, i.e. under or over reinforcement and prestressed; (f) extent of beam cracking; (g) loading condition; and (h) environmental exposure.

Similar strengthening performance due to FRP bonding were also shown in sagging and hogging strengthening of continuous RC beams, El-Refaie et al., [58]. The magnitude of the performance increase was influenced by the composition of the concrete beams, as well as the type and amount of external FRP reinforcement. In general, the strength and stiffness of the beam increased with the modulus and thickness of applied external reinforcement. In most cases, there was a limit of FRP strip thickness, beyond which no further increase in beam strength could be obtained. And the effectiveness of FRP external reinforcement decreased as the thickness of the FRP strip was increased.

In fact, specimens with identical properties and quantities, except for different configurations of the FRP strips, exhibited different flexural responses. It was reported that the deflection of specimens bonded with FRP of wider plates was up to 60% larger than those having an equal area of FRP but with narrower plates, Brena et al. [57]. The main reason is that with the increase in plate width, the FRP-concrete contact area was increased, distributing the bond stress over a larger area thus introducing a higher load-carrying capacity, Thomsen et al. [59]. Also, the failure mode of the strengthened beams was strongly dependent on the ratio of flexural stiffness of the RC element to the flexural stiffness of the FRP strip. A large loss in beam ductility occurred with a significant increase of load-carrying capacity, probably due to the linear stress strain behaviour of FRP strips up to failure.

Many different types of FRP composite bonded location and geometry have been studied to strengthen beams, such as longitudinal bonding at the tensile soffit, longitudinal bonding on the sides, transverse straps wrapping combined with other longitudinal bonding, Brena et al., [57]. All these FRP bonded location and geometry increased the load carrying capacity and stiffness.

In practice, strengthening of ageing or damaged structure is more common than strengthening of new structures. From the viewpoint of rehabilitation of damaged and /or ageing structures, precracked RC beams have also been studied extensively. While significant research has been carried out on this topic, only inconsistent conclusions are available, mainly due to large differences in experimental conditions, Sharif et al. [60], Arduini and Nanni [46], Bonacci and Maalej [61], Shahawy et al. [62], Arvil et al. [63].

Arduini and Nanni [46] concluded that the performance of a strengthened precracked specimen was not significantly different from that of a strengthened virgin specimen; there were only about 10% reductions in ultimate strength and stiffness for the former specimens. Bonacci and Maalej [61] showed that precracked strengthening affected the load carrying capacity marginally, only 5%. This conclusion correlates very well with the results obtained from a study conducted by Stepanel and Podolka [64].

2.3.1. Failure Modes

Regarding the existing experimental studies in the literature, the failure modes of concrete beams/slabs strengthened by plate bonding can be classified into the following two main categories, FIB [1].

i. Full composite action or classical failure modes

This category comprises the failure modes where the full composite action of the concrete and the bonded plate is maintained until failure occurred due to one of the following.

- Concrete crushing: Concrete crushes in the compression zone before or after the yielding of the inner reinforcing steel, while the FRP composite is intact. This mode of failure will be brittle and undesirable particularly if the concrete crushes before steel yielding;
- FRP rupture: For relatively low ratios of both internal and external reinforcements, failure may occur through tensile fracture of the FRP strip; and
- Shear failure: The reinforced concrete beam may reach its shear limit prior to any kind of flexural failure if it is not properly reinforced in shear.

ii. Loss of composite action or debonding

This category describes the failure where debonding or loss of composite action takes place at the interface between the adherents prior to the classical failure modes. Debonding failure may occur at one of the following different interfaces:

- Cohesion failure in the adhesive layer.
- Inside the FRP between fibers and resin (interlaminar shear failure).
- At the concrete/adhesive interface or at the FRP strip/adhesive interface.
- At the top surface of the concrete along a weakened layer or along the embedded reinforcing steel.

Figure 2.1 illustrates the possible failure modes for strengthened flexural RC member. Whereas, probable debonding scenarios are illustrated in Figure 2.2.

Further details regarding failure modes can be found in Teng et al. [25], Buyukozturk and Hearing [65], El-Mihilmy and Tedesco [66], El-Mihilmy and Tedesco [67], Chaallal et al. [68], Chaallal et al. [69], Triantafillou [70], Triantafillou and Antonopoulos [71], Chen and Teng [72], Luk and Leung [73] and Triantafillou and Plevris [74].

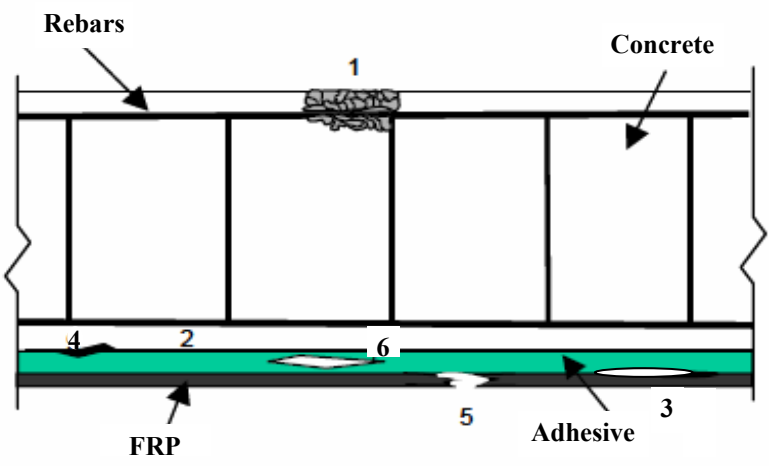

1. **Concrete compressive failure.**
2. **Failure of concrete layer between inner reinforcing and FRP strip.**
3. **Adhesive failure at FRP strip adhesive interface.**
4. **Adhesive failure at concrete adhesive interface.**
5. **Rupture of FRP strip.**
6. **Cohesion failure in the adhesive**

Figure 2.1: Possible failure modes in RC beam externally strengthened with FRP

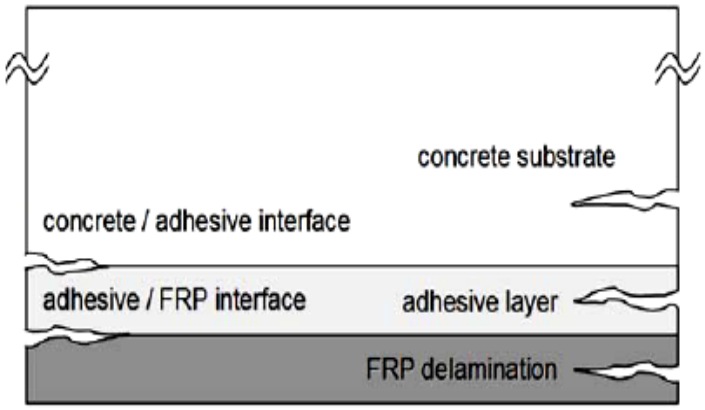

Figure 2.2: Possible debonding locations, Reeve et al. [75]

2.3.2. Debonding

In experimental studies, debonding is observed to be a dominate failure mode, Teng et al. [25], Arduini and Nanni [46], Buyukozturk and Hearing [65], Chen and Teng [72], and Reeve et al. [75]. Once the FRP strip begins to debond from the member it can no longer fully contribute to the member's load carrying capacity. Therefore debonding is an undesirable failure because the retrofitted member is not allowed to reach its full flexural capacity. Thus, FRP strengthening systems are often used inefficiently. Efficiency of the FRP can be measured as the ratio of the FRP strain that may be obtained in situ to the rupture strain of the FRP. FRP rupture would be considered 100% efficiency of the FRP strip. Debonding failures greatly limit the strains observed in the FRP, FIB [1] and ACI [13]. Thus it is important to understand, and hopefully mitigate debonding failures. There are two main areas where debonding can initiate: at the end (curtailment) of the FRP reinforcement, or within the span of FRP

reinforcement. Teng et al. [25] report that while end debonding is more commonly observed in the experimental literature, intermediate crack induced debonding (often referred to as "midspan debonding") will, for the most part, determine beam flexural strength in practical applications where flexural elements will typically have relatively long shear spans (as discussed below).

FRP debonding will occur in sudden bursts and not as a continuous process, Reeve et al. [75]. It will usually initiate in areas of stress concentrations, which are commonly due to material inconsistencies and/or the location of existing cracks in the concrete substrate. Mixed mode (Modes I and II) loading conditions on FRP strengthening systems has been found to initiate debonding in flexural members anywhere that a moment gradient is present (non-zero shear). Debonding will then propagate along the length of the beam following the path of least resistance. Propagation is dependant on loading conditions, material properties (strength and elasticity), and the fracture properties at the debonding crack tip.

Therefore, failure in the FRP/RC beam system can take place through materials or at the interface of two materials and may "jump" from one "plane" to another, as shown in Figure 2.2.

i. Plate End Debonding

Plate end debonding initiates at the end (curtailment) of the FRP strip and propagates toward midspan as illustrated in Figure 2.3. This debonding can be characterized as interfacial debonding or concrete cover delamination (although, cover failure is not exactly a "debonding" failure, as it occurs away from the bond line, it is referred to as such). Both of these plate end debonding types are caused by high stresses at the end of the FRP strips.

Interfacial debonding occurs at the interface between the concrete substrate and the FRP strip. This is caused by high normal stresses that occur at the end of the plate which cause a tension failure in the system's weakest component (usually concrete). A thin layer of concrete will usually come off with the FRP strip indicating that the adhesive-to-concrete bond is stronger than the concrete tensile capacity, Teng et al [25]. On the other hand, concrete cover delamination is initiated by cracks forming in the concrete, on the beam soffit, at the end of the FRP strips. These cracks form because of the sudden termination of the FRP strip which causes high normal stresses and high interfacial shear in the flexural tension region of the beam. At the soffit of a beam in flexure, an axial strain exists in the beam, which increases with distance from the supports. The end of the FRP strip is "free" and has zero axial strain at its curtailment. The adhesive and FRP strip then try to "catch up" and achieve the same strain as that of the directly adjacent concrete substrate. So even when there is a very small distance between the end of the FRP strip and the support, there may still be significant stresses being imparted in the adhesive and FRP. This stress will cause a Mode II failure in which the opposing sides of a crack will slide against each other (in the plane of the crack) in opposite directions. The "free" ends of the FRP strip also have zero curvature, unlike the concrete beam which does have curvature under loading. As the beam bends, the FRP attempts to remain straight and a vertical stress (normal to the FRP) is put on the adhesive which pulls on the concrete substrate cover, Teng et al [25]. This will cause Mode I cracking in which the opposite sides of a crack open and separate away from the crack plane, and each other. An element of peeling stress (Mode I) is present throughout a member and is proportional to the shear to moment ratio (i.e. increasing near supports).

These two types of stresses at the end of the FRP strip induce the mixed mode failure of end debonding, Reeve et al. [75]. A crack will propagate vertically at first to the elevation of the steel reinforcement (a weak plane) and then continue horizontally away from the beam end (toward midspan), separating the

concrete cover from the rest of the beam as shown in Figure 2.3. These cracks propagate towards midspan as this is where the highest induced moment occurs. This flexural peeling will eventually detach the entire FRP strip along with the cover concrete and leave the beam un-retrofit. Such debonding is found to occur in beams with low span to depth (a/h) ratios or in beams where the FRP is not terminated close to the supports, Triantafillou and Plevris [74].

ii. Midspan Debonding

Midspan debonding occurs in the shear span of the beam and is initiated at locations of high moment-to-shear ratio. It propagates in the direction of decreasing moment (towards the support) as shown in Figure 2.3. Large shear stresses are developed along the interface in order for tensile stresses to be transmitted from the FRP through the adhesive and concrete substrate to the internal reinforcing steel. The satisfactory transmission of stresses through the strengthening system must be reliable in order to ensure the continued participation of the FRP in the force resisting system and to ensure the desired failure behaviour. Failure will occur in one of the systems layers, usually in the concrete as it has a lower ultimate strength than the FRP or adhesive. This failure through concrete will be brittle, propagating rapidly with little warning, Triantafillou and Plevris [74].

In the beam shear span, near the location of the maximum moment, diagonal flexural cracks or flexural-shear cracks will form in the concrete substrate, as illustrated in Figure 2.3. Midspan debonding will initiate at the toes of these cracks. Cracking in the concrete will cause axial stress variations in the areas of uncracked concrete and consequently in the attached FRP (higher stresses at the cracks, with stresses decreasing away from the cracks). These stress variations must be transferred across the interface as shear (Mode II) stresses.

Midspan debonding is categorized as occurring in two steps: initiation and propagation. During initiation, at the toes of the beam's flexural cracks, inclined cracks begin to appear through the concrete cover. As the beam continues to deflect due to an increasing loading, the inclined cracks open and the bonded FRP is stretched across the opening. As the inclined cracks continue to open, the concrete cover on the side of the inclined cracks closest to the span center will be at an increasingly lower elevation relative to the concrete cover on the side of the crack furthest from the span center. Therefore, local bending begins to occur in the FRP at the inclined crack opening, as shown in Figure 2.3. The concrete cover on the side of the crack closest to center span will continue to drop in elevation relative to the other side of the crack and the FRP will be pushed in front of the dropping concrete cover. The section of the FRP being pushed will pull the FRP on the other side of the crack, and cause a stress in the adhesive interface that is normal to the FRP (Mode I). This normal stress, in conjunction with the large shear stresses (Mode II) induced by shear transfer between FRP and concrete will eventually peel the FRP and a thin layer of the concrete cover away from the beam as described above. This will create a horizontal crack, starting at the inclined crack, which will propagate towards the end of the FRP.

At first, the crack will propagate relatively steadily, with a steady increase in load. Since fracture initiation requires greater energy than fracture propagation, the debonding may be arrested as the stress falls or even as the debonding passes across another crack in the concrete substrate. Thus with increasing applied load, the debonding propagation appears somewhat intermittent.

Eventually, a critical condition is reached and the debonding crack will instantly propagate along the remaining length of the FRP, completely detaching it from the beam, taking with it a thin layer of concrete and sometimes even the concrete wedges between the flexural and inclined cracks.

As described, there is a peeling stress (Mode I) associated with midspan debonding in addition to the shear stress (Mode II). It has been shown that Mode II bond toughness, as measured by the critical fracture energy at the concrete/FRP interface, is significantly reduced in the presence of even a small amount of Mode I stress. Thus, the presence of very low peeling stresses will still have a very significant effect on bond performance, Reeve et al. [75].

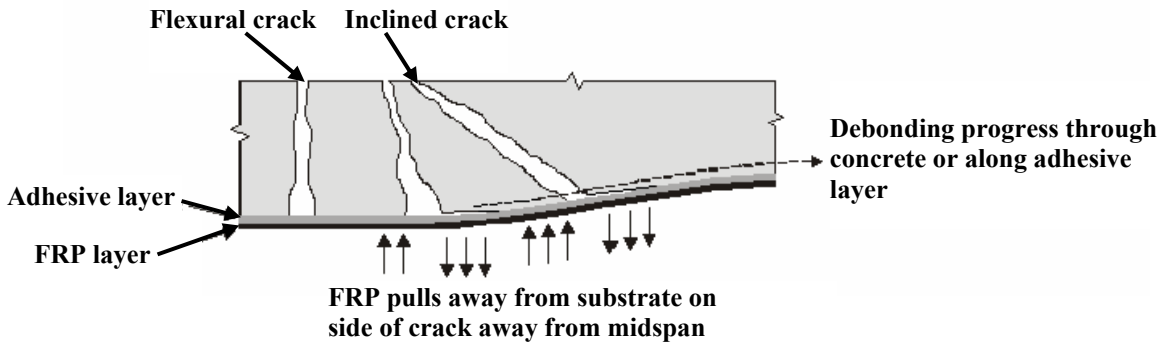

Figure 2.3: Intermediate crack induced debonding, Reeve [75]

2.3.3. Bond Strength Models

A number of bond strength models have been set and developed in the last twenty five years to predict the bond strength of FRP or steel plates-to-concrete. These models can be roughly sorted out into three categories: empirical models based directly on regression of test data, e.g. Tanaka [76], Maeda et al. [77] and Khalifa et al. [82]; fracture mechanics models, e.g. Holzenkämpfer [6], Täljsten [78], Neubauer and Rostásy [79], and Yuan et al. [80]; and design proposals that are based on some assumptions, Van Gemert [81], Chaallal et al. [68] and Roberts [83]. Previous fruitful research works have revealed some of the characteristics of the behaviour of the bonded joints between the external reinforcing plates and the concrete elements. However, research work on characterizing and quantifying the interfacial bond is still ongoing because of the importance of this topic.

Under the theoretical point of view various one-dimensional models have been proposed for estimating stress concentrations in the adhesive layer. Roberts [83] proposed one of the first formulations for evaluating normal and shear stress in the adhesive layer that most of the models neglect.

It is noted that most of the experimental based models reported were empirically calibrated against specific experimental data and were thus reported to be very accurate at predicting the behaviour against which they were calibrated. The accuracy of theses models may be degraded when applied to other experimental data.

Teng et al [25] examined twelve different approaches available in the scientific literature for assessing their strengths and weaknesses. They set a new model and identified most of the models developed for steel plated beams to be the more accurate ones, while those specially developed for FRP plated beams give poorer predictions. To verify the statement above, the model set by Holzenkämpfer [6], which has been developed by Neubauer and Rostásy [79]; Robert's model [83] and the model developed by Teng et al. [25] will be reviewed and verified with the obtained experimental results. The same terminology and notations would be used for all the above analytical models to facilitate their application.

3. Experimental Program

3.1. Introduction

To achieve the main objective of this research project, that is to evaluate the consequences of severe environments on the CFRP strengthened structures, an intensive experimental work was conducted at the following organizations: Institute for Building Materials, Concrete Structures & Fire Protection (iBMB) at the Carolo-Wilhelmina Technical University of Germany, and Building Research Center (BRC) at the Royal Scientific Society (RSS) of Jordan.

The accomplished experimental work was divided into three main work packages as follows.

1. Examinations on single materials, epoxies and CFRP plates;
2. Examination of the long term behaviour of RC slabs with high salt concentrations and CFRP externally bonded reinforcement under bending stress; and
3. Examinations on composite specimens, CFRP plates, epoxy adhesive and concrete.

The mechanical properties of three selected types of structural adhesives and one type of CFRP plates were evaluated after exposing representative test specimens to different environmental conditions, which included humidity, water, salt solutions and alkaline solutions, all associated with an ambient temperature of 23 ºC and a high temperature of 50 ºC.

The behaviour of the bond between concrete substrate and CFRP plates was studied and evaluated by testing CFRP strengthened RC slab specimens in bending under three-point loading, and testing CFRP strengthened concrete prisms in pure shear. Slab and prism specimens were subjected to two exposure regimes before testing. The first exposure regime started directly after the slab and prism specimens were manufactured and cured for 28 days and lasted for four months, whereas the second exposure regime was extended for almost one year after the specimens were strengthened with CFRP plates. The encountered environments included real-life environments prevailing at Amman city, Dead Sea region and Aqaba region of Jordan. In addition to laboratory simulated severe exposure conditions that included salt solutions, 50 % humidity combined with 50 ºC, and normal laboratory conditions of 65 % humidity and 20 ºC temperature.

Testing of similar specimens under-real life exposure conditions and simulated laboratory conditions allowed for a detailed evaluation of the durability and the behaviour of the bond between the CFRP plates and concrete in terms of bond strength and failure modes.

Before testing started certain procedures have been carried out, such as collecting environmental data, i.e. ambient maximum and minimum temperatures and humidity prevailing at Amman, Dead Sea and Aqaba regions of Jordan, in addition to some measurements to quantify the concrete surface temperatures and chloride contents for some reinforced concrete structures located at the three considered sites mentioned above. Furthermore, selecting the required materials, structural adhesives and CFRP plates, and preparing the needed test specimens, as will be shown in the following sections.

3.2. Materials

As this investigation aims at studying the long-term behaviour of CFRP strengthened structures under severe environments, it is important to be acquainted with the materials that have been used in this investigation.

This is especially true for the adhesives. There are many different types of structural adhesives that are used as bonding agents, which may react differently under different environments.

The concrete, FRP composites and adhesive materials selected for this research work were mostly representative of typical materials used in previous concrete repair and plate bonding research programmes.

Furthermore, the FRPs and adhesives were selected from good reputation materials available at the market place, on the basis of their well defined properties for providing a balance of suitable performance under severe environmental conditions.

FRP plates, structural adhesives and the stainless reinforcing steel used in this investigation were from the same sources for both the experimental work that was performed at BRC laboratories of Jordan and at iBMB laboratories of Germany. Whereas, concrete was produced at each of BRC and iBMB laboratories from the locally available cement and aggregates, but following the same mix design

3.2.1. Fiber Reinforced Plastic Materials

Carbon fiber reinforcing plastic composites in the form of unidirectional plates were used in this project. CFRP plates were chosen because they have higher mechanical properties as compared to other types of FRP composites. Moreover, CFRP composites have recognized an outstanding durability.

The selected CFRP composites were obtained from a manufacturer at Germany. They were in the form of continuous prefabricated plates, which consisted of unidirectional carbon fibers soaked in epoxy resin, and cured through heating. Fiber volumetric content was more than 70 % according to the manufacturer's data sheet. These CFRP plates were designed for strengthening concrete, timber, as well as masonry members by bonding onto the structure as external reinforcement.

The thickness and width of the CFRP plates as specified by the manufacturer were 1.4 mm and 50 mm, respectively. The plates were supplied in a roll form as shown in Figure 3.1. The mechanical properties of the plates as furnished by the manufacturer are shown in Table 3.1.

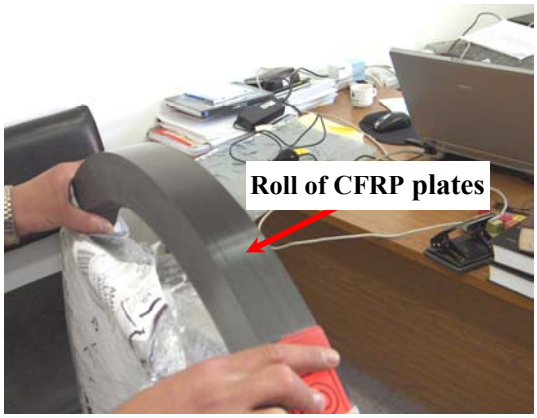

Figure 3.1: CFRP plates used in the research project

Table 3.1: Mechanical properties of CFRP plates as given by the manufacturer

Tensile strength	3360 MPa
Modulus of elasticity	168,000 MPa
Ultimate strain	0.02 mm/mm

The dimensions of the delivered CFRP plates were measured using a micrometer to evaluate the actual thickness and width. Measured values confirmed a width of 50 mm, but an average depth of 1.47 mm compared by 1.4 mm as per manufacturer's data sheet.

Furthermore, the CFRP plates were tested at the iBMB laboratories to obtain the actual mechanical properties. Twenty coupon test specimens of 15 mm wide and 300 mm long were tested in accordance with the recommendations of CEN 1996 [84]. Testing was performed under normal laboratory conditions using a Universal Testing Machine, Walter and Bai-LFV 100, and at a loading rate of 2 mm/min, as shown in Figure 3.2. The obtained tensile strength, rupture strain and the elastic modulus are shown in Table 3.2.

Figure 3.2: Failure of CFRP plate in tension

Table 3.2: Measured mechanical properties of CFRP plates

Tensile strength	3350 MPa
Modulus of elasticity	167,500 MPa
Ultimate strain	0.02 mm/mm

3.2.2. Structural Adhesives

The adhesive used for bonding a reinforcing plate to a concrete substrate is perhaps the most essential part for the success of the strengthening process. The adhesive must be capable of bonding the adherents, FRP plates and concrete, and has retain its strength when exposed to environmental conditions. This dictated that the adhesive should be resistant to moisture, temperature fluctuations, salt solution and concrete pore solution to ensure that the bond does not degrade during the service life.

To achieve the objectives of this investigation, it was essential to select the correct adhesives from a plethora of structural adhesives available at the market place. Investigating each type of these adhesives would have proven to be a monumental task well beyond the scope of this investigation.

A selection process was developed for selecting three adhesives with high glass transition temperature and with proved durability laboratory tests. In addition to be compatible with the chosen type of the CFRP plates.

In order to reduce the list of potential candidates that fit into the selection criteria for this application, previous studies involving the use of structural adhesives for the application of strengthening reinforced concrete structures were referenced, in addition to reviewing the information submitted from several manufactures taking into consideration the general adhesive requirements for structural bonding specified in specifications, e.g. CEN 2001a [85].

Three different types of adhesives were selected. They are cold curing epoxy based resin adhesives, which normally attained their full strength in 7 days at temperature of about 20 °C.

In order to maintain confidentiality, the commercial names, manufacturers' data sheets and the product properties can not be identified in this study. Each adhesive has been given an arbitrary label; Type 1, Type 1 Modified and Type 2.

Type 1 and Type 1 modified are produced by the same manufacturer which also produces the CFRP plates used in this investigation. Type 1 adhesive consisted of two components, epoxy resin and hardener. Type 1 Modified was similar to Type 1 as per the type and mixing ratios for the epoxy resin and hardener components, but differed from Type 1 with respect to the extra additives to enhance its properties. Whereas, Type 2 adhesive is produced by another manufacturer and also consisting of two components, epoxy resin and hardener.

Mix proportions of the selected adhesives are illustrated in Table 3.3.

Table 3.3: Adhesive types and their mixing proportions

Adhesive	Mixing Proportions
Type 1	Komp A: Komp B = 4:1 (w/w)*
Type 1 Modified	Komp A: Komp B = 4:1 (w/w) + 10 % of the weight of Komp C (additive)
Type 2	Komp A: Komp B = 3:1 (w/w)

***: weight to weight ratio**

Since the mechanical properties of the adhesives play a major role in this research project, a test program was set up to determine their mechanical properties. Tests were conducted at iBMB laboratories in accordance with the relevant standards and under normal laboratory conditions.

Tensile strength tests were performed according to the CEN 1999b [85] specification, elastic moduli according to ISO 178 [86] specification and glass transition temperature in accordance with CEN 1998c [87] specification.

Test results of the mechanical properties for the adhesives after 47 days curing under normal laboratory condition of 23 °C temperature and 65 % humidity, are presented in Table 3.4.

Table 3.4: Measured mechanical properties for the selected adhesives

Adhesive	Glass Transition Temperature (°C)	Tensile Strength (MPa)	Elastic Modulus (MPa)
Type 1	53.1	25.13	7905
Type 1 Modified	57.1	14.87	5716
Type 2	58	25.17	8995

3.2.3. Concrete

As stated earlier in section 3.2, the concrete used to produce the test specimens needed at BRC laboratories of Jordan, was prepared from Jordan local aggregates and cements. Similarly for the test specimens manufactured at iBMB laboratories of Germany, concrete was produced from German local aggregates and cement. The same concrete mix design, minimum compressive strength of 35 MPa with cement content of 350 kg/m^3 and w/c ratio of 0.5 was adopted and used for the production of concrete at both laboratories.

For the Jordanian specimens, the concrete was supplied by a local ready-mix supplier. The concrete strength was 35 MPa for all specimens. The actual mean 28-day cube strength of 45 MPa was obtained from testing three standard cubes of 150 x 150 x 150 mm^3 in dimension, which were cast at the time of casting and placement of the test specimens to characterize the concrete quality.

For Germany specimens, the concrete was prepared at iBMB laboratory following the same mix design described here above, and the actual mean 28-day cube strength was about 44.3 MPa.

3.2.4. Stainless Steel Reinforcing Bars

Stainless steel rebars were chosen instead of black rebars because corrosion of reinforcing steel is undesirable in this study. The presence of black reinforcing steel would complicate the otherwise straightforward evaluations if corrosion exists and loss of bond between the inner steel and concrete exists during different environmental conditioning. The focal point of this investigation is to study the behaviour of the bond between CFRP laminates and concrete, therefore, it is vital to protect the test specimens from corrosion and subsequent concrete deterioration.

Stainless steel rebars having diameter of 10 mm were used for reinforcing the slab specimens in both longitudinal and transverse directions.

According to the manufacturer, the steel exhibits a yield strength of 545 MPa and a tensile strength of 707 MPa.

The mechanical properties of the stainless steel rebars were tested at the mechanical laboratories of RSS to characterize the yield strength and ultimate strength. Test results revealed a value of 561.67 MPa for yield strength and a value of 688.33 MPa for ultimate strength.

3.3 Specimens for Single Materials Tests and Exposure Conditions

Representative test specimens were prepared from the selected types of CFRP composites and epoxies according to the respective specification. Test specimens were exposed to several environments, e.g. humidity, water, salt solutions, alkaline solutions and ultra violet radiations, all associated with ambient temperature of 23 °C and high temperature of 50 °C. According to the literature, these exposures are considered to be the most severe environments on CFRP composites and epoxies for outdoor applications.

The desired exposure regimes were identified according to the environmental conditions prevailing at the Middle East regions, particularly at the Dead Sea region of Jordan. This area is one of the most severely corrosive environments in the world. It is characterized by high temperature and humidity, in addition to the severe ground and ambient salinity with high levels of chlorides in soil and ground water.

Temperature values and humidity levels were estimated based on field measurements conducted by the researcher on several structures at Jordan, in addition to monthly recorded data collected from three different meteorological stations at Amman, Dead Sea and Aqaba regions, as illustrated in Appendix A.

Furthermore, chloride contents were assessed based on field measurements conducted by the researcher at one of the salt extracting plants operating at the Dead Sea region. Representative concrete powder samples were collected at various depths from footings and slabs of several units at the plant. Typical chloride ion contents as percentage of cement weight in concrete are outlined in Appendix A.

Based on the obtained data, several exposure conditions were identified and considered for conditioning and testing the selected single materials, as will be discussed in the following sections.

3.3.1. CFRP Plates

Standard representative test specimens having dimension of 15 mm width, 1.47 mm thickness and 300 mm length were prepared from the selected type of CFRP composites in accordance with the requirements of CEN 1996 [84].

Based on the literature review, and the need for evaluation the feasibility of utilizing CFRP composites in retrofitting deteriorated and substandard RC structures in Jordan, the test specimens were immersed in water, salt solutions and an artificial concrete pore solution, and in addition to 65 % moisture. All the exposures were performed at two different temperatures, ambient temperature of 23 °C and high temperature of 50 °C. The selected high temperature represents a realistic upper bound of service temperature that could be reached in the soffit of RC structural members in severe environment, such as the Dead Sea region.

The saline solution was composed of 0.5 mole KOH and 3 moles NaCl dissolved in a saturated Ca $(OH)_2$ solution. Whereas, concrete pore solution was composed of 0.5 mole KOH and 3 moles KCl dissolved in a saturated Ca $(OH)_2$ solution.

Mainly 4 different environments were considered for the conditioning of the test specimens, i.e. moisture, water, salt solutions and alkaline solutions, all associated with two different temperatures, 23 °C and 50 °C.

Additionally, test specimens were placed in an ultra violet chamber, and were exposed to two different environments, 250 MJ energy associated with 23 °C temperature and 500 MJ energy associated with 50 °C. The choice of these energies was based on the fact that, the UV components of solar radiation incident on the earth surface are in the band of (290 to 400) nm. The energy of these UV photons is comparable to the dissociation energies of polymer covalent bonds, which are typically (290 - 460) MJ, Mays and Hutchison [23].

Therefore, the number of test variables encountered for assessing the effects of environments on CFRP composites is ten, as outlined in Table 3.5.

Table 3.5: Exposure conditions for conditioning CFRP test specimens

Exposure No.	Details of exposure environments and storage
Exposure No.1	Temperature: 23° C; humidity: 65%; storage: in air
Exposure No.2	Temperature :23° C; storage: soaked in water
Exposure No.3	Temperature :23° C; storage: soaked in salt solution
Exposure No.4	Temperature :23° C; storage: soaked in alkaline solution
Exposure No.5	Temperature: 50° C; humidity: 50%; storage: in humidity chamber
Exposure No.6	Temperature :50° C; storage: soaked in water
Exposure No.7	Temperature :50° C; storage: soaked in salt solution
Exposure No.8	Temperature :50° C; storage: soaked in alkaline solution
Exposure No.9	Ultra Violet radiation; = 250 MJ ; Temperature :23° C
Exposure No.10	Ultra Violet radiation; = 500 MJ; Temperature :50° C

The mechanical properties were tested after conditioning the test specimens under the aforementioned environments for almost 96 days, and the test results are presented herein.

3.3.2. Epoxy Specimens

Test specimens were prepared by hand-mixing the required proportions of the components for each adhesive of the three selected materials in strict conformance with the manufacturer's instructions. Specimens were made according to the size and shape requirements of ASTM D 638 [88] Standards. Test specimens in dogbone-shape were produced for the mechanical testing in a custom mechanical testing device.

Produced test specimens were cured according to their related manufacturer's data sheet. Cured specimens were exposed to environments No. 1 to No. 8 shown in Table 3.5.

Measurements of the mechanical properties for the conditioned specimens were performed at two different ages, i.e., at 47 days and at 97 days. This was necessary for the evaluation of the effect of aging on the mechanical properties, in addition to the effect of exposure environments.

Since the testing temperature has a considerable effect on the properties of the adhesives and for the sake of obtaining accurate results, care has been taken to carry out testing at a temperature equivalent to the conditioning temperature.

Glass transition temperatures for the three adhesive types were determined via differential scanning calorimetry in accordance with ASTM D 4065 [89] Standards.

Additionally, water absorption measurements were performed at ages of (0, 1, 4, 7, 12, 19, 26, 32, 42, 56, 68 and 84) days from exposing representative samples of all selected adhesives to all environments, except environments No.1 and No.5. since specimens were not soaked in solutions. Measurement intervals were shorter at the beginning to capture the faster moisture uptake behaviour.

Test results for mechanical properties, glass transition temperatures and water uptakes for all adhesives are included herein.

3.4 Concrete Test Specimens and Exposure Conditions

3.4.1. Reinforced Concrete Slab Specimens

Thirty RC concrete slab specimens having dimensions of (1600 x 500 x 120) mm were prepared and cast in plywood moulds pre-fabricated to the required dimensions, of which twelve specimens were manufactured at iBMB laboratories and the rest were manufactured at BRC laboratories.

Deformed stainless steel rebars having 10 mm diameter were used to reinforce each specimen, five rebars in the longitudinal direction and eight rebars in the transverse direction, with a small concrete cover of approximately 25 mm, as illustrated in Figure 3.3.

Figure 3.3: Moulds and reinforcing details

Four stainless steel thin plates of 25 mm height and 2 mm thick were fixed at the bottom surface of each mould at locations where debonding of CFRP plates is likely to start. These plates were used to serve as crack raisers. They were placed at both sides from the center line of each mould at distances of 200 mm and 300 mm, as illustrated in Figure 3.4. This is to ensure that all slabs will have the same crack pattern at the critical locations and consequently the test results could be comparable.

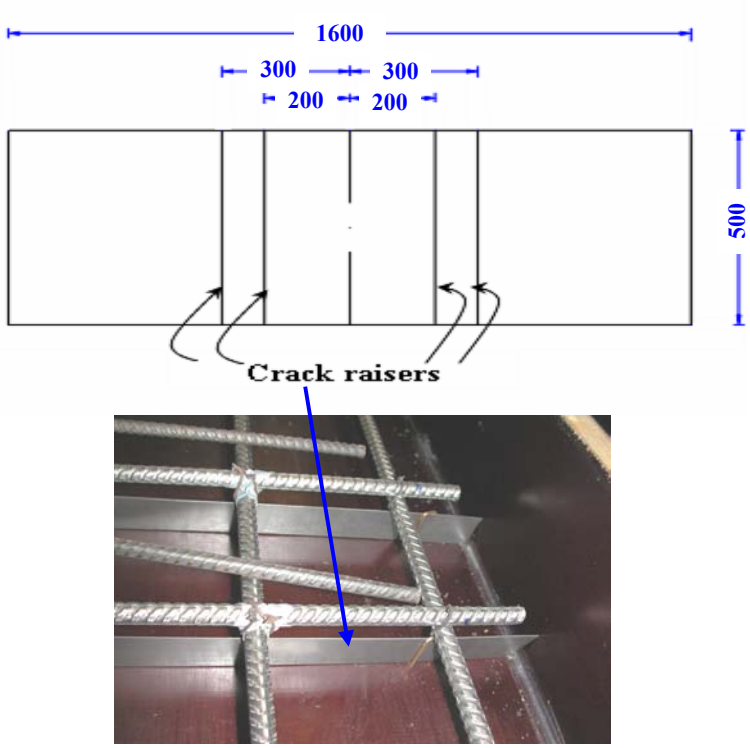

Figure 3.4: Location of crack raisers along slab specimens

Slab specimens were prepared from the concrete batches explained earlier in section 3.2.3. After 24 hours from casting, water sprays were applied to the specimens in order to cure them in a fashion similar to conventional construction. Wet curing of the specimens continued by covering the finished surfaces and moulds with damp burlap mats and plastic sheets for 7 days. This wet curing method kept the concrete continuously wet throughout the curing period.

After the 28-days curing, each pair of RC slab specimens were bonded together back-to-back with their tension faces outside in a sandwich form, and were subjected to sustained long-term loading using a steel-loaded fixture, which mainly consisted of four tie rods and spring plates as illustrated in Figure 3.5. This was necessary to force the slab specimens to crack at the predefined locations by the crack raisers.

All specimens were loaded in excess of the theoretical predicted cracking moment M_{cr}, being 5 kNm. They were subjected to initial sustained bending moment of 7.7 kNm, which is approximately equal to 40 % of the predicted slab capacity, being 19.4 kNm. This load was stipulated as 7.29 kN force per each tie-rod. This force was applied via a torque wrench using 8 spring plates, as shown in Figures 3.6 and 3.7. This mainly serves the purpose to create a realistic crack pattern to simulate the condition of deteriorated and cracked RC slabs at site. Also, to increase accessibility of salt solutions through the concrete as found in practice.

Figure3.5: Slab specimens placed back- to-back in sandwich form

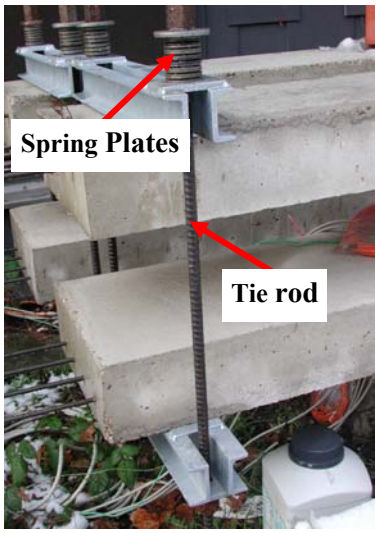

Figure 3.6: Tie rods and spring plates used to apply loads

Following the application of the sustained load, slab specimens in the sandwich form were exposed to real-life severe exposure conditions and normal laboratory conditions for a period of four months, as illustrated in Table 3.6.

The eighteen RC slabs that were produced at BRC laboratories were exposed to real-life environments prevailing at Jordan. Of which, 6 specimens were allocated at one of the salt extracting plants operating at the shore of the Dead Sea as shown in Figure 3.8. The chosen location was away from direct contact with chemical spills that are produced due to manufacturing processes. Another 6 specimens were allocated at the splash and tidal zone at the shore of the Red Sea of Aqaba region, as shown in Figure 3.9. This zone reflects the most severe type of chloride induced corrosion exposure for marine structures. Specimens at both locations were subjected to all the seasonal conditions throughout the storage period, including typical high temperatures of (37 – 49.5) °C in the summer and typical humidity of about 80 %, in addition to chlorides. And, the last six specimens were exposed to Amman environment by storing them at BRC laboratories, as shown in Figure 3.10.

On the other hand, the twelve specimens that were produced at iBMB laboratories were exposed to normal laboratory conditions, i.e. 23 °C temperature and 65 % humidity by storing them at iBMB laboratories. These specimens were considered as reference specimens.

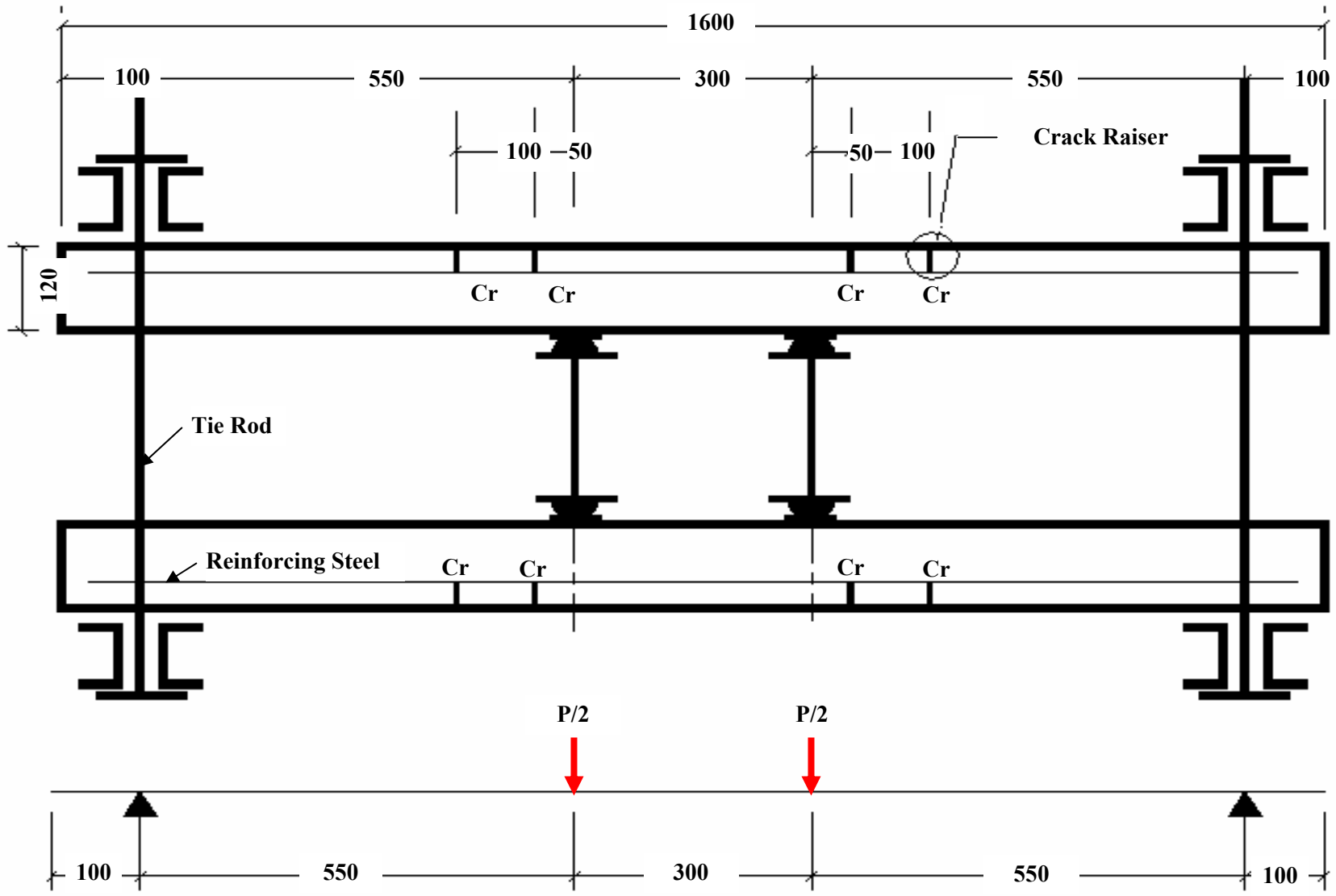

Figure 3.7: Four-point bending scheme test setup used for cracking slab specimens

Table 3.6: Exposure conditions for slab specimens for a period of four months

Slab Specimens Produced and Stored at Germany	Slab Specimens Produced and Stored at Jordan
Twelve slab specimens were stored at iBMB laboratories under normal laboratory conditions of 20 °C temperature and 65% humidity.	- 6 slabs were exposed to Dead Sea environment. - 6 slabs were exposed to Aqaba environment. - 6 slabs were exposed to Amman environment.

Figure 3.8: Slabs stored at Dead Sea region

Figure 3.9: Slabs stored at Aqaba region

Figure 3.10: Slabs stored at BRC laboratories – Amman city

CFRP plates of the length of 1200 mm were applied to the slab specimens after 4 months of exposure at the respective environments mentioned earlier. Composites were glued to the tension side of the specimens using the three selected types of epoxy adhesives. Application of the plates and surface preparation are detailed in Section 3.5 herein.

The applied load was increased by 20 % of its initial value, which accounts to a value of 8.75 kN per each tie rod. This new load was applied to each tie rod via a torque wrench and the spring plates after curing and hardening of the epoxy adhesive.

Slab specimens were stored again at the respective environments as shown in Table 3.7 for almost 12 months. Except six of the specimens that produced and stored at iBMB laboratories were exposed to chlorides by ponding their top surfaces with salt solutions (9.6 % NaCl solution) confined in rectangular wood dikes as shown in Figure 3.11.

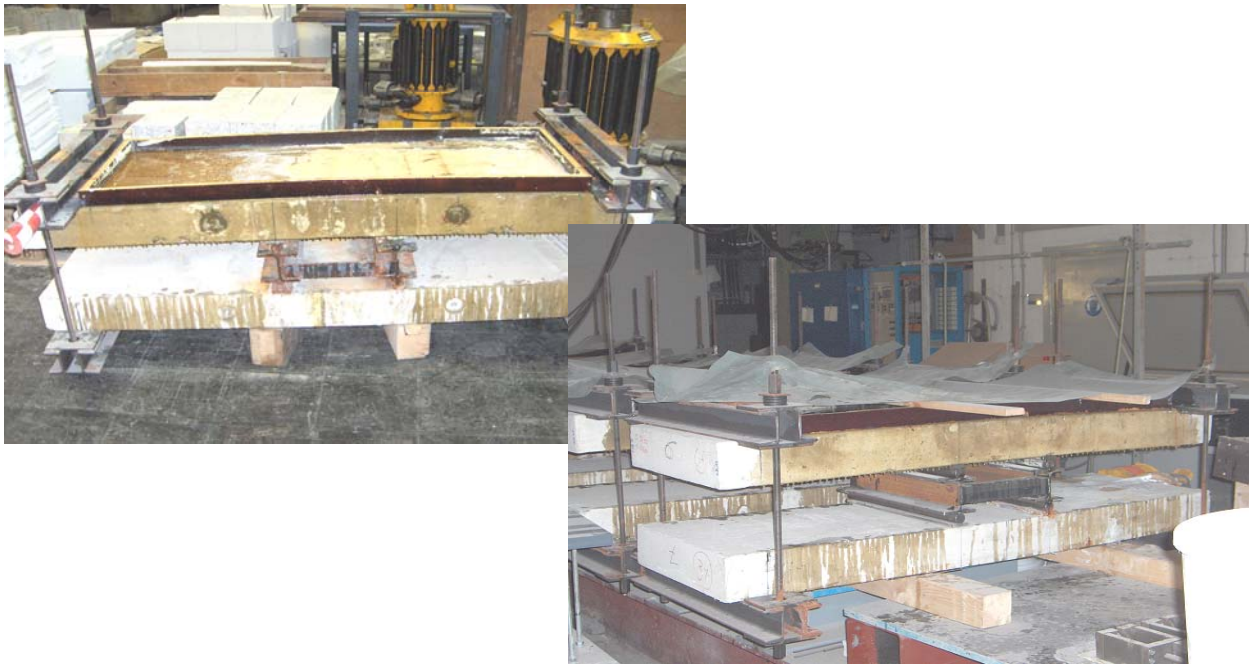

Figure 3.11: Exposing top specimens to salt solutions

Table 3.7: Exposure conditions of slab specimens after the application of CFRP plates for one year

Slab Specimens Produced and Stored at Germany	Slab Specimens Produced and Stored at Jordan
- 6 slab specimens were exposed to normal laboratory conditions of 20 °C temperature and 65% humidity, at iBMB laboratories. - 6 slab specimens were exposed to chlorides by ponding their top surfaces with salt solutions, and were stored at normal laboratory conditions of 20 °C temperature and 65% humidity, at iBMB laboratories.	- 6 slab specimens were exposed to Dead Sea environment. - 6 slab specimens were exposed to Aqaba environment. - 6 slab specimens were exposed to Amman environment

3.4.1.1. Testing of Reinforced Concrete Slab Specimens

a. General

Mechanical and electrical gauges as well as monitoring equipments were used to measure loads, deflections and CFRP strains. The following sections describe the system of instrumentation used prior to testing the strengthened slab specimens.

A computerized data-logging system was utilized to collect all electronic measurements by obtaining output in separate channels through Data Acquisition System. A supporting software known as Cat Man was installed on a laptop computer for monitoring the sensor signals.

Instrumentation and testing procedure for all slab specimens were kept the same for all types of exposure conditions.

b. Loads

All slab specimens were loaded using a universal testing machine of 250 kN capacity jack. Force-control was used for loads up to failure. Loads were applied in 10 kN increments during testing.

c. Strains

Electrical strain gauges of 120 ohm resistance were used to measure strains in the CFRP plates. Five strain gauges were used for each plate, of which four gauges were glued at the external surface of the CFRP plate exactly above the predefined cracks. Whereas, the fifth strain gauge was placed at the center of each plate, i.e. the location of the maximum moment. Figure 3.12 illustrates the location of the strain gauges.

Further more, demountable mechanical gauges, Demec strain gauges (DMC), were employed to measure strains along the CFRP plate. Twelve Demec targets were glued to one of the CFRP plates for each slab specimen, as shown in Figure 3.13.

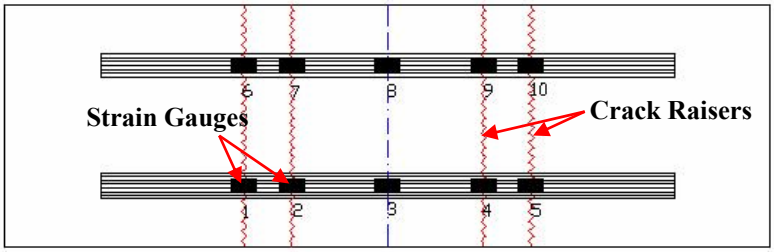

Figure 3.12: Location of electrical strain gauges along the CFRP plates

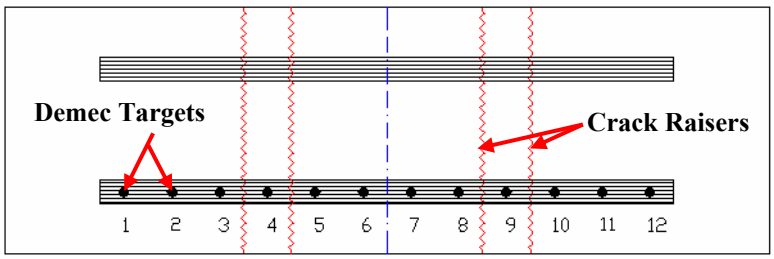

Figure 3.13: Location of Demec targets along one of the CFRP plates

d. Deflections

Deflections were measured at the midspan of each slab specimen by four linear variable differential transducers (LVDTs) connected to the data logging system. Two LVDTs were located at the center of the specimen and one LVDT was placed under each of the supports, as shown in Figure 3.14.

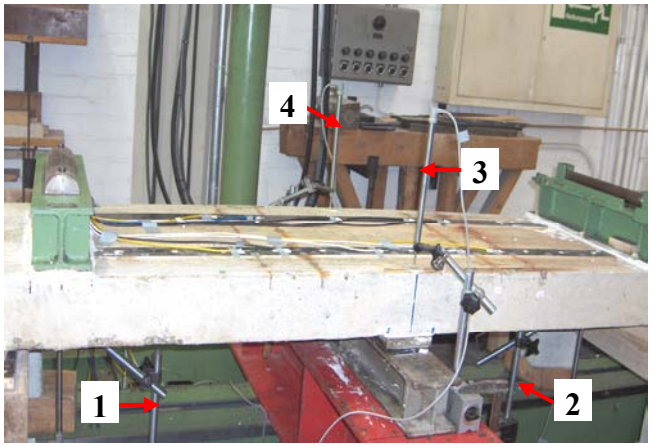

Figure 3.14: Location of LVDTs for all slab specimens

e. Testing

Following the conditioning, slab specimens were carefully unloaded and instrumented by the electrical strain gauges and the Demec targets at the locations explained earlier.

It was anticipated to test the slab specimens in a four-point bending scheme, with 1400 mm center-to-center between supports and 300 mm constant moment region, in a setup similar to the testing scheme used earlier to crack the specimens; but after testing the first specimen under four-point bending, premature concrete shear failure impaired the testing while the CFRP plates were still intact with the concrete surface, as shown in Figure 3.15.

Figure 3.15: Concrete shear failure

Such a failure mode is not favorable in this study as the main issue of the experimental work is to study the behaviour of the bond and to evaluate the effectiveness of different exposure conditions on it. Therefore, it was decided to change the setup to three-point loading in order to increase the shear span,

hence reducing shear forces on the concrete. On the other hand, the clear span between supports was reduced to 1320 mm by moving the supports 50 mm in the direction of the end of the plates. This was necessary to reduce the clear distance between the ends of the CFRP plates and the supports as much as possible and to have larger shear span. It was very difficult to locate the plates very closed to the supports when first applied to the bounded specimens in the sandwich form under the sustained loads.

The slab specimens were cast with compression side up, but tested with the tension side up. This was necessary for facilitating monitoring the CFRP plates and measuring the mechanical strains. The instrumented specimens were tested under three-point loading setup as shown in Figure 3.16.

Before testing, the LVDTs were located at the desired locations explained earlier. Load was applied in increments of 10 kN. At each load increment, crack development was observed and marked with a heavy felt pen. Additionally, cracks widths were measured and extensions between each two successive Demec targets were also measured.

The process of reading the Demec gauges, marking the observed cracks and measuring the widths of the major cracks took approximately five to ten minutes for each load increment. Loading was resumed to the next load step once the process was completed.

The Demec gauge readings were measured as near as possible to the peak load, however, these measurements could only be done with careful supervision to avoid any possibility of injury from a sudden failure of the CFRP plates. The electronic strain measurements, loads and deflections were taken continuously throughout each test. Test results are included in the next chapter.

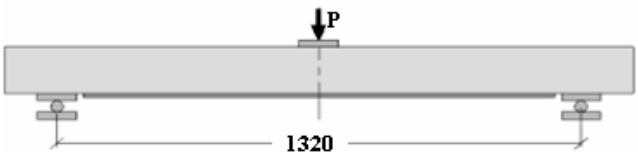

Figure 3.16: Three-point loading scheme for testing retrofitted slabs

f. Concrete Tensile Strength

The tensile strength at the concrete surface was measured by means of a pull-off test. Concrete tensile strength tests were performed after the testing slab specimens under three-point loading in accordance with EN1542 [90] Standards. Small steel cylinders of 50 mm diameter are glued onto the concrete surface. The fracture surface is bordered by coring just over the cylinder into the concrete. Then the fracture load that represents concrete tensile strength was measured as illustrated in Figure 3.17.

Figure 3.17: Concrete tensile strength measurements

g. Total chloride ion contents

This test was performed to determine chloride ion contents and the chloride-ion concentration profiles for slab specimens exposed to salt solutions, in addition to specimens exposed to real-life environments prevailing at Amman, Aqaba and Dead Sea regions. Concrete powder samples were collected from three different holes drilled at the top surface of the concrete tensile zone, of which one hole was drilled directly under each of the CFRP plates and the third hole was drilled in the concrete between the CFRP plates, as can be seen in Figure 3.18. Extractions were performed at three different depth levels along slab-depth, i.e. (0 – 10) mm, (10 – 30) mm and (30 – 60) mm.

Total chloride ion contents were determined by analyzing the collected powder samples at the chemical laboratories at iBMB institute for specimens exposed to salt solution, and at the chemical laboratories at RSS institute for specimens exposed to real-life environments.

Figure 3.18: Collecting concrete powder samples

3.4.2. Concrete Prism Specimens

A total of sixty six concrete prisms in all having nominal dimension of (150 x 150 x 450) mm were prepared and cast at both iBMB and BRC laboratories. Twenty one prism specimens were produced at iBMB laboratories and fourty five specimens were produced at BRC laboratories.

Prism specimens were cast and cured at the same time of producing the slab specimens and from the same concrete batches detailed in Section 3.2.3. Water sprays were applied to the specimens in order to cure them in a fashion similar to conventional construction, after 24 hours of casting. Wet curing of the specimens continued by covering the finished surfaces and moulds with damp burlap mats and plastic sheets for 28 days.

After the age of 28 days of curing, prism specimens were exposed to real-life environments and laboratory conditions for almost 4 months. Twelve specimens out of the twenty one prisms prepared at the iBMB laboratories were preconditioned by salt solution, by ponding their top surfaces with 9.6 % NaCl solution. Whereas, the fourty five prism specimens prepared at RSS laboratories were exposed to real-life environments prevailing at the Dead Sea region, Aqaba region and BRC laboratories; fifteen specimen at each location, as illustrated in Table 3.8.

CFRP plates of 500 mm length were applied to the prism specimens after 4 months of exposure at the respective environments mentioned earlier. Composites were bonded to the specimens for a length of 300 mm using the three selected types of epoxy adhesives. Whereas, the remaining 200 m length of the plates

were remaining free, as shown in Figure 3.19. Application of the plates and surface preparation are detailed in Section 3.5 herein. The 300 mm bonded length was chosen to satisfy the needed effective bond length according to the models developed by Neubauer and Rostásy [79], and Teng et al. [25].

After application of the CFP plates, all concrete prisms were stored again for another period of one year at the respective environments shown in Table 3.9, and illustrated in Figures 3.19, 3.20, and 3.21.

Table 3.8: Exposure environments of prism specimens for four months

Prism Specimens Produced and Stored at Germany	Prism Specimens produced and Stored at BRC
- 12 specimens treated with salt solutions and stored at iBMB laboratory under normal laboratory conditions. - 9 specimens were stored at iBMB laboratory under normal conditions.	- 15 specimens were exposed to Dead Sea environment. - 15 specimens were exposed to Aqaba environment. - 15 specimens were exposed to Amman environment.

Table 3.9: Exposure environments of prism specimens after CFRP Application for one year

Prism Specimens Produced and Stored at Germany	Prism Specimens Produced and Stored at Jordan
- 6 specimens pre-treated with salt solutions were exposed to normal laboratory conditions of 20 °C temperature and 65 % humidity. - 6 specimens pre-treated with salt solutions were exposed to 50 °C temperature and 50 % humidity at a humidity chamber. - 9 specimens were exposed to normal laboratory conditions.	- 15 prism specimens were exposed to Dead Sea environment. - 15 prism specimens were exposed to Aqaba environment. - 15 prism specimens were exposed to Amman environment.

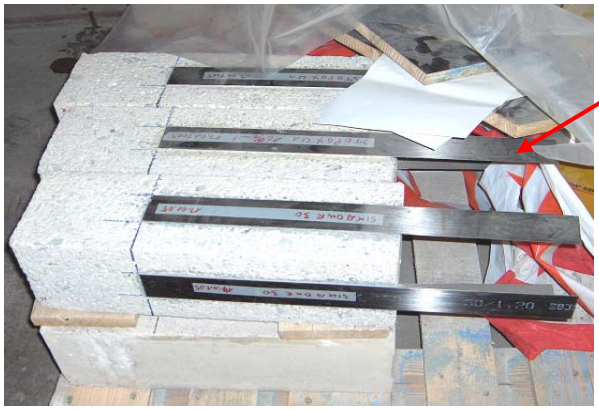

Figure 3.19: Storage of specimens at iBMB laboratories

Figure 3.20: Storage of specimens at the humidity chamber

Figure 3.21: Storage of specimens at Aqaba region

3.4.2.1. Testing of Concrete Prism Specimens

Bond strength of all prism specimens were measured by direct shear strength test using the DSS-TEST instrument manufactured by Germann Instruments.

The un-bonded 200 mm part of the CFRP plate was fixed to a pair of gripping jaws and emery papers to increase friction and prevent slippage of the plate. The jaws were firmly tightened to the plate in between with transverse fasteners. A pull assembly with coupling attachment was connected to the jaws, and a counter pressure was governed over the transverse fasteners and made to rest against the pedestal. A hydraulic pull machine was attached to the coupling and made to rest against the counter pressure. The loading was increased until rupture occurs between the plate and the substrate. Figure 3.22 illustrates the testing process.

This machine is operated manually by hand and the pull machine is loading the CFRP plate in shear.

Furthermore, concrete tensile strength and total chloride ion contents were performed for each concrete prism as per the procedure explained earlier in items f and g of section 3.4.1.1 respectively.

Figure 3.22: Testing process for measuring CFRP plate-concrete bond strength

3.5 Application of CFRP Plates

Concrete surfaces were sand blasted using a hand grinder to remove the surface cement paste and expose the aggregates, in order to allow ensuring proper bonding for the CFRP plates through the epoxy layer. In particular, the surfaces of the tension side (soffit) of the slab specimens, and the casting face of the prism specimens were thoroughly sanded to remove the surface cement paste with minor exposure of aggregates, as shown in Figure 3.23. Dusting from surface grinding was removed using compressed air blower to achieve dust free and clean surface.

Next, the roll of the 50 mm wide CFRP was cut into lengths of 1200 mm for the slab specimens and 500 mm for the prism specimens using a manual saw as shown in Figure 3.24.

Figure 3.23: Exposed aggregate

Figure 3.24: Cutting CFRP plates

Surface preparation for the CFRP plates was performed in accordance with the manufacturer's instructions. CFRP plate surface was wiped with an acetone-soaked cloth until ensured removal of all carbon dust.

Selected types of epoxy adhesives were prepared in accordance with the respective manufacturer's published mixing instructions, regarding mix ratio of components, proper temperature, mixing tools, speed and time. Adhesive components were mixed thoroughly according to the manufacturer's prescribed mixing time and visually inspected for uniformity of colour. Adhesive components were contrasting colours, so full mixing was achieved when colour streaks are eliminated and homogenous mixture is attained. Care was taken to mix only the quantity of epoxy adhesive which can be used within its pot life.

The adhesive was applied as a thin layer with a trowel to the concrete immediately after mixing. Also, the adhesive was applied to the roughest face of the plate in a dome shape, having slightly more thickness along the center line of the plate. This reduces the risk of forming voids when the plate is applied. The plate was positioned to the concrete surface without applying pressure until checking its correct place. Pressure was applied starting from the center of the plate going to the far ends using a rubber roller to insure intimate contact with the concrete, and not allowing the formation of voids. Figure 3.25 detailed the application procedure.

For the slab specimens, two CFRP plates were applied at the tension side for each specimen. The distances from both edges to the plates were 100 mm, and the distance between the two plates was 200 mm, as shown in Figure 3.26a. Whereas, for the prism specimens, the CFRP plate was centered along the longitudinal axis of the concrete prism and a 50 mm shoulder was left on either side of the bond

to remove edge effects. The bond length was 300 mm and the cantilever free length was 200 mm, as illustrated in Figure 3.26b.

It worth mentioned here, the application of the CFRP plates to the slab specimens were performed while the specimens were bounded together in the sandwich form and under the applied sustained loads. This was necessary to simulate the retrofitting of real structures at site, as dead loads are always present on the structure while strengthening.

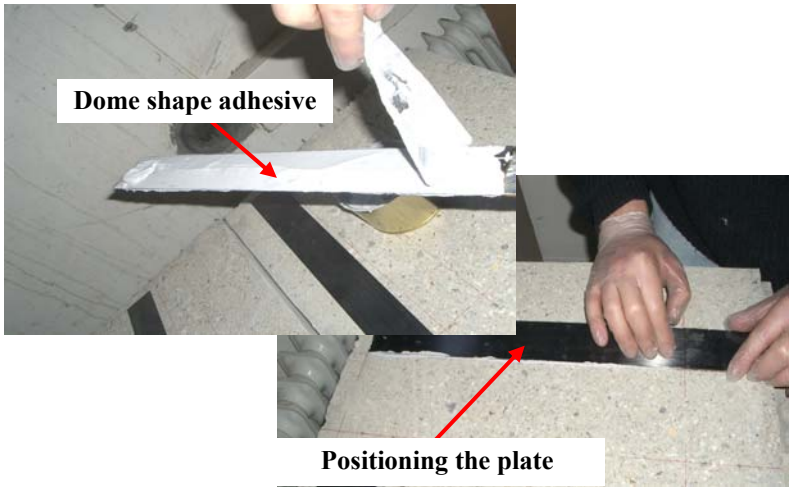

Figure 3.25: Application of CFRP plates to concrete substrate

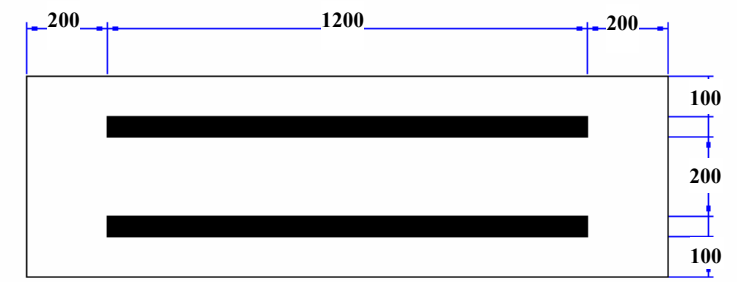

a. Slab specimen

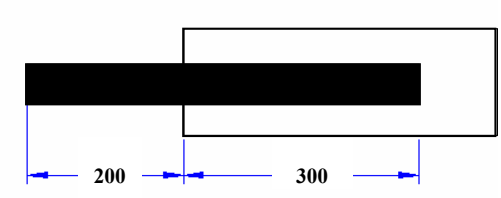

b. Prism specimen

Figure 3.26: Location of CFRP plates

3.6 Ultimate Strength Analysis

In this section, ultimate strength analysis of the retrofitted slab specimens is performed and the calculated flexural load capacities are given as a basis for the following comparison with the attained test results and calibration studies, ACI [13] and Chaallal et al [68].

The fundamental assumptions of this approach are full composite action, i.e. perfect bond at the concrete-FRP interface, and strain compatibility, i.e. plane sections remain plane. In what follows, basic compatibility and equilibrium equations are presented to determine the flexural capacity of an FRP strengthened slab.

The stress and strain distribution in a strengthened slab/beam at or close to ultimate state is shown in Figure 3.27. From the equilibrium and strain compatibility conditions, the nominal moment capacity, M_n, is as given in equation 3.1.

$$M_n = A_s f_s\left(d - \frac{\beta_1 c}{2}\right) + A_f f_f\left(h - \frac{\beta_1 c}{2}\right) \tag{3.1}$$

The steel stress, f_s, can be determined from strain assuming an elastic-perfectly plastic behaviour as,

$$f_s = E_s \varepsilon_s \le f_y \tag{3.2}$$

and the FRP stress, f_f, can be determined from the FRP strain assuming a linear elastic behaviour as,

$$f_f = E_f \varepsilon_f \tag{3.3}$$

From strain compatibility, the FRP strain, ε_f, is related to the concrete strain, ε_c, by the following relation

$$\varepsilon_f = \varepsilon_c\left(\frac{h}{c} - 1\right) \tag{3.4}$$

and the relation between the steel strain, ε_s, and the FRP strain, ε_f, can be written as,

$$\varepsilon_s = \varepsilon_c\left(\frac{d}{c} - 1\right) = \varepsilon_f\left(\frac{d-c}{h-c}\right) \tag{3.5}$$

From equilibrium, the depth of the neutral axis, *c*, is given by

$$c = \frac{A_s f_s + A_f f_f}{\gamma \beta_1 f_c' b} = \frac{\left(\rho_s f_s + \rho_f f_f\right) d}{\gamma \beta_1 f_c'} \tag{3.6}$$

where the steel reinforcement ratio ρ_s, and the FRP reinforcement ratio, ρ_f, are defined as analogous dimensionless forms as

$$\rho_s = \frac{A_s}{bd} \quad , \rho_f = \frac{A_f}{bd} \tag{3.7}$$

When failure mode is controlled by concrete crushing, γ and β_1 can be taken as the values associated with the equivalent Whitney stress block, i.e. $\gamma = 0.85$ and β_1 as defined in ACI [99];

$$\beta_1 = 1.09 - 0.008 f_c' \tag{3.8}$$

If failure is through FRP rupture, cover delamination or FRP debonding, which means the maximum concrete strain at failure is below the ultimate strain of concrete; use of the Whitney stress block may still give reasonably accurate results, ACI [13]. However, more accurate values for γ and β_1 can be obtained by considering the nonlinear behaviour of concrete below ultimate strain. For an arbitrary concrete stress-strain model, the parameters α and β can be given by

$$\alpha = \frac{\int_0^{\varepsilon_{cm}} f_c d\varepsilon_c}{f'\varepsilon_{cm}}, \qquad \beta = 1 - \frac{\int_0^{\varepsilon_{cm}} f_c d\varepsilon_c}{\varepsilon_{cm} \int_0^{\varepsilon_{cm}} f_c d\varepsilon_c} \tag{3.9}$$

From which γ and β_1 can easily be determined as

$$\beta_1 = 2\beta \ , \quad \gamma = \frac{\alpha}{\beta_1} \tag{3.10}$$

Analysis of the flexural failure modes involves solution of equations 3.1 to 3.6 simultaneously which may be performed through an analytical or an iterative approach. The analytical approach is taken here, as the iterative approach is more suited for computer application. As flexural failure of a FRP strengthened element may occur through one of three possible failure modes, which are associated with different ultimate stress and strain conditions, identifying the failure mode is an integral part of the solution. A conceptual analysis of the flexural failure modes suggests that at low FRP reinforcement ratio, failure occurs through reinforcement yielding followed by FRP rupture. With increasing FRP reinforcement ratio, one expects a transition in the failure mode, first to reinforcing steel yielding followed by concrete crushing, and then to concrete crushing before steel yielding. Thus, by determining the transition points, one can determine the failure mode from the FRP reinforcement ratio.

Flexural failure of unstrengthened beams may occur through one of two different modes. Concrete crushing before steel yielding for over reinforced sections, or concrete crushing after steel yielding for under reinforced sections.

The balanced steel ratio is determined as the steel ratio that causes concrete crushing and steel yielding to take place simultaneously. As there are three possible flexural failure modes for strengthened beams, there are two different balanced FRP ratios, namely balanced FRP ratio for steel yielding and the balanced steel ratio for FRP rupture.

The balanced FRP ratio for steel yielding, ρ_{fp}, is defined as the FRP reinforcement ratio that causes concrete crushing and steel yielding to take place simultaneously in flexurally strengthened under reinforced sections. Thus, ρ_{fp}, specifies the maximum FRP area that can be used for strengthened beam to fall in a ductile manner. Setting $\varepsilon_c = \varepsilon_u$ and $\varepsilon_s = \varepsilon_y$, the balanced FRP ratio for steel yielding, ρ_{fp}, can be determined from equilibrium and strain compatibility as

$$\rho_{fb} = \frac{A_{fp}}{bd} = \frac{0.85 f'_c \beta_1 \eta_s - \rho f_y}{E_f \varepsilon_u \left(\frac{h}{\eta_s d} - 1 \right)} \tag{3.11}$$

where $\eta_s = \dfrac{\varepsilon_u}{\varepsilon_u + \varepsilon y}$,

The balanced FRP ratio for FRP rupture, ρ_{fr}, or simply the balanced FRP ratio can be defined as the FRP ratio that results in concrete crushing and FRP rupture to take place simultaneously. Setting $\varepsilon_c = \varepsilon_u$ and $\varepsilon_f = \varepsilon_{fu}$, ρ_{fr} can be determined from equilibrium and strain compatibility as

$$\rho_{fr} = \frac{A_{fr}}{bd} = \frac{0.85 f'_c \beta_1 \eta_f \dfrac{h}{d} - \rho f_y}{f_{fu}} \tag{3.12}$$

where $\eta_f = \frac{\varepsilon_u}{\varepsilon_u + \varepsilon_{fu}}$, A_{fr}, is the FRP area that results in the balanced condition of FRP rupture and f_{fu} is the ultimate tensile strength of the FRP. Implicit in equation 3.12 is the assumption that the steel reinforcement yields before FRP ruptures take place, which is a valid assumption for all practical sizes of flexural members considering that the typical ultimate strain of FRP composites are much larger than the yield strain of steel.

In view of equations 3.11 and 3.12, the flexural failure mode of strengthened element can be identified based on the FRP ratio such as if $\rho_f > \rho_{fb}$, a brittle mode of failure through concrete crushing before steel yielding is expected; $\rho_{fr} < \rho_f < \rho_{fb}$, failure occurs through steel yielding followed by concrete crushing; and if $\rho_f \le \rho_{fr}$, steel yielding followed by FRP failure mode will take place.

Once the failure mode of the strengthened beam is identified, its flexural capacity can be determined using equation 3.1 and the compatibility conditions associated with the identified failure mode.

For $\rho_f > \rho_{fb}$, concrete crushing before reinforcing steel yielding (CCBRY), depth of the neutral axis is given by,

$$c = \frac{-B + \sqrt{B^2 - 4AC}}{2A} \qquad 3.13$$

where

$$A = 0.85 f_c' \beta_1 b \ ; B = A_s E_s \varepsilon_u + A_f E_f \varepsilon_u \text{ and } C = -\left(A_s E_s \varepsilon_u d + A_f E_f \varepsilon_u h\right)$$

with c known, f_s and f_f are calculated from equations 3.2 to 3.5, setting $\varepsilon_c = \varepsilon_u$, substituting f_s and f_f in equation 3.1, the nominal moment capacity for $\rho_f > \rho_{fb}$ is given by

$$M_n = A_s E_s \varepsilon_u \left(\frac{d}{c} - 1\right)\left(d - \frac{\beta_1 c}{2}\right) + A_f E_f \varepsilon_u \left(\frac{h}{c} - 1\right)\left(h - \frac{\beta_1 c}{2}\right) \qquad 3.14$$

For $\rho_{fr} < \rho_f < \rho_{fb}$, concrete crushing followed by reinforcing steel yielding (CCFRY), and the depth of the neutral axis is given by

$$c = \frac{-B + \sqrt{B^2 - 4AC}}{2A} \qquad 3.15$$

where

$$A = 0.85 f_c' \beta_1 b \ ; B = -A_s f_y + A_f E_f \varepsilon_u \text{ and } C = -\left(A_f E_f \varepsilon_u h\right)$$

and the nominal moment capacity for $\rho_{fr} < \rho_f < \rho_{fb}$ is given by

$$M_n = A_s f_y \left(d - \frac{\beta_1 c}{2}\right) + A_f E_f \varepsilon_u \left(\frac{h}{c} - 1\right)\left(h - \frac{\beta_1 c}{2}\right) \qquad 3.16$$

For the case where $\rho_f \le \rho_{fr}$, yielding of reinforcing steel followed by FRP rupture (RYFFR) will be the failure mode and the neutral axis will be

$$c = \frac{A_s f_y + A_f f_f}{\gamma f_c' \beta_1 b} \qquad 3.17$$

and the nominal moment capacity for $\rho_f \le \rho_{fr}$ is given by

$$M_n = A_s f_y \left(d - \frac{\beta_1 c}{2} \right) + A_f f_{fu} \left(h - \frac{\beta_1 c}{2} \right) \qquad 3.18$$

3.6.1. Analysis of Test Specimens

The analysis procedure described above was implemented for the evaluation of the expected failure loads for the retrofitted slabs. Considering material properties, geometry of slab specimens and test setup provided in the previous sections, the following results are obtained.

$\rho_s = 0.0083$

$\rho_f = 0.0031$

$\rho_{fr} = -0.0002$

A negative ρ_{fr} means that FRP rupture is theoretically not expected to take place regardless of the FRP ratio, and the FRP plate will never reach its ultimate strain. Thus, the expected flexural failure mode of the strengthened FRP slabs will be concrete crushing before yielding of the reinforcing steel.

For this failure mode, the neutral axis at failure is given by

$$c = \frac{-B + \sqrt{B^2 - 4AC}}{2A}$$

where,

$A = 12240$; $B = 321457.5$ and $C = -32385150$

$c = 40\ mm$

$$\varepsilon_f = \varepsilon_u \left(\frac{h - c}{c} \right) = 0.006\ mm/mm$$

$$M_n = A_s E_s \varepsilon_u \left(\frac{d}{c} - 1 \right) \left(d - \frac{\beta_1 c}{2} \right) + A_f E_f \varepsilon_u \left(\frac{h}{c} - 1 \right) \left(h - \frac{\beta_1 c}{2} \right) = 46.16\ kNm$$

Accordingly maximum load at failure $P = 140\ kN$

On the other hand, the predicted failure loads for the original slabs before retrofitting are as follows.

$M_n = 19.4\ kN/m$

$P = 58.8\ kN$

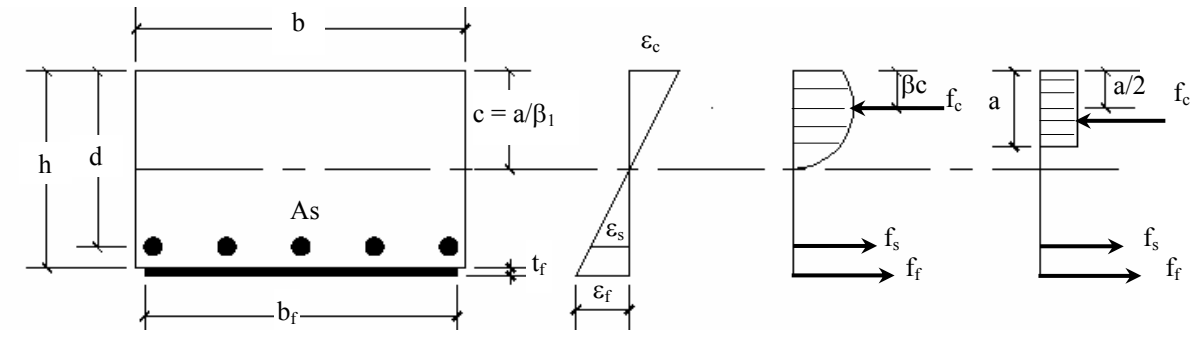

Figure 3.27: Stress and strain distribution in a strengthened slab section

4. Test Results and Discussion

4.1. Introduction

This chapter presents and compares the results obtained from the experimental work conducted to achieve the main objective of this research project. This investigation intended to study the effect of severe environmental conditions, such as high temperature and salt solutions, on the performance of CFRP-bonded concrete slabs and on the interfacial bond between the composites and the concrete substrate.

As stated earlier in the previous chapter, and will be repeated here again for the comprehensiveness of this report, the conducted experimental work was divided to the following main work packages,

1. Examination on single materials (epoxies and CFRP plates);
2. Examinations of the long term behaviour of RC slabs with high salt concentrations and CFRP externally bonded reinforcement under sustained bending loading; and
3. Examinations on composite specimens (CFRP plates, epoxy adhesive and concrete).

Accordingly, this chapter is divided into the following sections.

Section 4.2 shows the results obtained from testing the mechanical properties of the single materials, CFRP composites and structural adhesives, after conditioning representative samples into moisture, water, salt solutions, and alkaline solutions, all associated with two different temperatures, ambient temperature of 23 ºC and high temperature of 50 ºC. Additionally, the mechanical properties of the CFRP composites were evaluated after exposure to UV – 500 and UV – 250 ultra violet radiations.

Observed failure modes and measured loads at failure for flexural tests, along with the corresponding deflections and strains were presented and discussed in section 4.3. Measured values for chloride contents and concrete tensile strength values were also included. Additionally, shear stresses along one of the CFRP plates for each slab were predicted and included.

Results obtained from direct shear tests are outlined in section 4.4. It included the observed modes of failure, failure loads, chloride contents and concrete tensile strength.

Obtained test results are summarized in section 4.5

4.2. Test Results of Single Materials

4.2.1. Test Results of CFRP Plates

The mechanical properties of the CFRP plates were tested after conditioning representative specimens for almost 96 days under different environments, as illustrated in a schematic format in Figure 4.1. Five test specimens were used for each environment. The consequences of the severity of the encountered environments on the mechanical properties of the CFRP composites are shown hereunder.

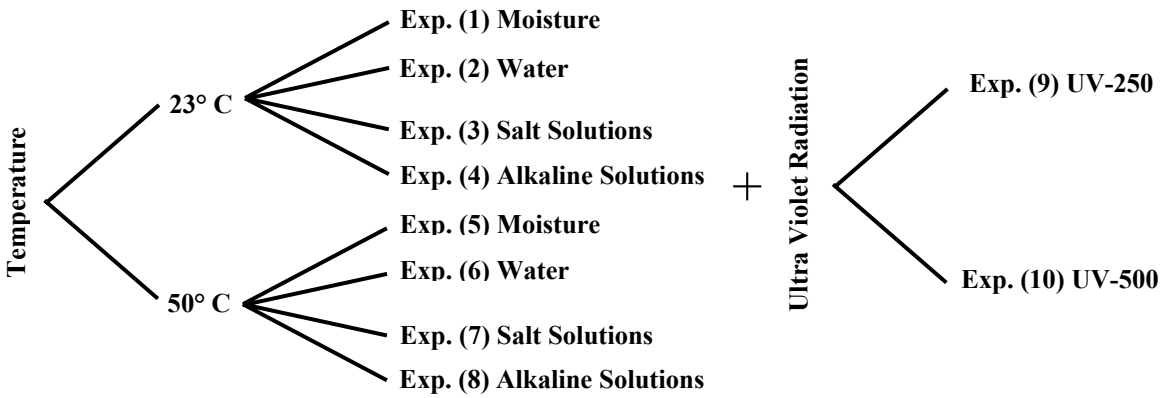

Figure 4.1: Exposure conditions used for conditioning CFRP plate test specimens

4.2.1.1. Tensile Strength

Measured values of tensile strength for test specimens that were conditioned under all the encountered environments are presented in Figure 4.2.

The following observations could be drawn from the collected measured values.

Average tensile strength values were in the range of (2983.5 - 3171.5) MPa for specimens conditioned under environments No.1 – No.4 combined with 23 °C temperature. As it should be, the highest value was for specimens exposed to normal laboratory conditions, followed by a value of 3061.5 MPa for specimens soaked in water, and a value of 3027.5 MPa for specimens soaked in salt solutions. Whereas, specimens immersed in alkaline solutions got the lowest average tensile strength.

For specimens conditioned at environments No.5 – No. 8 associated with high temperature of 50 °C, the average tensile strength values were in the range of (2972 – 3176) MPa. The highest value was for specimens exposed to moisture, followed by a value of 3125 MPa for specimens immersed in water and a value of 3095 MPa for specimens immersed in salt solution, respectively. The lowest value was for specimens immersed in alkaline solution respectively.

Whereas, specimens exposed to environments No. 9 and No.10 showed an unexpected trend; specimens exposed to UV-500 had higher strength with an average value of 3058.7 MPa as compared to an average value of 3040 MPa for specimens exposed to UV-250.

Insignificant increase in the measured tensile strength was observed for specimens exposed to moisture, immersed in water and salt solutions, all associated with 50 °C temperature when compared to their corresponding specimens conditioned under the same environments but at 23 °C temperature. Percentage increase in tensile strength was about 0.15 %, 2 % and 2.2 % for specimens exposed to moisture, immersed in hot water and immersed in hot salt solutions, respectively. Also, a slight increase in tensile strength of 0.62 % was observed for specimens exposed to UV-500 as compared to their corresponding specimens but exposed to UV-250. A possible reason for this insignificant enhancement on tensile strength could be attributed to beneficial post-curing by high temperature for the resin matrix that holds and encapsulates the carbon fibers. Similar observations were obtained by previous researchers, e.g. Shahrooz et al. [91].

On the other hand, specimens immersed in alkaline solutions associated with 50 °C temperature showed reduction in tensile strength of about 6.3 % when compared with their corresponding reference specimens. Also, specimens exposed to ultra violet radiations showed an insignificant reduction of about 4 % and 3.6 % for specimens exposed to UV – 250 and UV – 500, respectively. However, these reductions in strength are not considered large enough to significantly affect the durability performance of the CFRP plate, taking into consideration the severity of environments.

All the recorded values for tensile strength are reasonable and far above the stringent limits set by the code of practice, ACI [14]. The code suggests 15 % reduction on the tensile strength of CFRP plates when exposed to outdoor severe environments.

Roughly, we could say that there is no detrimental effect from the encountered environments on the tensile strength of the CFRP composites.

4.2.1.2. Modulus of Elasticity

Average values of the elastic moduli for all specimens conditioned under all the encountered environments are shown in Figure 4.3.

The following observations could be made from the obtained results.

Obtained values were in the range of (160.2 – 167.5) kN/mm^2 for all specimens conditioned under environments No.1 to No. 4 at ambient temperature of 23 °C. The highest value was for specimens exposed to normal laboratory conditions, followed by a value of 165.5 kN/mm^2 for specimens immersed in water, then a value of 161.5 kN/mm^2 for specimens immersed in salt solution. Specimens immersed in alkaline solution got the lowest value.

For specimens conditioned under environments No. 5 to No. 8 associated with high temperature of 50 °C, elastic moduli were in the range of (163.6 – 167.3) kN/mm^2. The highest value was for specimens exposed to moisture, followed by a value of 166.9 kN/mm^2 for specimens immersed in water, and then a value of 164.6 kN/mm^2 for specimens immersed in salt solution. The lowest value was for specimens immersed in alkaline solution.

Furthermore, specimens exposed to UV-500 got higher values, being 161.2 kN/mm^2, when compared to a value of 158.9 kN/mm^2 for specimens exposed to UV-250.

Generally, specimens exposed to high temperature, 50 °C, got higher values when compared with their corresponding specimens conditioned under the same environments but at 23 °C temperature. Insignificant increase in the measured elastic moduli in the order of 0.4 % and 0.8 % for specimens exposed to moisture and immersed in water, respectively. Whereas, specimens immersed in salt solutions and alkaline solutions have similar increased value of 2% on the measured elastic modulus. This trend correlates very well with the trend observed for tensile strength, and again is related to the effect of post-curing of the resin matrix.

Insignificant reduction on the measured elastic moduli in the range of (0.12 – 5.13) % is observed when comparing the results obtained from testing specimens conditioned under all environments with the reference specimens. The lowest reduction value is for specimens immersed in water at ambient temperature, whereas, the highest value was for specimens conditioned in alkaline solutions associated with high temperature. However, this reduction is not considered large enough to significantly affect the performance of the composite material.

4.2.1.3. Maximum Strain at Failure

Average measured rupture strains for all test specimens following the environmental exposure are shown in Figure 4.4. No significant changes in the measured strains compared to the reference specimen were observed. All the measured values fall in the range of (0.019 – 0.02) mm/mm. This observation indicates that the composite material is stiff and generally being not affected by the different exposure environments, thus confirming the previous observations that there is no detrimental effect from the encountered environments.

As a general conclusion, the findings obtained so far are very encouraging because of the satisfactory performance of CFRP composite under the encountered environments, which represent the most severe environmental conditions. This result could be attributed to the high glass transition temperature of the polymer matrix that bounded the carbon fibers, taking into consideration that carbon fibers are very durable material. Additionally, it proofs the high quality of the manufacturing, processing and curing of the composite material. Therefore, the molecular chain of the resin material is more restrained and stiff.

Accordingly, the chosen type of CFRP composite proved an adequate performance under harsh environments, and can be used for retrofitting structures such as those located at the Dead Sea and Aqaba regions of Jordan. This conclusion is further reinforcing comparable previous conducted studies by Rahimi [14], Rostásy [17], Karbhari et al. [24], Tommaso et al. [22] and David and Neuner [36].

It is prudent to state that this conclusion is specifically devoted for the chosen type of CFRP plates and may not be generalized to other types. For every specific application of CFRP plates, particularly at severe environment, it is recommended that the mechanical properties have to be checked and evaluated.

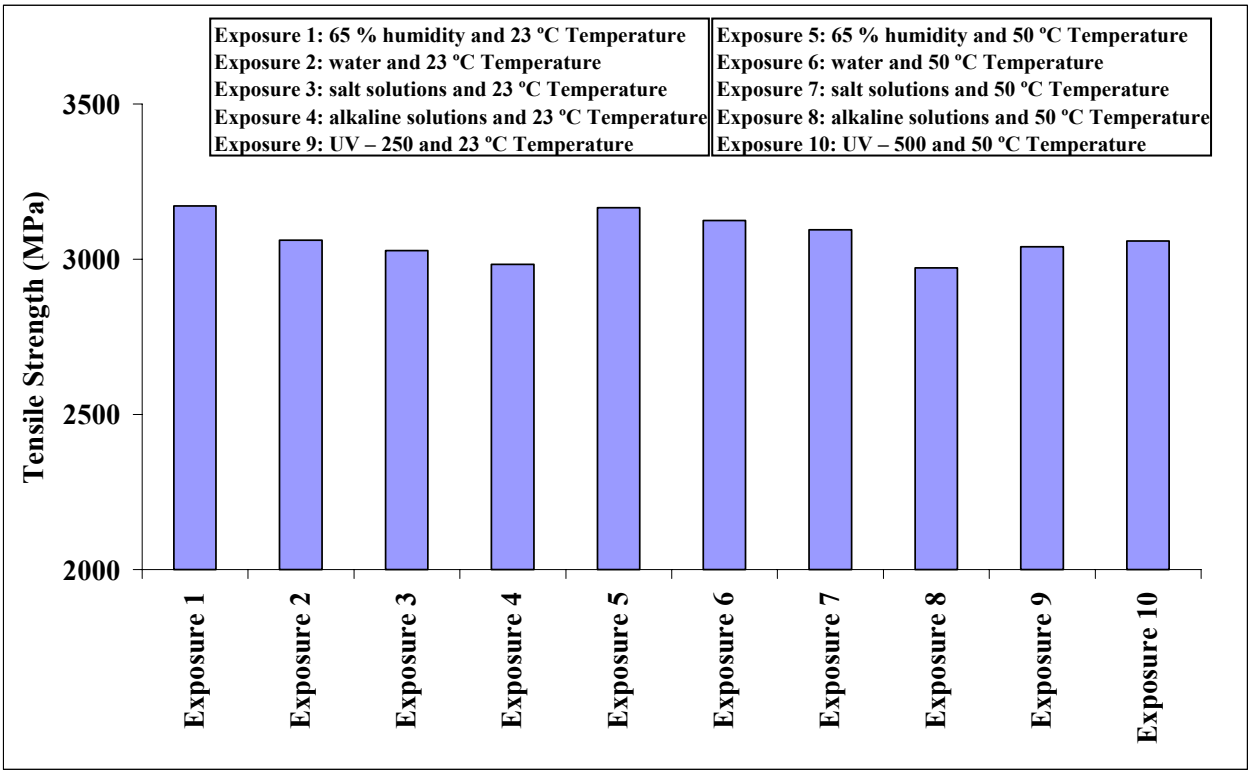

Figure 4.2: Average tensile strength values of CFRP plates after 96 days conditioning

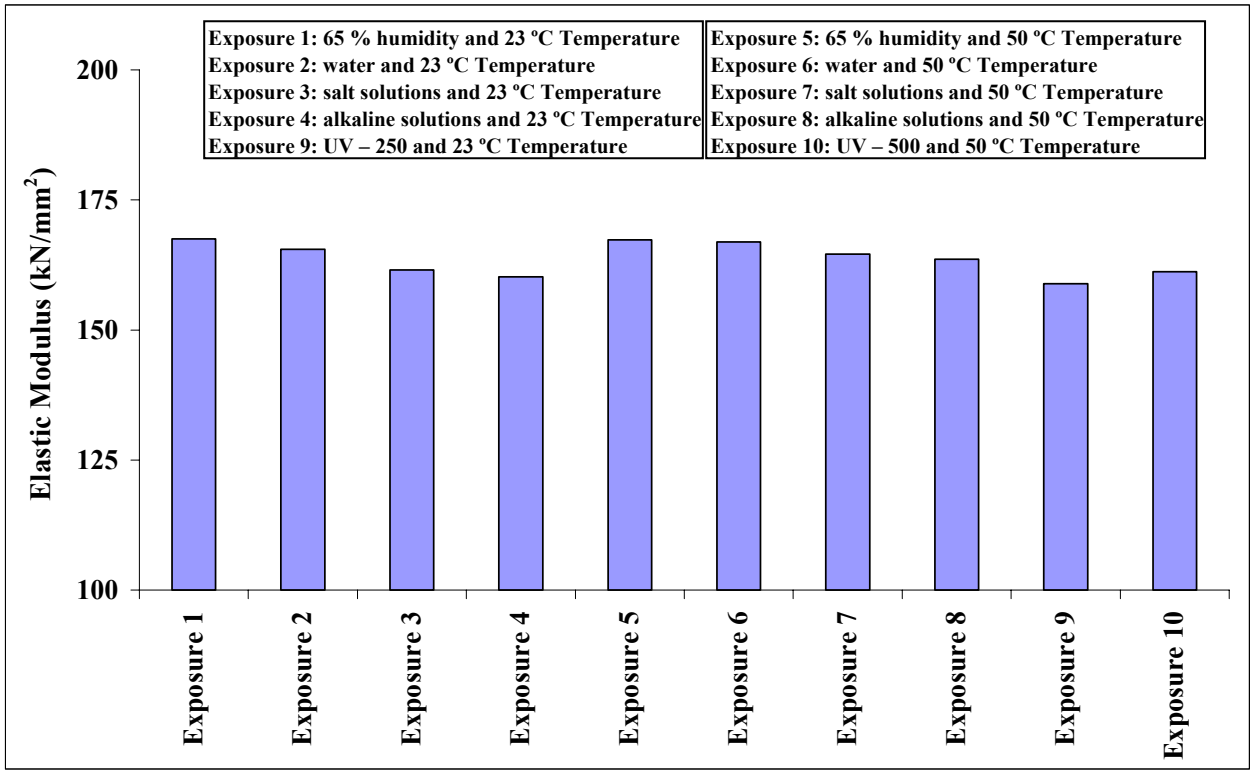

Figure 4.3: Average elastic modulus values for CFRP plates after 96 days conditioning

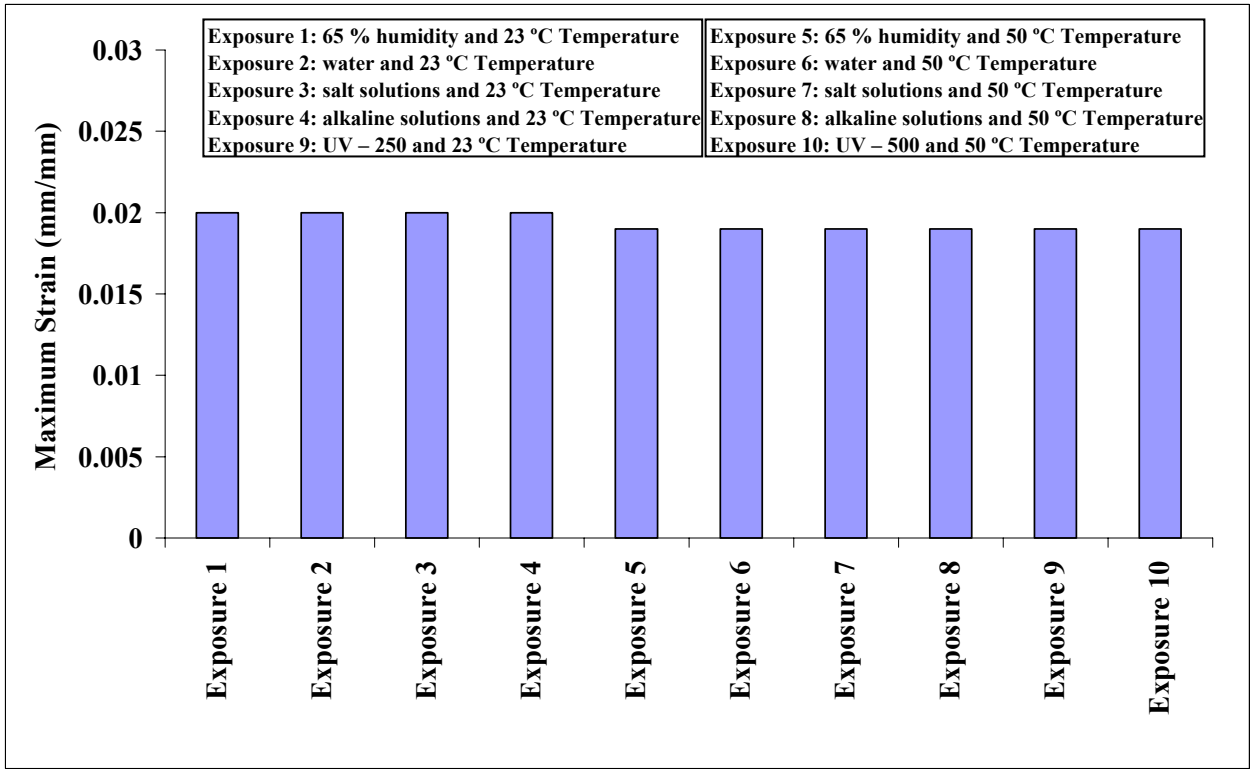

Figure 4.4: Average ultimate strain values of CFRP plates after 96 days conditioning

4.2.2. Test Results of Epoxy Adhesives

All the obtained results from testing the glass transition temperature, mechanical properties and the water uptake of representative specimens of the three selected epoxy adhesives are presented in the following sections. Measurements were performed after conditioning representative test specimens to different environments as shown schematically in Figure 4.5.

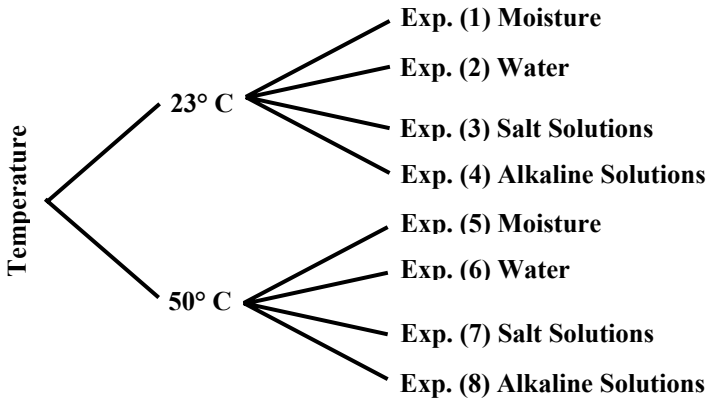

Figure 4.5: Exposure environments used for conditioning epoxy test specimens

4.2.2.1.Glass Transition Temperature

Measured values of the glass transition temperatures, T_g, for all epoxy types are shown in Figure 4.6. The following observation may be drawn from the obtained results.

Variation in performance is observed with gain or loss on the measured T_g for all test specimens made from all epoxy types and exposed to environments No. 5 to No. 8 as compared to the original T_g given by the manufacturers.

For Type 1 epoxy, there is no reduction on the measured T_g when test specimens were exposed to 65 % moisture or immersed in water, both combined with 50 °C temperature. Measured T_g values were in close proximity with the manufacturer's T_g. On the other hand, insignificant loss of about 1.5 % in the measured T_g was observed for specimens immersed in salt solutions associated with high temperature of 50 °C, and a substantial loss of 11.5 % on the measured T_g was observed for specimens immersed in alkaline solutions combined with 50 °C temperature.

On the contrary, higher values for T_g were measured for specimens made from Type 1 Modified when exposed to 65 % moisture or immersed in water, all combined with 50 °C temperature. The measured values were higher than the manufacturers T_g by a value of 4 % when specimens exposed to moisture associated with high temperature and by a value of 6.5 % when specimens immersed in hot water. But, reduction on the measured T_g as compared to the manufacturers T_g was observed when specimens were immersed in salt and alkaline solutions, both combined with high temperature of 50 °C. Reduction values were about 0.71 % and 8.76 % for specimens immersed in salt solutions and alkaline solutions, respectively.

For Type 2, there is no reduction on the measured T_g when test specimens exposed to moisture or immersed in water, all combined with 50 °C temperature. But, a reduction on the measured T_g in the

order of 9.48 % and 19.5 % when specimens were exposed to salt and alkalines solutions associated with 50 °C temperature, respectively.

Generally, there is no significant reduction on the measured T_g for all types of epoxies when exposed to moisture and water associated with high temperature, but quite the opposite the values were found higher than the values given by the manufacturers. This was unexpected because moisture and water generally attributed to reduce T_g and mechanical properties of adhesives. A reasonable explanation is that, since these epoxies were ambient cured and there was no post-cure treatment given, there may still present many open chain sites and there was upside potential for further crosslink formation. Hydrogen bonding might have occurred at these non cross-linked sites, thus raising the T_g.

On the other hand, reduction on the measured T_g of 1.5 %, 0.7 % and 9.48 % was observed for epoxies, Type 1, Type 1 Modified and Type 2, respectively when exposed to chloride solutions associated with high temperatures. Almost insignificant reduction of T_g on specimens made from Type 1 and Type 1 Modified as compared to the reduction in the T_g for specimens made from Type 2 epoxy. Whereas, alkaline solutions at high temperatures could be considered the most harmful environment for all types of epoxies, as a reduction in the measured T_g was 11.5 %, 6.5 %, and 19.5 % for specimens made from Type 1, Type 1 Modified and Type 2, respectively. This observation implies that the chemical composition of the epoxies may be affected by the salts and alkalines to such an extent that conquered any beneficial post-curing that may be attained from the high temperature. The absorbed salts complex with the resin groups and at the same time interferes with hydrogen bonding thus making the chain more flexible, hence decreasing the glass transition temperatures, Hollaway [31].

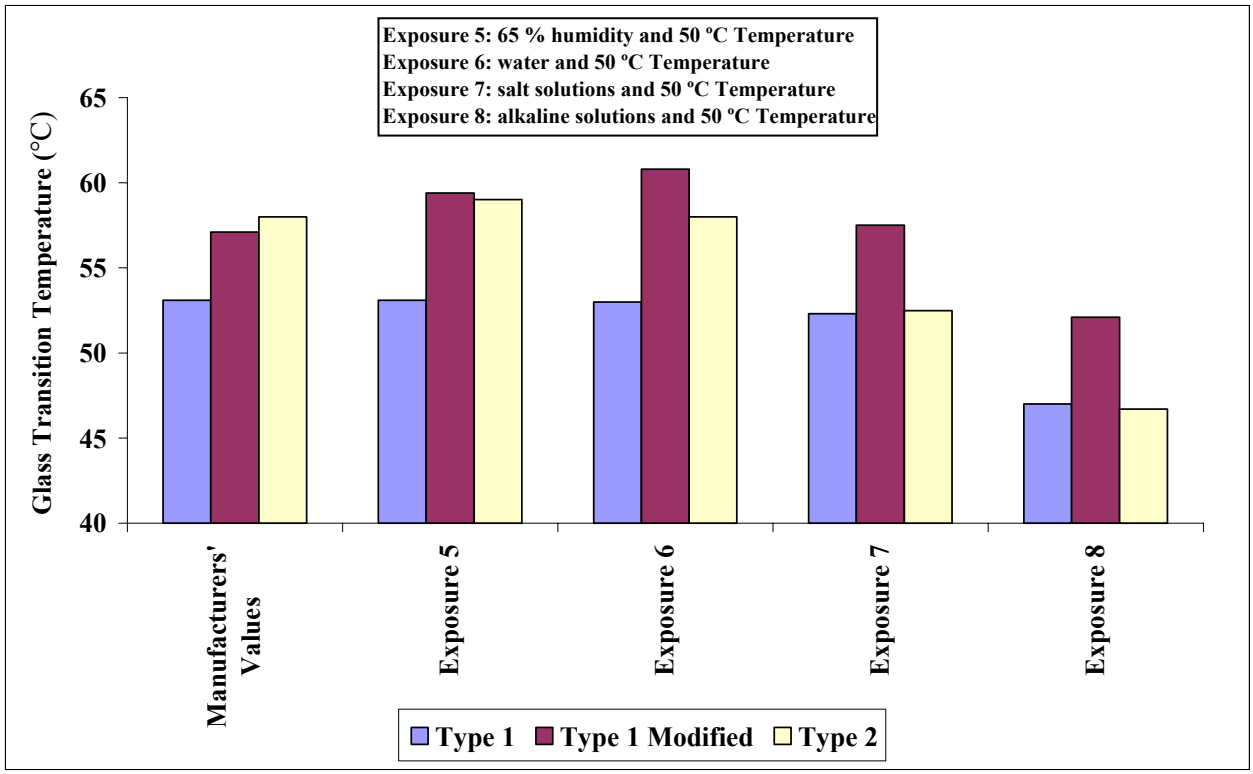

Figure 4.6: Measured values of glass transition temperatures for all epoxy types

4.2.2.2. Mechanical Properties

Mechanical properties for all epoxy types were tested at temperatures equivalent to their respective conditioning temperatures, thus eliminating temperature gradients along the test section. Specimens conditioned under environments No. 1 to No. 4 were tested at temperature of 23 °C at ages of 47 days and 95 days. Whereas, specimens conditioned under environments No. 5 to No. 8 were tested at temperature of 50 °C at ages of 48 days and 96 days.

Test results obtained after conditioning representative samples are presented in Figures 4.7 to 4.14.

Generally, tensile strength and elastic moduli curves showed variations and fluctuations in the measured values. Significant drop in the measured values for both the tensile strength and elastic moduli are obvious due to conditioning of the specimens in solutions, which was aggravated by ageing and high temperatures.

The following observations may be drawn from the obtained test results.

a. Specimens conditioned for 47 days under exposures No. 1 to No. 4 and tested at 23 °C

- For normal laboratory conditions, tensile strength values were in the range of (14.87 – 25.17) MPa with the highest value for specimens made from Type 2, followed by a comparable value of 25.13 MPa for specimens made from Type 1 and the lowest strength was for specimens made from Type 1 Modified. Whereas, elastic moduli were 7905 N/mm2, 5716 N/mm2 and 8995 N/mm2 for specimens made from Type 1, Type 1 Modified and Type 2, respectively. These values for both the tensile strength and elastic modulus were considered the reference values.
- For specimens immersed in water, loss in the mechanical properties for all test specimens was observed. The loss in strength was about 8.8 %, 10.47% and 13 % for specimens made from Type 1 Modified, Type 1 and Type 2, respectively. And the loss in the elastic moduli was about 20 %, 21.2 % and 19.7 % for specimens made from Type 1 Modified, Type 1 and Type 2, respectively.
- Further reduction in the measured mechanical properties was observed for specimens immersed in salt solutions. The loss was about 21.4 %, 27.13 % and 40.2 % for specimens made from Type 1 Modified, Type 1 and Type 2, respectively. And the loss in the elastic moduli was 42.5 %, 52.44 % and 60.37 % for specimens made from Type 1 Modified, Type 1 and Type 2, respectively.
- Significant loss in strength was observed for specimens soaked in alkaline solutions. The loss in strength was 29.8 %, 38.44 % and 47.34 % for specimens made from Type 1 Modified, Type 1 and Type 2, respectively. And the loss in the elastic moduli was 59.67 %, 63.25 % and 87.6 % for specimens made from Type 1 Modified, Type 1 and Type 2, respectively.

Water and chemical solutions had an adverse effect on the mechanical properties for all epoxy types, even at ambient temperature and short period of exposure. The severity of each specific environment depends on the chemical composition of each epoxy type. But, generally for such exposures, alkaline solutions are the most severe on the mechanical properties, followed by chloride solutions, and then water.

b. Specimens conditioned for 95 days under exposures No. 1 to No. 4 and tested at 23 °C

- Enhancement on the mechanical properties was observed for all test specimens exposed to moisture. An increased in the obtained tensile strength of 3.82 %, 23.53 % and 6.08 % was observed for specimens made from Type 1, Type 1 Modified and Type 2, respectively. Also, an increased in the

elastic moduli of 7.5 %, 9.7 % and 12.5 was observed for specimens made from Type 1, Type 1 Modified and Type 2, respectively. This was less than expected given higher values for both the tensile strength and elastic modulus at the age of 95 days as compared to those at age of 47 days. Ageing has a beneficial effect in enhancing the mechanical properties. This could be attributed to complexion between the water molecules with resin groups, thus stiffening the chains and subsequently increasing the mechanical properties to an extent that certainly depends on the chemical composition of each type.

- On the other hand, reduction in tensile strength and elastic moduli was observed for all epoxy types when soaked in water. The reduction in strength was about 7.68 %, 5.65 % and 11.8 % for specimens made from Type 1, Type 1 Modified and Type 2 respectively. Also, in the same order there was reduction of 17.6 %, 5 % and 18.7 % on the elastic moduli. But by comparing these reduction values with those at age of 47 days, these values are lower and confirming the previous observation regarding to ageing.

- Substantial loss in measured values for both tensile strength and elastic moduli was observed for specimens immersed in salt solutions. The loss in tensile strength was 69.4 %, 43.04 % and 71.4 % for specimens made from Type 1, Type 1 Modified and Type 2, respectively. Whereas, the loss in the elastic moduli was of 85 %, 54 % and 81 % for specimens made from Type 1, Type 1 Modified and Type 2, respectively. The loss in tensile strength at age of 95 days is greater than that at the age of 47 days. Long exposure to salt solution could affect the chemical composition of the epoxies defeating any gain of strength could be attributed from ageing.

- Tensile strength and elastic moduli are observed to reduce more when specimens are immersed in alkaline solutions. The loss in strength was of 74 %, 43.43 % and 77.38 % for specimens made from Type 1, Type 1 Modified and Type 2, respectively. And in the same order a loss of 91 %, 65.5 % and 96 % in the elastic moduli. Long exposure to alkaline solutions is very detrimental on the mechanical properties of all adhesives.

c. Specimens conditioned for 48 days under exposures No. 5 to No. 8 and tested at 50 °C

- Considerable loss in the mechanical properties was observed for specimens exposed to moisture. Type 1 loses 40.47 % of its tensile strength and 86.25 % of its elastic modulus, and Type 1 Modified loses 29.18 % and 66 % of its tensile strength and elastic modulus, whereas Type 2 loses 49.54 % of its strength and 97 .4 % of its elastic modulus. It is clear that exposure to moisture combined with hot temperature has an adverse effects on the mechanical properties. This observation does not agree with the higher glass transition temperature values measured when specimens were exposed to moisture at 50 °C.

- Further losses in strength and moduli were observed for specimens soaked in water. The loss in strength was of 52.6 %, 36.18 % and 85.9 % for specimens made from Type 1, Type 1 Modified and Type 2, respectively. And in the same order a loss of 86.9 %, 83.5 % and 97.2 % in the elastic moduli. Also, this observation contradicts the gain in the measured T_g.

- Significant loss in the mechanical properties when specimens are soaked in salt solutions. The loss in strength was 93.1 %, 79.2 % and 93.8 % for specimens made from Type 1, Type 1 Modified and Type 2, respectively. While the loss in the moduli was of 99.4 %, 97 % and 98.7 % for specimens made from Type 1, Type 1 Modified and Type 2, respectively. This observation agrees very well with the reduced values of measured T_g. Salt solutions had an adverse effect on epoxy materials by

depression their T_g values, thus epoxy specimens are exposed to temperature that is very closed to their T_g values. Therefore, epoxy material is transformed from relatively hard glassy-like material to relatively viscous rubbery-like material, thus losses almost all of its properties.

- Adhesives almost lost most of their properties when immersed in alkaline solution, Type 1 loses 94.2 % of its strength and 99.7 % of its modulus, while Type 1 Modified loses 80.4 % of its strength and 98.9 % of its modulus, and Type 2 loses 93.13 % of its strength and 99.5 % of its modulus. Also, this observation agrees very well with the depression on the measured T_g values.

It is known that polymers absorbed larger quantities of solutions at higher temperatures, and the chemical reactions between the polymeric chain and either the water molecules, or salts and alkalines are increased at higher temperatures; this may explain the significant loss in mechanical properties when exposed to water and chemical solutions at high temperatures. Again the most severe environment is the alkaline solutions followed by the salt solution, water and moisture, respectively.

d. Specimens conditioned for 96 days under exposures No. 5 to No. 8 and tested at 50 °C

- Considerable loss in mechanical properties is observed for specimens exposed to moisture. Type 1 loses 78.75 % of its strength and 98.9 % of its elastic modulus, while Type 1 Modified loses 36.45 % in its strength and 87 % of its elastic modulus, and Type 2 loses 56.18 % of it strength and 97 % of its elastic modulus. Reduction in the mechanical properties is much higher than that at the age of 48 days. Long exposure to moisture had an adverse effect on the properties if accompanied with high temperature.

- Further losses in mechanical properties were observed for specimens soaked in water. The loss in tensile strength was of 90.6 %, 83.2 % and 87.8 % for specimens made from Type 1, Type 1 Modified and Type 2, respectively. And in the same order, the loss in the elastic moduli was 98.9 %, 89.9 % and 99.3 %.

- Significant loss in strength was observed when specimens are soaked in salt solutions. The loss in strength was 93.3 %, 74.51 % and 91.7 % for specimens made from Type 1, Type 1 Modified and Type 2, respectively. Whereas, the loss in the elastic modulus was 99.3 %, 95.2 % and 99.5 % for specimens made from Type 1, Type 1 Modified and Type 2, respectively.

- Adhesives lost most of their mechanical properties when immersed in alkaline solutions; Type 1 loses 93.75 % of its strength and 99.6 of its modulus, while Type 1 Modified loses 84.4 % of its strength and 98.6 % of its elastic modulus, and Type 2 loses 92.1 % of its strength and 99.6 % of its elastic modulus.

Generally, the following conclusions could be drawn based on the results obtained so far.

- Exposure to 65 % moisture at ambient temperature for longer periods was found to enhance the mechanical properties for the specific selected types of adhesives.

- All studied adhesives were found to suffer an apparent trend of deterioration when exposed to high temperatures particularly if close to their glass transition temperature. At elevated temperatures adhesives soften, degrade and suffer reduction in strength and stiffness.

- Exposure to 65 % moisture combined with high temperature of 50 °C was found to reduce the mechanical properties to considerable values that been aggravated by ageing.

- Adhesives lost considerable amount of their mechanical properties when soaked in water and chemical solutions at ambient temperature. But, ageing helped in decreasing the amount of loss in the mechanical properties when adhesives were conditioned in water. On the contrary, the loss in the mechanical properties was found to increase with ageing when adhesives were immersed in salt and alkaline solutions.
- Adhesives were found to loose significant amount of their strength and stiffness when immersed in hot solutions that was aggravated with ageing.
- Generally, alkaline solutions were found to be the most severe environment followed by salt solution and then water. The severity of all encountered environments was found to be aggravated if associated with high temperatures and ageing.
- The percentage of deterioration in strength and stiffness varies between the different types of epoxies depending mainly on the chemical composition of each type. Comparatively, under all the encountered environments, Type 1 Modified has the best performance notwithstanding its low initial mechanical properties as compared to the other types, followed by Type 1 and Type 2, respectively.

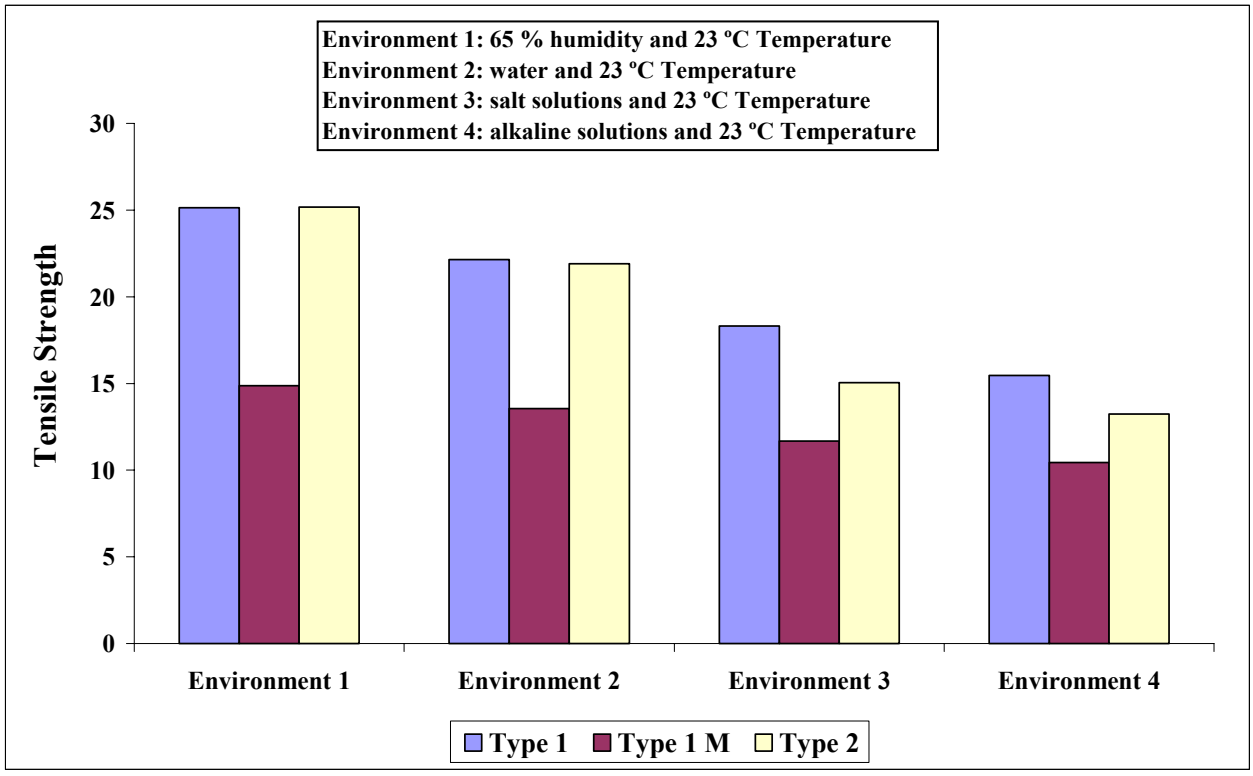

Figure 4.7: Results of tensile strength tests for all specimens conditioned under environments No. 1 – No. 4 for 47 days and tested at 23 °C

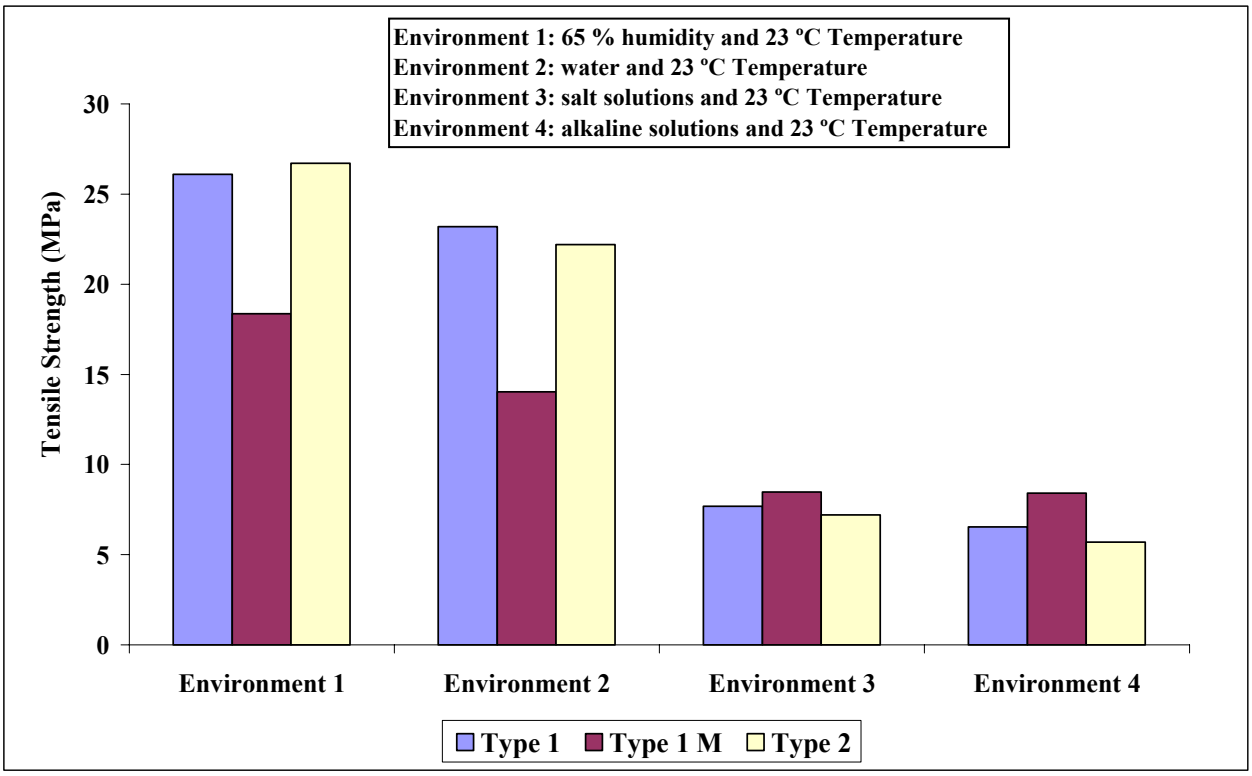

Figure 4.8: Results of tensile strength tests for all specimens conditioned under environments No. 1 – No. 4 for 95 days and tested at 23 °C

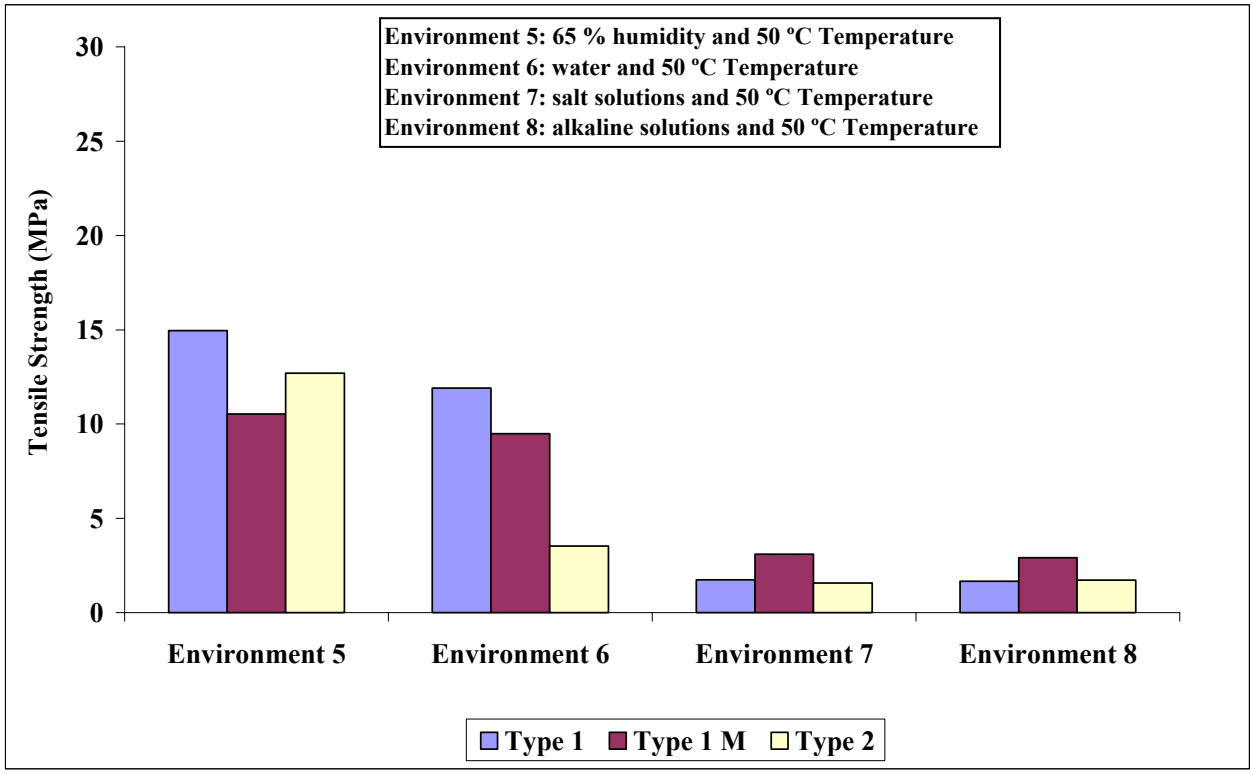

Figure 4.9: Results of tensile strength tests for all specimens conditioned under environments No. 5 – No. 8 for 48 days and tested at 50 °C

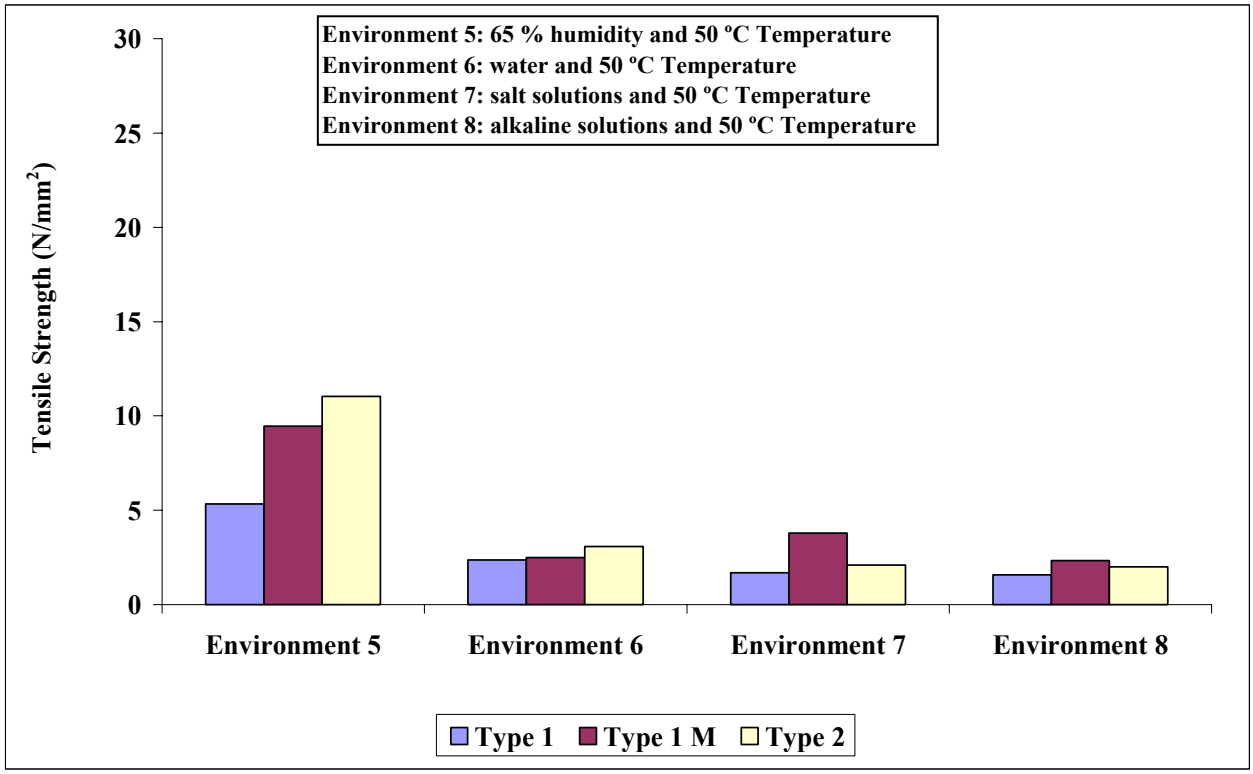

Figure 4.10: Results of tensile strength tests for all specimens conditioned under environments No. 5 – No. 8 for 96 days and tested at 50 °C

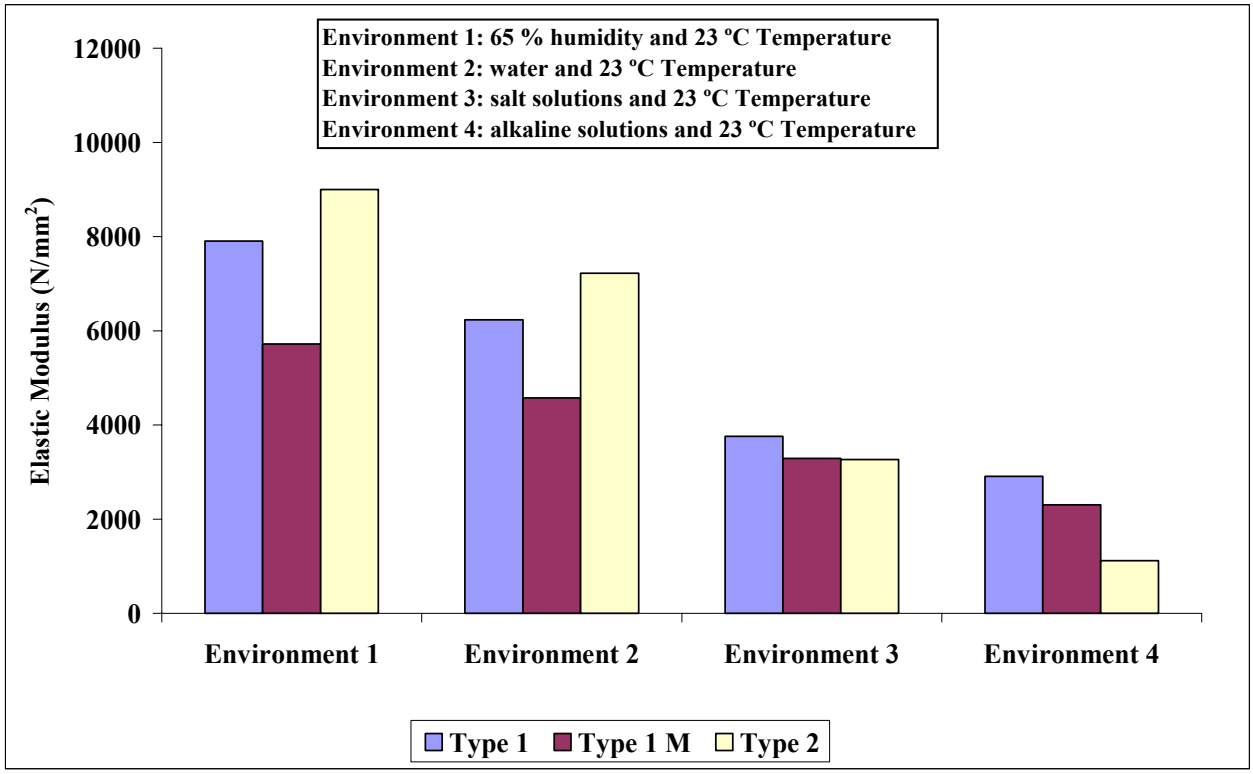

Figure 4.11: Results of elastic modulus tests for all specimens conditioned under environments No. 1 – No. 4 for 47 days and tested at 23 °C

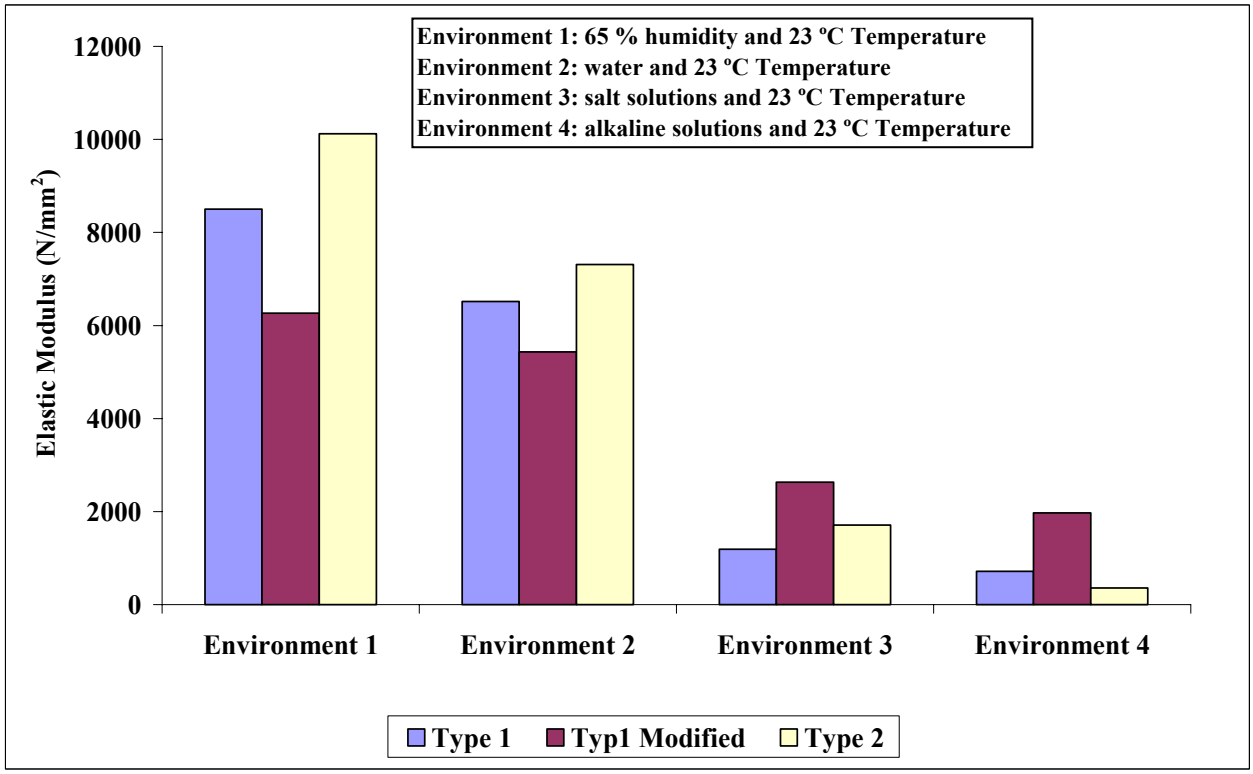

Figure 4.12: Results of elastic modulus tests for all specimens conditioned under environments No. 1 – No. 4 for 95 days and tested at 23 °C

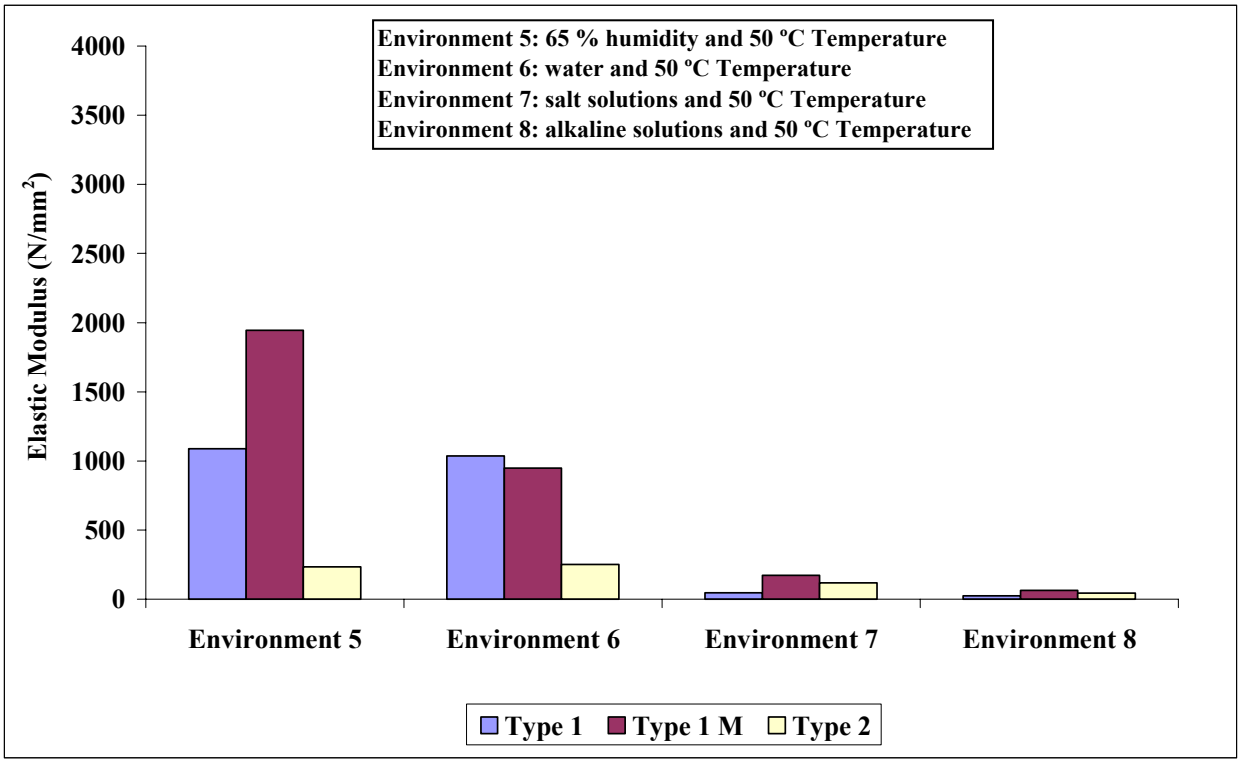

Figure 4.13: Results of elastic modulus tests for all specimens conditioned under environments No. 5 – No. 8 for 48 days and tested at 50 °C

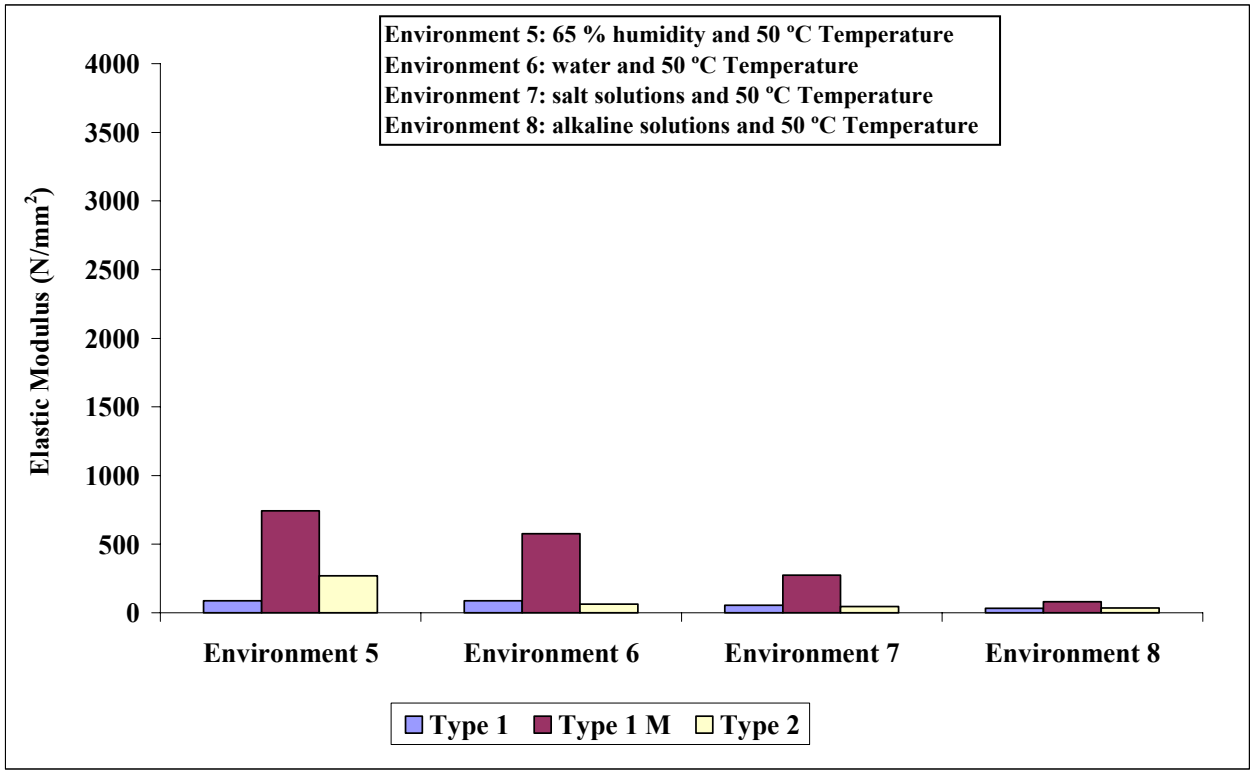

Figure 4.14: : Results of elastic modulus tests for all specimens conditioned under environments No. 5 – No. 8 for 96 days and tested at 50 °C

4.2.2.3. Moisture Uptake

Data collected from water uptake measurements for all epoxy types are presented in Figures 4.15 to 4.17. These figures show plots of the percentage of weight gain for all exposure conditions versus the square root of time, measured in hours.

In general, the curves show an initial linear region, followed by a region concave to the abscissa, and then a relatively stable but slower uptake until saturation, hardly resembling Fickian-Diffusion behaviour. This type of behaviour is called the Pseudo-Fickian curve. These types of curves are of the same general shape as in Fickian diffusion, except the initial linear portion persists for a shorter time. Note here that for the ideal Fickian diffusion, the mass uptake curve would exhibit the following characteristics: initial slope is linear and the linear limit exceeds 60 % of the equilibrium mass, Hollaway [31].

It is observed that higher conditioning temperature has generally led to faster moisture diffusion, as indicated from the higher saturation values as can be seen in Figures 4.15 – 4.17.

Additionally, the existence of the catalyst ions, chlorides and alkalines, increased the diffusion at both conditioning temperatures, 23 °C and 50 °C. Test specimens reach saturation at the age of 56 days but at different percentages, as shall be discussed hereunder. This observation explains the significant reduction in the measured mechanical properties of the adhesives.

The following observations are made for each epoxy type from the obtained results.

- **Type 1**

- Expected trend can be seen in Figure 4.15, as it should be higher values of moisture uptake for specimens immersed in baths associated with high temperature of 50 °C as compared to their corresponding specimens immersed in the same solutions but at ambient temperature of 23 °C. Also, the existence of chlorides and alkalines ions enhancing the sorption at both temperatures, as measured values of water uptake for specimens soaked at baths containing chlorides and alkalines are much higher than those immersed in water at both temperatures.

- Saturation rate was in the range of (4.1 – 7.5) % for specimens conditioned under ambient temperature of 23 °C. The lowest rate was for specimens immersed in water followed by a value of 5.1 % for specimens immersed in salt solution, whereas specimens immersed in alkalines had the highest rate value. On the other hand, a higher saturation rate in the range of (8.77 – 10.92) % was observed for specimens conditioned at 50 °C temperature, the lowest value was again for specimens immersed in water, followed by a value of 9.2 % for specimens immersed in salt solution and the highest rate was for specimens immersed in alkalines.

- No material deterioration was observed for any specimen after 84 days from conditioning in all the encountered environments.

- **Type 1 Modified**

- Specimens made from Type 1 Modified epoxy followed the same trend mentioned earlier for Type 1 epoxy, but at a lower level of sorption, as can be seen in Figure 4.16. Also, higher values for water up take were observed for specimens soaked at 50 °C temperature as compared to their corresponding specimens exposed to the same environments but at 23 °C.

- Saturation rate was in the range of (2.9 – 4.08) % for specimens conditioned under 23 °C temperature. The lowest rate was for specimens immersed in water followed by a value of 3.5 % for specimens immersed in salt solution, whereas specimens immersed in alkalines got the highest rate value. On the other hand, higher saturation rate in the range of (4.8 – 6.54) % was for specimens conditioned under 50 °C temperature, the lowest value was for specimens immersed in water, followed by a value of 5.14 % for specimens immersed in salt solution and the highest rate was for specimens immersed in alkalines.

- Generally, the measured values of water uptake were smaller than those measured for Type 1 epoxy, as can be seen in the difference for both ranges even at both conditioning temperatures, 23 °C and 50 °C

- No material deterioration was observed for any specimen after 84 days from conditioning in all the encountered environments.

- **Type 2**

- Again, higher values of water uptake for specimens immersed in solutions associated with high temperature as can be seen in Figure 4.17. Also, higher sorption for specimens immersed in salt and alkaline solutions as compared to those immersed in water for both temperatures, 23 °C and 50 °C.

- Saturation rate was in the range of (0.253 – 2.041) % for specimens conditioned under ambient temperature of 23 °C. The lowest rate as usual was for specimens immersed in water followed by a value of 1.01 % for specimens immersed in salt solution, whereas specimens immersed in alkalines

had the highest rate value. On the other hand, higher saturation rate in the range of (2.356 – 5.03) % is for specimens conditioned under 50 °C temperature, again the lowest value was for specimens immersed in water, followed by a value of 4.02 % for specimens immersed in salt solution and the highest rate was for specimens immersed in alkalines.

- Generally, the measured values of water uptake are smaller than those measured for both Type 1 and Type 1 Modified epoxies, as can be seen in the difference for both ranges at temperatures, 23 °C and 50 °C.
- No material deterioration was observed for any specimen after 84 days from conditioning in all the encountered environments.

4.2.2.4. Diffusion Coefficient and Activation Energy

Moisture diffusion in its broad meaning is defined as the process by which water molecules flow from a moist environment, i.e. a water bath, to a dryer environment, i.e. core of the material. The rate at which a diffusion process takes place is defined as the diffusion coefficient, which is expressed by Fick's law described in equation 4.1.

$$F = -D\frac{\partial C}{\partial x} \qquad 4.1$$

Where F is the rate of transfer per unit area of section, i.e. the amount of water diffusing; C is the concentration of solution; x is the space coordinate measured normal to the section; and D is the diffusion coefficient. By solving Fick's second law properly, an approximate relationship as illustrated in equation 4.2 can be obtained, which describes the moisture mass uptake behaviour relatively accurate, Hollaway [31].

$$\frac{M_t}{M_s} = \frac{4}{\sqrt{\pi}}\left(\frac{Dt}{h^2}\right)^{0.5} \qquad 4.2$$

Where M_t is the mass of water absorbed at time t; M_s the mass absorbed at saturation; h the thickness of the material coupon; and D is the diffusion coefficient.

Predicted values of diffusion coefficient for all types of epoxies under all the encountered environments are illustrated in Figure 4.18.

It is observed that higher conditioning temperatures have generally led to faster moisture diffusion, as indicated from the higher diffusion rates.

Furthermore, higher diffusion coefficients could be observed for specimens soaked in salt and alkaline solutions as compared to those values for specimens immersed in water for all epoxy types. This observation applies for both conditioning temperatures, 23 °C and 50 °C. The highest diffusion rates are for specimens immersed in alkaline solutions for all epoxy types, albeit the differences are comparable for specimens made from Type 1 and Type 1 Modified.

Comparatively, specimens made from Type 1 Modified got the lowest diffusion rates for all environments encountered except environment No. 6.

From the sorption curves shown in Figures, 4.15 to 4.17, it is observed that moisture diffusion in epoxy materials is a thermally activated rate process, as conditioning temperature gets higher led to more and

faster mass uptake at a given time. Such dependence on temperature can be quantified by an Arrhenius relationship as expressed in equation 4.3, Hollaway [31].

$$D = D_{\circ} e^{\frac{-A}{RT}} \qquad 4.3$$

Where $D_{\circ}$ is the pre-exponential coefficient; A is the activation energy for moisture diffusion; R the universal gas constant; and T the temperature on Kelvin scale at which moisture diffusion takes place. The estimated activation energies are shown in Figure 4.19.

By definition, the higher activation energy of epoxy implies a higher energy barrier that needs to be overcome. This might possibly be explained by a higher crosslink density, which is defined as the number of the sites chemically joined among adjacent polymer chains, crosslink per unit volume. However, a higher crosslink density also implies less water uptake at saturation.

It is obvious that the activation energy is higher for specimens made from Type 1 Modified followed by specimens made from Type 1, and then Type 2 for all environments and at both the conditioning temperatures. Albeit, for specimens exposed to salt solution comparable values are observed for specimens made from Type 1 and Type 1 Modified.

As a general conclusion based on results obtained from evaluating the epoxy bulk materials under severe environments; Type 1 Modified showed comparatively the best performance among other types, although it has the lowest initial properties. This result suggests that adhesives which show a lower viscosity in the workability stage may have better potential for bonding CFRP plates for outdoor applications. This result will be further evaluated based on the results that will be obtained from testing the performance of the CFRP externally bonded concrete specimens.

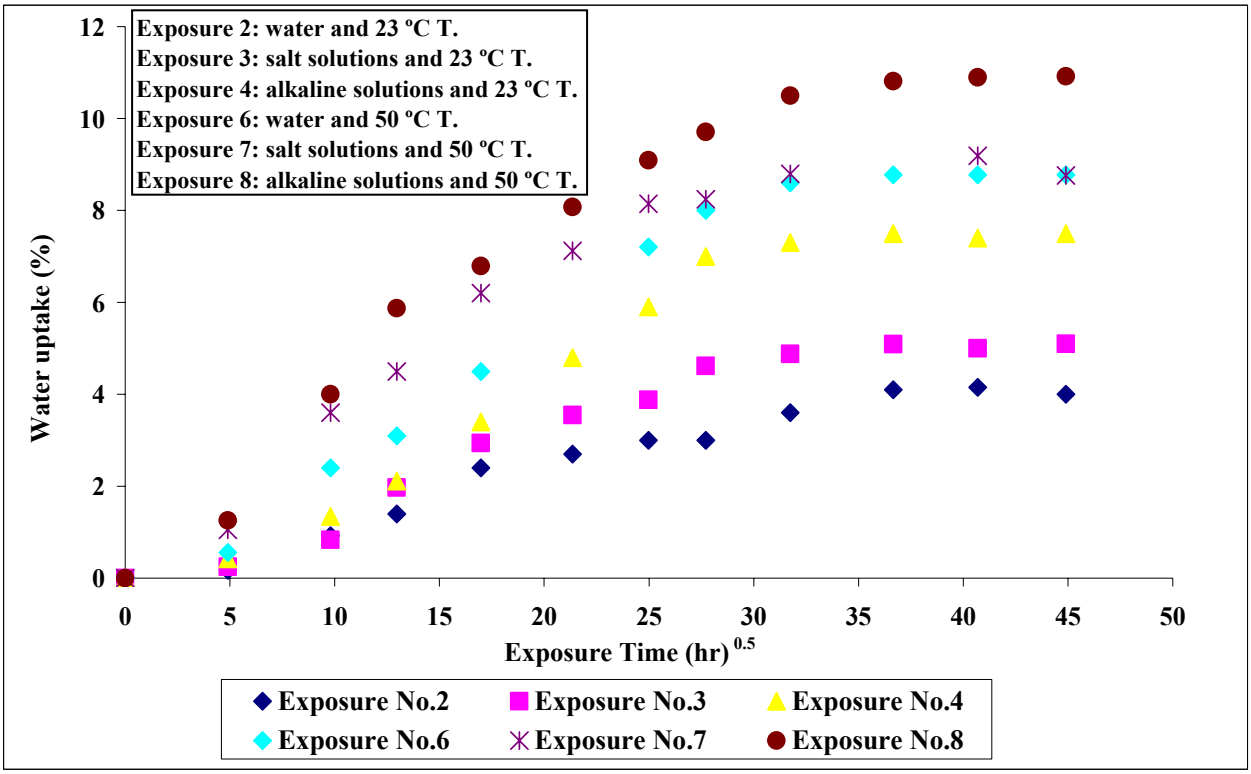

Figure 4.15: Measured values of water uptake for Type 1 epoxy

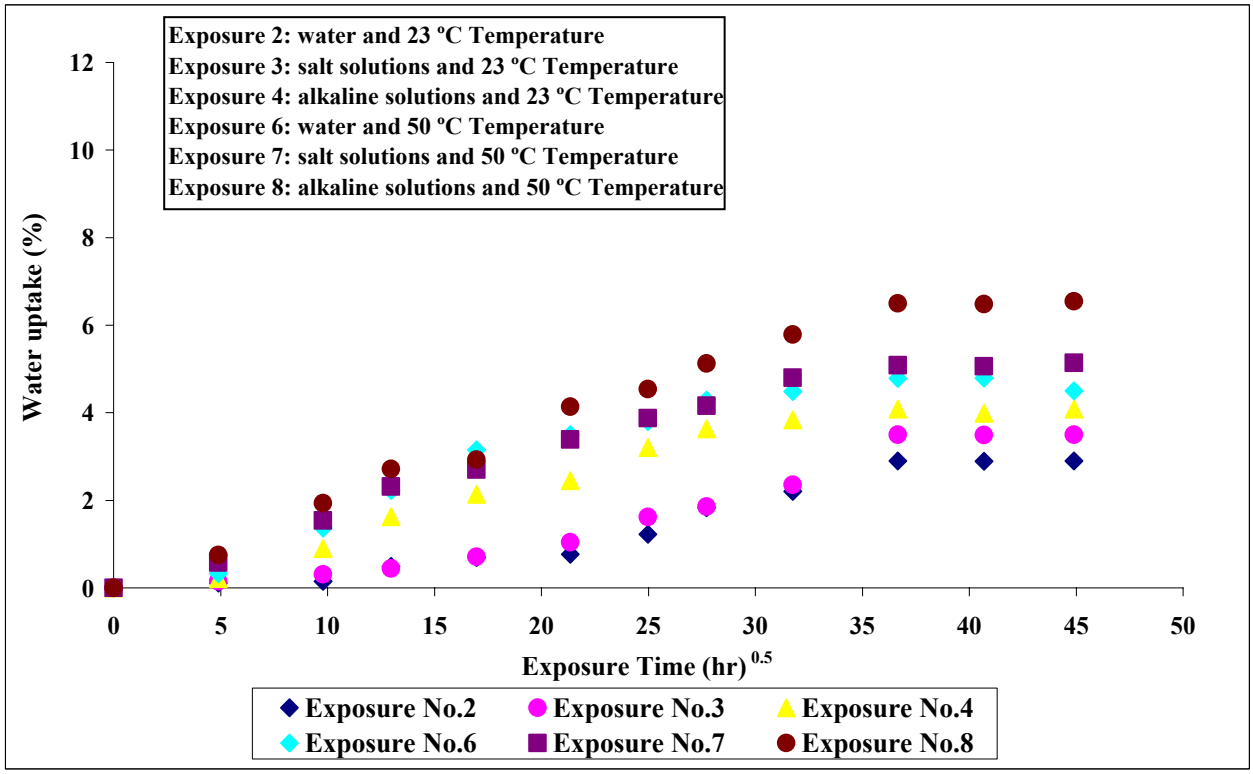

Figure 4.16: Measured values of water uptake for Type 1 Modified epoxy

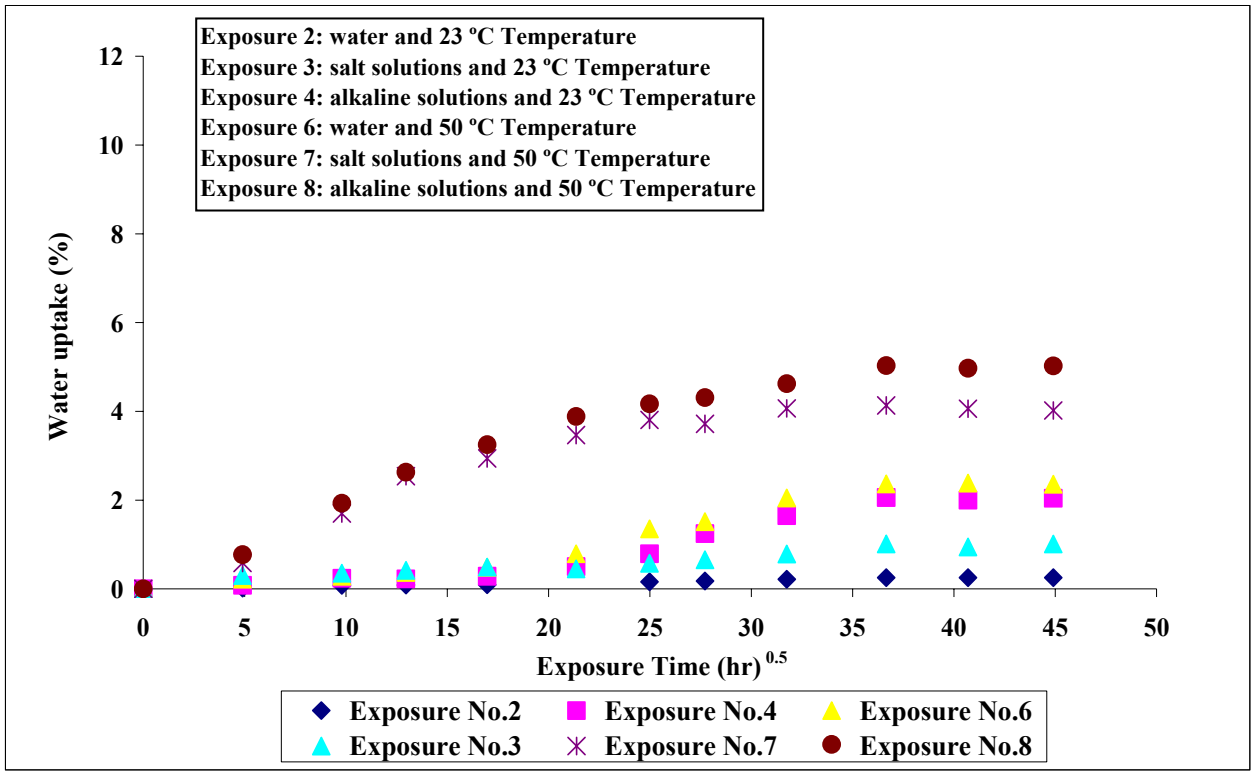

Figure 4.17: Measured values of water uptake for Type 2 epoxy

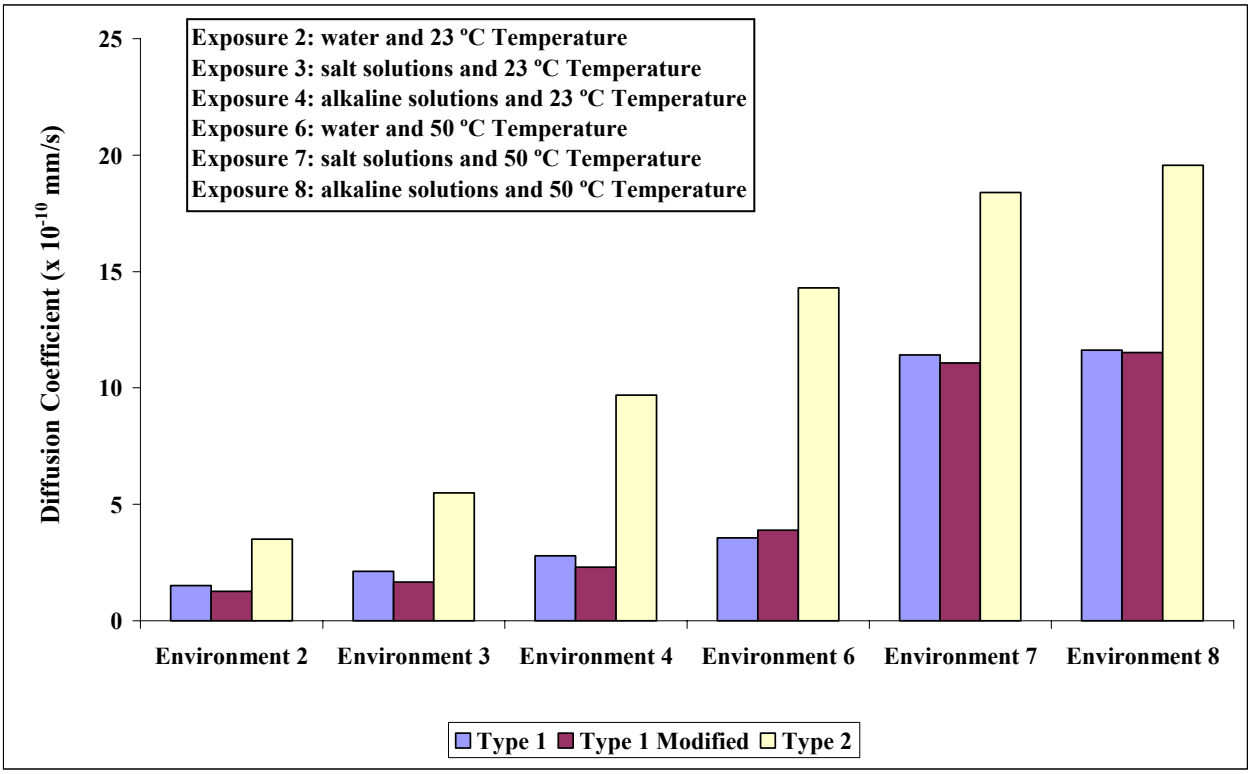

Figure 4.18: Predicted values for the diffusion coefficient

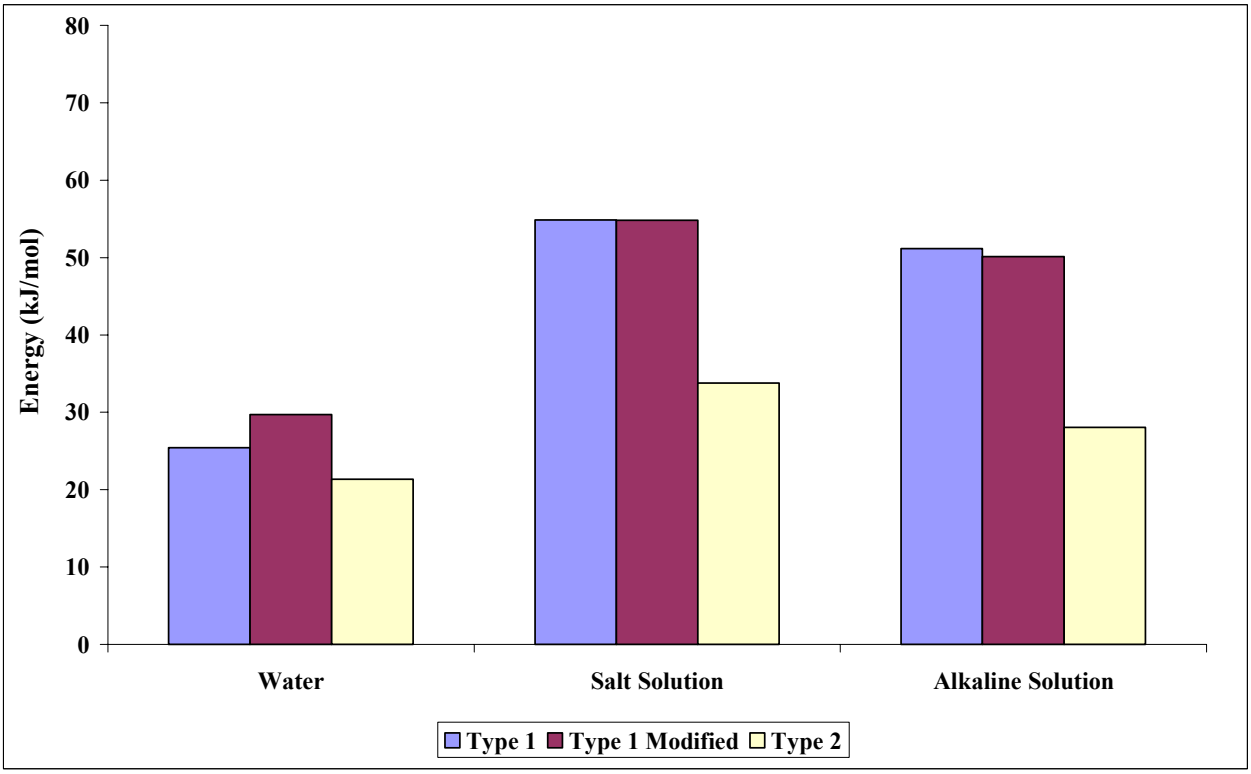

Figure 4.19: Predicted values for the activation energy

4.3. Test Results of Slab Specimens

4.3.1. Introduction

The obtained results are discussed subsequently hereunder in terms of the observed failure modes, ultimate failure loads, deflections, strains, concrete tensile strengths and chloride ion contents.

It is worthy to mention here that the slab specimens that were produced and stored at iBMB laboratories are considered the reference specimens as they were exposed to normal laboratory conditions.

4.3.2. Visual Inspection and Failure Modes

All specimens were in good conditions without signs of deterioration along the adhesive joints between the CFRP plates and concrete substrate, but one specimen, J_E2_D_2 that was allocated at the Dead Sea region showed signs of deterioration represented by debonding of a distance of 50 mm along the adhesive/concrete interface, as can be seen in Figure 4.20. This specimen was rolled out of testing as the major issue of this investigation is to study the bond behaviour. Corrosion stains were visible at the tension faces and sides of the specimens that were exposed to salt solutions and stored indoors at iBMB laboratories, in addition to specimens that were exposed to real-life severe environments prevailing at Aqaba and Dead Sea regions, as illustrated in Figure 4.21. These stains are related to the corrosion of the steel loaded fixture that has been used to crack the specimens during the storage period.

For all specimens, expected cracks appeared at the predefined locations, in addition to other flexural cracks that appeared in close vicinity to the maximum moment region. The initial widths for these cracks were in the range of (0.04 - 0.16) mm. Typical crack pattern is illustrated in Figure 4.22. During testing the cracks increased in number, widths and depths as loads increased. Measured crack widths at a load step just before failure were in the range of (0.1 – 0.7) mm.

Midspan debonding of the CFRP plates from the concrete substrate was the dominating failure mode, as illustrated in Table B.1 of Appendix B. Generally, all the slabs failed by intermediate flexural or flexural/shear crack induced interfacial debonding of the CFRP plate, as shown in Figure 4.23. More photos of the failure modes for all specimens are shown in Figures B.1 - B.6 of Appendix B.

These modes were considered undesirable because there was little warning before the sudden failure. The only indication of the incipient failure was a few popping sounds as the debonding cracks propagated quickly to one of the ends of the composite, while the concrete cover was intact at the other end, as shown in Figure 4.23.

It was observed that the pattern of the initial crack doesn't change until reaching a load of ~ 85 kN, which is the load at which the inner reinforcing steel started to yield. Debonding of the CFRP composites from the surface of the concrete occurred shortly after yielding of the inner reinforcement. In some cases, flexural cracks are associated with shear cracks near the supports causing ultimate shear failure in the concrete directly after debonding of the reinforcing plates, as shown in Figure 4.24.

The mechanism by which such a failure occurs can be explained as follows. When a major flexural or flexural-shear crack is formed in the concrete, the tensile stresses released by the cracked concrete are transferred to the CFRP plate, causing high local interfacial stress concentration areas near the crack. With the increase in the applied load, the tensile stresses in the plate and accordingly the interfacial stress

concentrations are increased. Upon reaching critical values of stresses, debonding initiates at the high stress concentration areas, i.e., crack locations, then propagates towards one of the plate ends driven forward by the widening of the crack and the relative displacement between the two crack faces, Teng et al [25].

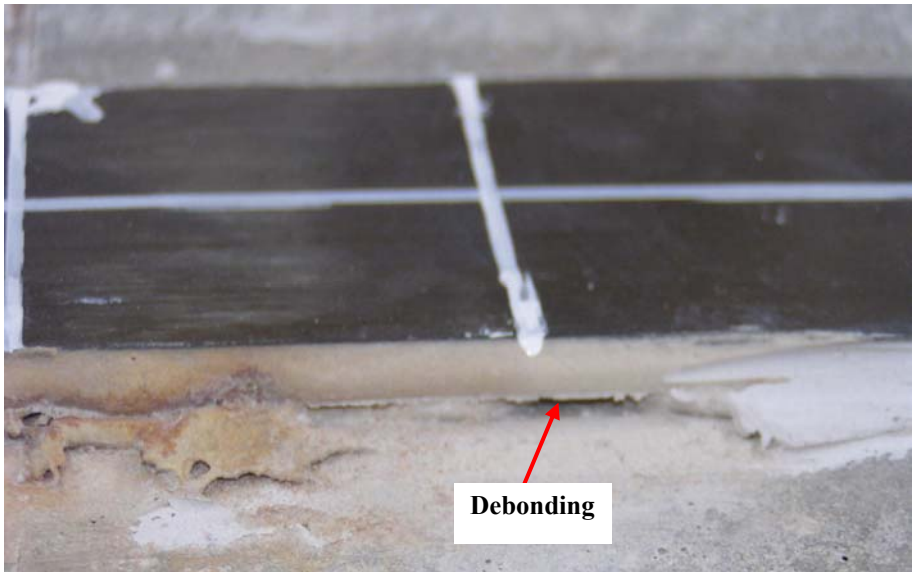

Figure 4.20: Deterioration along the adhesive bond

Figure 4.21: Corrosion stains at the top and sides of slabs exposed to salt solutions

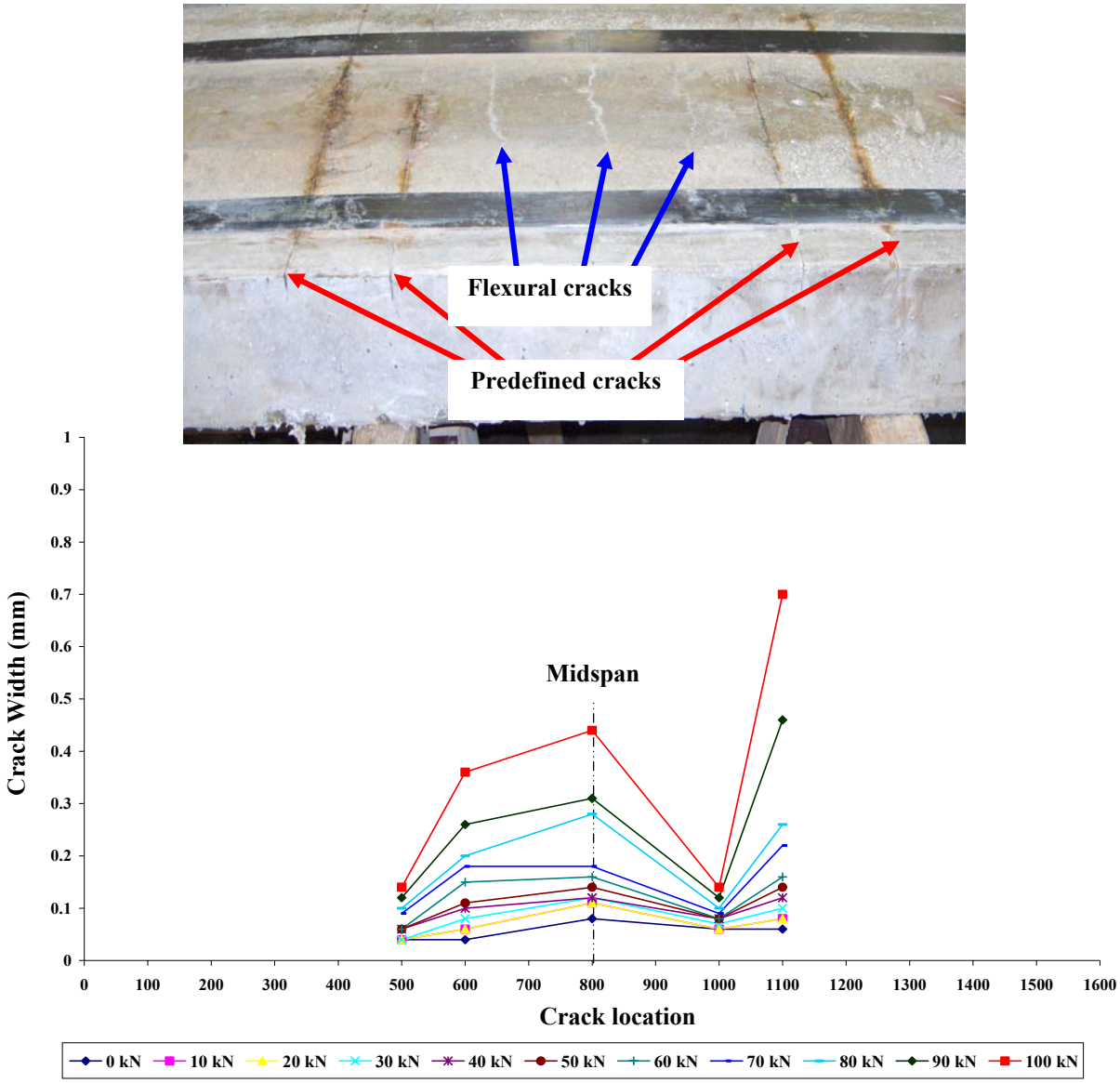

Figure 4.22: Typical crack pattern for slab G_E1_N

Although the global behaviour of the failure modes for all slabs were similar regardless of which environment they were exposed to, but upon closer examination a shift in the failure mode from material decohesion to interface separation was observed. For specimens exposed to indoor and outdoor severe environments, clean epoxy/concrete interface separation mode was observed with no concrete debris adhered to the debonded plates, as illustrated in Figure 4.25. This observation was consistent for all specimens regardless the type of adhesive being used to bond the CFRP plates to concrete and under all severe environments. Whereas, the failure occurred within a few millimeters in the concrete cover for slabs exposed to normal laboratory conditions at iBMB laboratories and those exposed to Amman environment as can be seen in Figure 4.26, this failure ensuring a sound adhesive joint.

The shift in debonding mode from concrete delamination to epoxy/concrete interface separation has revealed the fact that; when slabs are exposed to normal conditions, the strength of the epoxy layer was much higher than that for concrete leading to cohesive failure in concrete. On the contrary for specimens exposed to salt solutions, the ingress of moisture and chlorides causes a substantial loss in the strength of

the adhesive bond to such a certain level that it couldn't withstand the generated high shear and normal stresses in the CFRP plate across cracks, thus leading to failure at the adhesive materials. This observation correlates very well with the results obtained from testing adhesive materials after exposure to severe environments shown earlier in section 4.2.2, as the exposure to salt solutions causes a considerable loss in the mechanical properties of adhesives.

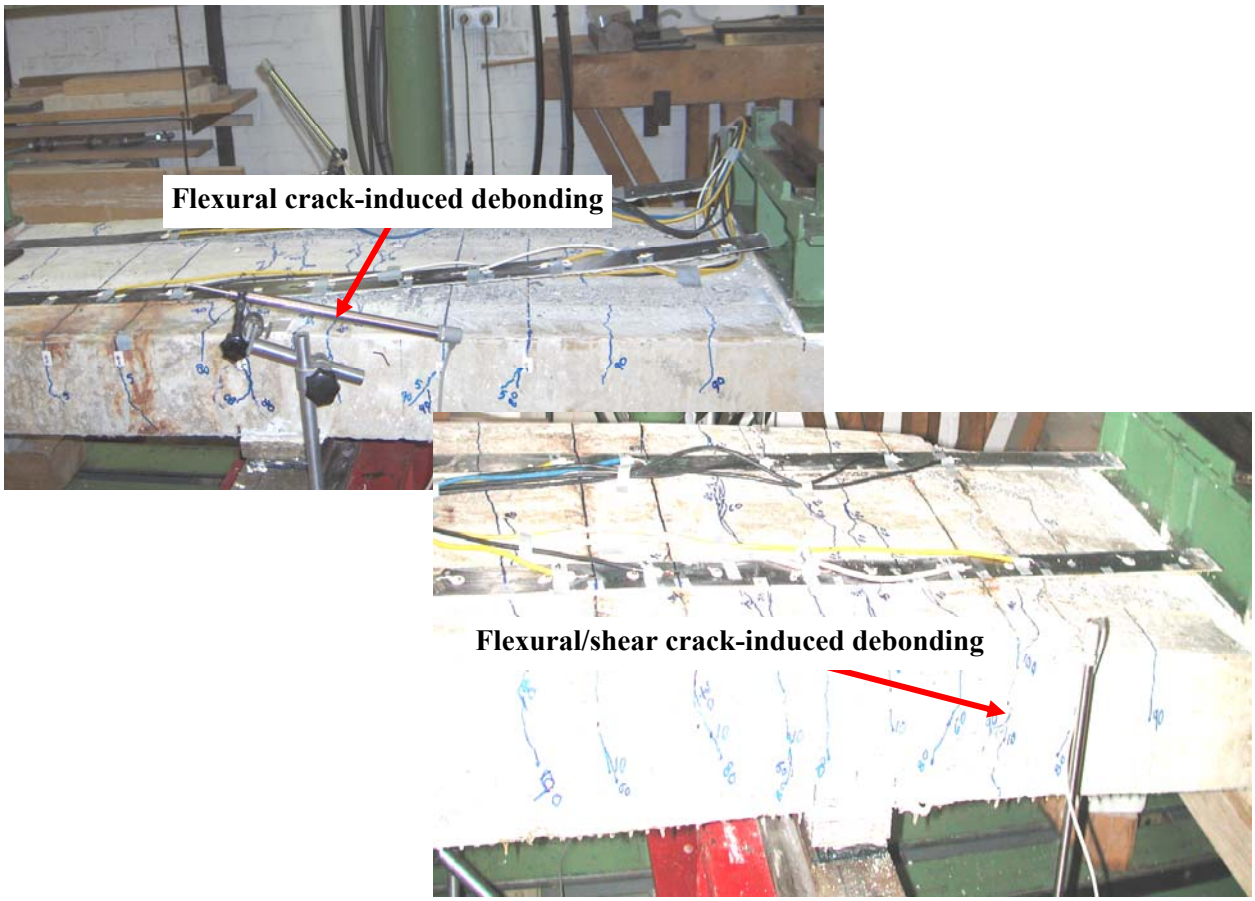

Figure 4.23: Typical Failure Modes

Figure 4.24: Ultimate concrete shear failure after debonding

Figure 4.25: Failure plane along epoxy/concrete interface

Figure 4.26: Failure plane along the concrete layer

4.3.3. Capacities and Failure Loads

Measured failure loads for all test specimens are shown in Table B.1 of Appendix B and in Figure 4.27. Failure loads were measured at the onset debonding of CFRP plates from the concrete substrate. Loading was stopped immediately after debonding is initiated.

The following observations may be drawn from Figure 4.27 and Table B.1.

- Measured failure loads for all slab specimens were in the range of (88.26 – 110.03) kN. These values were lower than the theoretical predicted load, being 140 kN. This result is attributed to the early debonding failures that limited the capacity of the slabs to lower levels than predicted.
- Generally, debonding initiated for almost all slabs at an approximate load of about 100 kN. Except slabs G_E1M_S and J_E1M_A that failed at higher loads of 110.03 kN and 101.57 kN, respectively. And slabs J_E1_D, J_E1M_D and J_E2_D that failed at lower loads of 89.16 kN, 96.31 kN and 88.26 kN, respectively.
- Roughly, the highest measured loads were for specimens exposed to salt solutions when compared with their corresponding reference slabs. Slabs G_E1_S, G_E1M_S and G_E2_S failed at loads of 100.27 kN, 110.03 kN and 99.98 kN, respectively. This observation may be attributed to concrete post-curing that results in higher concrete strength. Additionally, post-curing could improve concrete tensile strengths that may lead to higher bond strength, as concrete is normally the weakest

component in CFRP-adhesive-concrete joint. Hence delaying debonding and increased failure loads. Similar results are obtained by other researchers, Jia et al. [92], Grace [93] and Bo et al. [94].

- For slab specimens that were exposed to real-life environments, there is no marginal difference in the performance between specimens that were exposed to Amman or Aqaba environments. Failure loads of 99.84 kN, 99.96 kN and 99.61 kN were measured for specimens J_E1_A, J_E1M_A and J_E2_A, respectively as compared to values of 99.52 kN 99.78 kN and 99.24 kN measured for specimens J_E1_Q, J_E1M_Q and J_E2_Q, respectively. On the other hand, specimens exposed to Dead Sea environment attained the lowest failure loads. Measured loads for specimens J_E1_D, J_E1M_D and J_E2_D were 89.16 kN, 96.31 kN and 88.26 kN respectively.
- By comparing the measured failure loads for specimens J_E1_D, and J_E2_D, that attained the lowest loads with their corresponding reference specimens, the loss in the measured load was about 10.8 % and 11.7 % for specimens J_E1_D, and J_E2_D, respectively. This loss in the measured load was considered insignificant taking into consideration the severity of the Dead Sea region and assuming that the adhesives are saturated with solutions and hopefully there is no further reductions on strength
- Measured capacities for all slab specimens were in the range of (29.13 - 36.31) MPa, with an increase in capacities of approximately (150 – 190) % as compared to the predicted capacities of the original not retrofitted specimens. The highest incremental increase in strength was observed for precracked specimens exposed to salt solutions, followed by specimens exposed to normal laboratory conditions, then specimens exposed to Amman and Aqaba with no marginal difference between them. The lowest incremental increase in strength was observed for specimens exposed to Dead Sea environment, which is about 90 % of the increased in capacities attained for specimens exposed to normal laboratory conditions. This significant increase in capacities is good enough, and suggests that bonding CFRP plates at the soffit of cracked slabs has an acceptable potential for retrofitting deteriorated slabs even at the very harsh environments, such as the Dead Sea region that characterized by high temperature, humidity and salinity and considered one of the most corrosive environments around the world. But, it is prudent to take into consideration when a retrofitted RC structure is to be placed at a place like the Dead Sea region, not the full expected capacity will be attained, may be 90 % as the case for this study.
- Measured failure loads don't really represent the observed failure modes and expected deterioration along the adhesive bond. For specimens exposed to salt solutions either simulated at the laboratory or real-life exposures, the failure planes were along the adhesive/concrete interface suggesting that severe deterioration had occurred to the adhesive material to such an extent that its strength is equal to the concrete strength, or even lower to get such a failure. Albeit, the adhesive is still intact with the CFRP plate and able to transmit stresses between the adherents.
- As a comparative performance between the adhesives that have been used to bond the CFRP plates to the concrete substrate, specimens retrofitted with CFRP plates utilizing Type 1 Modified adhesive always attained the highest measured load for every single exposure environment, followed by specimens utilizing epoxy Type 1 and specimens utilizing epoxy Type 2 respectively. Although, there is no marginal difference between the results obtained for specimens utilizing Type1 and Type 2 adhesives. These observations correlate very well with the results obtained from testing adhesive materials explained earlier and confirming that viscous adhesive with initially lower mechanical

properties could retain more of its properties under severe exposures when compared with stiff adhesive with much higher initial mechanical properties.

4.3.4. Load-Deflection Response

Obtained values for the midspan deflections are presented in Table B.1and illustrated in Figures 4.28 and 4.29. Additionally, flexural stiffness values were predicted based on the failure loads and maximum deflections at failure and illustrated in Figure 4.30.

The following observations may be drawn from studying deflection curves.

- All curves demonstrate quite similar deflection profiles with very limited deformations before reaching the failure loads. This observation agrees very well with the least desirable brittle failure mode observed while testing the specimens.
- Measured maximum midspan deflections for all slab specimens were in the range of (9.9 – 12.52), which is lower than the predicted midspan deflection of about 15 mm. These lower values of measured deflections are attributed to the early failure of slabs by debonding before reaching the expected maximum failure loads. The lowest measured value was for specimen J_E2_D and the highest value was for specimen G_E1M_S.
- For the reference specimens that were exposed to normal laboratory conditions, the highest midspan deflection was for specimen G_E1M_N with a value of 11.84 mm, followed by a value of 11.8 mm for specimen G_E1_N and specimen G_E2_N got the lowest deflection value of 11.5 mm. Albeit there is no marginal difference between the measured values for deflections for specimens G_E1M_N and G_E1_N, being 0.08 mm.
- For specimens exposed to salt solutions, the highest deflection was for specimen G_E1M_S with a value of 12.52 mm, followed by a value of 11.364 for specimen G_E1_S, and the lowest deflection value of 11.25 mm was measured for specimen G_E2_S.
- For specimens exposed to Amman environment, the highest deflection was for specimen J_E1M_A with a value of 11.43 mm, followed by a value of 11.3 mm for specimen J_E2_A, and the lowest value of 11.24 mm was measured for specimen J_E1_A. Although, there is an insignificant difference in the measured deflection values for specimens J_E2_A and J_E1_A, being 0.06 mm.
- For specimens exposed to Aqaba environment, the highest deflection was for specimen J_E1M_Q with a value of 11.36 mm, followed by a value of 11.01 mm for specimen J_E1_Q, and the lowest deflection of 10.95 mm was measured for specimen J_E2_Q. Although, there is a trivial difference in the measured deflection values for specimens J_E1_Q and J_E2_Q, being 0.06 mm.
- For specimens exposed to Dead Sea environment, the highest deflection was for specimen G_E1M_D with a value of 11.29 mm, followed by a value of 10.09 mm for specimen G_E1_D, and the lowest deflection of 9.903 mm was measured for specimen G_E2_D.

On the other hand the following observations are made from Figure 4.30 regarding the flexural stiffness values for all slabs.

- The values fall in the range of (406.44 – 434.26) kNm^2, with the lowest stiffness for specimen G_E1M_N and the highest stiffness was for specimen G_E2_Q. There is no significant difference in the range, it is just 6.8 %.

- Slabs exposed to normal laboratory conditions got the lowest values as compared to their corresponding specimens but exposed to other environments.
- Specimens exposed to salt solutions have higher stiffness values when compared to their corresponding reference specimens. The percentage increase of 3.9 %, 3.6 and 2.25 % was for specimens retrofitted with CFRP plates utilizing Type 1, Type 1 Modified and Type 2, respectively.
- Specimens exposed to Amman environment have higher stiffness values as compared to their corresponding reference specimens. The percentage increase of 4.6 %, 3.6 % and 1.4 % was for specimens retrofitted with CFRP plates utilizing Type 1, Type 1 Modified and Type 2, respectively.
- Specimens exposed to Aqaba environment have much higher stiffness values as compared to their corresponding reference specimens. The percentage increase of 6 %, 3.6 % and 4.3 % was for specimens retrofitted with CFRP plates utilizing Type 1, Type 1 Modified and Type 2, respectively.
- Specimens exposed to Dead Sea environment have higher stiffness values as compared to their corresponding reference specimens. The percentage increase of 4.1 %, 0.57 % and 2.6 % was for specimens retrofitted with CFRP plates utilizing Type 1, Type 1 Modified and Type 2, respectively.
- Among all the exposure conditions, specimens at the tidal zone of the Red Sea, Aqaba, have the highest stiffness values. Whereas, slabs exposed to normal laboratory conditions got the lowest stiffness values. This observation could be attributed to beneficial concrete post-curing.
- The severity of the environments is not reflected on the test specimens; hence we could say that there is no obvious detrimental effect from all the encountered environments.

4.3.5. Strain Response

Strains were monitored for the two bonded CFRP plates using electrical resistance strain gauges at five locations along each plate as discussed earlier in section 3.4.1.1. These locations represent the four locations of the predefined cracks, and the fifth location represents the midspan crack at the location of the maximum bending moment.

Figures 4.31- 4.36 illustrate the average measured strains at the aforementioned locations. Additionally, average maximum measured strains at the midspan are presented in Table B.1, along with the theoretical predicted maximum strains.

The following observations could be drawn from Figures 4.31 – 4.36.

- Generally, strain curves for all test specimens show almost similar stiff profiles with limited ductility. This result confirms the results obtained from the load-deflection curves that also show stiff profiles.
- Average measured strains at midspan, i.e., at locations 3 and 8, are in the range of (0.0044 – 0.0058) mm/mm, which is smaller than the predicted value of 0.006 mm/mm. This observation is attributed to the early failure caused by the debonding of the CFRP plates from the concrete substrate. Early debonding failure modes limit the capacity of the slabs below the theoretical predicted capacity. Additionally, the obtained values of strains are much below the ultimate strain of the CFRP plates being 0.02 mm/mm. Measured strains constituted about (22 – 29) % of the plate ultimate strain. The smallest recorded strain value was for specimen J_E2_D and the highest value was for specimen G_E1M_S.

- Average measured strains above the left crack closest to the left support, i.e. at locations 1 and 6, are in the range of (0.0023 – 0.0042) mm/mm for all test specimens. These values are well below the ultimate strain of the CFRP plates being 0.02 mm/mm. Measured strains constituted about (16.3 – 20.7) % of the plate ultimate strain. The smallest strain value was measured for slab G_E1_D, whereas, the highest strain value was measured for slab J_E1M_N.

- Average measured strains above the left crack closest to midspan are in the range of (0.00354 – 0.0051) mm/mm for all test specimens. These values represent (17.7 – 25.5) % of the ultimate strain of the CFRP plate, being 2 %. The smallest strain value was measured for slab J_E1_D, whereas, the highest strain value was measured for slab G_E1M_S.

- Average measured strains above the right crack closest to the midspan are in the range of (0.00345 – 0.005) mm/mm for all test specimens. These values represent (17.25 – 25) % of the ultimate strain of the CFRP plate, being 0.02 mm/mm. The smallest strain value was measured for slab J_E1_D, whereas, the highest strain value was measured for slab G_E1M_S.

- Average measured strains above the left crack closest to the right support are in the range of (0.002 – 0.004) mm/mm for all test specimens. These values represent (10 – 20) % of the ultimate strain of the CFRP plate, being 0.02 mm/mm. The smallest strain value was measured for slab J_E1_D, whereas, the highest strain value was measured for slabs G_E1M_N and G_E1M_A.

- It is noticed that the maximum usable strain for all tested slabs and under all encountered environments is less than 30 % of the ultimate strain of the plate.

- By comparing the maximum measured strains for specimens exposed to salt solution with their control counterparts; specimens exposed to salt solution have almost the same strains as the control specimens and even higher. Specimen G_E1M_S got about 3.4 % higher value of strain. Though more usable strain assures that there is no detrimental effect from exposure to salt solutions when combined with ambient temperature of 23 ºC (normal laboratory conditions).

- By comparing the maximum measured strains for specimens exposed to real-life environments prevailing at Amman with their control counterparts, specimens exposed Amman environment have almost the same strains as the control specimens, except for specimen J_E2_A that has a lower strain value of about 5 %. This environment can be considered as a non detrimental.

- By comparing the maximum measured strains for specimens exposed to real-life environments prevailing at Aqaba region with their control counterparts, specimen J_E1_Q got higher strain value of about 2 %, while specimens J_E1M_Q and J_E2_Q have lower strain of about 5 %.

- By comparing the maximum measured strains for specimens exposed to real-life environments prevailing at Dead Sea region with their control counterparts; specimen J_E1_D got a lower strain value of about 15 %, specimens J_E1M_D got a lower strain value of about 10 % and specimen J_E2_D has lower strain of about 21 %. This low strain values justify the reduced measured failure loads.

- As a comparison between the different types of adhesives used to retrofit the deteriorated slabs with CFRP plates, specimens retrofitted by CFRP plates using Type 1 Modified epoxy got the highest strain values under all encountered environments, followed by specimens using Type 1 adhesive and specimens using Type 2 adhesive, respectively. Albeit the difference in performance between Type 1 and Type 2 epoxies is insignificant.

Furthermore, strains were measured along one of the CFRP plates for each specimen using Demec strain gauges. Measurements were taken at load increments of 10 kN to detect variations in the distribution of strains along the CFRP plate. For safety purposes, strain measurements were stopped when debonding popping sounds are clearly heard, almost at one step earlier before failure. Therefore, the maximum recorded strains do not represent the failure strains.

Collected measurements were used to develop strain-location curves that illustrate the variation in the strains along one the CFRP plates at different stages of the applied load prior to debonding.

Strain location curves for all specimens are shown in Appendix B, typical strain-location curves are reproduced herein for the comprehensive of this report. Figure 4.37 and 4.38 illustrate the variation in strains at different load levels for representative specimens, J_E1M_A and J_E1M_Q.

The following observations may be drawn from the test results.

- It is evident from the plots for slab specimens that the strain pattern for specimens is depicting the three-point bending moment scheme.
- The pattern of strains did not change significantly for different load levels during the tests. Strains increased proportionally with load in all strain locations.
- For most of the specimens, the maximum measured strains at all load levels typically occurred at the center of the CFRP plate, i.e., the location of maximum bending moment.
- Strains measured using Demec targets fall in the range of (0.00594 – 0.0082) mm/mm, the highest strain value was for specimen G_E1M_S and the smallest value was for specimen J_E2_D. This observation correlates very well with the results obtained from measuring strains using electrical strain gauges regarding specimens that got higher and minimum strains, but there is difference in the measured strain ranges. The range of strains measured using electrical gauges is smaller than the range of strains obtained by using mechanical gauges. A possible explanation is that; for the case of strain measurements using electrical gauges, strains are recorded directly above the crack, but strains were obtained by dividing the measured extensions by the distance between each two successive Demec targets, where the deflected shape of the specimen under loading could affect the extension measurement.
- For the control specimens that were exposed to normal laboratory conditions, the highest measured strain of 0.00793 mm/mm was measured for specimen G_E1M_N, followed by a value of 0.00783 mm/mm for specimen G_E1_N and specimen G_E2_N has the lowest comparable value of 0.00758 mm/mm. This result agrees very well with the results obtained using electrical strain gauges except for the exact values for strains.
- For specimens exposed to salt solution under normal laboratory conditions, specimen G_E1M_S got the highest strain value of 0.0082 mm/mm followed by specimen G_E1_S with a value of 0.0079, and specimen G_E2_S has the lowest value of 0.00781. Albeit, there is no significant difference in the measured values for G_E1M_S and G_E2_S. This result agrees very well with the results obtained using electrical strain gauges except for the exact values for strains.
- For specimens exposed to real-life environments prevailing at Amman, specimen G_E1M_A got the highest strain value of 0.00699 mm/mm followed by specimen G_E1_A with a value of 0.00685, and specimen G_E2_A has the lowest value of 0.00678. This result agrees very well with the results obtained using electrical strain gauges except for the exact values for strains.

- For specimens exposed to Aqaba real-life environments, specimen G_E1M_Q got the highest strain value of 0.0072 mm/mm followed by specimen G_E1_Q with a value of 0.0065, and specimen G_E2_Q has the lowest value of 0.00636. This result agrees very well with the results obtained using electrical strain gauges except for the exact values for strains.
- For specimens exposed to Dead Sea real-life environment, specimen G_E1M_D got the highest strain value of 0.00664 mm/mm followed by specimen G_E1_D with a value of 0.006, and specimen G_E2_D has the lowest value of 0.00594. This result agrees very well with the results obtained using electrical strain gauges except for the exact values for strains.
- Roughly, exposure to salt solution has no detrimental effect as specimens exposed to salt solution have the highest measured strains.
- Generally, the best performance was for specimens retrofitted with CFRP plates utilizing Type 1 Modified adhesive, as it always got the highest values under all the encountered environments. Followed by specimens utilizing Type 1 adhesive and Type 2 adhesive, respectively.

As a general conclusion, it is shown that there is no significant effect of salt solutions on the performance of the CFRP retrofitted slabs. On the contrary, exposure to salt solution enhanced the performance by increasing the stiffness, strains and failure loads. This conclusion was reached with other researchers, Shahrooz et al. [91] and Grace [93].

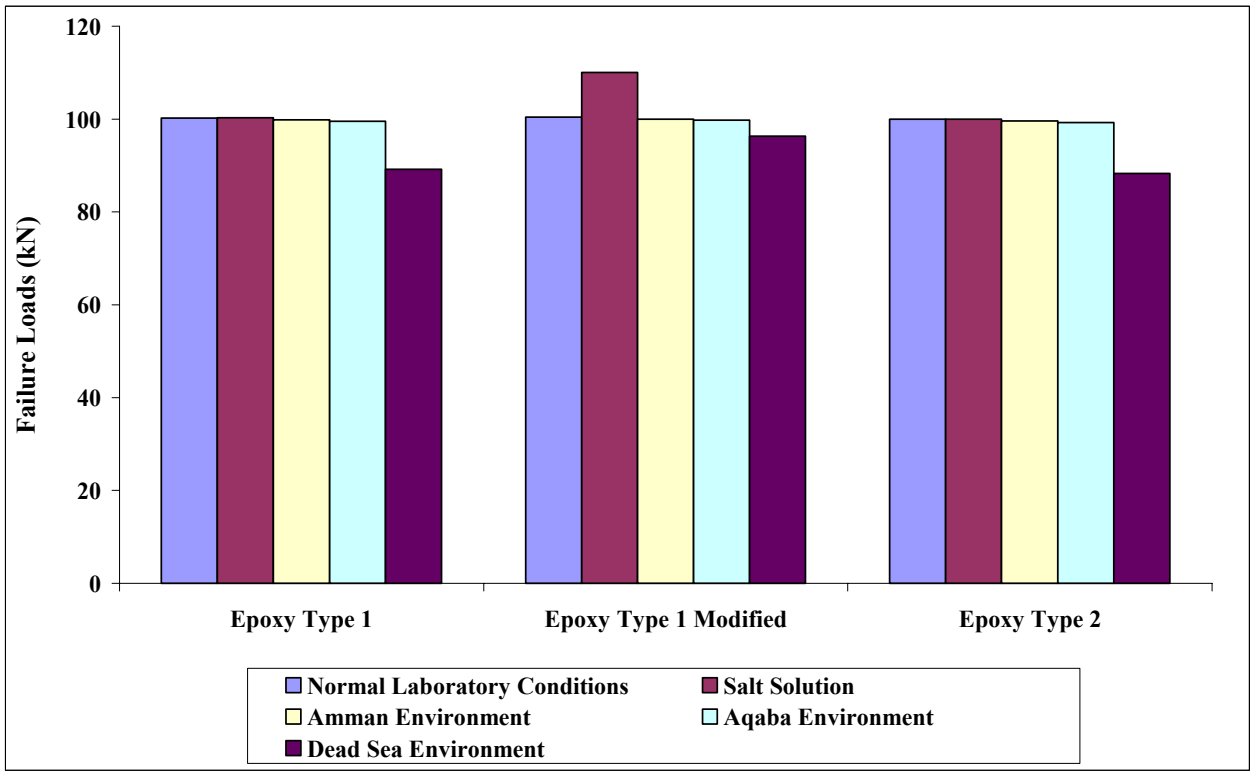

Figure 4.27: Average measured failure loads

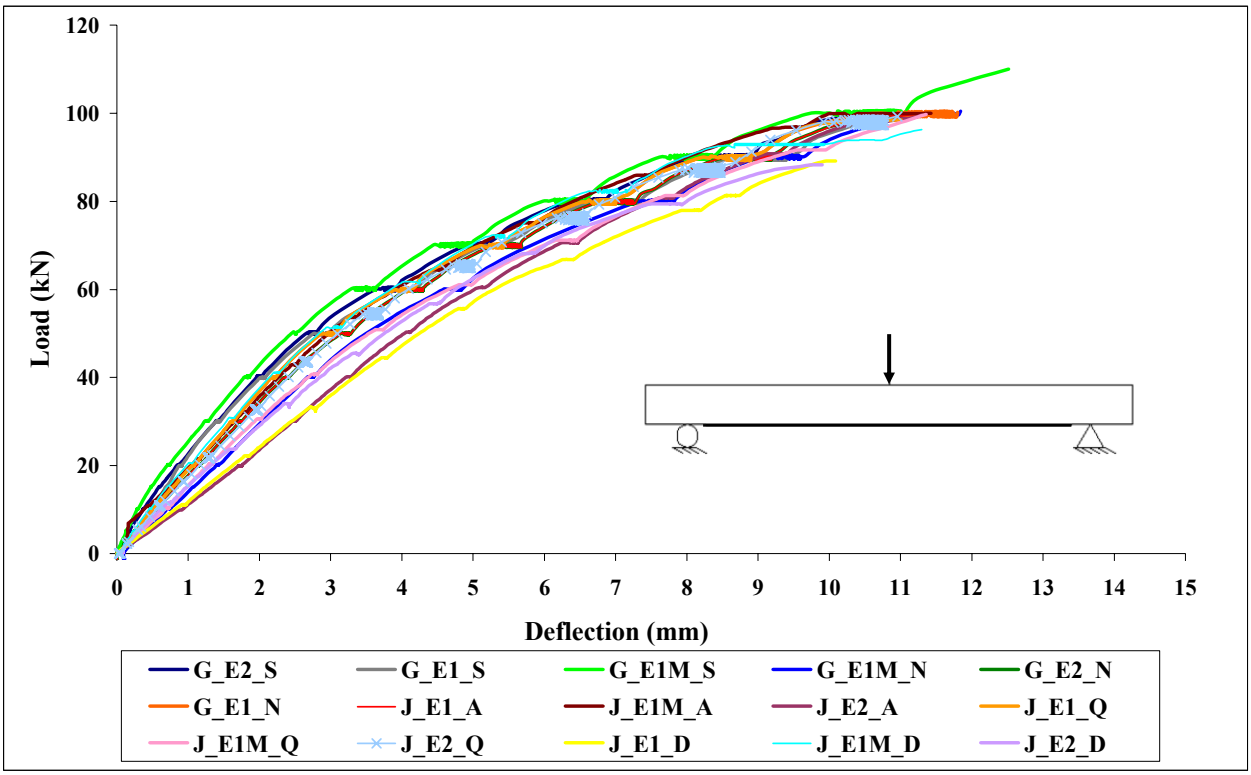

Figure 4.28: Average measured midspan deflections for all tested slab specimens

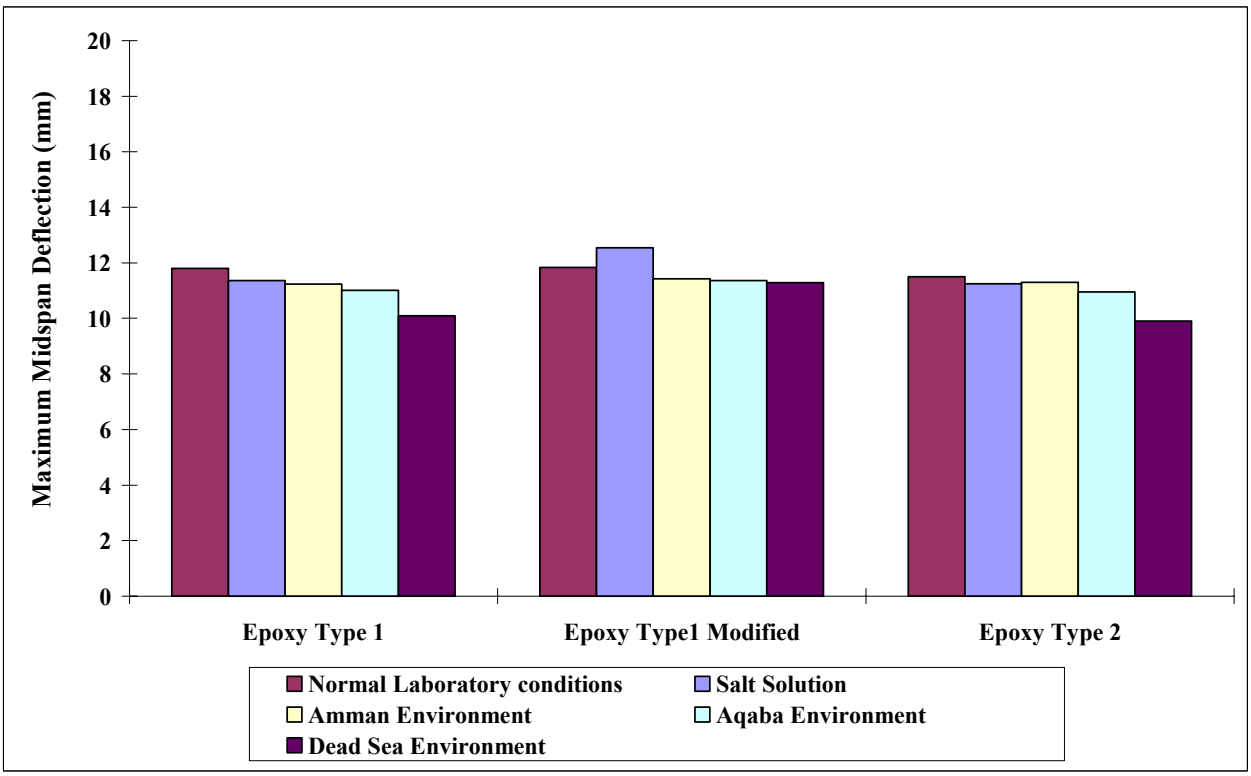

Figure 4.29: Average midspan deflection values for all tested slab specimens

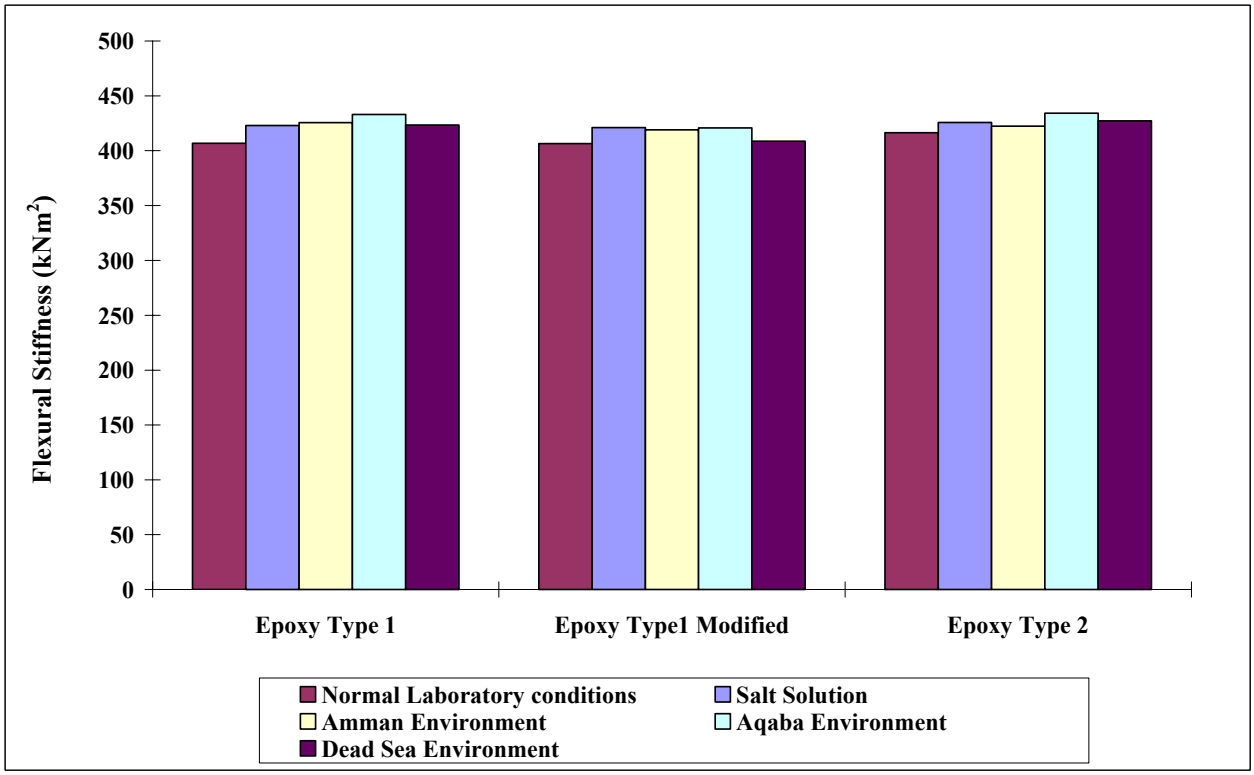

Figure 4.30: Average predicted values of flexural stiffness for all tested slab specimens

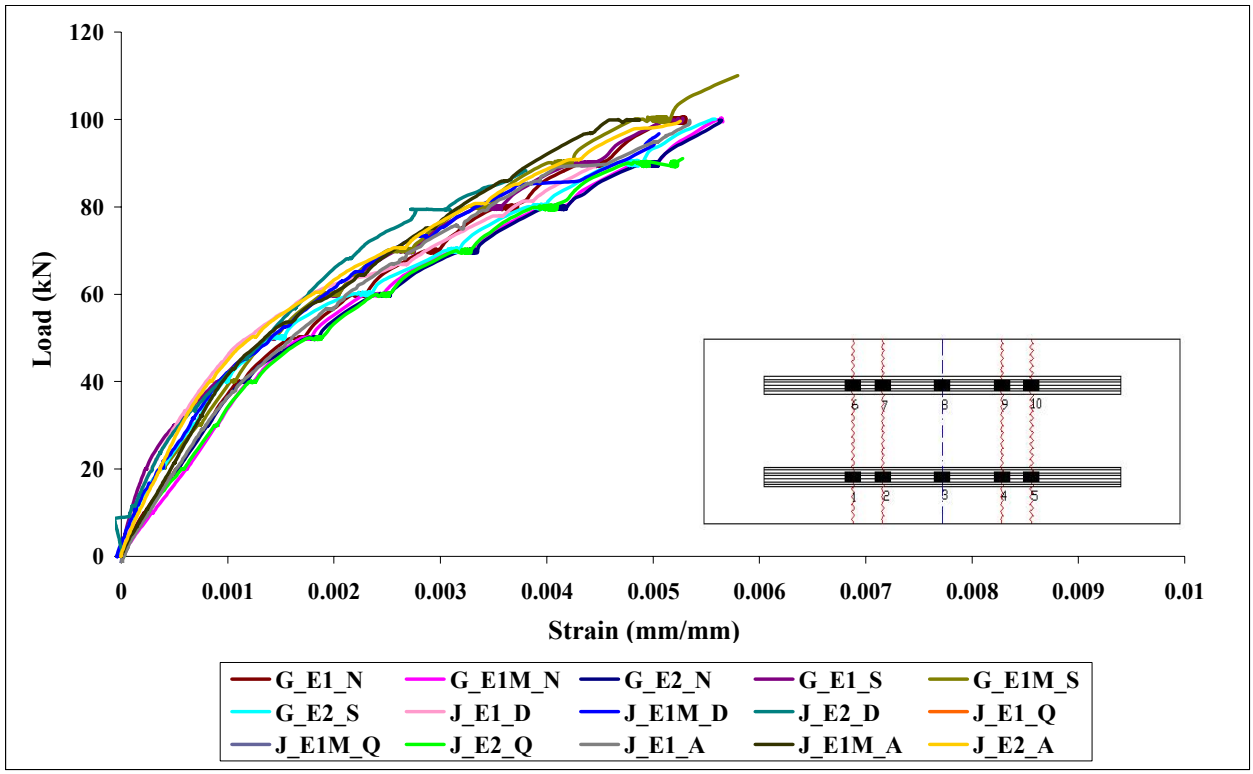

Figure 4.31: Typical average measured strains at slab midspan - locations 3 and 8

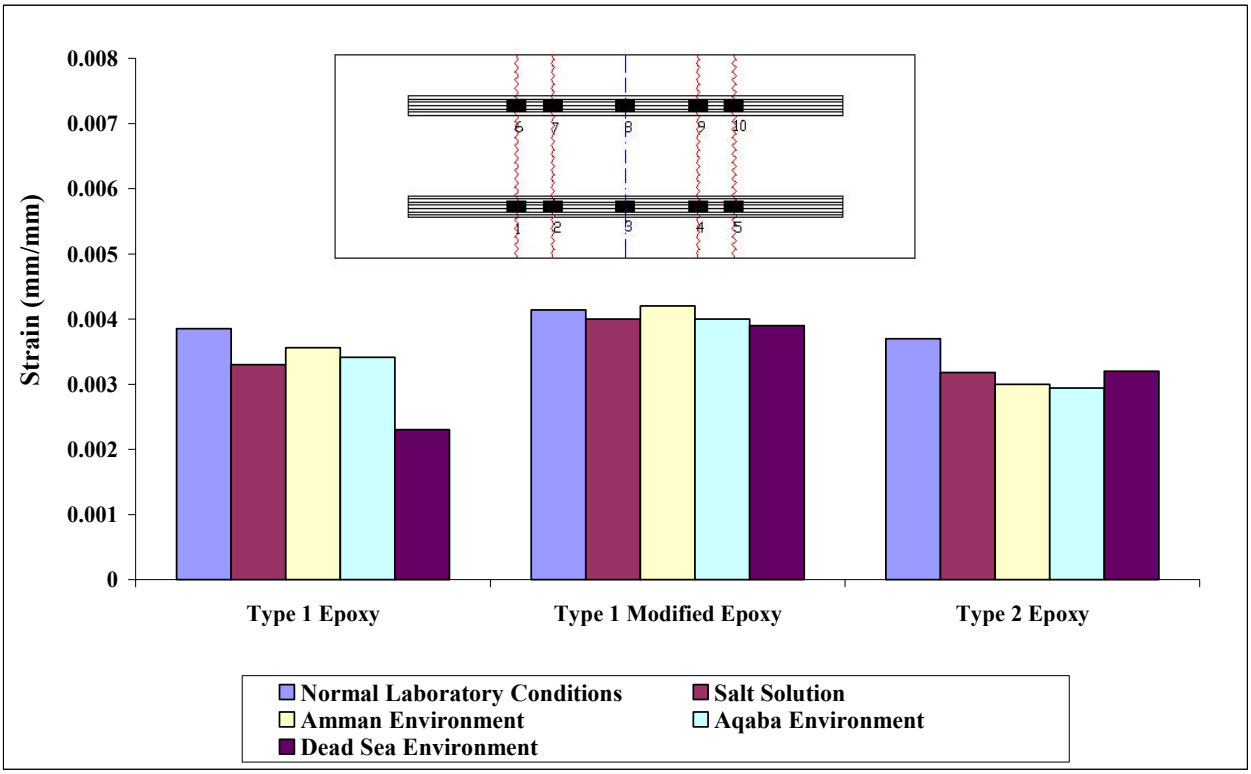

Figure 4.32: Average measured strains at locations 1 and 6

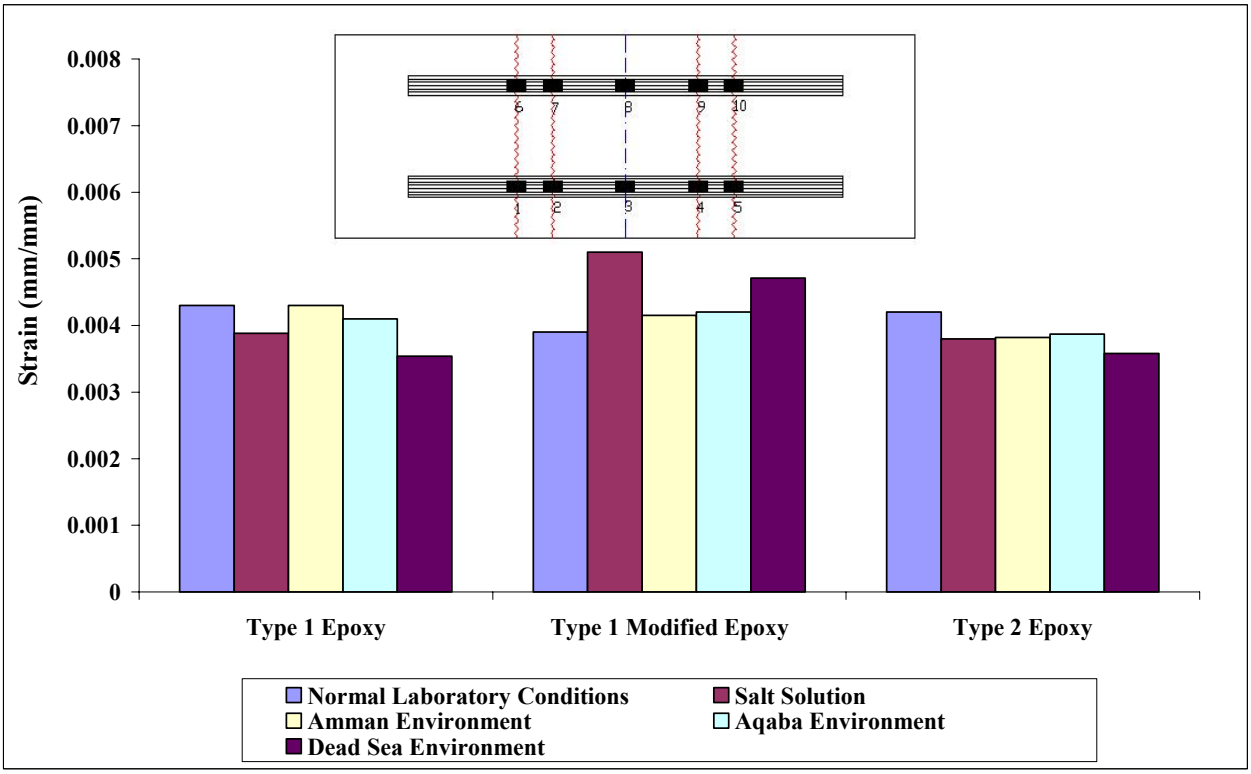

Figure 4.33: Average measured strains at locations 2 and 7

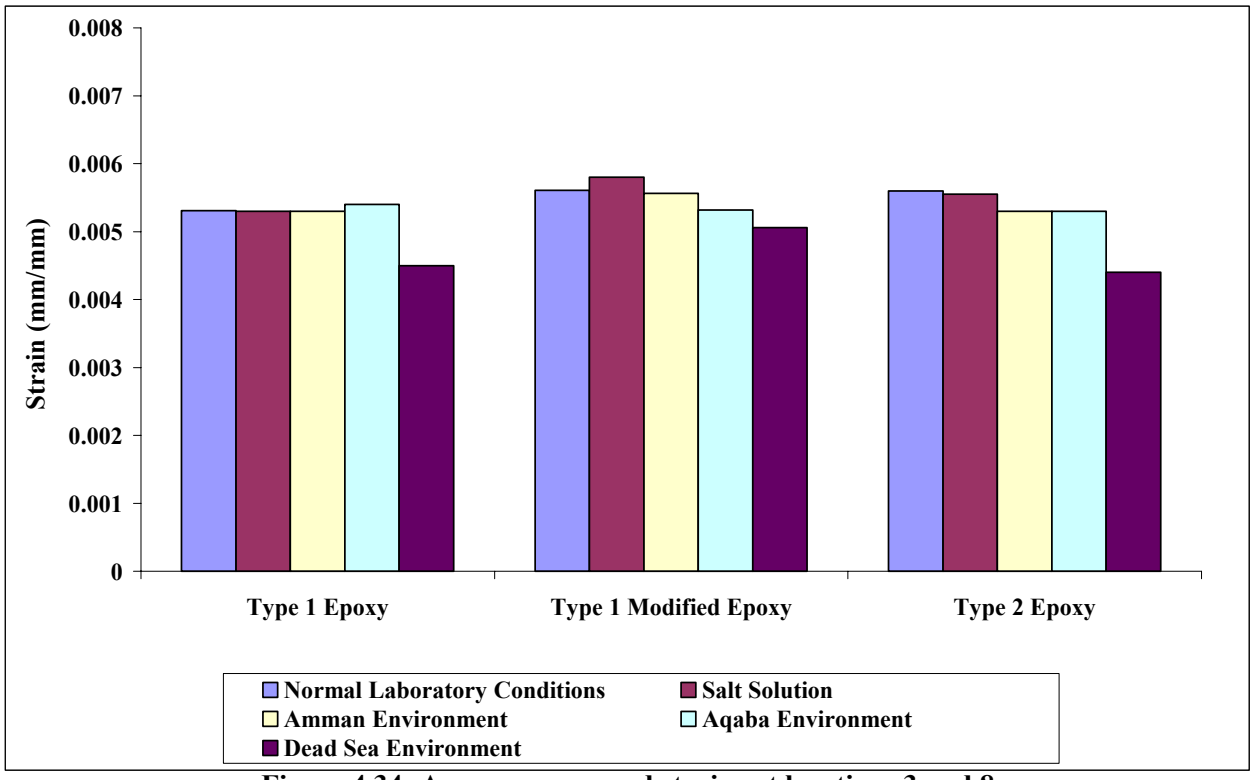

Figure 4.34: Average measured strains at locations 3 and 8

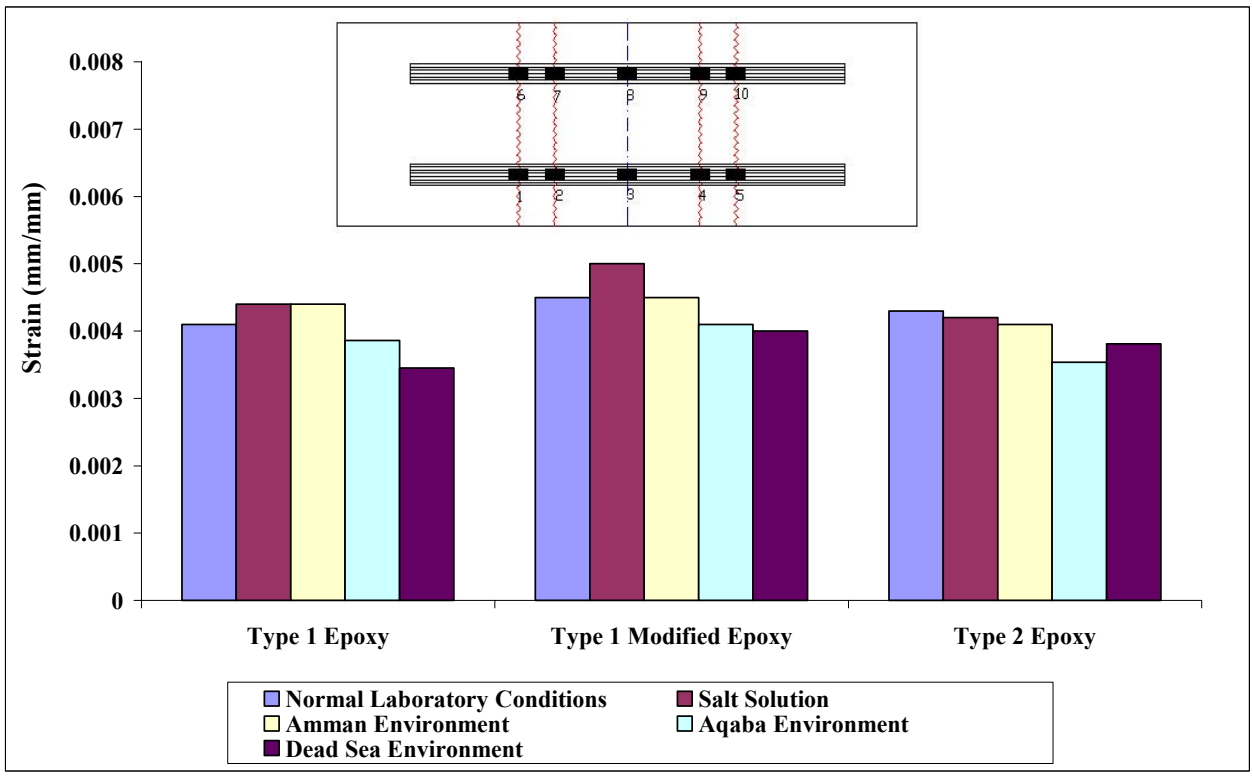

Figure 4.35: Average measured strains at locations 4 and 9

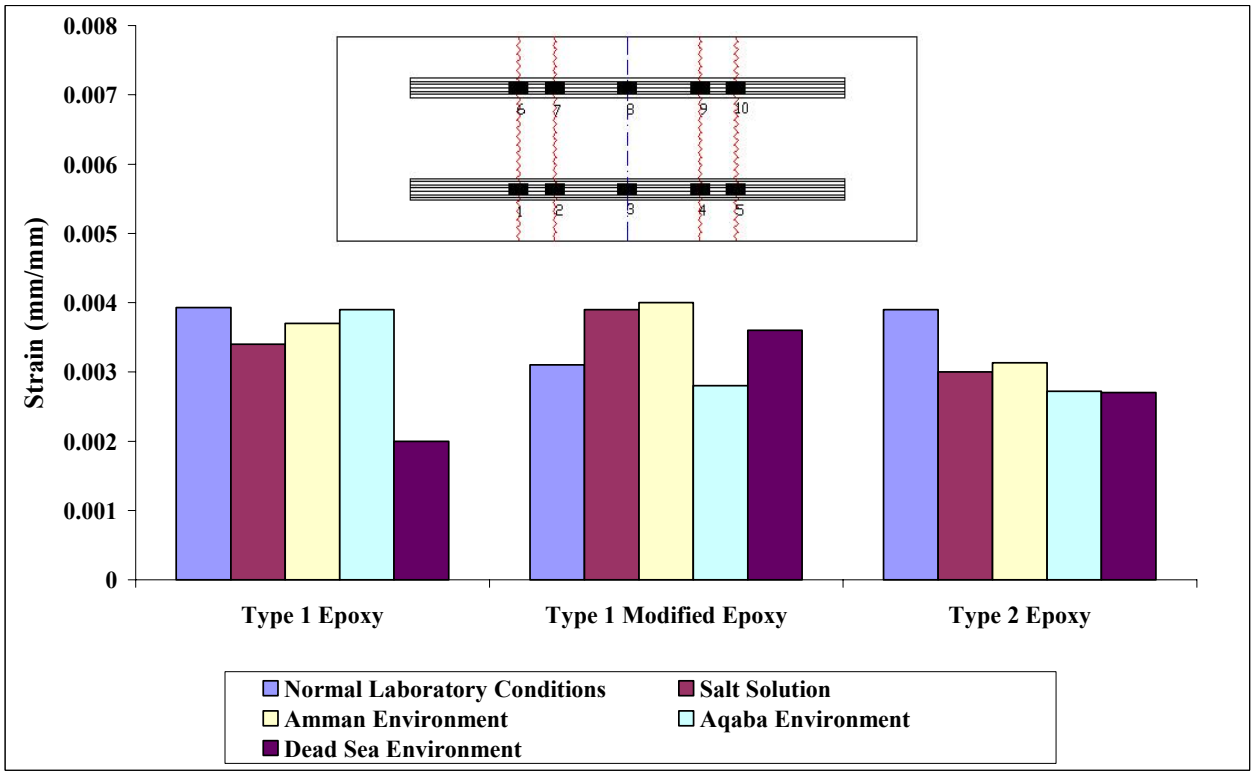

Figure 4.36: Average measured strains at locations 5 and 10

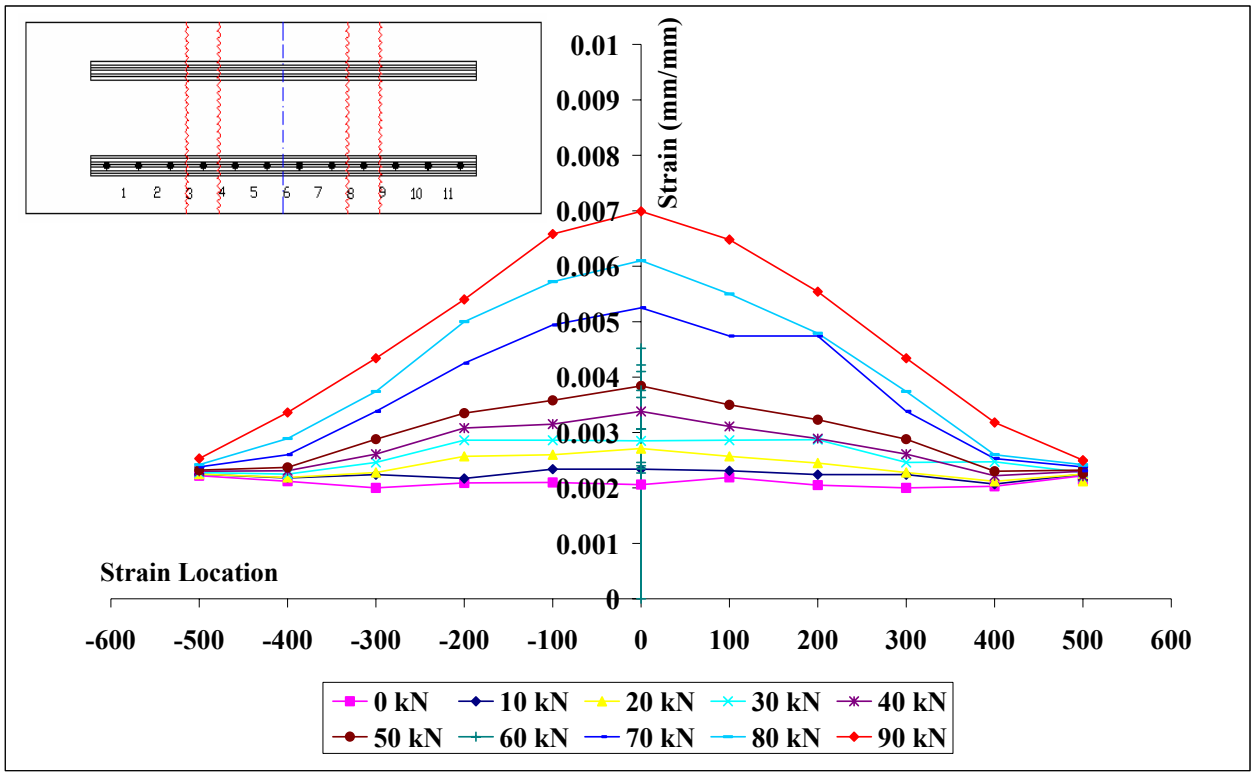

Figure 4.37: Measured strains along CFRP plate of slab J_E1M_A

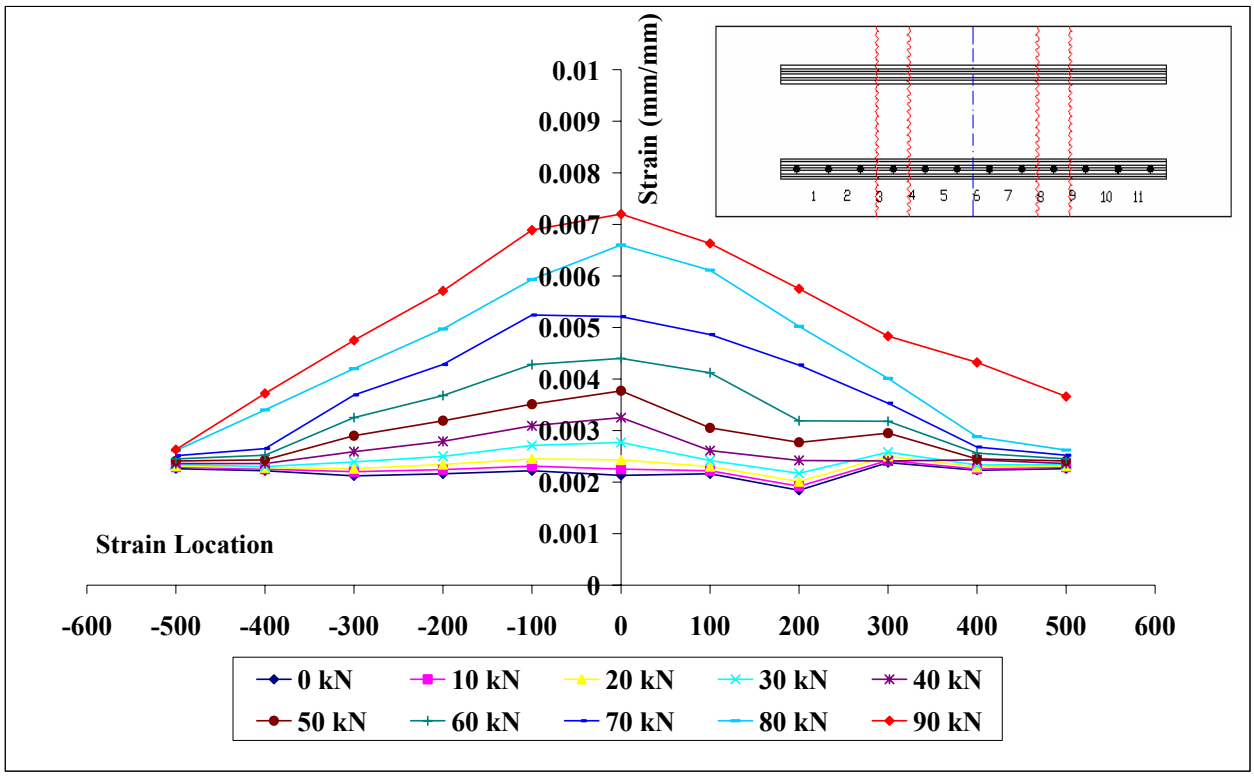

Figure 4.38: Measured strains along CFRP plate of slab J_E1M_Q

4.3.6. Shear Stresses Along the CFRP Plates

Strain measurements recorded at discrete locations along the CFRP plates were employed in founding the shear forces along the CFRP plates. The difference in tensile strain between gauge locations must be balanced by the shear force acting between the CFRP plate and the concrete substrate, as noted by Garden et al. [49]. Then, the average shear stress could be determined between the two gauge locations as,

$$\tau_{av} = E_p t_p \frac{(\varepsilon_2 - \varepsilon_1)}{(x_2 - x_1)} \qquad 4.4$$

Where, $(\varepsilon_2 - \varepsilon_1)$ is the difference in strain between two adjacent gauges, $(x_2 - x1)$ is the distance between gauges, E_p is the elastic modulus of the CFRP plate and t_p is the thickness of the plate.

By doing so, the shear stress is considered constant between the two strain gauges, and the calculated shear stress value is attributed to the middle of the two strain gauges.

The variation in shear stress along the CFRP plates and concrete substrate for all specimens at different load levels is presented in Figure 4.39 and in Appendix B. Also, typical curve is reproduced herein for specimen G_E1M_S as can be seen in Figure 4.40.

The following observations may be drawn from examining the predicted shear stress curves.

- Maximum value of the predicted shear stress along the CFRP plates for all specimens was in the range of (2.68 – 4.19) MPa. The highest value was for specimen G_E1M_S and the lowest value was for specimen J_E2_D. It is unexpected for specimen G_E1M_S that has been exposed to a very high

concentrated salt solution for almost 12 months to get the highest value of shear stress. This observation implies a very strong adhesive bond that correlates very well with the high observed failure load, but disagrees with the observed failure mode. Since the failure mode was at the adhesive/concrete interface. This suggests that the concrete strength is enhanced by exposure and ageing and the adhesives were deteriorating to levels that are equivalent or lower than the enhanced concrete strength.

- For specimens stored under normal laboratory conditions, shear stresses were in the range of (2.91 – 3.94) MPa, the highest value was for specimen G_E1M_N, followed by a value of 3.08 MPa for specimen G_E1_N and the lowest value was for specimen G_E2_N.
- For specimens exposed to simulated salt solution and stored under normal laboratory conditions, shear stresses were in the range of (2.89 – 4.186) MPa, the highest value was for specimen G_E1M_S, followed by a value of 3.0 MPa for specimen G_E1_S and the lowest value was for specimen G_E2_S.
- For specimens exposed at real-life environments prevailing at Amman, shear stresses were in the range of (2.93 - 2.954) MPa, the highest value was for specimen G_E1M_A, followed by a value of 2.94 MPa for specimen G_E1_A and the lowest value was for specimen G_E2_A, although insignificant difference between the predicted shear stress for all specimens.
- For specimens exposed at real-life environments prevailing at Aqaba region, shear stresses were in the range of (2.87 - 2.9) MPa, the highest value was for specimen G_E1M_Q, followed by a value of 2.88 MPa for specimen G_E1_Q and the lowest value was for specimen G_E2_Q, although insignificant difference between the predicted shear stress for all specimens.
- For specimens exposed at real-life environments prevailing at Dead Sea region, shear stresses were in the range of (2.61 - 2.81) MPa, the highest value was for specimen G_E1M_D, followed by a value of 2.71 MPa for specimen G_E1_D and the lowest value was for specimen G_E2_D, although insignificant difference between the predicted shear stress for all specimens.

Furthermore, Figure 4.40 shows the distribution of shear stresses along the CFRP plates. The curve shows a peak value at 150 mm to the left of midspan. This is the location where debonding was observed to be initiated during testing, then it propagated along the shear span in the direction of the left support as clarified in Figure 4.41.

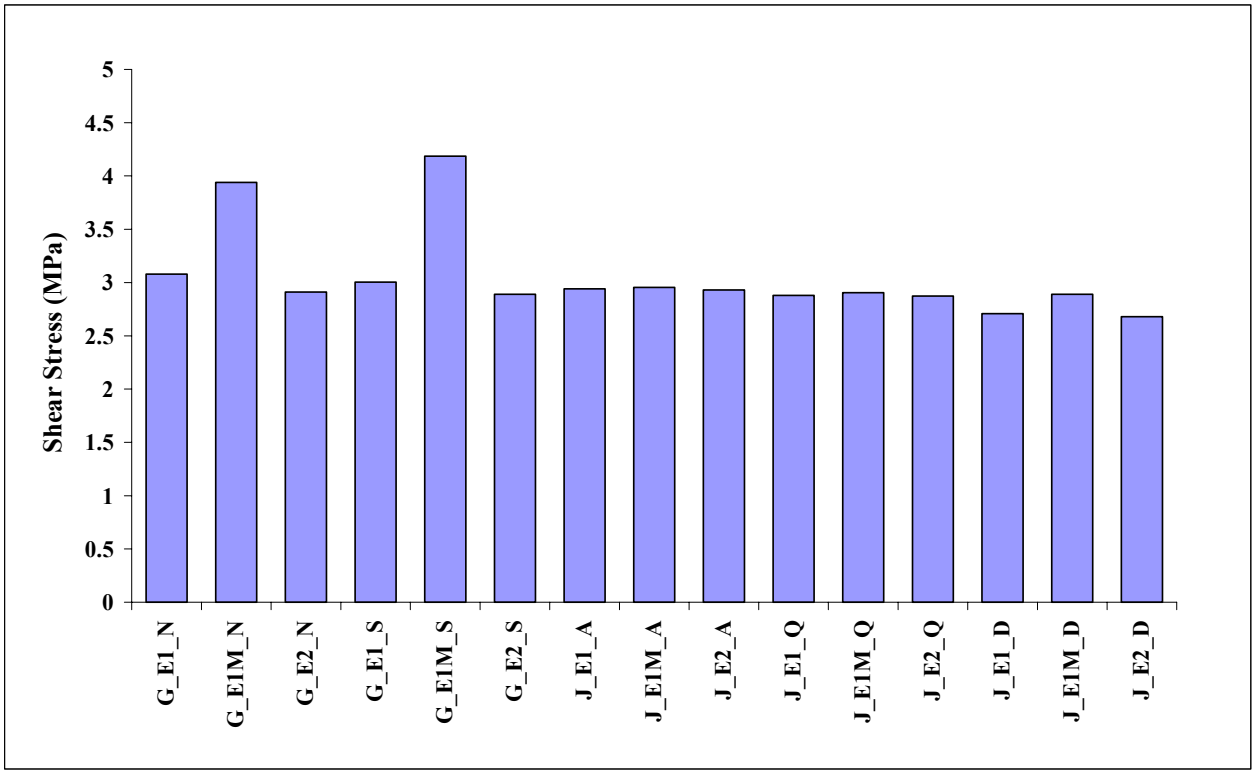

Figure 4.39: Predicted maximum shear stresses along CFRP plates for all slab specimens

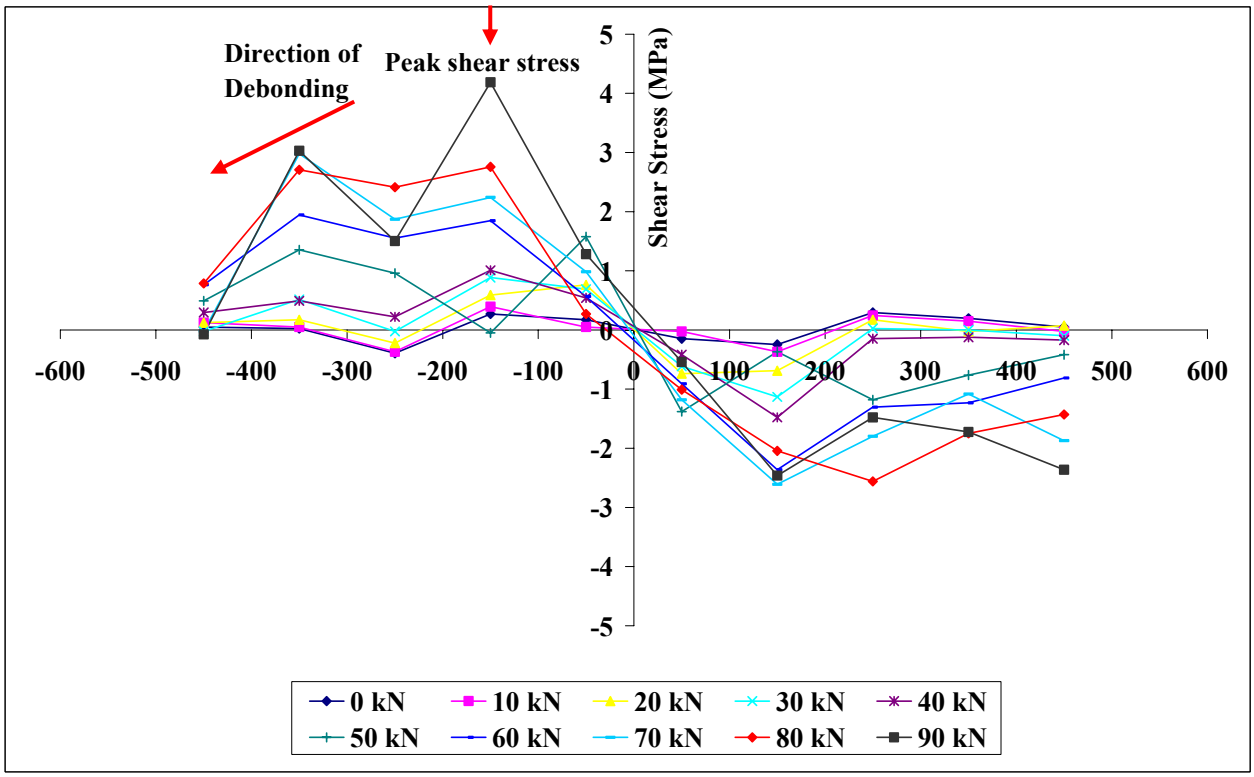

Figure 4.40: Predicted shear stresses along CFRP plate of slab G_E1M_S

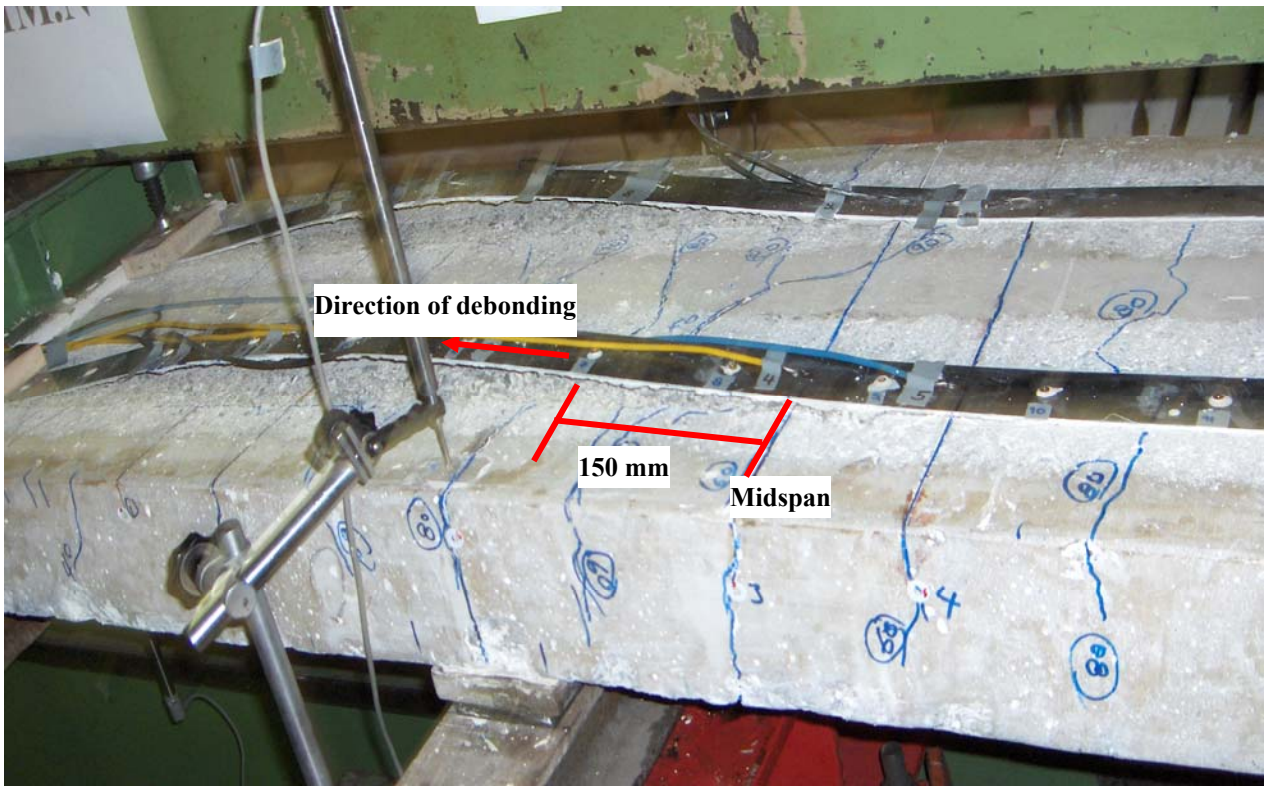

Figure 4.41: Location of debonding along the CFRP plate for slab G_E1M_N

4.3.7. Concrete Tensile Strength

Obtained results for concrete tensile strength for all specimens are shown in Table B.1 of Appendix B and Figure 4.42 herein.

The following observations may be drawn from the test results.

- Average measured values for concrete tensile strengths were in the range of (2.92 – 3.45) MPa, with the highest value measured for specimen J_E2_D and the lowest value is for specimen J_E1_D. It is less than expected for specimen J_E2_D to have the highest concrete tensile strength of 3.45 MPa and at the same time to have the lowest failure load of 88.26 kN, as compared with specimen G_E1M_S results, which got the highest failure load of 110.03 kN and attained concrete tensile strength of 2.95 MPa.
- There is consistency and direct relation between concrete tensile strengths and the measured failure loads for specimens exposed to normal laboratory conditions and those exposed to the real-life environment at Amman; higher failure loads were attained at higher concrete tensile strengths. This observation correlates very well with the observations obtained by previous researchers, Teng et al. [25], Hollaway and Leeming [31], Neubauer and Rostásy [77] and [78], and Bo et al. [94]. On the other hand, there is no conformity between the measured failure loads and the concrete tensile strengths for specimens exposed to salt solutions, and those exposed to real-life environments at Aqaba and Dead Sea region. Lower failure loads were measured for specimens with higher concrete tensile strength. Therefore concrete tensile strength is not the dominate parameter for bond strength for specimens exposed to severe environments. Adhesives were considered the control failure

parameters for specimens exposed to severe environments since the failure planes were along the adhesive/concrete interface. This observation ensures that adhesives were deteriorated by exposure to severe environments to such an extent that their strengths were reduced to be similar or even lower than those for concrete.

- A possible explanation for higher loads measured for specimens exposed to salt solution is that, concrete strength is enhanced by post-curing and the adhesive strength is deteriorated to the level of the enhanced concrete, consequently failure will be at higher levels when compared to specimens exposed to normal conditions, where there is no enhancement for concrete strength and the concrete is the controlling parameter of failure.

This observation suggests that the existing bond models should take into consideration the mechanical properties of the adhesives. Most of bond models are based only on the mechanical properties of the adherents, CFRP plate and concrete.

4.3.8. Total Chloride Ion Content

Chloride profiles that depict the measured chloride contents at three different levels along the depth of the concrete cover of the tested specimens are shown in Figure 4.43.

The following observation can be drawn from the obtained test results.

- All curves showed an expected general trend of decreasing chloride contents with increased depths.
- Chloride contents measured for all specimens exposed to salt solutions were in the range of (0.341 – 0.644) % of concrete weight at depth of (0 -10) mm in concrete cover. The minimum value was for specimen G_E1M_S and the highest value was for specimen J_E1M_Q. A reasonable threshold value is 0.4 % by weight of cement in concrete, Lin and Olek [98]. This threshold value is equivalent to 0.058 % in this study, assuming 350 kg cement weight in concrete. Although corrosion is not an issue in this investigation, but comparison of chloride contents with a threshold value enlighten the significance of the measured quantities of chlorides. It is obvious now that the measured chloride contents are quite significant if compared with chloride threshold needed for the initiation of corrosion.
- A lower range of chloride contents is observed at depth of (10 – 30) mm inside the concrete cover, i.e. at the level of reinforcing steel. Measured chloride contents were in the range of (0.036 – 0.286) %, with the highest value for specimen J_E2_Q and the lowest value for specimen J_E1M_D. Chloride contents for all specimens were much higher than the chloride threshold value, except specimens J_E1_D and J_E1M_D that showed lower values of chloride contents being, 0.04 % and 0.036 %, respectively.
- At depth of (30 – 60) mm inside the concrete cover, substantial reduction on the measured chloride contents was observed. Chloride contents were in the range of (0.023 – 0.148) % with the lowest value measured for specimen J_E1M_D and the highest value was measured for specimen J_E2_Q. Also, this range of chloride contents is higher than the chloride threshold value for all specimens exposed to salt solution, except for all specimens exposed to the real-life environment at the Dead Sea region, i.e. specimen J_E1_D, J_E1M_D and J_E2_D.
- Specimens exposed to real-life environments at Aqaba region got the highest chloride contents for all the three depth levels as compared to those ponded with the 9.6 % NaCl solution and those exposed to real-life environments at the Dead Sea region. This result could be attributed to the fact that,

specimens allocated at the tidal zone of the Red Sea of Aqaba are exposed to more than 600 dry and wet cycles during the exposure period which extends for almost one year. Alternate wetting and drying cycles result in higher chloride accumulation due to sea water movements that continuously washing chlorides from the surface and pushing them further deeper into the concrete. Additionally, these specimens allowed chloride penetration from all sides. Whereas, for the other specimens where there is no water movements, chloride accumulation and crystals formulation on the top surface of the concrete blocks further chloride ingress deeper into the concrete.

- For further evaluating the measured chloride contents, chloride tests were performed on concrete powder samples extracted from specimens exposed to Amman environment to be considered as reference specimens. Chloride contents measured for the first 10 mm depth into the concrete cover were in the range of (0.022 – 0.029), and in the range of (0.018 – 0.027) at steel level. Whereas, chloride contents were in the range of (0.01 – 0.022) % at depth level of (30 – 60) mm. These values are well below the chloride threshold and insure that the measured chloride contents are only due to diffusion of chlorides into the concrete and are not initially or exist in the concrete ingredients.
- As per a comparison between the epoxy types being used to retrofit cracked slab specimens, the lowest values for chloride contents at the three depth levels were measured for specimens using Type 1 Modified adhesive. Followed by Type 1 and Type 2, respectively. This result correlated very well with the predicted values of diffusion rates for the bulk materials.

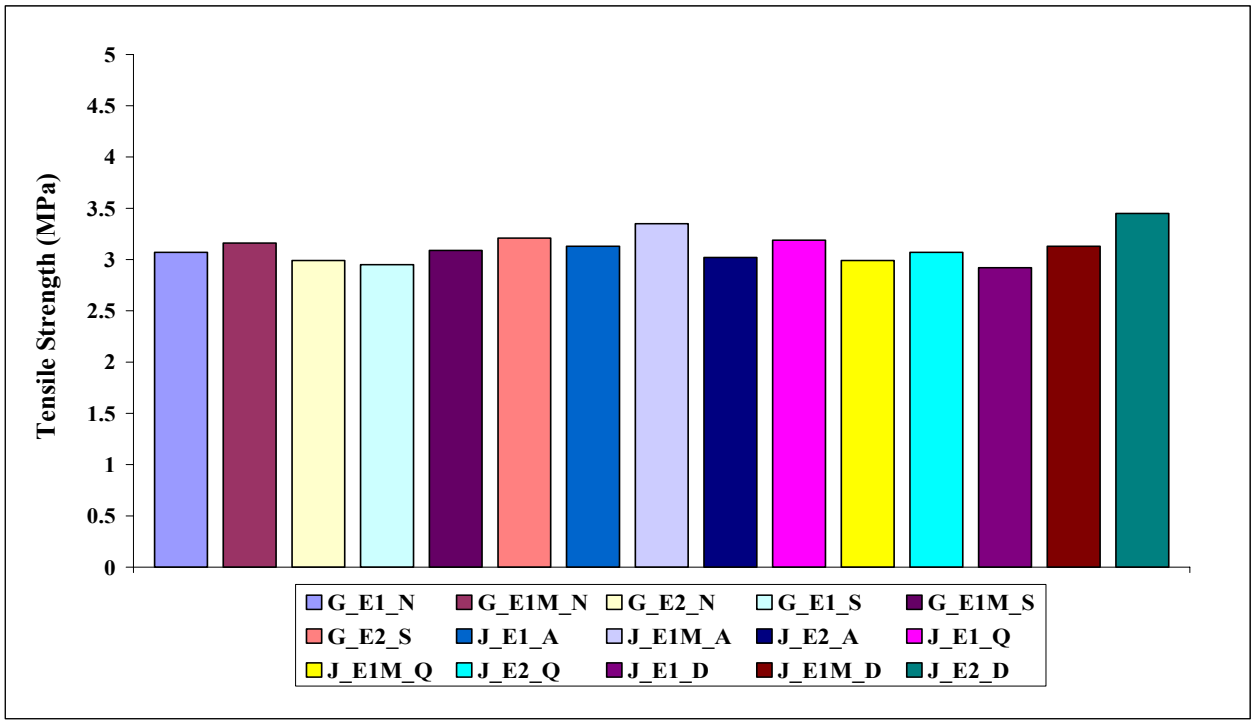

Figure 4.42: Average measured values for concrete tensile strength

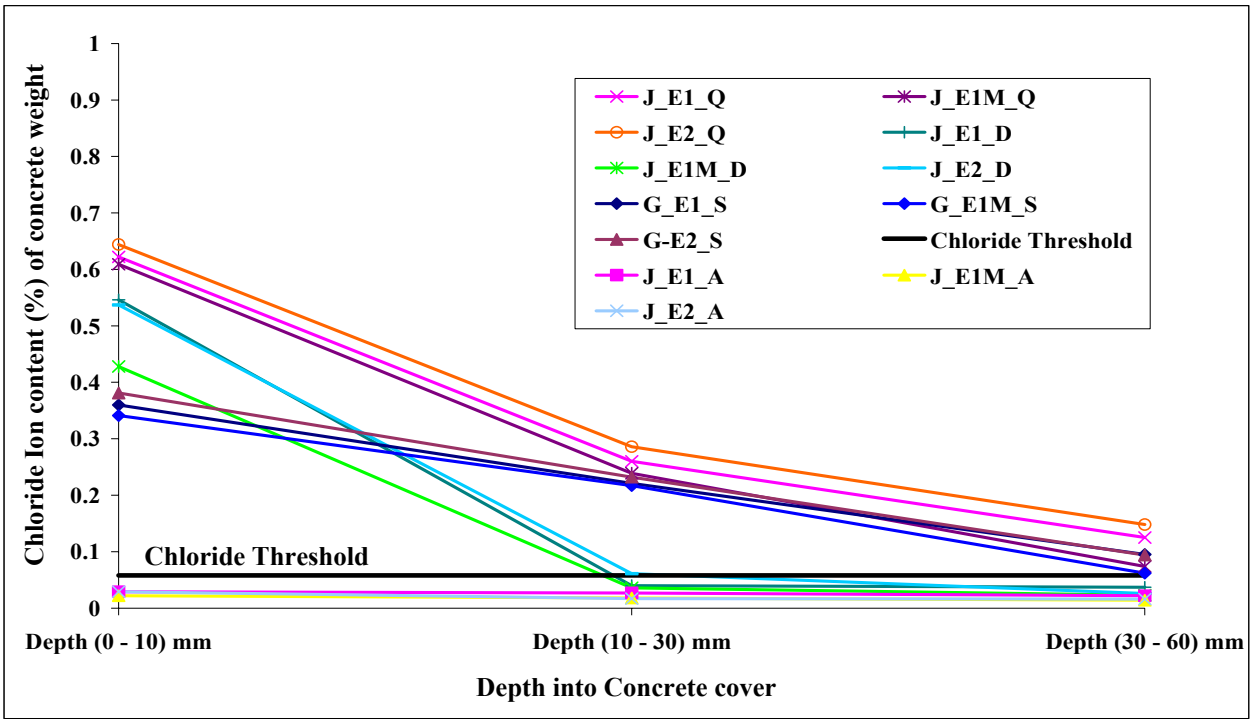

Figure 4.43: Total chloride contents in slab specimens

4.4. Test Results of Prism Specimens

4.4.1. Introduction

The obtained experimental results are discussed subsequently hereunder, in terms of the observed failure modes and ultimate failure loads, concrete tensile strengths and chloride ion concentration.

It's worthy to mention here that the nomenclature system used to designate the prism specimens is similar to the nomenclature system used to designate slab specimens, in addition to "TH" that refers for specimens that were stored in the humidity chamber at 50 °C temperature and 50 % humidity for almost one year after the application of the CFRP plates.

Prism specimens produced and stored at iBMB laboratories under normal laboratory conditions are considered the reference specimens.

4.4.2. Failure Modes and Ultimate Failure Loads

All specimens were in very good conditions after conditioning under all encountered environments. There were no signs of deterioration along the adhesive bond line or for the adherent materials, i.e. concrete and CFRP plates, as can be seen in Figure 4.44 for a typical representative specimen.

Generally, all tested specimens failed by the debonding of the CFRP plate as a whole from the concrete substrate. Debonding took place all at once in a brittle manner. By further inspection on the debonding interface after failure, two major failure planes were observed as will be explained hereunder.

For specimens that were preconditioned with salt solutions and exposed to Aqaba and Dead Sea environments, clean epoxy/concrete interface separation plane was observed with no concrete debris adhered to the debonded plate, as illustrated in Figure 4.45. This observation was consistent for all indoor specimens pretreated with salt solution under all encountered environments, and also for specimens exposed to outdoor severe environments. On the other hand, failure occurred within a few millimeters in the concrete cover, concrete shearing, for all prism specimens exposed to normal laboratory conditions and Amman environment, as can be seen in Figure 4.46.

These observations for the location of failure planes correlate very well with the observed locations of failure planes for slab specimens, as discussed earlier in section 4.3.2. It is important to state that, conditioned specimens were exposed to 9.6 % concentration NaCl solution for almost four months before the application of the CFRP plates.

Figure 4.44: Typical prism specimen before testing

Figure 4.45: Typical failure modes for salt solution pre-conditioned prism specimens

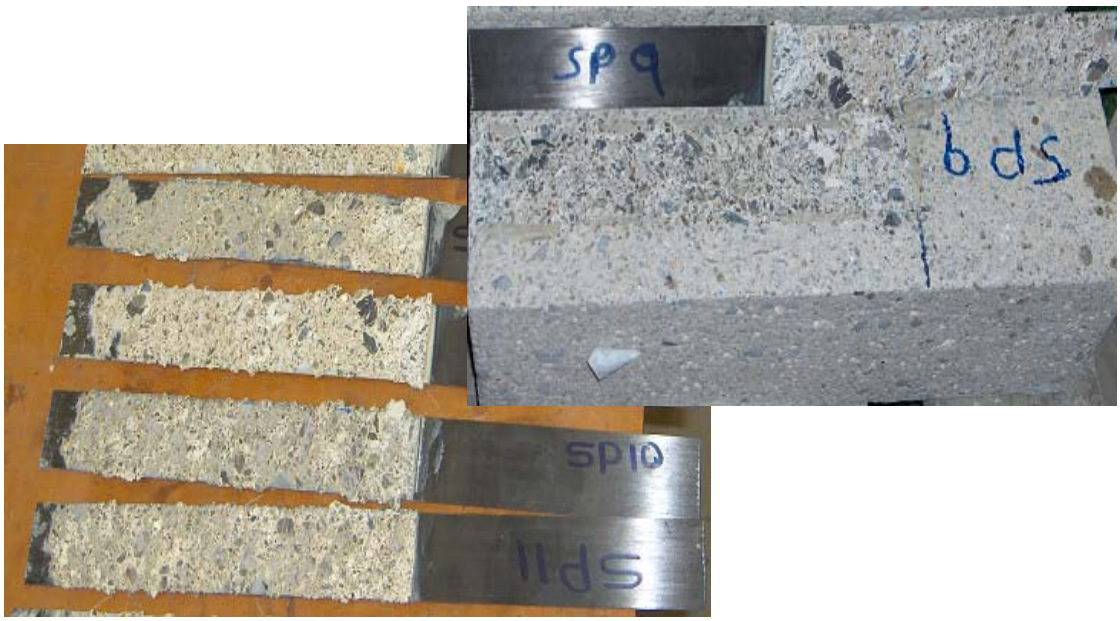

Figure 4.46: Typical failure modes for un-conditioned prism specimens

Average measured failure loads and concrete tensile strengths for all test specimens are shown in Figures 4.47 and 4.48, respectively.

The following observations may be drawn from the obtained test results.

- Measured failure loads for all prism specimens under all encountered environments were in the range of (19.93 – 31.97) kN, with the highest measured value for specimen J.E1M.Q and the lowest value is for G.E2.N. Whereas, the average values for tensile strengths were in the range of (2.91 – 4.46) MPa, with the highest value for specimen G.E2.Q and the lowest was for specimen G.E1M.D. There is direct relation between measured failure loads and concrete tensile strengths only for specimens exposed to normal laboratory conditions and Amman environment. On the other hand, for specimens exposed to severe environments indoor and outdoor, there is no direct relation between measured failure loads and concrete tensile strengths. For example, specimen J.E1M.Q that got the highest measured load of 31.97 kN has 3.95 MPa concrete tensile strength, when compared to specimen J.E2.Q that got the highest tensile strength of 4.46 MPa obtained 26.87 kN failure load. This observation is highly reinforced the previous observation obtained from testing slab specimens, i.e. is no direct relation between concrete tensile strength and bond strength for specimens exposed to severe environments.
- For the reference specimens that were exposed to normal laboratory conditions, the average failure loads were in the range of (19.93 – 22.3) kN. Specimen G.E1M.N has tensile strength of 3.11 MPa and got the highest failure load, followed by a failure load of 20.23 kN for specimen G.E1.N that got 3.05 MPa tensile strength. Whereas, specimen G.E2.N has the lowest failure load and 2.94 MPa tensile strength. Here we can see a direct relation between concrete tensile strength and failure loads. Also, this observation agrees very well with the results obtained from testing slab specimens, i.e. there is a direct relation between tensile strengths and failure loads.

- Measured failure loads fall in the range of (20.15 – 25.3) kN for specimens pre-conditioned with salt solutions and exposed to normal laboratory conditions. Maximum failure load was measured for specimen G.E1M.S.N that has 3.02 MPa tensile strength, followed by a value of 21.9 kN for specimen G.E1.S.N that has a tensile strength of 2.97 MPa, and the lowest failure load was measured for specimen G.E2S.N that got 3.24 MPa tensile strength. There is no direct relation between the attained failure loads and concrete tensile strengths.
- For specimens that were pre-conditioned with salt solutions and stored in the humidity chamber under 50 °C temperature and 50 % humidity, the average measured failure loads were 25.35 kN, 29.45 kN and 25.1 kN for specimens G.E1.S.TH, G.E1M.S.TH and G.E2.S.TH, respectively and their corresponding tensile strengths were 3.01 MPa, 2.95 MPa and 3.2 MPa, respectively. Also, here there is no direct relation between the attained failure loads and concrete tensile strengths.
- For specimens exposed to real-life environment prevailing at Amman, the measured failure loads were in the range of (20.85 – 24.43) kN. The highest measured load was recorded for specimen J.E1M.A that has 4.02 MPa, followed by a value of 21.5 kN for specimen J.E1.A that has 3.26 MPa tensile strength, and the lowest value was for specimen J.E2.A that has 3.08 MPa. Direct relation between concrete tensile strengths and failure loads is observed as these specimens are away from salt solutions.
- For specimens exposed to real-life environment prevailing at Aqaba region, the measured failure loads were in the range of (26.87 –31.97) kN. The highest measured load was recorded for specimen J.E1M.Q that has 3.95 MPa, followed by a failure load of 28.95 kN for specimen J.E1.Q that has 4.25 MPa, and the lowest value was for specimen J.E2.Q that has 4.46 MPa. There is no direct relation between concrete tensile strengths and the measured failure loads.
- The same trend is also observed for specimens exposed to Dead Sea region environment, but at a lower range being (20 – 23) kN. The highest recorded failure load was for specimen J.E1M.D that has 2.91 MPa tensile strength, followed by a failure load of 20.65 kN for specimen J.E1.D that has 3.27 MPa tensile strength, and specimen J.E2.D got the lowest failure load and has tensile strength of 3.04 MPa. Albeit the difference in the measured loads for J.E1.D and J.E2.D is insignificant. Indirect relation between tensile strength and the failure loads is also observed.
- There is no good agreement between the measured failure loads and the measured tensile strengths. Specimens that got higher failure loads for each group of specimens not necessarily to have the highest tensile strengths. This observation agrees very well with the previous observation obtained from correlating the failure loads of slab specimens with their respective tensile strengths.
- There is no reduction on the measured failure loads when specimen were exposed to indoor and outdoor severe conditions, on the contrary there is enhancement for the bond strength that could be attributed to beneficial post-curing for the adhesives and the concrete.
- As usual, specimens utilizing Type 1 Modified adhesive for bonding the CFRP plates got the highest failure loads for all exposure environments. Whereas, specimens utilizing Type 1 and Type 2 adhesives in bonding the CFRP plates have almost comparable performance.

Generally, from the test results obtained so far, there is no detrimental effect from exposure to severe environments. The only influence is the location of failure planes and the relation between failure loads and concrete tensile strengths.

4.4.3. Total Chloride Ion Content

Chloride profiles that represent the measured chloride contents at three different levels along the depth of the concrete cover of the tested specimens, namely: (0 -10) mm, (10 -30) mm and (30 -60) mm are illustrated in Figure 4.49. We should state that specimens exposed to Amman environment were considered the reference specimens.

The following observation can be drawn from the obtained test results.

- All curves as it should be showed an expected general trend of decreasing chloride contents with increased depths.
- Measured values for the reference specimens along depth of (0 – 60) mm in the concrete cover were in the range of (0.01 – 0.026) %. These values are well below the chloride threshold value being 0.058 % by concrete weight.
- Measured values of total chloride ion content at a level of (0 – 10) mm along the depth of the concrete cover for all test specimens were in the range of (0.31 – 0.61) % as compared to a range of (0.015 – 0.026) % for their counterpart reference specimens. The highest value was measured for specimen J.E2.Q, while the lowest value was for specimen G.E1M.S.TH.
- At level of (10 – 30) mm along the concrete cover, chloride ion contents for all specimens were in the range of (0.063 – 0.21) % as compared to a range of (0.01 – 0.015) % for the reference specimens. The highest measured value was also for specimen J.E2.Q and the lowest value was for specimen J.E1M.D. All values are well above the chloride threshold except for specimen J.E1M.D.
- All measured chloride contents were in the range of (0.013 – 0.049) % at depth level of (30 – 60) mm in the concrete cover. These chloride contents were higher than the obtained values for the reference specimens being in the level of (0.01 – 0.012) % and lower than the chloride threshold value.
- Specimens exposed to real-life environment at Aqaba region got the highest amount of chlorides, followed by specimens exposed to real-life environment at the Dead Sea. Whereas, specimens exposed to salt solutions and stored at normal laboratory conditions and at the humidity chamber got comparatively the same amounts of chlorides. The possible reason for this observation is that specimens stored at the Aqaba and Dead Sea regions were exposed to chlorides for longer period, being 12 months compared to a preconditioned period of 4 months for indoor specimens. Aqaba specimens got higher chloride values than those exposed to Dead Sea environment as we said earlier in section 4.3.8. Aqaba specimens were stored at the tidal zone, whereas Dead Sea region specimens were stored at the atmospheric zone.

Generally, for every specific environment the lowest values for chloride contents were measured for specimens using Type 1 Modified adhesive for bonding the CFRP plates and at the three considered levels along the depth of the concrete cover, followed by Type 1 and Type 2, respectively. This result correlates very well with the predicted values of diffusion rates for the bulk materials.

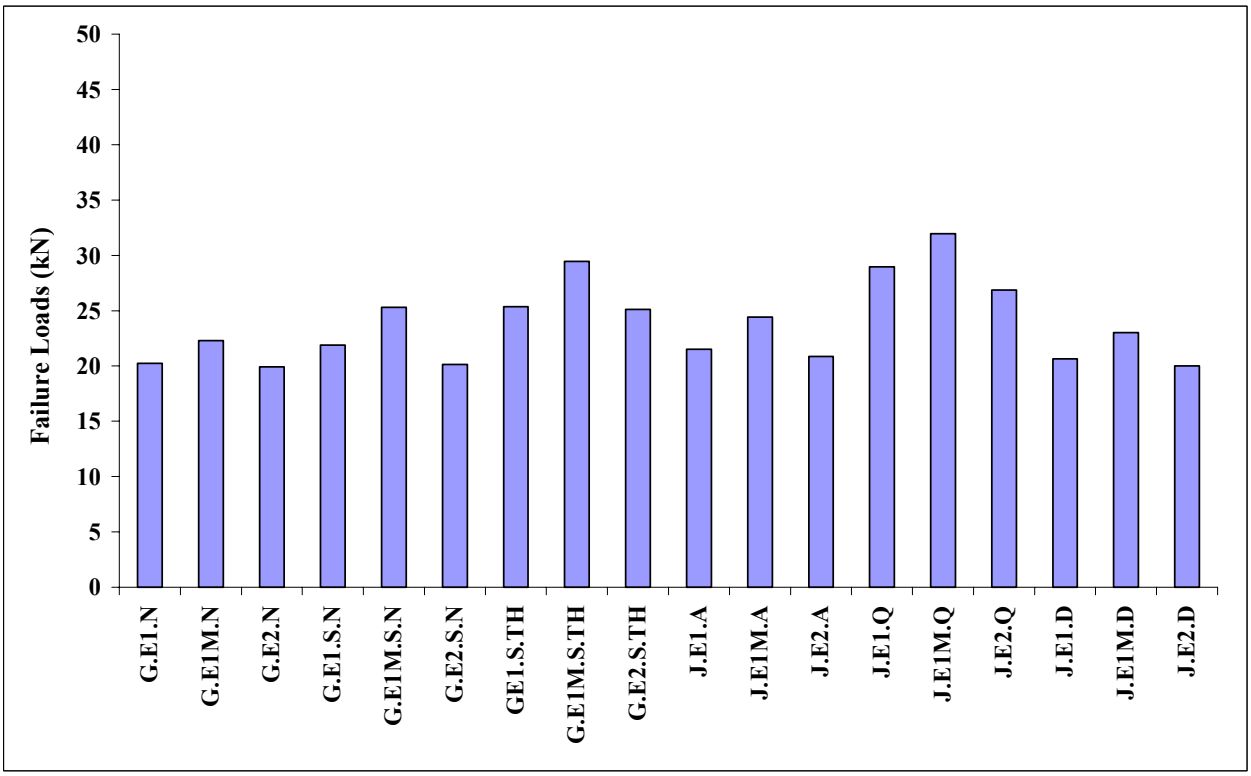

Figure 4.47: Average measured failure loads

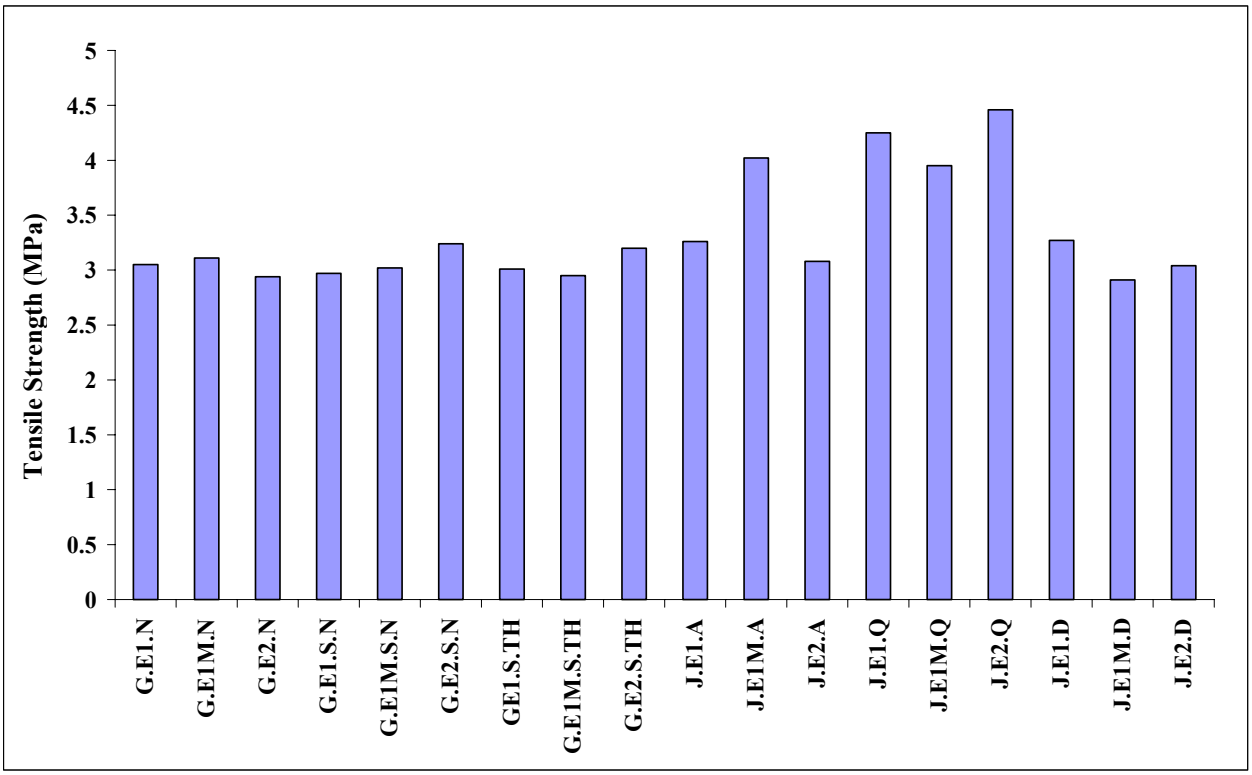

Figure 4.48: Tensile Strengths for all specimens

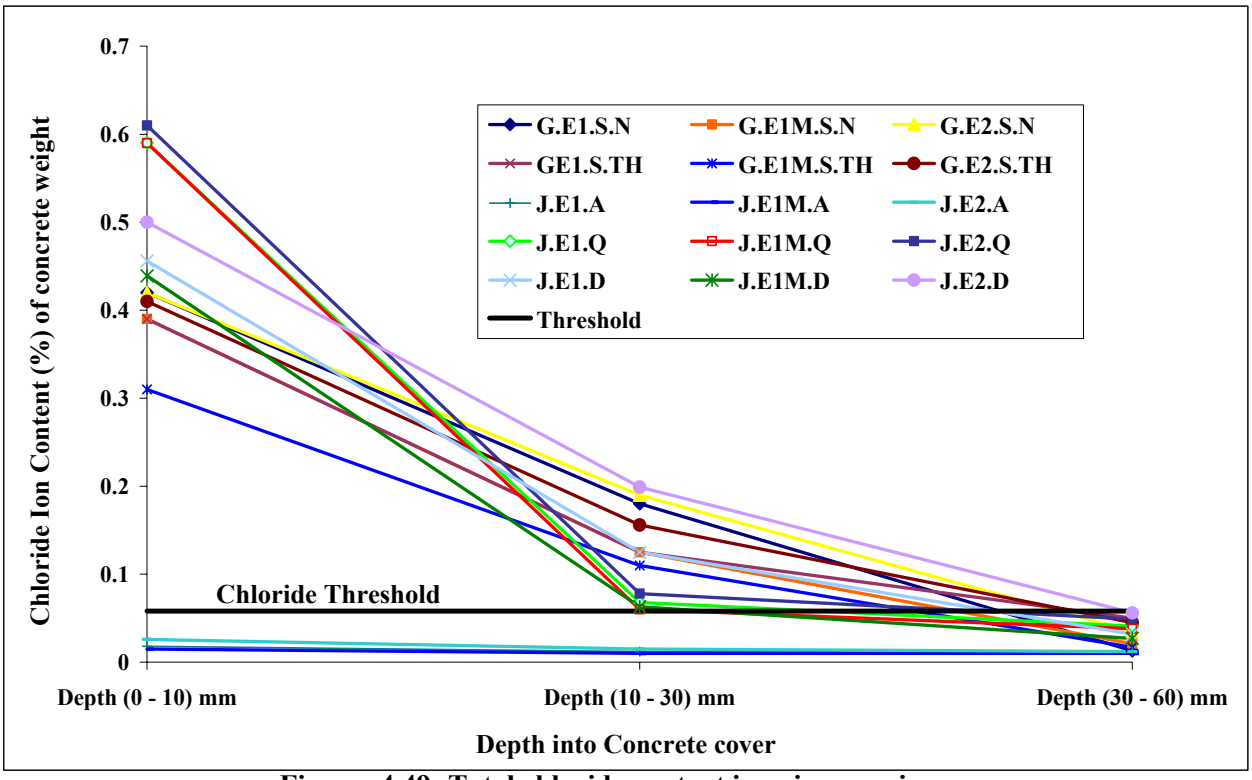

Figure: 4.49: Total chloride content in prism specimens

4.5. Summary of Test Results

To achieve the research objectives, an intensive experimental program was conducted to evaluate the effect of indoor and outdoor severe environments on the durability performance of CFRP composite retrofitted systems.

The work included studying the effect of moisture, water, chloride and alkaline solutions at two different conditioning temperatures, 23 ºC and 50 ºC, on the mechanical properties of the polymeric bulk materials, CFRP plates and three different types of structural adhesives. The effect of UV - 250 and UV - 500 ultra-violet radiations on the mechanical properties of CFRP composites was also studied.

Furthermore, the effect of severe environments on the adhesive bond was evaluated through flexural and shear tests performed on concrete specimens after one year of exposure to different environments.

The following results were achieved.

1. CFRP Plates

- No detrimental effects were observed on the mechanical properties of the chosen type of CFRP plates when exposed to moisture, water and salt solutions at both conditioning temperatures, 23 ºC and 50 ºC. On the contrary enhancement on the mechanical properties was observed when exposed to the previous mentioned environments particularly when associated with high temperatures. This result was attributed to post curing of the polymer matrix that binding the carbon fibers.

- Insignificant reduction on the measured mechanical properties when exposed to alkaline solutions and 250- UV ultra violet radiation. Whereas, exposure to 500 – UV ultraviolet radiation has enhanced the mechanical properties.
- Reduction on mechanical properties is well below the stringent limits set by design codes.
- The chosen type of CFRP plates proofs to be adequate for application in severe environments.

2. Structural Adhesives

- Temperature has enormous consequences on the mechanical properties of epoxy materials. Exposure to moisture combined with high temperature at longer duration enhances the mechanical properties as a result of post-curing that can conquer any contribution that will occur from moisture-induced degradation.
- On the contrary, exposure to water and chemical solutions combined with high temperatures has serious consequences on the mechanical properties of all selected adhesive types. One of the tested adhesives lost more than 85 % of its tensile strength, and showed viscous behaviour with very low modulus of elasticity, with loss more than 95 %.
- Exposure to alkaline solutions had a significant effect on adhesives. All studied types of adhesives had lost most of their mechanical properties when exposed to alkaline solutions, which was aggravated when combined with high temperature and ageing.
- Salt solutions had also an adverse effect on the chemical and mechanical properties of studied adhesives, but to a lesser extent if compared with the effect of alkalines. Also, if salt solutions are combined with high temperatures and ageing, the reduction in adhesives mechanical properties is escalated. Also, water had a substantial effect on the mechanical properties particularly if associated with high temperature
- Test results revealed that Type 1 Modified showed the best performance among the selected types of adhesives, albeit it has the lowest initial mechanical properties. Followed by Type 1 and Type 2, respectively. Sometimes comparable performance was observed for both Type 1 and Type 2 adhesives.

3. Flexural and Shear tests

- Bonding of CFRP plates at the soffit of intentionally cracked RC slab specimens has potentially increased the capacity to acceptable limits even under the most severe environments.
- All tested slab specimens failed suddenly in a brittle debonding mode.
- Relatively high chloride contents were measured under the CFRP plates for all specimens exposed to salt solutions and real-life severe environments, particularly at the first 30 mm depth along the depth of the concrete cover.
- The severity of degradation of the mechanical properties of the adhesives when exposed to severe environments was not reflected in the obtained results. There is no much difference in the measured failure loads for all test specimens, being in the average of 100 kN. Albeit, some specimens that were exposed to severe environments attained 10 % higher or lower loads than the reference specimens, depending on the adhesive type.

- The only reasonable difference between specimens exposed to normal laboratory conditions and those exposed to severe environments is the failure mode. Delamination at the top of the concrete layer for specimens exposed to normal laboratory conditions and separation along the adhesive/concrete interface for specimens exposed to salt solutions and severe environments.
- For specimens exposed to normal laboratory conditions, there is a direct relation between the tensile strength of concrete and the obtained failure loads. Whereas, no dependency from concrete strength was observed for specimens exposed to salt solutions and severe environments.
- Viscous adhesives with initially low elastic modulus and strength performed better than stiff adhesives with initially high mechanical properties.
- Not much difference in the measured values of deflections and strains under all encountered environments. The usable strains at failure for all specimens were less than 30 % of the CFRP composites ultimate strains. These results applied only for flexural tests.
- It was concluded that there was no detrimental effect from exposure to salt solution and severe environments either indoor or outdoor.

5. Interpretation of Test Results

5.1. General

Test results and discussion in the previous chapter illustrates the significance and importance of the early debonding failures of the slab specimens. The efficiency of the retrofitted concrete slabs was degraded to approximately 70 % of the theoretical expected capacity. Only about 30 % of the initial strain of the CFRP plates was utilized, this implies that the CFRP plates were used inefficiently and debonding should be mitigated for cost-effective retrofitting.

Early debonding failures and almost the similar relative performance for all tested slabs made the identification of the environmental effects on the retrofitted systems difficult and challenging. Although most of the slabs failed at about 100 kN and got almost comparable values of strains and deflections, there was a difference in the failure planes. The failure planes for specimens exposed to normal laboratory conditions were at the top of the concrete layer, whereas the failure planes were at the adhesive/concrete interface for specimens exposed to severe environments.

Consequently, to provide a more insight about the effects of severe environments on the CFRP retrofitted systems particularly on the adhesive bond; shear, normal and peeling stresses along the adhesive bond were evaluated by using linear elastic analysis. A similar approach to Roberts' model [83], was developed and implemented.

On the other hand, unexpected performance for the prism specimens which have been tested under direct shear tests notwithstanding the severity of exposure conditions. Most of the specimens exposed to severe environment got much higher failure loads than their corresponding specimens exposed to normal conditions, with the highest loads for specimens preconditioned with salt solutions and exposed to 50 % moisture associated with 50 ºC temperature and those exposed to Aqaba environment for almost one year. This enhancement on failure loads was attributed to beneficial post-curing for the concrete. Fracture energies were predicted for all specimens and used to characterize the effects of environmental conditions on the CFRP/concrete interface.

5.2. Interpretation of Test Results of Slab Specimens

Many researchers have done significant work on the premature failure of steel/FRP plates strengthened beams and developed the corresponding failure criteria for predicting failure load. The most common formula is that from Holzenkämpfer [6] as referenced by Teng et al. [25], which has been modified in different occasions afterwards by Täljsten [78], Neubauer and Rostásy [79], and Teng et al. [25].

Most of the derivations of the Holzenkämpfer [6] model, which was basically formulated for evaluating the maximum shear stresses for steel bonding by using fracture mechanics, neglect the effect of adhesive mechanical properties by assuming constant performance of the adhesive layer and related the failure load to concrete strength, Täljsten [78] and Neubauer and Rostásy [79]. The model developed by Neubauer and Rostásy [79] has been adopted by the FIB [1] and CSTR [26] in their design guidance for strengthening concrete structures using fiber composite materials.

Täljsten [78] used the linear elastic theory to derive shear and peeling stresses at the externally reinforced plate. Roberts [83] stated that "the shear and normal stresses in and adjacent to the adhesive layer can be reduced significantly by using a more flexible adhesive, reducing the thickness of the plate, and for a

simply supported system, by terminating the plate as close to the support as possible". Arduini [47] simulated and predicted the failure mode of FRP strengthened beams by taking into account the influence of concrete confinement in the compression zone due to the presence of the stirrups, and the tensile softening properties of concrete. Until now, a nonlinear closed-form formula has not yet been derived for FRP strengthened flexural structures.

Teng et al. [25] reviewed several existing models for plate debonding in FRP strengthened RC beams using available test data and identified most of the models developed for steel plated beams to be the more accurate ones, while those specially developed for FRP plated beams give poorer predictions.

Roberts' analytical model will be implemented to predict the shear and normal stresses along the adhesive bond, Roberts [83]. The choice of this model was based on the fact that, it is the only available model that takes into account the mechanical properties and dimensions of the adhesive layer. Other existing models assume constant performance for the adhesive.

Roberts' model is based on partial interaction theory to predict the shear and normal stress concentrations in adhesive joints for steel plates, Roberts [83]. His analytical model was developed in three stages. During the first stage, stresses were determined assuming full composite action between the reinforced concrete beam and the adhesive bonded steel plate. During the second and third stages, the analysis was modified to take into account the actual boundary conditions at the ends of the steel plate. The complete solution was then obtained by superposition. Roberts found that the shear and normal stress concentrations in the adhesive layer depend significantly on the shear and normal stiffness of the adhesive and on the thickness of the steel plate.

Robert's model could be used to predict the shear and normal stresses at the crack location by predicting the values of shear force and bending moment at each crack location, and considering the employment of CFRP plate instead of steel plate, the modified model will be as shown hereunder.

$$\tau_{\max} = \left(V_0 + \left\{ \frac{K_s}{E_f b_f t_f} \right\}^{1/2} M_0 \right) \frac{b_f t_f}{I_{fr} b_a} \left(\overline{Y} \right) \tag{5.1}$$

$$\sigma_{\max} = \tau_{\max} t_f \left(\frac{K_n}{4 E_f I_f} \right)^{1/4} \tag{5.2}$$

$$K_s = G_a \frac{b_a}{t_a}, \qquad K_n = E_a \frac{b_a}{t_a} \tag{5.3}$$

where:

V_0: shear force acting on the crack location

M_0: bending moment acting at the crack location

K_s: shear stiffness per unit length of adhesive

K_n: normal stiffness per unit length of adhesive

t_f: thickness of the CFRP plate

t_a: thickness of the adhesive layer

b_f : width of CFRP plate

b_a : width of adhesive

G_a : shear modulus of elasticity of the adhesive layer

E_f : elastic modulus of laminate plate

E_a : elastic modulus of adhesive

I_f : moment of inertia of FRP plate

I_{fr} : moment of inertia transformed section based on FRP plate

$\bar{Y}$: distance from neutral axis of the strengthened section to center of FRP plate

5.2.1. Analytical Approach

At the crack location, the concrete slab undergoes biaxial stresses as shown in Figure 5.1. In this case, three components of stresses are present: σ_x, calculated from flexural analysis; σ_y and τ_{xy}, peeling and shear stresses, respectively, are calculated based on analytical models.

A simple calculation procedure was implemented to calculate the stresses at the adhesive bond between concrete and CFRP plate. The obtained stresses were used to predict the principal peeling stress, σ_p, which is calculated using stress transformation relation under plane stress condition, as shown in equation 5.4. The failure is assumed to begin when the principal stress, σ_p is equal to the concrete strength under the biaxial state of stresses.

$$\sigma_p = \frac{\sigma_x + \sigma_y}{2} + \sqrt{\left(\frac{\sigma_x - \sigma_y}{2}\right)^2 + \tau^2} \qquad 5.4$$

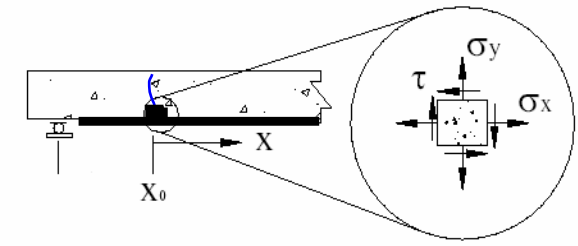

Figure 5.1: Stress acting at the adhesive-concrete interface

The geometric and material properties used to calculate the analytical shear and normal stresses along the CFRP plate for all slabs are shown in Figures 5.2 and 5.3, and Table 5.1.

The detailed procedure to determine the distribution of the shear and normal stresses in the adhesive layer, along slab G_E2_N, is shown in Appendix C.

The following stresses were found along the adhesive joint for specimen G_E2_N;

$\sigma_y = \sigma(x) = 4.46 \quad N/mm^2$

$$\sigma_x = \frac{M_0.(h_c - h)}{I_c} \Rightarrow \sigma_x = 15 \quad N/mm^2$$

$$\tau = \tau(x) = 8.3 \quad N/mm^2$$

$$\sigma_p = \frac{\sigma_x + \sigma_y}{2} + \sqrt{\left(\frac{\sigma_x - \sigma_y}{2}\right)^2 + \tau^2} \quad \Rightarrow \quad \sigma_p = 19.56 \quad N/mm^2$$

Measured tensile strength, $f_t = 2.99 N/mm^2$

Since $\sigma_p > f_t$, delamination will surely occur.

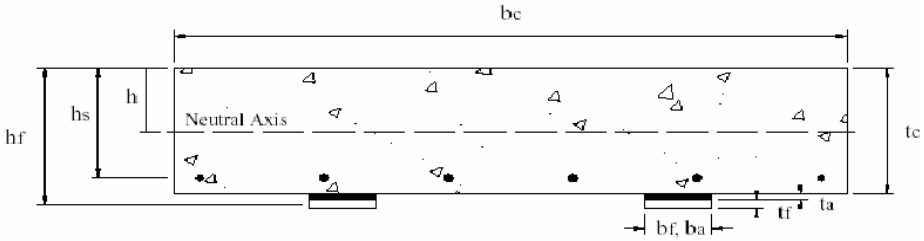

Figure 5.2: Cross section of slab specimens

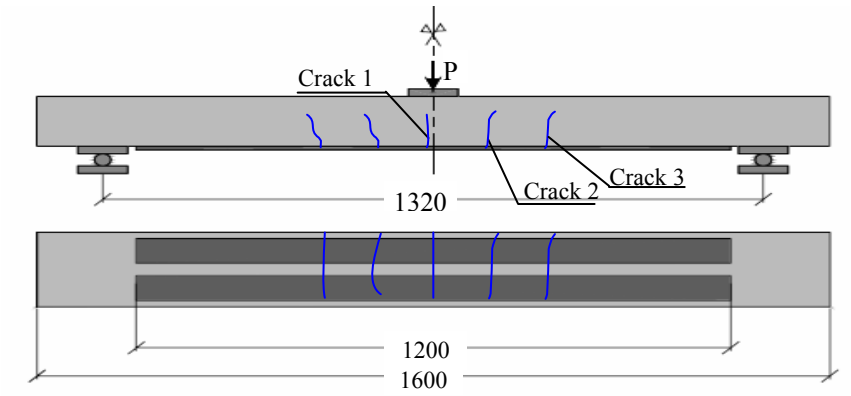

Figure 5.3: General view of the test setup and crack pattern

Table 5.1: Dimensions and material properties

Material	Width (mm)	Thickness (mm)	Height (mm)	Elastic Modulus (N/mm^2)	Shear* Modulus (N/mm^2)	Area (mm2)
Concrete	b_c: 500	t_c: 120	-	27000		
CFRP	b_f: 50	t_f: 1.47	h_f: 121	167500		147
Epoxy Type 1	b_a: 50	t_a: 3	-	7905	2927.8	
Epoxy Type1 Modified	b_a: 50	t_a: 3	-	5716	2117	
Epoxy Type2	b_a: 50	t_a: 3	-	8995	3331.5	
Steel	-		h_s: 90	210000		393

Epoxy poisonous ratio, $\nu = 0.35$; Shear modulus, $G = \frac{1}{2(1+\nu)}$

5.2.2. Results

The predicted values for shear, normal and peeling stresses for all specimens at crack locations 2 and 3 are shown in Tables 5.2 and 5.3, respectively.

The following observations could be drawn from the predicted stress values.

- High peeling stresses at the crack locations 2 and 3 were observed, with higher values at crack location 2 as it is closer to midspan. Predicted peeling stresses at crack 2 are in the range of (22 – 25.42) MPa, and in the range of (17.2 – 19.96) MPa at crack 3. For all cases the lowest values were for specimen J_E2_D and the highest were for specimen G_E1M_S. This observation agrees very well with measured failure loads, as specimen J_E2_D got the lowest failure loads and specimen G_E1M_S got the highest load. Regardless of adhesive types, the lowest values were for specimens exposed to the Dead Sea environment.
- Predicted peeling stresses are much higher than the measured concrete tensile strengths by pull-off tests for all tested specimens. This implies that the CFRP plates should peeled out from the concrete substrate and the failure plane should be somewhere along the concrete layer, since it is the weakest component in the bonded joints. On average, concrete tensile strengths constitute only about 12 % - 20 % of the tensile strengths of the adjoined adhesives, as can be seen in Tables 5.2 and 5.3. This fact was not fulfilled upon a closer examination of the location of the failure planes for specimens exposed to normal conditions and those exposed to severe environments. Regardless of adhesive systems used, there was a shift in the location of failure planes and two different locations could be distinguished; the first was concrete shearing at the top of the concrete layer for specimens exposed to normal conditions and the other was separation along the adhesive/concrete interface for specimens exposed to indoor and outdoor severe environments. Consideration of these two failure planes has led to the thinking of a possible degradation to the adhesive bond to the extent that its strength was no longer greater than the tensile strength of the concrete, so the bond strength controlled the results. But, this degradation assumption was not reflected in the measured failure loads, as they were comparable to each other. This implies that, the adhesive if degraded is still able to transmit stresses between the adherents and maintain the integrity of the retrofitted system.
- Assuming roughly that the adhesive strength of specimens exposed to severe environments has the same magnitude as the corresponding concrete; on average the reduction in adhesive strength could be estimated to be approximately in the range of (79 – 88) % depending on adhesive type. A reduction of about 88 % for Type 1, 79 % for Type 1 Modified and about 87 % for Type 2. This observation correlates very well with the results obtained from testing the neat adhesive materials as discussed earlier in section 4.2.2.2. Even if the adhesives had lost high percentages of their mechanical properties, but it is assumed that their strengths will not fall down below these levels. This assumption is in view with the fact that the adhesives should be fully saturated after one year of exposure. It was shown earlier in section 4.2.2.3 that the adhesives will be saturated in 56 days, and there was no noticeable deterioration after that age. Hence, it could be concluded that the degradation of the adhesive bond will not continue to fall further below the percentages shown above.
- By further inspection of the failure planes of the tested specimens which were exposed to severe environments, it was clear that the failure occurred along the adhesive/concrete interface and not in the adhesive material, i.e. the failure is adhesive failure and is not cohesive failure. This means that the material itself did not deteriorate greatly as it is still intact at the CFRP plate interface and could transmit stresses between the plate and concrete substrate, but the mechanical interlocking between

the adhesive and the concrete substrate has been degraded. This observation was rather reinforced by distinguishing a very thin shiny layer at the fractured planes directly after debonding failure, for both opposite surfaces of concrete and adhesive. Fractured surfaces for different specimens were further studied using X-Ray Fluorescence for element analysis, e.g. chloride ions. The study resulted in the existence of high amount of chlorides and some salts at the fracture surface. Accordingly, a possible explanation for the failure at the adhesive/concrete interface could be attributed to the existence of salt accumulation at the top concrete surface, taking into consideration that the test specimens were exposed to severe environments for about 4 months before the application of the CFRP plates. Although, the concrete surfaces were well prepared by mechanical abrasion of the top surfaces before the application of the plates, but this will not surely prevent the existence of salt accumulations that was increased by the long-term exposure to severe environments. Also, this result was further confirmed with the high chloride contents at the top concrete surfaces, particularly at the first 10 mm depth from the concrete cover, as outlined in section 4.3.8. This argument does not deny the existence of deterioration for the adhesive layer, in particular at the adhesive/concrete interface.

- When considering the shear stresses along the adhesive bonds, it is clear that Type 1 Modified adhesive always got the lowest stresses when compared to other types under all environments. This observation could be attributed to the flexibility and ductility of this type of adhesives as it has the lowest shear modulus. A more flexible adhesive layer will allow shear deformation of the adhesive to occur under the applied forces. This will let the plate to "slip" slightly in relation to the slab, which allows for better distributing stresses along the bond and results in improved FRP efficiency. The Task Group on Bond [101], newly reported that bond layer with a lower elastic shear modulus , G_a , but with good ductility and strength higher than that for concrete substrate could lead to higher interface bond strengths.
- Comparatively peeling stresses for all specimens utilizing Type 1 Modified are lower as compared to their corresponding specimens under the same exposure but utilizing other types of adhesives. And if considering the higher failure loads measured for specimens utilizing this type of adhesive discussed earlier in section 4.3.3., it could be concluded that the mechanical properties for Type 1 Modified adhesive are more retained as compared to other types, so it can withstand higher forces. This implies that softer adhesives with lower shear modulus could perform better than stiff adhesives with higher shear modulus under severe environments.

Table 5.2: Predicted stresses in the adhesive bond at crack 2 for all tested specimens

Specimen No.	Shear Stress (τ_x,Mpa)	Horizontal Principal Stresses (σ_x, Mpa)	Vertical Principal Stresses (σ_y, MPa)	Principle Peeling Sresses (σ_p, MPa)	Concrete Tensile Strength (Mpa)	Adhesive Tensile Strength (Mpa)
G_E1_N	10.43	18.92	5.48	24.61	3.07	25.13
G_E1M_N	8.94	18.96	4.34	23.20	3.16	14.87
G_E2_N	11.07	18.87	6.00	25.24	2.99	25.17
G_E1_S	10.44	18.93	5.48	24.62	2.95	25.13
G_E1M_S	9.80	20.77	4.75	24.42	3.09	14.87
G_E2_S	11.06	18.84	5.99	25.20	3.11	25.17
J_E1_A	10.39	18.85	5.46	24.52	3.13	25.13
J_E1M_A	8.90	18.87	4.32	23.09	3.35	14.87
J_E2_A	11.04	18.80	5.98	25.16	3.02	25.17
J_E1_Q	10.36	18.79	5.44	24.43	3.19	25.13
J_E1M_Q	8.89	18.84	4.3	23.05	2.99	14.87
J_E2_Q	10.10	18.74	5.96	25.07	3.07	25.17
J_E1_D	9.78	16.66	5.30	22.29	2.92	25.13
J_E1M_D	8.58	18.18	4.16	22.25	3.13	14.87
J_E2_D	9.28	16.83	4.87	21.89	3.45	25.17

Table 5.3: Predicted stresses in the adhesive bond at crack 3 for all tested specimens

Specimen No.	Shear Stress (τ_x,Mpa)	Horizontal Principal Stresses	Vertical Principal Stresses	Principle Peeling Sresses	Concrete Tensile Strength	Adhesive Tensile Strength
G_E1_N	8.24	14.81	4.327	19.30	3.07	25.13
G_E1M_N	7.07	14.84	3.437	18.20	3.16	14.87
G_E2_N	8.74	14.77	4.74	19.8	2.99	25.17
G_E1_S	8.24	14.81	4.33	19.30	2.95	25.13
G_E1M_S	7.75	16.26	3.76	19.1	3.09	14.87
G_E2_S	8.73	14.74	4.73	19.80	3.11	25.17
J_E1_A	8.21	14.75	4.31	19.26	3.13	25.13
J_E1M_A	7.04	14.77	3.42	18.14	3.35	14.87
J_E2_A	8.71	14.72	4.72	19.76	3.02	25.17
J_E1_Q	8.18	14.70	4.30	19.20	3.19	25.13
J_E1M_Q	7.03	14.74	3.41	18.10	2.99	14.87
J_E2_Q	8.68	14.66	4.70	19.69	3.07	25.17
J_E1_D	7.72	13.04	4.18	17.5	2.92	25.13
J_E1M_D	6.78	14.22	3.29	17.47	3.13	14.87
J_E2_D	7.33	13.17	3.85	17.2	3.45	25.17

5.3. Interpretation of Test Results of Prism Specimens

The performance of the prism specimens will be evaluated according to their interface fracture energy. It was pointed out earlier in section 5.2, that a number of researchers have developed models for the evaluation of the failure loads of retrofitted systems. The model shown in equation 5.5, which was developed by Brosens [7], Täljsten, [78] and Neubauer and Rostásy [79] after conducting single and double lap shear tests will be adopted to predict the fracture energy for the tested specimens.

$$P_{\max} = b_f \sqrt{2G_f E_f t_f}\, \tanh(\Omega^* L_f) \qquad 5.5$$

The above model is based on relating the fracture energy, and the mechanical and dimensional properties of the CFRP plates, where

b_f : width of FRP plate

G_f : fracture energy per unit area of the joint (N/mm)

E_f : elastic modulus of CFRP plate

t_f : thickness of plate

Ω^* : constant defined in the simplified linear approach to solve the differential equation governing plate tensile stresses, and is given by $\Omega^* = \sqrt{\frac{1}{E_p t_p}\frac{G_a}{t_a}}$

L_f : bonded length of the plate

Using the above model and experimental results of all tested specimens, the fracture energy for each bond specimen is calculated and outlined in Table 5.4, along with the measured tensile strengths and the adhesives shear moduli for easier comparison.

5.3.1. Results

The following observations could be drawn from studying Table 5.4.

- The obtained interfacial fracture energies were in the range of (0.32 – 0.83) N/mm with higher values for specimens exposed to severe environments. These values are of key importance in bond characterization and should therefore be compared and contrasted to related fracture parameters in the literature. For example, Karbhari et al. [9] reported values for interface fracture energy in the range of (0.45 – 3.5) N/mm based on pull-off tests of unconditioned and conditioned FRP bonded to concrete substrate, with higher values for conditioned specimens. Also, Savoia et al. [101] obtained interfacial fracture energies of about 1.5 N/mm based on single-lap shear tests of unconditioned CFRP plates bonded to concrete blocks and 2.2 N/mm for conditioned specimens. It is clear that the fracture energies obtained in this investigation are less than the fracture energy values reported in the literature. This discrepancy can be caused by different methods of computation of the interfacial fracture energy. Nevertheless, the obtained values of fracture energy agrees with those in the literature in that higher values of interfacial fracture energy are for conditioned specimens compared to their corresponding unconditioned specimens. Furthermore, in a comparative study by Zhao [102]

the author found a range of fracture energies of (0.21 – 0.78) N/mm, which is comparable to the range attained in this study.

- The highest values of fracture energy are for specimens exposed to Aqaba environment being in the range of (0.58 – 0.83) N/mm. The highest value was for specimen J.E1M.Q, followed by a value of 0.68 for specimen J.E1.Q and the lowest value was for specimen J.E2.Q. These high values of fracture energies are attributed to the enhancement of concrete strength due to beneficial post curing as these specimens were stored at the tidal zone of the Red Sea of Aqaba for almost one year.
- Almost comparative values of interface fracture energies is observed for specimens exposed to normal laboratory conditions, Amman environment and Dead Sea region; a range of (0.32 – 0.4) N/mm was found for specimens exposed to normal conditions compared to a range of (0.35 – 0.48) % for specimens exposed to Amman environment and a range of (0.32 – 0.43) N/mm for specimens exposed to Dead Sea environment. Highest values were observed for specimens utilizing Type 1M, followed by specimens utilizing Type 1 and Type 2, respectively.
- A range of (0.51 – 0.70) N/mm fracture energy is observed for specimens exposed to 50 % humidity and 50 ºC temperature for almost one year, after preconditioning with salt solution, the highest value was for G.E1M.S.TH, followed by a value of 0.52 N/mm for specimen G.E1.S.TH, and the lowest was for G.E2.S.TH.
- Upon a closer examination for the predicted values of fracture energies, it is obvious that the specimens that were conditioned in salt solution and those exposed to humidity and sea water attained higher values. A possible explanation for higher fracture energies for specimens exposed to severe environments is that, exposure to moisture enhances concrete strength due to post-curing, in addition to the post-curing of the adhesive bond caused by high temperatures, assuming service temperatures are below the glass transition temperature for each adhesive, and consequently the failure will occur at higher loads.
- For every single environment, specimens using Type 1 Modified got the highest values as compared to the other types, followed by specimens using Type 1 and specimens using Type 2, respectively.

It is usually assumed in the literature that the fracture energy increases with increased tensile strength of the concrete. In this investigation, the fracture energy increased with increased tensile strength only for specimens exposed to normal laboratory conditions and Amman environment. But for specimens exposed to severe environments, there is no direct relation between the measured concrete tensile strength and the predicted fracture energies, as shown in Figure 5.4. The direct relation is not satisfied because the failure was controlled by the adhesive and not the concrete, as the failure plane was along the adhesive/concrete interface. Other researchers reach such results in the literature, that there is no direct relation between the concrete tensile strength and the fracture energy when specimens are exposed to severe environments, Zhao [102] and Lorenzis et al. [103]. The researchers concluded that, “the concrete strength did not seem to affect the bond strength”. Also, they reported that adhesives with moderate shear modulus have better performance and rendered higher fracture energy than stiff adhesives with higher shear modulus.

In this investigation it is clear that for different fracture paths within a CFRP concrete bond, fracture energy, G_f, has different expressions; fracture energy is a function of concrete strength if the fracture path is within concrete, and if the fracture occurs in the interface and no concrete sheared off from the substrate, the fracture energy could be related to the specific epoxy used.

Table 5.4: Comparison of bond properties with different exposure conditions

Specimen No.	Concrete Tensile Strength (MPa)	Adhesive Shear Modulus (Mpa)	Failure Load (kN)	Fracture Energy (N/mm)
G.E1.N	3.05	2927.8	20.23	0.33
G.E1M.N	3.11	2117	22.3	0.40
G.E2.N	2.94	3331.5	19.93	0.32
G.E1.S.N	2.97	2927.8	21.9	0.39
G.E1M.S.N	3.02	2117	25.3	0.52
G.E2.S.N	3.24	3331.5	20.15	0.33
GE1.S.TH	3.01	2927.8	25.35	0.52
G.E1M.S.TH	2.95	2117	29.45	0.70
G.E2.S.TH	3.2	3331.5	25.1	0.51
J.E1.A	3.26	2927.8	21.5	0.38
J.E1M.A	4.02	2117	24.43	0.48
J.E2.A	3.08	3331.5	20.85	0.35
J.E1.Q	4.25	2927.8	28.95	0.68
J.E1M.Q	3.95	2117	31.97	0.83
J.E2.Q	4.46	3331.5	26.87	0.59
J.E1.D	3.27	2927.8	20.65	0.35
J.E1M.D	2.91	2117	23	0.43
J.E2.D	3.04	3331.5	20	0.32

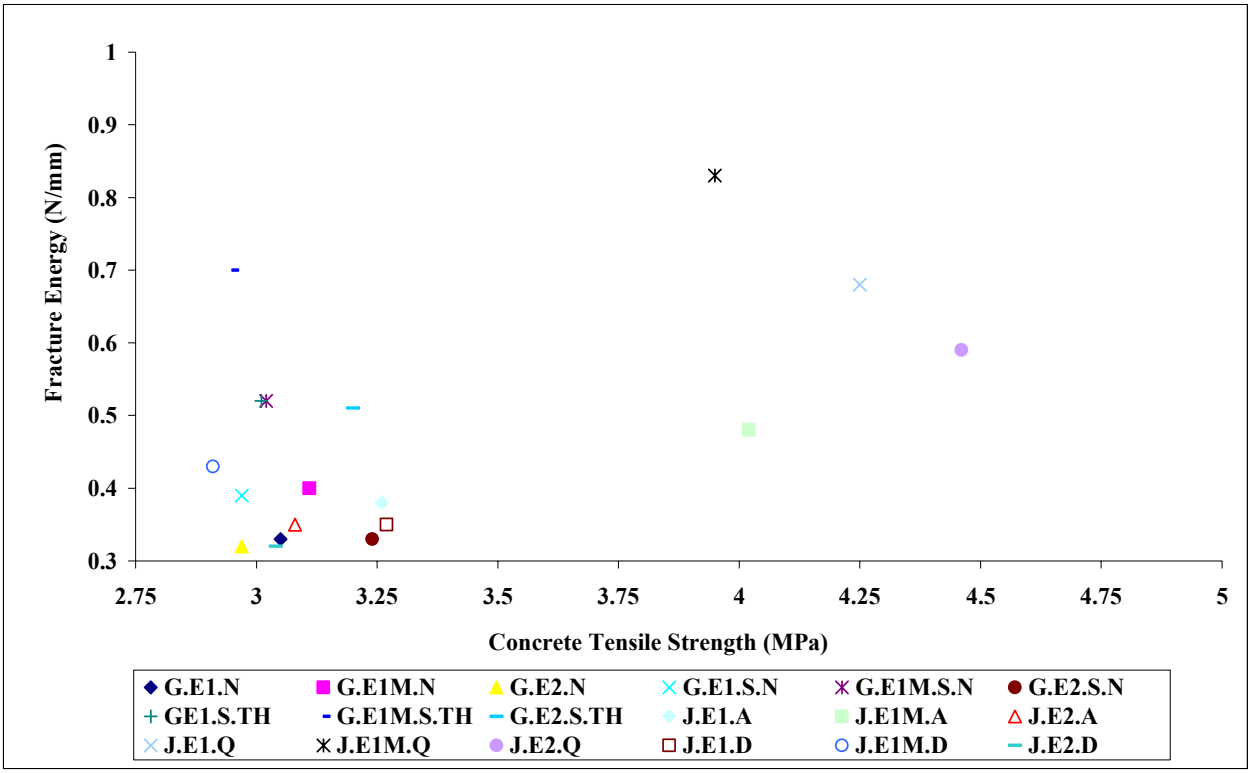

Figure 5.4: Relation between concrete tensile strength and fracture energy

5.3.2. Model Comparison and Development

The author reviewed and assessed the performance of some models available in the literature, and decided for the model developed by Teng et al. [25], and the model developed by Neubauer and Rostásy [79]. These models show a reasonable performance and give good prediction for the average bond strength. Also, theses models were identified by a comparative study conducted by Teng et al. to be among the best models to characterize bond strength.

The chosen models were employed to predict the ultimate loads and the results are shown in Figure 5.5. The performed calculation takes into consideration the length of the bonded joint, i.e. 300 mm, which was larger than the minimum required effective length acquired by both models.

Both models agree reasonably well with the measured failure loads for specimens exposed to normal conditions and to those exposed to Amman and Dead Sea environments. On the other hand, the models show poor predictions for specimens exposed to Aqaba environment and to those exposed to 50 % moisture associated with 50 ºC temperature. These specimens showed much higher failure loads due to the beneficial post-curing of concrete.

For further evaluation the performance of the two models, the measured failure loads were plotted against the predicted failure loads, in addition to a 45º line that simulate the ideal relation between measured and failure loads, as shown in Figure 5.6. The plots are scattered around the 45º line. This is expected as the models assumed a direct relation between the failure loads and the concrete strength, which is valid only for specimens exposed to normal conditions when the tensile strength of concrete is the controlling parameter of failure. On the other hand, for the specimens exposed to severe environment the concrete is not the controlling failure parameter, it is the adhesive since the failure occurred at the adhesive/concrete interface. Therefore, it is important to include the mechanical properties of the adhesive into the models.

In order to investigate the relation between the failure loads and the failure controlling parameters, i.e. adhesive and concrete, Figure 5.7 shows plots for the measured failure loads versus the adhesives shear moduli, it seems that there is an indirect relation between the measured failure loads and the adhesives shear moduli for all tested specimens and under all environments. Adhesives with lower shear moduli attained higher failure loads as compared with adhesives with higher shear moduli. On the other hand, Figure 5.8 shows plots for concrete tensile strengths versus the measured bond strengths. The plots are scattered for specimens exposed to severe environments insuring that there is no relation between measured bond strengths and the measured tensile strengths. Whereas, for specimens exposed to normal environments, there is a direct relation between the concrete tensile strength and measured failure load.

It is clear now that both models adequately predict the failure load for specimens exposed to normal conditions, but they do not for specimens exposed to severe environment. The chief drawback of these models is that they underestimate the failure load for specimens exposed to severe environment. For example, for specimens exposed to Aqaba environment, the measured values for specimens J.E1.Q, J.E1M.Q and J.E2.Q, respectively were 28.95 kN, 31.97 kN and 26.87 kN; compared to predicted values of 25.57 kN, 24.65 kN and 26.2 kN using the model of the Neubauer and Rostásy model, and a predicted value of 20.81 kN for the three specimens using Teng et al model.

Variant behaviour and limitations are observed for the two models; in certain environments the accuracy is high while in others it is low. The variation in performance stems from the fact that the models didn't take into account the effects of the exposure conditions on the location of failure planes, which is sometimes through concrete and in other times at the adhesive/concrete interface. Therefore, it is

improper to neglect adhesive properties, in particular when the adhesive is the controlling failure parameter.

Accordingly, it is necessary to develop a model that can predict the failure loads under all environments with high accuracy that can depict the effects of the environments on bond strength. The proposed model will be a development of Neubauer and Rostásy model as its prediction accuracy was higher than the Teng et al. model, by introducing the adhesive properties and the environmental effects.

The linear elastic approach adopted by Neubauer and Rostásy [79], which follows Holzenkämpfer's model [6] and which has been adopted in the German Institute of Construction Technology [104], illustrates the relationship between maximum load and the main parameters affecting the bond behaviour. The main parameters directly proportional to the ultimate load are the bond length, width, stiffness of CFRP plate, in addition to the width and stiffness of concrete. These parameters were well defined for retrofitted systems exposed to normal laboratory conditions. This case is true as the concrete is the controlling parameter.

But, adhesives degrade when exposed to severe environment to such an extent that their strength could be reduced to that of concrete or below, hence controlling the failure. Therefore, their dimensional and mechanical properties in the form of thicknesses and shear moduli should be included in the model, since the adhesive layer is transmitting stresses between concrete and the reinforcing plates through shear stresses.

Considering the general model of Neubauer and Rostásy [79] shown in equation 5.6.

$$P_{\max} = \alpha \;\; c_1 \;\; k_b \;\; b_f \sqrt{E_f t_f f_{ctm}} \qquad 5.6$$

where,

α: is a reduction factor, approximately equal 1 for beams with sufficient internal and external shear reinforcement and in slabs;

c_1: constant obtained from the calibration of test results, and is usually set to 0.64 for CFRP plates;

b_f: breadth of the CFRP plate;

t_f: thickness of the plate;

k_b: factor to describe the introduction of bond force in the concrete member with the width of the plate, b_f, and is equals to

$$k_b = 1.06 \sqrt{\frac{2 - \frac{b_f}{b}}{1 + \frac{b_f}{400}}} \;, \qquad \frac{b_f}{b} \geq 0.33$$

E_f: elastic modulus of the FRP plate; and

f_{ctm}: mean concrete tensile strength

This model predicts the ultimate load when the available bonded length, l_b is equal to or greater than the maximum anchorage length, $l_{b\max}$. Maximum anchorage length is defined by Neubauer and Rostásy

[79] as the maximum bonded length beyond which there will be no further increase of the bond force. It is equal to

$$l_{b\max} = \sqrt{\frac{E_f t_f}{2 f_{ctm}}} \qquad 5.7$$

Accordingly, the maximum anchorage length is in the range of (189 – 204) mm depending on the concrete tensile strength. The bond length for all tested specimens is 300 mm, which is much greater than the maximum anchorage length.

Therefore, the general form of the proposed model after introducing adhesive properties will be as shown in equation 5.8.

$$P_{\max} = (\mathbf{constant}) b_f \left(\frac{G_a}{t_a}\right)^{-x} (E_f t_f)^{0.5} (f_c')^{0.67} \qquad 5.8$$

The only differences from the model developed by Neubauer and Rostásy [79] are the parameters of the adhesive, concrete compressive strength and constants.

Adhesive parameter is taken as the shear modulus per unit thickness raised to a power "-x". The value $\frac{G_a}{t_a}$ is deduced from the coefficient $\Omega^* = \sqrt{\frac{1}{E_p t_p}\frac{G_a}{t_a}}$ shown earlier in equation 5.5, in accordance to Täljsten, [78] whose model was based on Holzenkämpfer's model [6]. Herein, x is an experimental factor obtained through regression of test results. The negative sign is to simulate the indirect relation between the shear modulus and the measured failure loads. It has been shown earlier that adhesives with lower elastic modulus, but good ductility, can lead to higher interface bond strengths. Performing regression analysis for the test results, the factor *x* is found to be 0.36. This factor is close enough to a factor of 0.352, obtained by regression analysis conducted by other researchers, Ueda and Dai [105].

It is assumed to include concrete compression strength instead of tensile strength obtained by pull-off tests. The justification is that, concrete tensile strength is not always the controlling parameter for failure, as the case when failure is at the adhesive/concrete interface. Also, concrete tensile strength is not always available to the designer engineer, on the contrary concrete compressive strength is always available as it is a main parameter in design models. Furthermore, concrete tensile strength is related to concrete compressive strength, $f_{ctm} \cong (f_c')^a$, where the factor (a) has different values such as, 1/2 and 2/3 as shown by other researchers, e.g. Chajes et al. [106] and Horiguchi [107], respectively.

Now, upon a closer examination of the plots of Figure 5.7, it seems that there is a limit for adhesive strength that above which there is a reduction in the ultimate load. Considering Type 1 Modified adhesive to be the optimum, then using regression analysis for the test results and taking into consideration the environmental effects. The results of regression analysis are shown in Table 5.5. Comparing the obtained results together to account for concrete post-curing, assuming that the specimens exposed to Aqaba environment to be the optimum, the constant is equal to (1.238 - k_n), where k_n is the environmental as shown in Table 5.6.

More tests on different types of adhesives are needed to exactly determine the optimum adhesive.

Therefore, the proposed model assuming available bond length is larger than the effective transfer length as given by Neubauer and Rostàsy model will be as shown in equation 5.9.

$$P_{\max} = (1.238 - k_n) b_f \left(\frac{G_a}{t_a}\right)^{-0.36} (E_f t_f)^{0.5} (f_c')^{0.67} \quad 5.9$$

The predicted bond strength is regarded as an average force because the model basically is deterministic model taking only average values of the basic variables into consideration.

The overall accuracy of the developed model was 98.6 % under all encountered environments, 97.7 % for normal conditions, and 96.8 % for salt solution exposure, 99.5 % for 50 % humidity associated with high temperature of 50 ºC, 99.2 % for Amman environment, 99.1 % for Aqaba environment and 99.5 % for Dead Sea environment. Comparison between the measured failure loads and those predicted using the developed model, in addition to the models of Neubauer and Rostásy [79] and Teng et al [25] are illustrated in Figure 5.9. It is clear that the model could adequately predict the failure loads.

Table 5.5: Results of regression analysis

Exposure Conditions	Results
Normal Exposure	0.864
Salt Solution	0.980
Humidity with high temperature	1.141
Amman Environment	0.946
Dead Sea Environment	0.891
Aqaba Environment	1.238

Table 5.6: Environmental factor (K_n)

Exposure Conditions	Results
Normal Exposure	0.374
Salt Solution	0.258
Humidity with high temperature	.097
Amman Environment	0.274
Dead Sea Environment	0.347
Aqaba Environment	0*

***: the environmental factor = 0.0 to account for post curing**

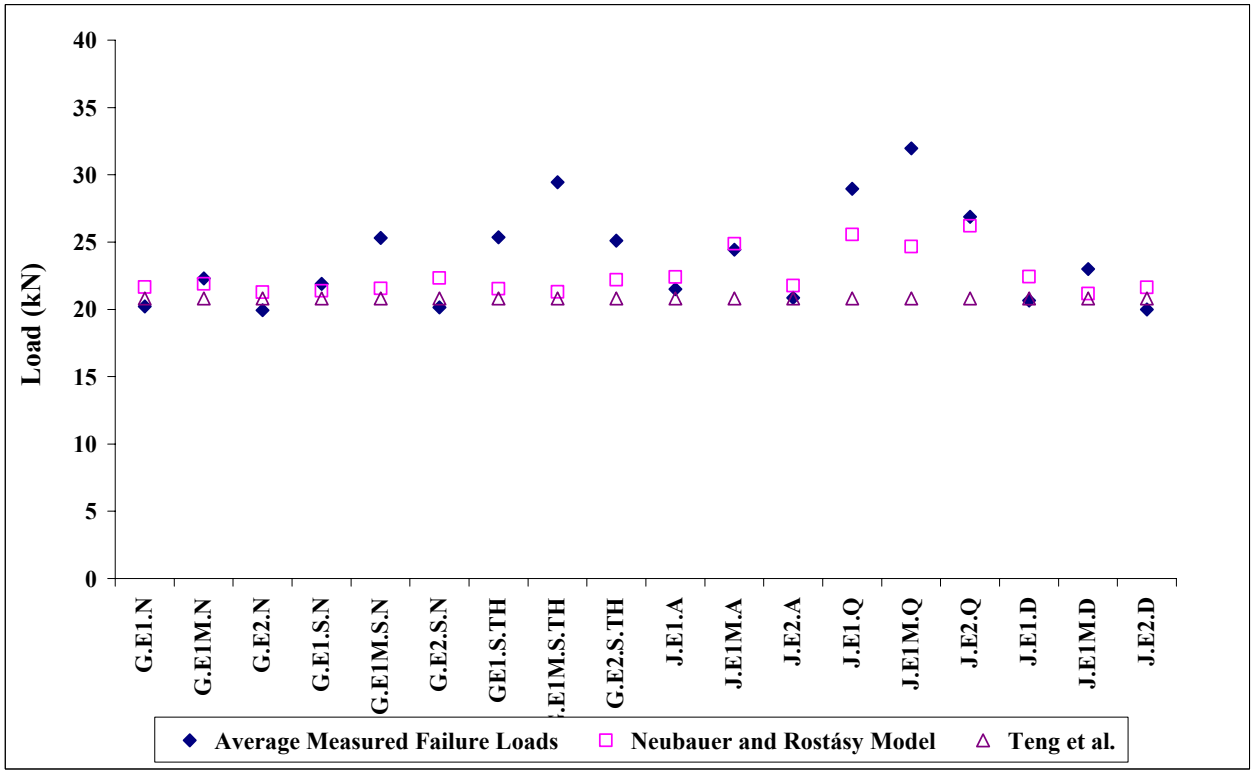

Figure 5.5: Measured and model predicted failure loads

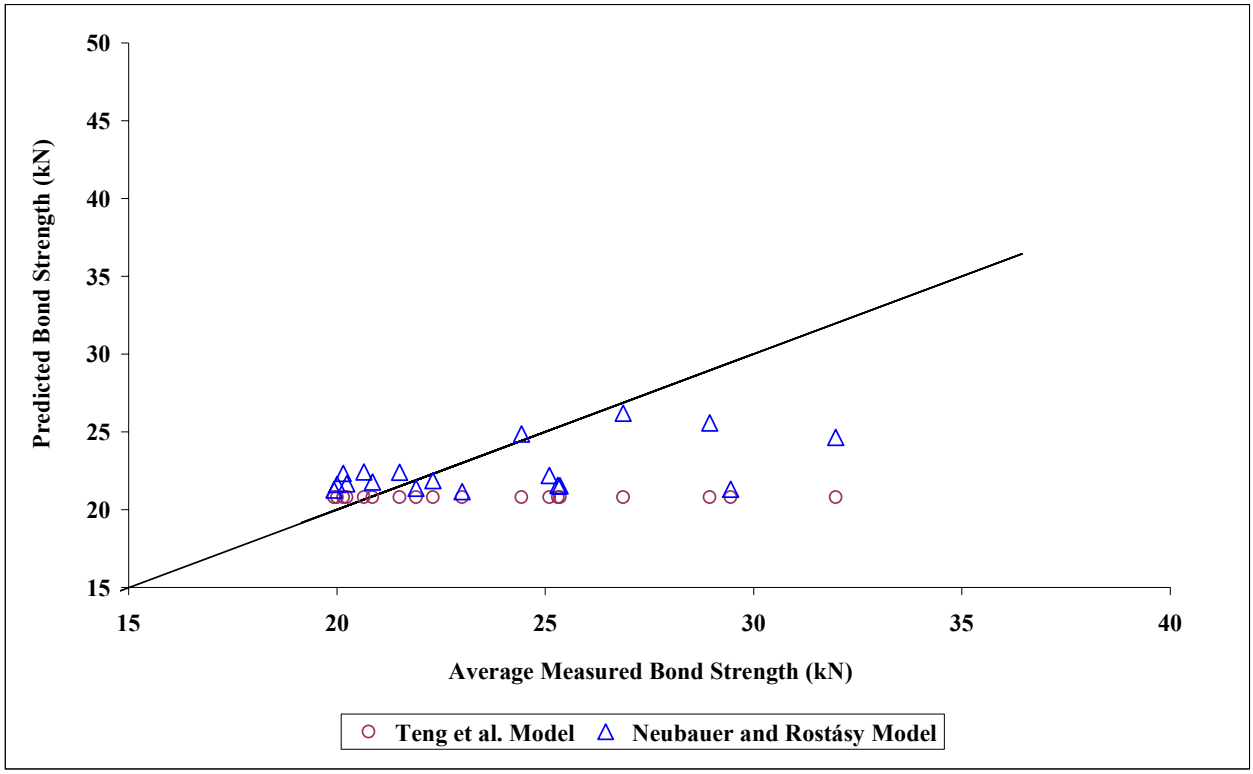

Figure 5.6: Measured bond strength versus predicted values

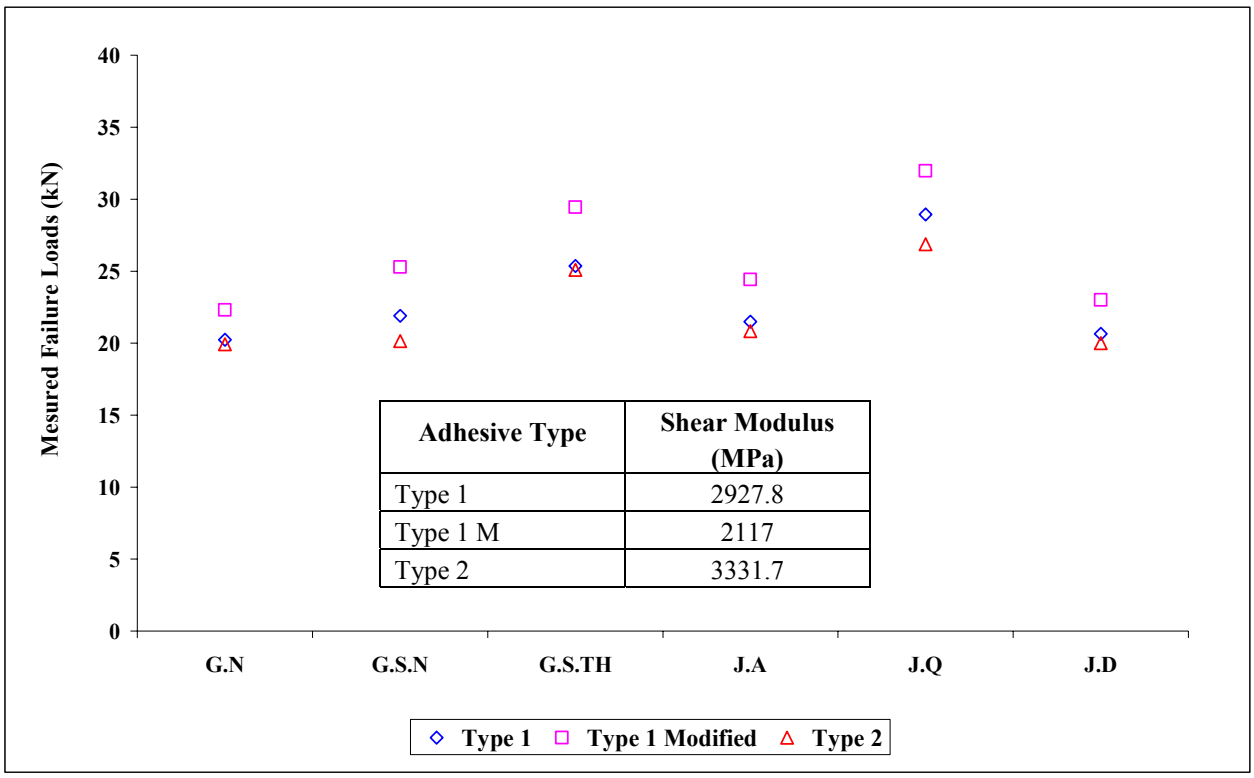

Adhesive Type	Shear Modulus (MPa)
Type 1	2927.8
Type 1 M	2117
Type 2	3331.7

Figure 5.7: Measured bond strength versus adhesives shear moduli

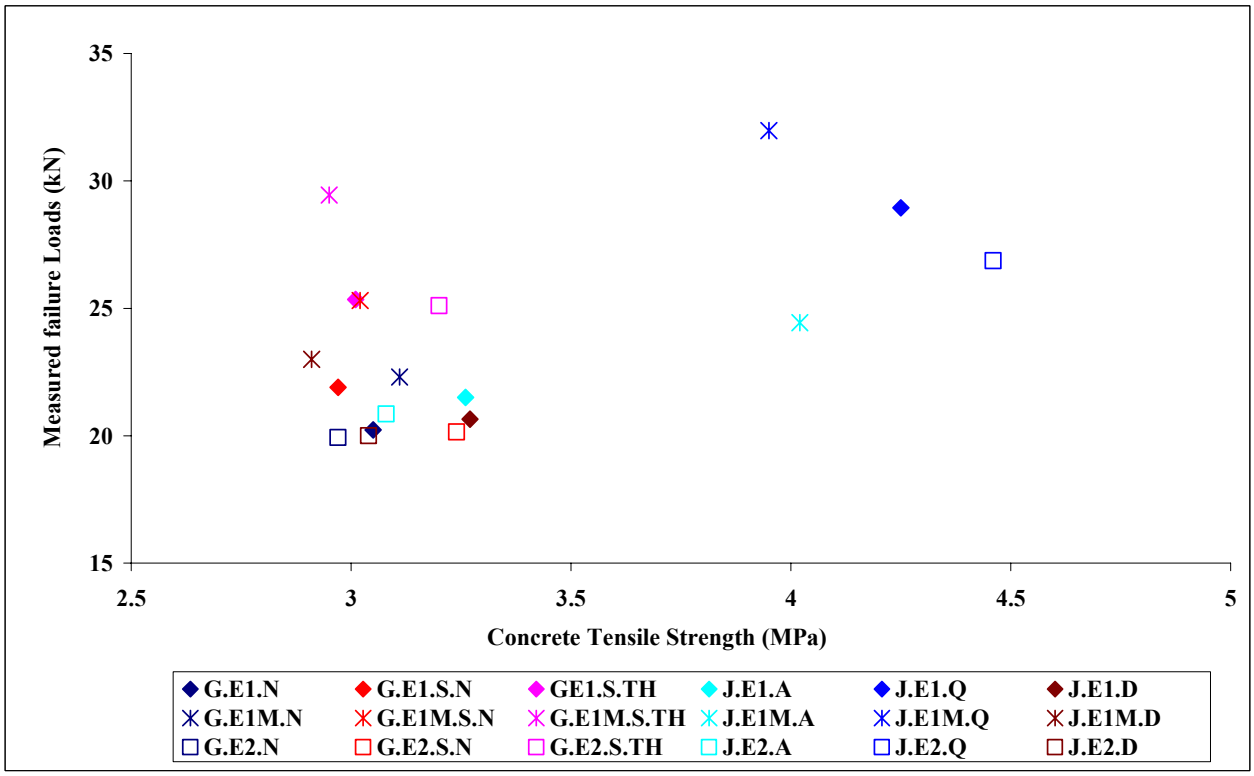

Figure 5.8: Measured bond strength versus concrete tensile strengths

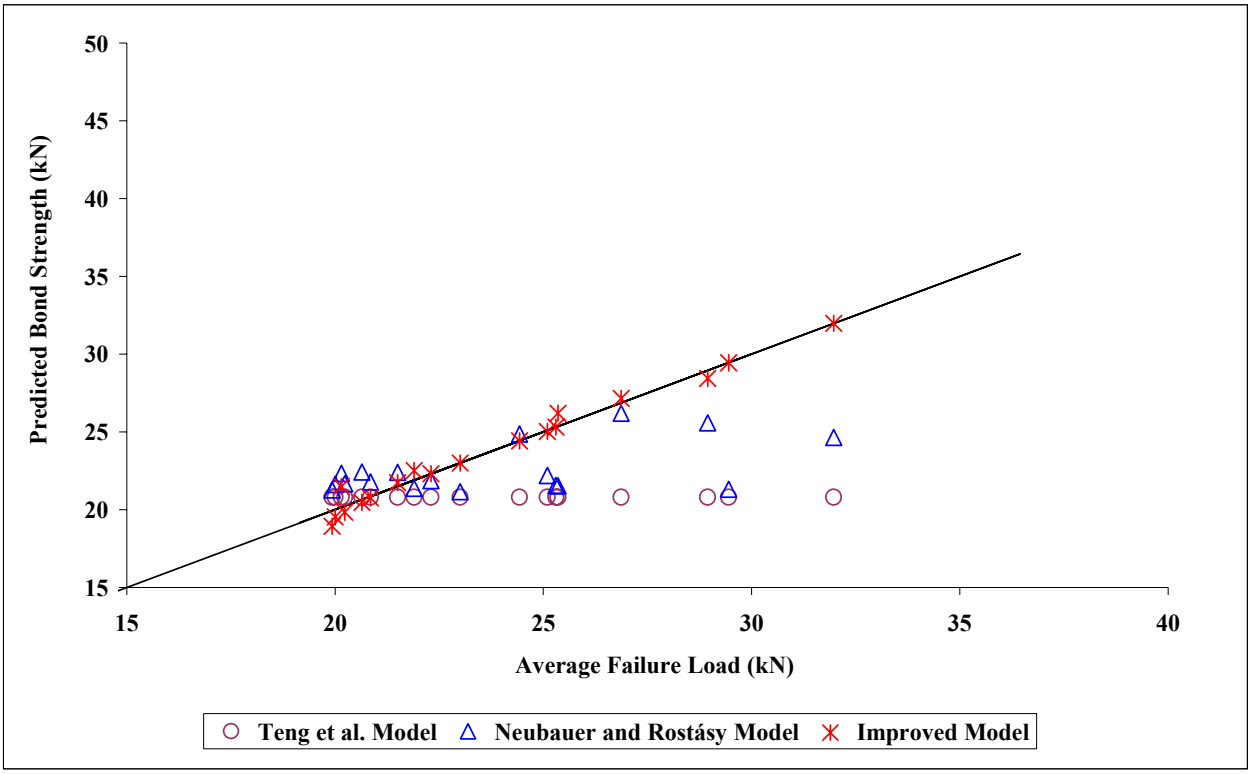

Figure 5.9: Measured bond strength versus concrete tensile strengths

5.4. Durability and Service Life Estimation

The forecast of service life of adhesive joints is quite risky. The problem is that an adhesive joint is not made up of just one material. It contains of several components that may interact with each other. In fact, in most adhesive joints at least five elements must be considered: three materials and two interfaces. Understanding and predicting the rate of degradation of each of these elements is challenging, but it can be done. The most difficult failure situations to predict are those resulting from interactive effects. Thus, it is important to consider and evaluate the adhesive joint as a complete system.

However, in this study only the adhesive component of the bonded system is considered and evaluated as it is the most sensitive element to degradation when related to severe environment.

Life prediction methodology embraces all aspects of the numerous processes that could affect the function of the element - in this case the adhesive material. The fist step is to define the function of the adhesive clearly enough for a failure criterion to be derived. This failure criterion may be an unacceptable reduction in tensile strength, reduction in elastic modulus due to moisture ingression, or a variety of other possible criteria. It is also important that the criteria can be related to practical adhesive joint performance. This is where it is difficult in view of the fact that these specific materials do not have long history of real life applications as other construction materials, e.g. concrete. Thus we must presume it, at least for this limited analysis, based on results and observations obtained from testing the slab and prism specimens.

Usually, to obtain reasonable durability estimates representative specimens are exposed to accelerated environments at elevated temperatures for a sufficient period of time, during which the degradation in any property is measured frequently at different intervals during the exposure period. In this way an

acceleration of any degradation is obtained partly as a result of the elevated temperature. Then the Arrhenius equation is commonly used to predict the rate of changes in combined effects of temperature and time from which the lifespan is predicted.

In this study, the prediction of life span will follow the method of Tannous and Saadatmanesh [95] taking into consideration the results obtained from testing the bulk materials and the observed modes of failure. It was shown earlier in this investigation that the mechanical properties of the bulk materials were severely degraded when soaked in water, salt and alkaline solutions. The higher losses were observed in the case of alkaline and salt solutions particularly when associated with high temperatures. This was in an agreement with the increased diffusivity, thus resulting in deeper moisture penetration. However, this severity of degradation was not reflected in the obtained results from the conducted pull-off and flexural tests, in particular for the flexural tests. The failure loads were comparable to each other and to the reference specimens with hardly any difference in the measured values, or even the loads were little bit higher for specimens exposed to severe environments. This observation ensures that the adhesive joint is still intact and capable of transmitting shear stresses between concrete substrate and CFRP plates, which has been imitated in the measured strains and shear stresses. Nonetheless, there was a difference in the failure modes; delamination at the top of the concrete layer for specimens exposed to normal conditions insuring very strong bond, and separation at the adhesive concrete interface for specimens exposed to severe environments.

Since the failure modes were shifted from concrete shearing to adhesive/concrete interface, there is surely a reduction on the elastic properties of the adhesives when exposed to sever environment, either real-life exposure or simulated laboratory sever exposure conditions.

According to the study performed by Tannous and Saadatmanesh [95], the loss in adhesive properties could be related to the rate and depth of penetration of contaminants. The depth of penetration can be described by Fick's law, as shown in equation 5.10.

$$x = \sqrt{2DCt} \qquad 5.10$$

Where x is the depth of penetration (mm); D is the diffusity, (mm^2/sec), C is the normalized or relative alkaline or chloride concentration (mol/l) / (mol/l), and t is the elapsed time (s). The loss in strength is evaluated on the assumption that the load carrying capacity in the penetrated area only is destroyed.

The depth of moisture penetration in all adhesive types after exposure to the encountered environments will be as shown in Table 5.7, taking into consideration the concentration of the conditioning solutions; concentration for chloride solution was 9.6 % and 14 .6 % for alkaline solutions.

The loss in strength of the adhesive materials is evaluated on the assumption that only the load carrying capacity of the penetrated area is destroyed. Considering the initial thickness and width of the original specimen to be, t_o (mm) and b_o (mm) as shown in Figure 5.10; the depth of penetration x (mm), and the initial tensile strength, P_o (kN) are used to predict the residual tensile strength P_r (kN) from equation 5.11. Residual tensile strengths for all adhesives immersed in salt and alkaline solutions at the two conditioning temperature are presented in Table 5.7. No calculation could be made for specimens immersed in water since there is no concentration, i.e. $C = 0$.

$$P_r = P_o\left(\frac{(b_o - 2x)(t_o - 2x)}{(b_o t_o)}\right) \qquad 5.11$$

The prediction of the long life of bulk materials followed the empirical equation No. 5.12, Maxwell et al. [97].

$$\log P(t,T) = A(T) - B(T)t \qquad 5.12$$

Where P represents the level of material property, T is the absolute temperature in Kelvin, A is a constant and B is the degradation rate obtained from plotting material property data against time for one temperature-moisture level.

The expected lifetime of the selected adhesives is shown in Table 5.8. These predictions were based on acceptable functioning limits given by ACI [13], which assumes that tensile strengths are reduced to 85 % of their initial values when operating outdoor and under severe environment.

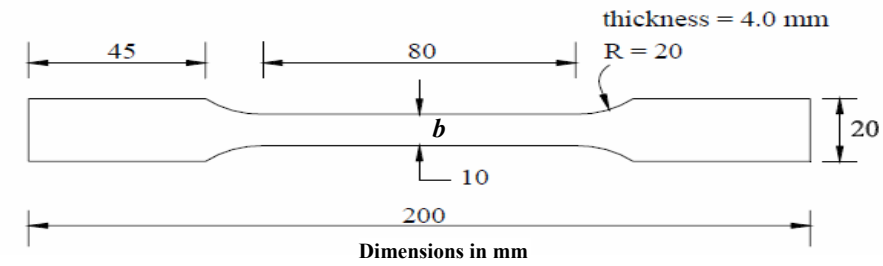

Figure 5.10: Dog-bone specimen used for measuring diffusion rate

Table 5.7: Penetration depth and residual tensile strength

Environment	Type 1		Type 1 Modified		Type 2	
	Penetration Depth (mm/year)	**Residual Strength (%)**	**Penetration Depth (mm/year)**	**Residual Strength (%)**	**Penetration Depth (mm/year)**	**Residual Strength (%)**
Exposure (3)	0.0358	97.5	0.0317	97.8	0.0577	96
Exposure (4)	0.0506	96.5	0.046	96.8	0.0945	93.5
Exposure (7)	0.0831	94.3	0.0819	94.3	0.1056	92.7
Exposure (8)	0.1037	92.8	0.103	92.8	0.134	90.8

Table 5.8: Predicted lifespan of the selected adhesives in identified environments

Environment	Lifetime (Years) based on 85 % of residual tensile strength		
	Type 1	Type 1 Modified	Type 2
Exposure (3)	40.3	45.1	24.9
Exposure (4)	28.5	31.1	15.4
Exposure (7)	17.6	17.6	13.7
Exposure (8)	13.9	13.9	11

Actual calibration of accelerated aging to natural weathering is not complete in this study. However, it is cited from previous studies that the expected service life for retrofitted systems using adhesives similar to Type 1 to be about 30 years for exposure similar to No. 4, Horiguchi, [107], Litherland et al. [108] and Maeda et al [109]. Therefore the results presented in Table 5.8 are reasonable.

Adhesive Type 1 Modified, which got the best performance under all environments among other types as been proved in this investigation, could retain about 85 % of its strength in 45.1 years if exposed to salt solutions at ambient temperature of 23 ºC, compared to 35.1 years if exposed to salt solutions associated with high temperature of 50 ºC. This 10 years reduction in the adhesive life is attributed to the higher absorption rates of solutions caused by higher temperature, which had an adverse effect on the adhesive properties by reducing its glass transition temperature to levels closed to service temperature.

It is clear that the most severe environment for the retrofitted systems is the exposure to alkaline solutions, particularly if associated with high temperatures. This is manifested by the short lifespan of all adhesives. Type 1 adhesive could loose about 34 % of its service life; Type 1 Modified could loose about 30 %, while Type 2 could loose about 44 %.

This life estimate enlightened the consequences of severe environments on the CFRP externally retrofitted systems, for example exposure like No. 8 could shorten the service life of retrofitted systems using Type 2 adhesive to 11 years. This is rather a short period if compared to the expected life of civil structures in service, which is in the range of (50 – 100) years.

But, in the author's opinion based on the results obtained so far, the real lifetime for the retrofitted systems could be longer than the predicted lifetime if taking the following into consideration.

- The degradation in the bond strength for specimens located in severe environment, either simulated laboratory conditions or real-life environment were not as the severity of degradation in testing the bulk materials.
- The rate of diffusion measured for the bulk materials is really not depicting the real diffusion in real structures at site. The diffusion in bulk materials was based on fully immersion of the dog-bone specimens in solutions. In this case the specimen is absorbing solutions from all its sides, which is not representing the adhesive enfolded between concrete and CFRP plates, taking into consideration that the CFRP material is an impermeable material, and the thickness and the quality of concrete

substrate. Design codes set recommendations regarding the minimum acceptable strength for concrete in severe environments to be not less than 35 MPa, ACI [99], this implies a high quality and nearly impermeable concrete. Furthermore, in cases where the concrete is cracked or deteriorated, the application of CFRP plates should not be performed on the deteriorated and contaminated concrete. Cracks should be injected, delamination and spalls should be removed and contaminated concrete should be cleaned or removed to a depth of acceptable low contamination content. And if there is corrosion in the inner steel, corroded areas should be cleaned or compensated with new reinforcing steel. Then the concrete is patched with new high quality concrete in order to get sound concrete before the application of the CFRP plates for retrofitting.

- The concentration of the conditioning solutions was very high if compared to seawater or concrete alkalinity.
- The diffusion rate will not continue on a constant scale for the whole life of the adhesives. It has been shown earlier that all adhesives reach saturation level in about 84 days.
- Usually the CFRP plates are placed at the soffit of beams, girders and slabs, except in cases of negative moments where they may be exposed to higher quantities of solutions, ultraviolet and direct exposure to sun. In such cases the system must be protected and sealed for extending its lifespan.
- Also, it is important to point out that the temperature in real-life environments is not constant at the same degree throughout the year. For an example, the temperatures at the three areas of interest Amman, Dead Sea and Aqaba regions as shown in Appendix A from data collected for 10 years, are varying from day to day and season to season. This means that the diffusion rate should be less than the values obtained from testing the bulk materials and surely the lifetime should be longer.

Furthermore, these lifetime predictions were based on the performance of the adhesive materials alone, as there are no much data available at hand regarding the diffusion rates for concrete and CFRP plates. It was not planned at the early beginning when the experimental work starts to evaluate the diffusion rates for CFRP plates and concrete.

6. Conclusions and Recommendations

6.1. General

The use of CFRP in civil engineering is relatively new compared to conventional materials. The amount of experimental data and level of confidence concerning durability of CFRP composites in civil engineering applications is comparatively low; the influence of environmental exposure on the durability of CFRP and its composites is a major concern. Furthermore, there is growing interest in exploring the application of CFRP in severe environments such as Middle East countries, in particular Dead Sea and Aqaba of Jordan. For these environments, the level of durability information is limited and not publicly available.

Response of CFRP retrofitted RC structures, in particular the adhesive bonds, to real-life severe environments and sustained loading is another area in civil engineering application where the level of knowledge and scientific data ranges from very limited to non-existant. The research reported in this thesis was undertaken to address the growing demand for information and experimental data from the civil engineering industry regarding the mechanical response and durability of CFRP and its bonds. Furthermore, to provide valuable insight into the feasibility of utilizing CFRP plates in retrofitting Jordanian deteriorated and substandard structures, particularly industrial structures located at the shore of the Dead Sea region, which is one of the most corrosive areas throughout the world. Thus, the primary purpose of this study was to evaluate the effects of various environmental conditions on the long-term behaviour of CFRP retrofitted structures, and thus add further valuable information in this area.

This study is composed mainly of three parts; (1) Examinations on single materials, epoxies and CFRP plates, (2) Examinations of the long-term behaviour of slabs with high salt concentrations and CFRP externally bonded reinforcement under bending stress, and (3) Examinations on composite specimens, CFRP plates, epoxy adhesive and concrete.

The experimental program entailed evaluating the performance of three different types of structural adhesives and one type of CFRP plates after conditioning representative specimens in moisture, water, salt solutions, alkaline solutions and ultra violet radiations. All associated with ambient temperatures of 23 ºC and high temperatures of 50 ºC. Additionally, the durability performance of the bond between CFRP plates and concrete substrate was evaluated by exposing retrofitted RC slab specimens and concrete prism specimens to indoor simulated severe conditions and real-life severe conditions. The encountered simulated environments were salt solution, humidity and high temperature. Whereas, the real-life encountered environments included Amman environment, Dead Sea environment and Aqaba environment.

Testing similar specimens under real-life exposure conditions and simulated laboratory conditions allowed for a detailed evaluation of the durability and the behaviour of the bond between the CFRP plates and concrete in terms of bond strength, failure modes and strength gain.

To simulate the real behaviour of deteriorated and substandard RC structures at site, slab specimens were cracked at predefined locations and exposed to different environments as above for a period of four months. Specimens were retrofitted with CFRP plates using the three selected adhesives while under sustained loading, and then went through long-term exposure for about one year. Conditioned specimens were tested under three-point loading scheme. Deflections and strains were measured, additionally crack widths at every load step.

Furthermore, the prism specimens were exposed to simulated severe and real-life severe conditions for almost 4 months before bonding the CFRP plates using the three selected adhesives. Afterwards they went through a long-term exposure for almost one year. Specimens were then tested under pure shear.

It is worthy to mention here that the indoor environments were chosen based on the real-life environments prevailing at Amman, Dead Sea and Aqaba regions.

An analytical model based on data regression analysis was proposed, using the model of Neubauer and Rostásy [79], taking into consideration the effects of the encountered environments on the bond strength.

6.2. Conclusions

6.2.1. Testing Single Materials

- This investigation confirmed the excellent durability of carbon fiber reinforced composites. The accelerated ageing tests showed that CFRP is long lasting, even when exposed to severe environmental conditions for long durations. The chosen type of CFRP composite proved to be adequate in harsh environments, and can be used to retrofit deteriorated and substandard structures such as those located at the Dead Sea and Aqaba regions of Jordan.
- All studied adhesives were found to suffer an apparent trend of deterioration when exposed to high temperatures particularly if close to their glass transition temperatures. At elevated temperatures adhesives soften, degraded and suffer reduction in strength and stiffness.
- For the specific chosen types of adhesives, exposure to 65 % moisture at ambient temperature of 23 ºC for longer periods was found to enhance their mechanical properties. On the contrary, considerable loss on the adhesives mechanical properties is attained when adhesives are exposed to moisture associated with high temperatures.
- Adhesives lost considerable amount of their mechanical properties when soaked in water and chemical solutions at ambient temperature. But, ageing helped in decreasing the amount of loss in the mechanical properties when adhesives were conditioned in water. On the contrary, the loss in the mechanical properties was found to increase with ageing when adhesives were immersed in salt and alkaline solutions.
- Adhesives were found to loose significant amount of their strengths and stiffness when immersed in hot solutions that was aggravated with ageing.
- Generally, alkaline solutions were found to be the most severe environment on adhesives mechanical properties, followed in severity by salt solution and water, respectively. The severity of all encountered environments was found to be aggravated if associated with high temperatures and ageing.
- The percentage of deterioration in strength and stiffness varies between the different types of epoxies depending mainly on the chemical composition of each type. Comparatively, under all the encountered environments, Type 1 Modified, which got the lowest mechanical properties, has found to have the best performance notwithstanding its low initial mechanical properties as compared to the other types, followed by Type 1 and Type 2, respectively.

6.2.2. Testing Slab Specimens

- Full composite action was observed between the CFRP plates and the concrete substrate for slab specimens exposed to ambient indoor and out door exposures.
- Debonding of CFRP plates from concrete substrate was the dominate failure mode. All tested specimens failed at almost the same loads with hardly any differences between them, not withstanding the severity of environments either simulated or real-life. Only two of the specimens that were exposed to Dead Sea environment failed at about 90 % of the failure loads of their corresponding control specimens. On the other hand, specimens exposed to salt solution failed at higher loads of 110 % as compared to their corresponding control specimens.
- Failure was described as undesirable brittle failure with low measured deflections and strains. Only 30 % of the rupture strain of the CFRP plates was utilized.
- Comparatively, under all exposure conditions the best performance was for specimens retrofitted with CFRP plates utilizing viscous adhesives with lower mechanical properties.
- The severity of degradation of the neat adhesive materials when exposed to severe environments was not reflected in the obtained results from testing slab specimens by flexure. Peeling failures had limited the capacity of slabs to about 70 % of the expected predicted capacity. The only difference was the location of the failure planes; delamination at the top of the concrete layer for specimens exposed to normal conditions insuring very strong bond, and separation at the adhesive/concrete interface for specimens exposed to severe environment. Therefore, there was no firm conclusion regarding the consequences from the severe environments on the retrofitted systems. But, according to the results obtained so far, it seems that, CFRP composites could be used to retrofit substandard structures at Jordan, taking into consideration the selected composite and adhesive types to have high glass transition temperatures and the retrofitted systems should be protected as much as possible from direct contact with solutions and high temperatures.

6.2.3. Testing Prism Specimens

- Full composite action was observed between the CFRP plates and the concrete substrate for prism specimens exposed to ambient indoor and out door exposures.
- Specimens failed in catastrophic brittle manner by peeling of the CFRP plates from the concrete surfaces, with different locations for the failure planes. Shearing failure along concrete layer with a thin layer of concrete adherent to the peeled plates for specimens exposed to normal conditions. On the other hand, failure planes were along the adhesive/concrete interfaces with no concrete adherent to the peeled plates for specimens exposed to severe environments.
- Higher failure loads were measured for specimens exposed to Aqaba environment and humidity combined with high temperature. This result was attributed to the beneficial post curing for the concrete and adhesives.
- The direct relation between concrete tensile strengths and the interfacial fracture energies is only existed for specimens exposed to normal conditions; concrete is the controlling failure parameter in the bonded joint as it is the weakest component. On the other hand, for specimens exposed to severe environments, there is no direct relation between concrete tensile strengths and the interfacial fracture energies, but rather an indirect relation between adhesive shear modulus and fracture energies; adhesive is the controlling failure parameter. This result insures that the adhesive joints had lost

considerable strengths to such an extent that their strengths are similar to that of concrete or even lower.

- Adhesives with lower mechanical properties got the higher failure loads, assuring that viscous adhesives with enough strength can distribute concentrated stresses through deformations under higher loads.
- The study on the effects of indoor and outdoor exposure on the performance of CFRP-concrete bond showed that the specimens had good resistance to severe environments, and there were no detrimental effects from the service environments in Jordan; on the contrary higher failure loads were measured for specimens exposed to severe environments. Thus reinforcing the conclusions drawn from testing slab specimens, i.e. CFRP composites could be used to retrofit deteriorated and substandard structures in Jordan.

6.2.4. Contributions

As one of the early attempts to characterize the effects of severe environment on the behaviour of the FRP-bonded concrete system, the following contributions have been made.

- Build up new knowledge and data on material deterioration due to the effects of indoor and outdoor exposure conditions.
- Enlighten the consequences of the severe environments on the CFRP- retrofitted systems for the engineering community.
- Realize debonding mode of epoxy/concrete interface separation that can be observed consistently.
- Establish the relation between concrete tensile strength, adhesive properties and bond strength through developing an empirical model, which could predict the ultimate maximum load for every single environment.
- Devise a robust research methodology for quantifying the durability of CFRP retrofitted systems.

It is also believed that this thesis research will directly impact professional practice, as the findings have formed the basis for future directions and development of design guidelines.

6.3. Recommendations

Based on the results and observations acquired from the entire investigation, the following recommendations could be made.

- Further studies on retrofitted RC elements should include viscous adhesives and take into consideration as an aim to prevent debonding failure for better quantifying the bond strength. Specifically in this experimental work, the adverse effects of the environments is not very well clear as most of the specimens failed at almost the same failure load and in the same fashion. Early debonding of the plates has limited the capacity of the retrofitted slabs to about 70 % of the expected capacity and causing failure to occur at lower loads. The only clear difference between the tested slabs is the location of the failure planes. Therefore, the author suggests mitigating debonding as much as possible for better utilizing the CFRP plates.

- Growing concrete strength due to exposure and age (beneficial post-curing) has mitigated the effects of the severe environments on bond strength. The exact mechanisms for these changes need to be investigated and addressed.
- The real mechanism of the bond cannot be explained because exposure to service temperatures enhances the mechanical properties of the adhesives; considering service temperatures below the glass transition temperatures of the adhesives. Therefore, there is a need for chemical and micro-mechanical examination of the exposed specimens.
- The proposed empirical model should be checked for various bond lengths and types of adhesives. Additionally, other environmental factors should be established for combined environmental conditions, since the proposed environmental factors were estimated for each single environment.
- Also, the optimum adhesive shear modulus needs to be determined through conducting more tests with different adhesives.
- Time-dependent behaviour of CFRP and its bond under load while subjected to various environmental conditions is a very important aspect of durability that needs to be evaluated.
- The real need is to find, consider, investigate, and improve new materials to be used as bonding agents. The debonding failure along the adhesive/concrete interface for specimens exposed to severe environments establishes the need of further research in order to find a better compatible material to bond the CFRP to the concrete.
- Most of the available data are from a limited set of fatigue conditions and do not consider combined effects of fatigue and other environmental conditions. The range of fatigue conditions (frequency, amplitude, stress levels) and interactions needs to be further investigated and documented.
- Creep, relaxation, and stress rupture are significantly affected by stress level, environmental conditions, and interactions thereof; effects of synergistic conditions need to be evaluated at both the materials and structural level.
- In order to select materials that will be durable for 30 -100 years, the development of a procedure is required which can verify service life via a representative exposure, which can be completed within a reasonable lapse of time. The development of analytical tools based on finite element analysis that can assist in this process at the structural level is also needed.
- This experimental work presents a first step in the study of CFRP-concrete durability. Studies considering a variety of other factors are required to establish adequate durability design data. Concerted efforts are required to fully address all durability issues, as the various parameters involved in durability investigations are numerous. Strategic planning among researchers in the durability field is essential to ensure that all critical topics are adequately covered and that unnecessary duplication is avoided. Collaborative endeavours to standardize accelerated laboratory test conditions would undoubtedly contribute greatly towards improving our basic understanding of the durability characteristics of CFRP strengthening technologies. Also, coordinated activities with regard to establishing controlled exposure test sites for CFRP repair materials and CFRP-repaired elements would be of great value.

7. References

[1] FIB Bulletin, 2001, "Externally Bonded FRP Reinforcement for RC Structures", Technical Report, Bulletin 14, Task Group 9.3 FRP (Fiber Reinforced Polymer) Reinforcement for Concrete Structures, International Federation for Structural Concrete (FIB), Lausanne, Switzerland, p.130.

[2] Mehta, K., 1986, "Concrete: Structure, Properties, and Materials", Prentice-Hall, Upper Saddle River, N.J.

[3] Al Far, A., and Kahhaleh, K., I., 2004, "Development of Repair Materials and Techniques for Extending the Lifespan of Industrial Structures", Technical Report No. CS/2004/DUR.01, Building Research Center, Royal Scientific Society, Amman, Jordan.

[4] Ranisch, E., 1982, "Zur Tragfähigkeit von Verklebungen zwischen Baustahl und Beton - Geklebte Bewehrung", Heft 54, T.U-Braunschweig, Germany.

[5] Ranisch, E., and Rostásy, F., 1986, "Bonded Steel Plates for the Reduction of Fatigue Stresses of Coupled Tendons in Multi-span Bridges", Adhesion between Polymers and Concrete (Bonding, Protection, Repair), Proceeding of an International Symposium Organized by RILEM Technical Committee 52-Resin Adherence to Concrete and Laboratoire Central des Ponts et Chaussees, Paris France, pp. 561-570.

[6] Holzenkämpfer, O., 1994, "Ingenieurmodelle des Verbundes Geklebter Bewhrung für Betonbauteile", Ph.D. Dissertation, Technical University of Braunschweig, Germany.

[7] Brosens, K., 2001, "Anchorage of Externally Bonded Steel Plates and CFRP Laminates for the Strengthening of Concrete Elements", Ph.D. Dissertation, Keatholieke Universsteit Leuven Faculteit Toegepaste Wetenschappen, Department Burgerlijke Bouwkunde, Belgium.

[8] Meier, U., 1992, "Carbon Fiber-Reinforced Polymers: Modern Materials in Bridge Engineering", Structural Engineering International, Vol.1, pp. 7-12.

[9] Karbhari, V., and Engineer, M., 1996, "Investigation of Bond between Concrete and Composite: Use of Peel Test", Journal of Plastics and Composites, Vol. 15, No. 2, pp. 208-227.

[10] Rostásy, F., 1990, "State-of-the-Art of FRP Materials", FIP Report, Draft.

[11] Nanni, A.; and Dolan, C., 1993, "FRP Reinforcement for Concrete Structures," Proceedings, ACI SP-138, American Concrete Institute, Detroit.

[12] Rostásy, F., Holzenkämpfer, P. and Hankers, C., 1996, Geklebte Bewehrung für die Verstärkung Von Betonbauteilen, In Betonkalender, II, 547-576.

[13] ACI 440.2R-02, 2002, "Guide for the Design and Construction of Externally Bonded FRP Systems for Strengthening Concrete Structures," American Concrete Institute, Farmington Hills, Michigan, USA, p. 45.

[14] Rahimi, H., 2004, "Environmental Durability of Materials and Bonded Joints Involving Fiber Reinforced Polymers and Concrete, 1st Conference on Application of FRP Composites in Construction and Rehabilitation of Structures, Tehran, Iran.

[15] Darby, J., 1999, "Role of Bonded Fiber-Reinforced Composites in Strengthening of Structures", Strengthening of Reinforced Concrete Structures Using Externally-Bonded FRP Composites in Structural and civil Engineering, Edited by L. C. Hollaway and M. B. Leeming, woodhead Publishing, Cambridge, UK.

[16] Meier, U., and Kaiser, H., 1991, "Strengthening of Structures with CFRP Laminates", Advanced Composite Materials in Civil Engineering Structures, ASCE Specialty Conference, pp.224-232.

[17] Rostásy, F., 1997, "On Durability of FRP in Aggressive Environments", Non-Metallic FRP Reinforcement for Concrete Structures, Proceeding of the Third Symposium, Vol.2 pp. 107-114.

[18] Neubauer, U., 1998, Carbon Fiber Reinforced Plastics-Plates for Strengthening of Structural Members, Concrete Precasting Plant, pp. 58- 63.

[19] Nanni, A., 1999, "Composites: Coming on Strong", Concrete Construction, Vol. 44, p. 120.

[20] Rostásy, F., and Neubauer, U., 1999, "Strengthening of Bridges with Externally Bonded CFRP Plates", Technical Report, Technical University of Braunschweig, Germany.

[21] Alkhrdaji, T., Nanni, A., Chen, G., and Barker, M., 1999, "Upgrading the Transportation Infrastructure: Solid RC Decks Strengthened with FRP", Concrete International: Design and Construction, Vol. 21, No.10, pp. 37-41.

[22] Tommaso, A., Neubauer, U., Pantuso, A., and Rostásy, F., 2001, "Behaviour of Adhesively Bonded Concrete-CFRP Joints at Low and High Temperatures", Mechanics of Composite materials, Vol. 37, No., 4, pp. 327-338.

[23] Mays, G., and Hutchinson, A., 1992, "Adhesives in Civil Engineering", Cambridge University Press, Redwood Press ltd, UK.

[24] Karbhari, V.; Chin, J.; Hunston, D.; Benmokrane, B.; Juska, T.; Morgan, R.; Lesko J.; Sorathia U.; Reynaud, D., 2003, "Durability Gap Analysis for Fiber-Reinforced Polymer Composites in Civil Engineering", Journal of Composite Construction, ASCE, Vo. 7, No. 3, pp.238-247.

[25] Teng, J., Chen, J. and Lam L., 2002, "FRP-Strengthened RC Structures", John Wiley & Sons, LTD., Baffins Lane, Chichester, West Sussex, PO19 1UD, England.

[26] Concrete Society, 2000, "Design Guidance for Strengthening Concrete Structures with Fiber Berkshire, UK.

[27] ISIS, 2001, "Strengthening Reinforced Concrete Structures with Externally-Bonded Fiber Reinforced Polymers", Design Manual No. 4, The Canadian Network of Centers of Excellence on Intelligent Sensing for Innovative Structures, ISIS Canada Corporation, Manitoba, Canada.

[28] Japanese Society of Civil Engineers, 1997, "Recommendation for Design and Construction of Concrete Structures Using Continuous Fiber Reinforcing Materials", Concrete Engineering Series 23, Research Committee on Continuous Fiber Reinforcing Materials, Tokyo, Japan, p.325.

[29] Japan Concrete Institute, 1997, "Non-Metallic (FRP) Reinforcement for Concrete Structures", Vol.1 and 2, Tokyo, Japan.

[30] Civil Engineering Research Foundation, CERF, 2001, "Gap Analysis for Durability of Fiber Reinforced Polymer Composites in Civil Infrastructure", Report No. 40578, ASCE.

[31] Hollaway, L., and Leeming, M., 2000, "Strengthening of Reinforced Concrete Structures", Washington DC., CRC press.

[32] Bisby, L., and Green, M., 2002, "Resistance to Freezing and Thawing of Fiber-Reinforced Polymer Concrete Bond" ACI Structural Journal, Vol. 99, No.2, pp. 215-223.

[33] Juska, T., Dutta, P., Carlson, L., and Weitsman, J., 2000, "Thermal Effects: Gap Analysis for Durability of Fiber Reinforced Polymer Composites in Civil Infrastructure", ASCE Publications, pp. 40-45.

[34] Kumhara, S., Masuda, Y., and Tanano, Y., 1993, "Tensile Strength of Continuous Fiber Bar under High Temperature", International Symposium on Fiber-Reinforced Plastic Reinforcement for Concrete Structures, SP-138, American Concrete Institute, Michigan, pp. 731-742.

[35] Leung, H., Balendran, R., and Lim, C., 2001, "Flexural capacity of Strengthened Concrete Beams Exposed to Different Environmental Conditions", proceedings of the International Conference of FRP Composites in Civil Engineering, Hong Kong, China, pp. 1597-1606.

[36] David, E. and Neuner, J., 2001, "Environmental Durability Studies for FRP Systems- Definition of Normal Conditions of Use of FRP for Structural Strengthening Applications", Proceedings of the International Conference of FRP Composites in Civil Engineering, Hong Kong, China, pp. 1551-1558.

[37] Zheng, Q., and Morgan, R., 1993, "Synergistic Thermal-Moisture Damage Mechanics of Epoxies and Their Carbon Fiber Composites", Journal of Composite Materials, pp. 1465-1478.

[38] Woo, M., and Piggot, M., 1988, "Water Absorption of Resins and Composites II: Diffusion in Carbon and Glass Reinforced Epoxies", Journal of Composite Technology and Research, pp. 162-166.

[39] Chin, J., Haight, M., Hunghes W., and Nguyen, T., 1998, "Environmental Effects on Composite matrix Resins Used in Construction", Proceedings of CDCC-98, Sherbrooke, Canada, pp. 229-242.

[40] Rahman, A., Lauzier, C., Kingsley, C., Richard, J., and Crimi, J., 1998, "Experimental Investigation of the Mechanism of Deterioration of FRP Reinforcement for Concrete", Proceedings of the Second International Conference on Composites in Infrastructure: Fiber Composites in Infrastructure. V. II. Tucson, AZ, pp. 501-511.

[41] Sonawala and Spontak, 1996, "Degradation Kinetics of Reinforced Polyesters in Chemical Environments, Part 1: Aqueous Solution", Journal of Material Science, pp. 4745-4756.

[42] Swamy R., Jones, R., and Charif, A., 1989, "The Effect of External Plate Reinforcement on the Strengthening of Structurally Damaged RC Beams", The Structural Engineer, Vol. 67, pp. 45-56.

[43] Ritchie, P., Thomas, D., Lu L., and Connelly G., 1991, "External Strengthening of Concrete Beams Using Fiber Reinforced Plastic", ACI Structural Journal, Vol. 88, pp. 490-500.

[44] Quantrill, R., Hollaway L., and Thorne A, 1996, "Experimental and Analytical Investigation of FRP Strengthened Beam Response: part I", Magazine of Concrete Research, Vol. 177, pp. 331-342.

[45] Quantrill, R., Hollaway L., and Thorne A., "Predictions of the Maximum Plate end Stress of FRP Strengthened Beams: Part II", Magazine of Concrete Research, Vol. 177, pp. 343-351.

[46] Arduini M., and Nanni, A., 1997, "Behaviour of Precracked RC Beams Strengthened with carbon FRP sheets", Journal of Composite for Construction, Vol. 1, No. 2, pp. 63-70.

[47] Arduini M., Tommaso, A., and Nanni, A., 1997, "Brittle Failure in FRP Plate and Sheet Bonded Beams", ACI Structural Journal, Vol. 94, No. 4, pp. 363-370.

[48] Garden H., and Hollaway, L, 1998, "An Experimental Study of the Influence of Plate end Anchorage of carbon Fiber Composite Plates Used to Strengthen Reinforced Concrete Beams", Composite Structures, Vol. 42, pp. 175-188.

[49] Garden H., Hollaway, L, and Thorne, A., 1997, "A preliminary Evaluation of Carbon Fiber Reinforced Polymer Plates for Strengthening Reinforced Concrete Members", Proceedings of the institution of Civil Engineers Structures and Buildings, Vol. 123, pp. 127-142.

[50] Spadea, G., Bencardino, F., and Swamy, R., 1998, "Structural Behaviour of Composites RC Beams with Externally Bonded CFRP", Journal of Composites for Construction, Vol. 2, No. 3, pp. 132-137.

[51] Maalej, M., and Bian, Y., 2001, "Interfacial Shear Stress Concentration in FRP-Strengthened Beams", Composite Structures, Vol. 54, pp. 417-426.

[52] Nguyen, D., Chen, t., and Cheong, H., 2001, "Brittle Failure and Bond Development Length of CFRP Concrete Beams", Journal of Composites for Construction, Vol. 5, pp. 12-17.

[53] Ritchie, P., Thomas, D., Lu, L., and Connelly G., 1991, "External Strengthening of Concrete Beams Using Fiber Reinforced Plastic", ACI Structural Journal, Vol. 88, pp. 490-500.

[54] Fanning, P., and Kelly, O., 2001, "Ultimate Response of RC Beams Strengthened with CFRP Plates", Journal of Composites for Construction, Vol. 5, pp. 122-127.

[55] White, T., Soudki, K., and Erki, M., 2001, "Response of RC Beams Strengthened with CFRP Laminates and Subjected to a High Rate of Loading", Journal of Composites for Construction, Vol. 5, pp. 153-162.

[56] Pham H. and Al-Mahaidi, R., 2004, "Experimental Investigation into Flexural Retrofitting of Reinforced Concrete Bridge Beams Using FRP Composites", Composites for Construction, Vol. 8, No. 352, pp. 352-359.

[57] Brena, S., Bramblett, r., Wood, S., and Kreger, M., 2003, "Increasing Flexural Capacity of Reinforced Concrete Beams Using CFRP Composites", ACI Structural Journal, Vol. 100, No. 1, pp. 36-46.

[58] El-Refaie, S., Ashour, A., and Garrity, S., 2003, "Sagging and Hogging Strengthening of Continuous RC Beams Using CFRP Sheets", ACI Structural Journal, Vol. 100, No. 4, pp. 446-453.

[59] Thomsen, H., Spacone, E., Limkatanyn, S., and Camata, G., 2004, "Failure Mode Analysis of Reinforced Concrete Beams Strengthened in Flexure with Externally Bonded FRP", Journal of Composites for Construction, Vol. 8, No. 2, pp. 123-131.

[60] Sharif, A., Al-Sulaimani, G., Basunbul, I., Baluch, M., and Ghaleb, B., 1994, "Strengthening of Initially Loaded Reinforced Concrete Beams Using FRP Plates", ACI Structural Journal, Vol. 91, No., 2, pp. 160-168.

[61] Bonacci, J., and Maalej, M., 2000, "Externally Bonded Fiber-Reinforced Polymer for Rehabilitation of Corrosion Damaged Concrete Beams", ACI Structural Journal, Vol. 97, No. 5, pp. 703-711.

[62] Shahawy, M., Chaallal, O., A., Beitelman, T., and El-Saad 2001, "Test and Modelling of carbon-Wrapped Concrete Columns", Composite: Part B, Vol. 33, pp. 471-480.

[63] Arvil, S., Vautrin, A., and Hamelin, P. 2003, "Mechanical Behaviour of Cracked Beams Strengthened with Composite: Application of Full-Field Measurement method", Materials and Structures, Vol. 36, No. 5, pp. 379-385.

[64] Stepanel, P., and Podolka, L., 2001, "Strengthening and Repair of RC Structures in the CZECH republic using CFRP Strips", Proceedings of the International Conference on FRP Composites in Civil Engineering, Hong Kong, China, Vol. 1, pp. 467-473.

[65] Buyukozturk, O., and Hearing, B., 1998, "Failure Behaviour of Precracked Concrete Beams Retrofitted with FRP", Journal of Composites for Construction, Vol. 2, No. 3 pp. 138-144.

[66] El-Mihilmy, M., and Tedesco, J., 2000, "Analysis of RC Beams Strengthened with FRP Laminates", Journal of Structural Engineering, Vol. 126, No. 6, pp. 684-691.

[67] El-Mihilmy, M., and Tedesco, J., 2001, "Prediction of Anchorage Failure for Reinforced Beams Strengthened with FRP laminates", ACI Structural Journal, Vol. 98, No. 3, pp. 301-314.

[68] Chaallal, O., Nollet, M., and Perraton, D., 1998, "Strengthening of RC Beams with Externally Bonded Fiber-Reinforced-Plastic Plates: Design Guidelines for Shear and Flexure", Canadian Journal of Civil Engineering, Vol. 25, pp. 692-704.

[69] Chaallal, O., Nollet, M., and Perraton, D., 1998, "Durability of Concrete Beams Using Externally Bonded Composite Materials", Construction and Building Materials, Vol. 8, pp. 191-201.

[70] Triantafillou, T., 1998, "Shear Strengthening of RC Beams Using Epoxy Bonded FRP Composites", ACI Structural Journal, Vol. 95, No. 2, pp. 107-115.

[71] Triantafillou, T., and Antonopoulos, C., 2000, "Design of Concrete Flexural Members Strengthened in shear with FRP", Journal of Composites for Construction, Vol. 4, No. 4, pp. 198-205.

[72] Chen, J., and Teng, J., 2003, "Shear Capacity of Fiber Reinforced polymer Strengthened RC Beams: Fiber Reinforced Polymer Rupture", Journal of Structural Engineering, Vol. 129, No. 5, pp. 615-625.

[73] Luk, H., and Leung, C., 2001, "Effect of Flexural Cracking on Plate End Shear Stress in FRP-Strengthened Beams", Proceedings of International Conference on the Use of Advanced Composite in Construction, Glamorgan.

[74] Sebastian, M., 2001, "Significance of Midspan Debonding Failure in FRP-Plated Concrete Beams", Journal of Structural Engineering, pp. 792-798.

[75] Reeve, B., Earls, C., Koubaa, A., and harries, K., 2005, "Effect of Adhesive Stiffness and CFRP Geometry on the Behaviour of Externally Bonded CFRP Retrofitted Measures Subject to Monotonic Loads", Report, University of Pittsburgh.

[76] Tanaka, T., 1996 "Shear Resisting Mechanism of Reinforced Concrete Beams with CFS as Shear Reinforcement", Graduation Thesis, Hokkaido University, Japan.

[77] Maeda, T., Asano, Y. Sato, Y. Ueda, T. and Kakuta, Y., 1997, "A Study on Bond Mechanism of Carbon Fiber Sheet", Non-Metallic (FRP) Reinforcement for Concrete Structures, Proceedings of the Third international Symposium, Sapporo, Japan, pp. 279-285.

[78] Täljsten, B., 1997, "Strengthening of Beams by Plate Bonding", Journal of Materials in Civil Engineering, Vol. 9, No. 4, pp. 206-212.

[79] Neubauer, U., and Rostásy, F., 1997, "Design Aspects of Concrete Structures Strengthened with Externally Bonded CFRP Plates", Concrete and Composites, proc. 7th International Conference on Structural Faults and Repair, Vol. 2, pp. 109-118, ECS Publication Edinburgh, Scotland.

[80] Yuan, H., and Wu, Z., and Yoshizawa, H., 2001, "Theoretical Solutions on Interfacial Stress Transfer of Externally Bonded Steel/Composite Laminates", Structural Engineering/Earthquake Engineering, pp. 27 - 39.

[81] Van Gemert, D., 1980, "Force Transfer in Epoxy-Bonded Steel-Concrete Joints", Journal of adhesives, No. 1, pp. 67-72.

[82] Khalifa A, Gold WJ, Nanni A, Aziz A., 1998 “Contribution of externally bonded FRP to shear capacity of RC flexural members”, Journal of Composites for Construction, ASCE Vol. 2, No. 4, pp. 195–203.

[83] Roberts, T., 1989, “Approximate Analysis of Shear and Normal Stress Concentration in the Adhesive Layer of Plated RC beams”, The Structural Engineer, Vol. 67, No. 12/20, pp. 229-233.

[84] CEN 1996, “Aeronautical - Plastics Reinforced with Carbon Fibers - Unidirectional laminates-Tensile test Parallel to the Fiber Direction”, EN 251, Comité Européen de Normalisation, Brussels, Belgium.

[85] CEN1999 b, “Products and Systems for the Protection and Repair of Concrete Structures: Test Methods – Determination of adhesion Steel – to – Steel for Characterization of Structural bonding Agents”, EN 12188, Comité Européen de Normalisation, Brussels, Belgium.

[86] ISO 178, 2001, “Plastics - Determination of flexural properties”, International Organization for Standardization.

[87] CEN1998 c, “Products and Systems for the Protection and Repair of Concrete Structures: Test Methods – Determination of the Coefficient of Thermal expansion”, EN 1770, Comité Européen de Normalisation, Brussels, Belgium.

[88] ASTM D638, 2002, “Standard Test Method for tensile Properties of Plastics”, ASTM International.

[89] ASTM D4065, 1995, “Standard Practice for Plastic: Dynamic Mechanical properties”, ASTM International.

[90] EN 1542, 1999, “Products and Systems for the Protection and Repair of Concrete Structures, Measurement of Bond Strength by Pull-off, EN Standards.

[91] Shahrooz, B., Pack, J., Baseheart, M., and Rieser, 2002, “Environmental Durability Evaluation of Externally Bonded Composites”, Report No. UC-CII 03/02, Federal Highway Administration And Ohio Department of Transportation, Cincinnati Infrastructure Institute, University of Cincinnati, College of Engineering, Cincinnati, Ohio 45221-0071.

[92] Jia, J., Boothby, T., Bakis, C., and Brown, T., 2005, “Durability Evaluation of Glass Fiber Reinforced-Polymer-Concrete Bonded Interfaces”, Journal of Composites for Construction, Vol. 9, No., 4, pp. 348- 359.

[93] Grace, N., 2003, “Environmental/Durability Evaluation of FRP Composite Strengthened Bridges, Civil Engineering Department, Lawrence Technological University, Southfield, MI 48075-1058, USA.

[94] Bo, G., Kim, J., and Leung, C., 2005, “Experimental Study on RC Beams with Strips Bonded with Rubber Modified Resins, Department of Mechanical Engineering and Department of Civil Engineering Hong Kong University of Science & Technology, Hong Kong.

[95] Tannous, F., and Saadatmanesh, H., 1998, “Environmental Effect on the Mechanical Properties of E-Class FRP Rebars”, ACI Materials Journal, V. 95, No. 2, pp. 87 – 100.

[96] Katsuki, F., and Uomoto, T., 1995, “Prediction of Deterioration of FRP Rods Due to Alkali Attack”, Non-metallic (FRP) Reinforcement for Concrete Structures, Proceedings of the Second International RILEM Symposium (FRPRCS-2), pp. 82 - 89.

[97] Maxwell, A., Broughton, W., Dean, G., and Sims, G., 2005, “Review of Accelerated Ageing Methods and Lifetime Prediction Techniques for Polymeric Materials”, NPL Report DEPC MPR 016, National Physical Laboratory, United Kingdom, London.

[98] Lin, R., and Olek, J., 2001, “Development and Evaluation of Cement-Based Patching Materials for Repair of Corrosion-damaged Reinforced Concrete Slabs”, FHWA/IN/JTRP-2000/10, Indiana Department of Transportation, Purdue University, Virginia, USA.

[99] ACI 318-02 and ACI 318R-02, 2002, “Building Code Requirements for Structural Concrete and Commentary,” American Concrete Institute, Farmington Hills, Michigan, USA.

[100] Task Group on Bond, 2005, “Current Recommendations and Guidelines for Mitigating Debonding Failures in Adhesively Bonded, Externally Applied FRP Applications.” ACI 440F, Version 1.0, pp 2-12.

[101] Savoia, M., Ferracuti, B., and Mazzoltti, C., 2003, “Non Linear Bond-Slip Law for FRP-Concrete Interface”, Proceeding of the Sixth International Symposium on FRP Reinforcement for Concrete Structures (FRPRCS), Vol. 1, World Scientific, Singapore, pp. 163-172.

[102] Zhao, L., 2005, “Characterization of RC Beams Strengthened with Carbon Fiber Sheets”, PhD. Dissertation, University of Alabama in Huntsville, USA.

[103] Lorenzis, L., Miller, B., and Nanni, A., 2001, “Bond of Fiber-Reinforced Polymer Laminates to Concrete”, ACI Material Journal, Vol. 98, No. 3, pp. 256-264.

[104] German Institute of Construction Technology, 2000, Authorization No. Z - 36.12-56.

[105] Ueda, T., and Dai, J., 2004, “Interface Bond between FRP Sheets and Concrete Substrates: Properties, Numerical Modelling in member Behaviour”, Published Online by Wiley Inter Science, www.intersciemnce.wiley.com , DO1: 10.1002/pse.187.

[106] Chajes, M., Finch, W., Januszka, T., and Thomson, T., 1976, “Bond and Force Transfer of composite Material Plates Bonded to Concrete”, ACI Structural Journal, Vol. 93, No.2, pp. 295-303.

[107] Horiguchi, T., 1997, “Effect of Test Methods and Quality of Concrete on Bond Strength of CFRP sheet”, Non-Metallic (FRP) reinforcement for Concrete Structures, proceedings of the Third International Symposium, pp. 165-270.

[108] Litherland, K., Oakley, R. and Proctor, B., 1981, “The Use of Accelerated Ageing Procedures to Predict the Long Term Strength of GRC Composites,” Cement and Concrete Research, Vol. 11, pp.455-466.

[109] Maeda, T., Asano, Y., Sato, Y., Ueda, T., and Kakuta, Y., 1997, "A Study on Bond Mechanism of Carbon Fiber Sheet", Proceedings of the Third International Symposium, Vol. 1.

Appendices

Appendix A

Environmental Data

Table A.1: Measured values for surface and ambient temperatures at some structures in Aqaba and Amman during October-2003

Location	Structure	Time	Ambient Temperature (° C)	Surface Temperature (° C)
Ports Cooperation	Observation Tower	8:00	27.4	28.8
		10:00	28.5	33.1
		12:00	29.7	33.9
		2:00	30.1	34.9
	Grain Silos Cluster No. 191	8:16	29	31.5
		10:15	33	38.8
		12:15	33.3	38.9
		2:10	33.8	35.8
	Grain Silos Cluster No. 177	8:20	29	34.5
		10:17	33	40
		2:17	33.3	38.9
		2:12	33.8	35.8
	Grain Silos Cluster No. 165	8:25	29	34.5
		10:20	33	39.8
		12:19	33.3	38.6
		2:14	33.8	35.4
Aqaba Gulf Hotel	Exterior East Facade	8:40	27.5	28.5
		10:40	31	33.4
		12:40	32.2	34.1
		2:46	32.6	35.6
RSS laboratories at Aqaba	Outside Surface	17:19	-	43.5
		18:19	-	38.1
		19:19	-	36
		20:19	-	34.3
		21:19	-	33.1
		22:19	-	32.1
		237:19	-	31.2
		24:19	-	30.4
		1:19	-	28.7
		2:19	-	28.1
		3:19	-	27.7
		4:19	-	27.1
		5:19	-	27.1
		6:19	-	27
		7:19	-	27.4
		8:19	-	28
		9:19	-	28.8
		11:19	-	30.2
		12:19	-	34.5
		1:19	-	37.8
		9:00	-	21.6
		11:30	-	25.8
		3:00	-	31.6
		5:00	-	28.1
RSS laboratories at Aqaba	Outside Surface	11:30	24.2	25.8
		3:00	27.2	31.6
		5:00	23.6	28.1

Table A.2: Recorded values for ambient temperature and humidity measured at Amman for the period of ten years (1993-2002)

Mean Maximum Air Temperature ° C

Year	Jan	Feb	Mar	Apr	May	Jun	Jul	Aug	Sep	Oct	Nov	Dec
1993	12.1	12.6	11.2	25.3	27.4	33.2	33.4	34.8	32.5	29.3	20.4	18.8
1994	14.7	14.4	11.3	27.3	30.5	31.8	32.0	34.0	32.5	29.8	17.8	11.8
1995	14.8	15.5	19.8	23.9	30.6	33.9	33.0	34.2	33.1	27.8	19.4	14.8
1996	13.8	18.8	16.7	22.8	31.0	32.1	34.8	34.4	32.3	26.2	21.3	17.4
1997	15.2	12.4	15.2	22.2	30.4	31.9	32.8	30.9	30.4	27.7	21.2	15.5
1998	12.5	15.0	16.5	25.7	29.4	32.6	34.6	35.5	32.8	29.3	24.9	17.7
1999	15.9	16.7	20.0	24.7	31.3	31.3	33.4	34.8	31.8	27.8	22.3	18.3
2000	12.4	15.0	17.7	26	28.9	33.0	37.7	33.7	31.4	26.4	20.7	15.3
2001	15.1	14.8	27.7	25.7	29.3	33.4	34.6	34.1	31.2	27.3	20.5	15.4
2002	11.3	17.2	20.8	22.8	28.1	31.8	35.0	33.7	32.8	30.0	21.2	14.3

Mean Minimum Air Temperature ° C

Year	Jan	Feb	Mar	Apr	May	Jun	Jul	Aug	Sep	Oct	Nov	Dec
1993	-0.4	-0.4	2.7	5.3	10.2	12.4	13.1	14.3	11.2	11.7	8.0	4.8
1994	4.1	20	3.7	8.5	10.8	12.0	14.1	13.4	14.4	13.8	8.8	1.9
1995	1.1	2.5	2.9	5.3	10.0	13.4	14.2	13.8	13.4	8.1	4.1	2.2
1996	2.8	3.3	4.3	6.6	11.9	11.9	17.1	14.9	13.1	8.9	8.0	3.5
1997	2.2	-0.2	2.8	5.5	11.2	12.7	14.5	13.6	11.5	10.9	8.1	3.5
1998	2.3	2.9	3.2	8.0	11.9	12.2	14.7	15.3	14.5	10.0	7.4	3.7
1999	2.4	2.1	4.2	7.3	12.5	13.2	15.3	15.1	13.9	10.5	5.5	2.7
2000	1.9	0.7	2.7	3.5	9.5	12.7	17.1	15.5	12.9	10.4	8.2	4.2
2001	2.2	2.3	0.8	3.7	11.0	13.3	15.0	15.9	12.9	10.1	5.5	3.7
2002	1.7	3.3	5.7	6.8	5.5	12.4	15.6	14.9	13.4	12.6	7.2	4.5

Daily Mean Relative Humidity %

Year	Jan	Feb	Mar	Apr	May	Jun	Jul	Aug	Sep	Oct	Nov	Dec
1993	83.0	85.0	75.0	51.0	54.0	57.0	65.0	64.0	73.0	72.0	76.0	83.0
1994	85.0	82.0	83.0	54.0	57.0	59.0	62.0	66.0	72.0	71.0	87.0	89.0
1995	83.0	83.0	73.0	62.0	57.0	57.0	63.0	63.0	62.0	67.0	62.0	84.0
1996	84.0	71.0	81.0	58.0	41.0	47.0	43.0	40.0	47.0	51.0	61.0	73.0
1997	72.0	71.0	72.0	54.0	37.0	44.0	47.0	58.0	52.0	54.0	70.0	78.0
1998	87.4	74.4	67.8	50.5	45.1	46.1	47.8	48.9	50.9	47.1	49.2	59.1
1999	66.0	68.0	63.0	47.7	44.7	67.7	56.6	56.9	57.5	63.5	57.1	54.1
2000	78.0	75.6	70.0	53.0	50.0	46.0	46.0	54.0	88.0	70.0	84.0	88.0
2001	78.7	79.2	50.5	68.2	60.5	42.2	66.0	67.0	72.3	66.0	71.5	83.1
2002	66.4	65.6	83.2	85.8	68.2	66.1	48.8	60.0	53.8	68.8	62.8	82.9

Table A.3: Recorded values for ambient temperature and humidity measured at Dead Sea region for the period of ten years (1993-2002)

Mean Maximum Air Temperature ° C

Year	Jan	Feb	Mar	Apr	May	Jun	Jul	Aug	Sep	Oct	Nov	Dec
1993	17.3	17.2	22.7	29.9	31.7	37.5	38.2	39.2	36.6	34.9	25.8	23.3
1994	20.6	20.5	23.3	32.4	35.4	36.5	38.2	38.9	38.3	34.9	23.2	17.9
1995	19.8	20.7	24.5	28.4	34.6	38.0	38.3	38.9	37.1	32.3	24.8	20.5
1996	19.1	21.6	22.5	28.0	35.4	37.4	39.3	49.4	37.3	31.7	27.8	22.3
1997	20.0	18.2	20.4	26.6	35.6	37.4	39.0	47.2	35.8	32.7	26.5	21.1
1998	18.6	20.5	22.1	30.4	34.6	37.4	39.9	40.8	38.1	34.6	29.6	23.2
1999	21.1	22.1	25.7	30.1	36.3	37.3	39.4	40.0	37.7	33.5	27.9	23.1
2000	17.6	20.0	22.5	30.4	34.3	38.3	41.5	39.2	38.8	31.5	27.4	20.8
2001	20.5	20.5	29.6	31.5	34.7	39.0	39.9	39.4	35.8	33.0	25.9	20.5
2002	17.3	22.5	26.5	27.5	33.2	37.5	40.5	49.3	38.1	33.9	27.9	20.1

Mean Minimum Air Temperature ° C

Year	Jan	Feb	Mar	Apr	May	Jun	Jul	Aug	Sep	Oct	Nov	Dec
1993	9.5	8.7	11.6	15.3	18.1	22.0	23.6	24.5	22.9	23.3	15.8	14.5
1994	13.4	11.8	12.5	16.1	19.6	21.9	24.0	24.7	25.4	23.9	16.0	11.1
1995	11.6	11.3	12.9	14.7	19.4	22.5	24.8	25.3	23.9	20.5	15.2	12.6
1996	11.7	12.1	12.5	14.7	19.2	22.0	25.1	25.0	23.8	20.4	18.6	14.4
1997	11.7	8.9	10.8	13.7	19.0	22.1	25.5	23.8	22.4	20.9	17.6	13.1
1998	10.9	10.8	12.2	16.6	19.9	21.9	24.4	25.6	24.8	21.9	19.0	15.0
1999	12.4	12.1	14.1	15.9	20.7	23.1	25.0	26.0	24.9	22.0	17.6	13.5
2000	10.1	10.9	11.4	16.3	18.6	22.7	26.2	25.7	24.2	20.9	17.4	13.9
2001	12.0	11.9	16.1	18.1	19.9	22.9	24.7	26.0	24.4	22.1	15.9	13.0
2002	10.5	11.4	14.8	14.6	18.3	23.1	26.1	26.1	24.6	22.3	18.3	12.7

Daily Mean Relative Humidity %

Year	Jan	Feb	Mar	Apr	May	Jun	Jul	Aug	Sep	Oct	Nov	Dec
1993	53.0	71.0	55.0	45.0	50.0	46.0	48.0	49.0	48.0	42.0	47.0	57.0
1994	63.0	62.0	65.0	42.0	48.0	51.0	52.0	57.0	50.0	47.0	53.0	58.0
1995	60.0	66.0	58.0	48.0	39.0	43.0	48.0	52.0	62.0	61.0	47.0	57.0
1996	65.0	63.0	68.0	54.0	53.0	55.0	48.0	50.0	49.0	44.0	36.0	50.0
1997	50.0	50.0	61.0	48.0	42.0	49.0	41.0	43.0	43.0	44.0	64.0	77.0
1998	76.5	70.1	66.6	58.5	56.4	63.0	61.0	66.5	63.5	60.1	56.2	53.1
1999	59.9	63.4	59.4	59.8	55.6	55.0	42.7	44.6	44.1	44.9	36.8	52.3
2000	68.0	63.0	63.0	58.0	55.0	57.0	58.0	64.0	65.0	59.0	44.0	74.0
2001	71.3	73.2	55.1	55.9	52.0	55.0	60.5	53.1	63.9	59.5	56.9	73.4
2002	69.1	54.8	57.3	60.0	65.9	62.4	61.8	58.6	56.1	86.9	52.7	80.0

Table A.4: Recorded values for ambient temperature and humidity measured at Aqaba for the period of ten years (1993-2002)

Mean Maximum Air Temperature ° C

Year	Jan	Feb	Mar	Apr	May	Jun	Jul	Aug	Sep	Oct	Nov	Dec
1993	18.2	19.7	24.7	31.0	33.7	38.9	39.5	40.4	36.5	34.1	26.8	22.7
1994	20.9	21.8	25.3	32.7	36.0	37.6	39.5	37.7	34.5	25.4	19.6	30.9
1995	20.6	22.0	26.2	29.3	35.1	39.8	39.4	37.4	31.5	30.9	24.5	30.6
1996	20.4	23.0	24.9	30.2	36.6	37.6	40.1	39.4	37.7	31.9	27.7	23.7
1997	21.8	20.2	23.8	28.9	35.4	38.6	40.0	38.3	35.8	32.5	27.6	22.1
1998	20.7	22.8	24.6	32.7	5.2	38.2	41.0	41.1	37.9	33.9	28.2	22.9
1999	26.41	21.9	26.4	30.9	35.7	37.8	39.5	40.2	36.9	37.5	28.0	23.2
2000	19.8	21.4	24.1	32.1	35.0	38.9	41.8	38.8	36.7	30.9	26.9	21.8
2001	21.2	22.7	29.6	31.0	34.9	34.9	38.9	49.5	39.4	36.6	32.1	22.2
2002	19.1	24.4	27.7	29.5	34.7	37.9	41.3	38.7	37.4	32.8	28.3	22.1

Mean Minimum Air Temperature ° C

Year	Jan	Feb	Mar	Apr	May	Jun	Jul	Aug	Sep	Oct	Nov	Dec
1993	7.3	8.1	12.1	16.6	20.8	23.8	24.7	25.9	23.3	21.3	14.9	12.1
1994	11.1	9.7	12.3	18.7	21.2	23.0	25.3	25.7	24.7	22.8	14.4	8.3
1995	8.4	10.4	13.7	15.4	20.7	24.5	25.7	25.8	24.5	19.6	13.1	9.9
1996	9.3	11.4	12.6	16.2	22.3	22.8	26.7	26.3	24.0	19.2	16.1	11.3
1997	9.4	7.8	11.5	15.0	21.9	24.2	25.4	24.6	22.9	20.2	11.2	10.6
1998	9.2	10.9	12.8	18.9	22.0	24.0	26.6	28.1	20.9	27.8	16.3	11.4
1999	10.0	11.2	13.8	16.9	22.5	24.2	26.2	26.9	24.3	20.9	15.6	10.8
2000	8.9	9.2	11.5	24.3	27.9	25.7	23.9	27.9	23.9	19.3	14.7	11.1
2001	8.9	9.9	16.6	18.2	21.5	24.8	26.3	24.1	20.5	21.3	13.9	11.8
2002	8.7	11.8	15.3	17.2	19.8	23.6	27.2	26.6	24.2	22.1	16.7	11.4

Daily Mean Relative Humidity %

18.2	20.4 124.	Feb	Mar	Apr	May	Jun	Jul	Aug	Sep	Oct	Nov	Dec
1993	62.0	57.0	50.0	37.0	35.0	30.0	34.0	36.0	45.0	44.0	52.0	53.0
1994	65.0	50.0	52.0	33.0	35.0	38.0	35.0	35.0	47.0	55.0	61.0	52.0
1995	63.0	63.0	55.0	48.0	43.0	37.0	36.0	41.0	47.0	54.0	45.0	55.0
1996	52.0	52.0	54.0	46.0	40.0	44.0	51.0	52.0	51.0	55.0	56.0	66.0
1997	65.0	63.3	53.3	43.1	52.6	44.2	40.4	51.0	58.5	59.7	68.1	65.2
1998	60.9	53.3	53.0	43.1	52.6	52.8	44.2	40.4	51.0	58.5	59.7	68.1
1999	62.0	71.0	67.0	47.0	45.0	46.0	50.0	59.0	65.0	73.0	64.0	58.7
2000	69.1	61.9	59.3	49.0	50.0	47.5	49.9	53.7	60.2	70.8	65.0	54.9
2001	69.1	61.1	56.8	56.9	50.4	46.9	50.2	62.3	68.5	74.5	72.0	77.1
2002	60.2	51.5	67.8	70.3	65.7	51.0	40.5	45.0	50.7	63.2	48.5	63.0

Table A.5: Typical values for chloride concentrations

Plant	Unit	Concrete Element	Location of Sample from Outer Surface (mm)	%Chloride Content by weight of concrete
Hot Leaching	Carnalite	Footing	0 - 30	0.359
			30 – 60	0.235
			60 – 90	0.465
			90 – 120	0.095
			120 - 150	0.083
		Slab 1	0 - 30	0.741
			30 – 60	0.599
			60 – 90	2.188
			90 – 120	2.576
			120 - 150	N.A.
		Slab 2	0 - 30	0.668
			30 – 60	0.302
			60 – 90	0.091
			90 – 120	0.05
			120 - 150	0.05
		Slab3	0 - 30	0.136
			30 – 60	0.531
			60 – 90	0.842
			90 – 120	1.207
			120 - 150	N. A.
	Sylvinite	Footing	0 - 30	0.151
			30 – 60	0.093
			60 – 90	0.091
			90 – 120	0.09
			120 - 150	0.084
		Slab 1	0 - 30	0.292
			30 – 60	0.173
			60 – 90	0.044
			90 – 120	0.026
			120 - 150	N. A.
		Slab 2	0 - 30	0.133
			30 – 60	0.043
			60 – 90	0.042
			90 – 120	0.032
			120 - 150	0.027
	Screening	Slab1	0 - 30	0.982
			30 – 60	0.857
			60 – 90	0.843
			90 – 120	0.834
			120 - 150	0.821
Cold Crystallization	Carnalite	Slab 1	0 - 30	0.509
			30 – 60	0.055
			60 – 90	< 0.01
			90 – 120	0.039
			120 - 150	0.017
		Slab 2	0 - 30	0.0444
			30 – 60	0.124
			60 – 90	0.074
			90 – 120	0.053
			120 - 150	0.046
	Product Centrifuge	Slab 1	0 - 30	0.45
			30 – 60	0.103
			60 – 90	0.088
			90 – 120	0.065
			120 - 150	0.037
		Slab 2	0 - 30	0.566
			30 – 60	0.101
			60 – 90	0.05
			90 – 120	0.035
			120 - 150	0.026

Appendix B

Experimental Test Results/RC Slabs

Table B.1: Summary of test results

Specimen No.	Average Measured Values					Predicted Theoretical Values				Failure Modes
	Tensile Strength (N/mm^2)	P_u (kN)	M_u (kNM)	Δ_{max} (mm)	$*\varepsilon_{max}$ (%)	P_u (kN)	M_u (kNM)	Δ_{max} (mm)	ε_{max} (%)	
G_E1_N	3.07	100.2	33.07	11.8	0.00531	140	43.97	15	0.006	**DIC
G_E1M_N	3.16	100.43	33.14	11.84	0.00502	140	43.97	15	0.006	DIC
G_E2_N	2.99	99.95	32.98	11.5	0.00562	140	43.97	15	0.006	DIC
G_E1_S	2.95	100.27	33.089	11.36	0.00528	140	43.97	15	0.006	**DIC-SF
G_E1M_S	3.09	110.03	36.31	12.52	0.0058	140	43.97	15	0.006	DIC-SF
G_E2_S	3.11	99.98	32.93	11.25	0.00559	140	43.97	15	0.006	DIC-SF
J_E1_A	3.13	99.84	32.95	11.24	0.00534	140	43.97	15	0.006	DIC
J_E1M_A	3.35	99.96	32.99	11.43	0.00556	140	43.97	15	0.006	DIC
J_E2_A	3.02	99.61	32.87	11.3	0.00526	140	43.97	15	0.006	DIC
J_E1_Q	3.19	99.52	32.84	11.01	0.00539	140	43.97	15	0.006	DIC
J_E1M_Q	2.99	99.78	32.93	11.36	.00544	140	43.97	15	0.006	DIC
J_E2_Q	3.07	99.24	32.75	10.95	0.00528	140	43.97	15	0.006	DIC
J_E1_D	2.92	89.16	29.42	10.09	0.00445	140	43.97	15	0.006	DIC
J_E1M_D	3.13	96.31	31.78	11.29	0.00506	140	43.97	15	0.006	DIC
J_E2_D	3.45	88.26	29.126	9.90	0.00426	140	43.97	15	0.006	DIC

Notes:

***: Average maximum strain measured at the middle of the CFRP plates using electrical strain gauges.**

****: DIC: debonding of the CFRP plate by intermediate flexural crack.**

*****: DIC-SF: debonding of the CFRP plate by intermediate flexural crack followed directly by shear failure.**

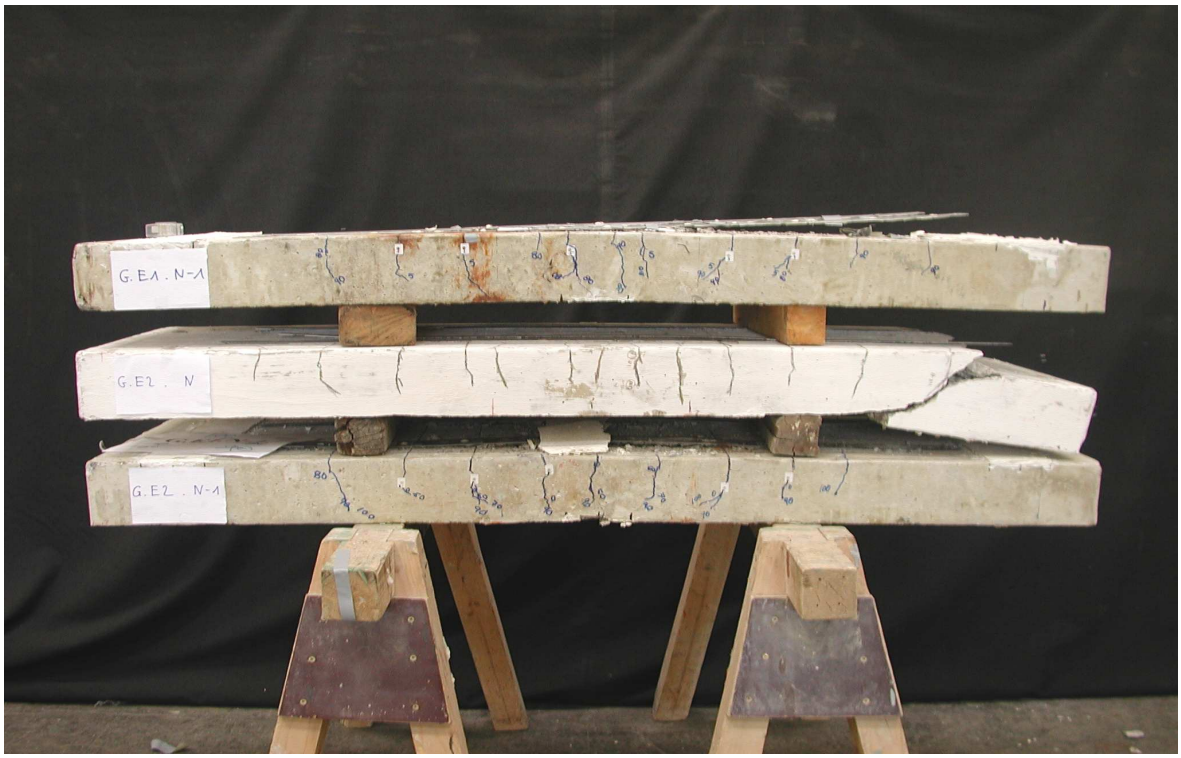

Figure B.1: Failure modes of specimens exposed to normal laboratory conditions at iBMB laboratory-Germany

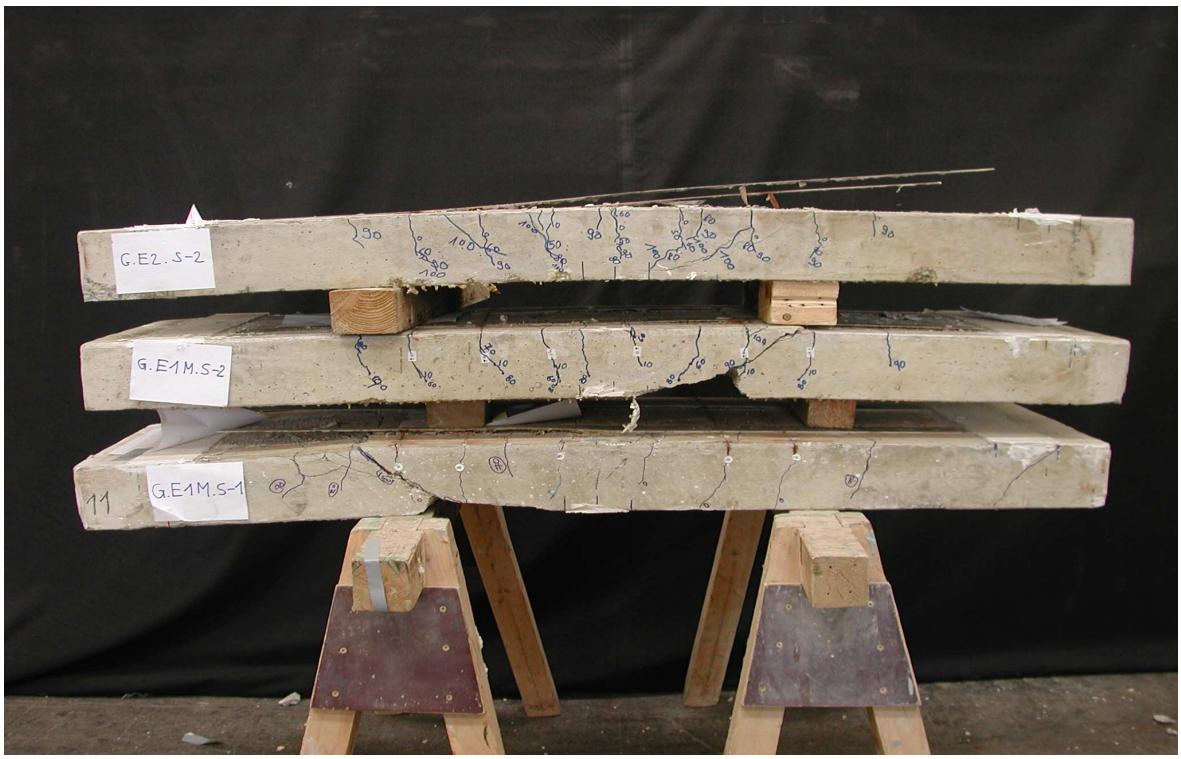

Figure B.2: Failure modes of specimens exposed to salt solution and normal laboratory conditions at iBMB laboratory-Germany

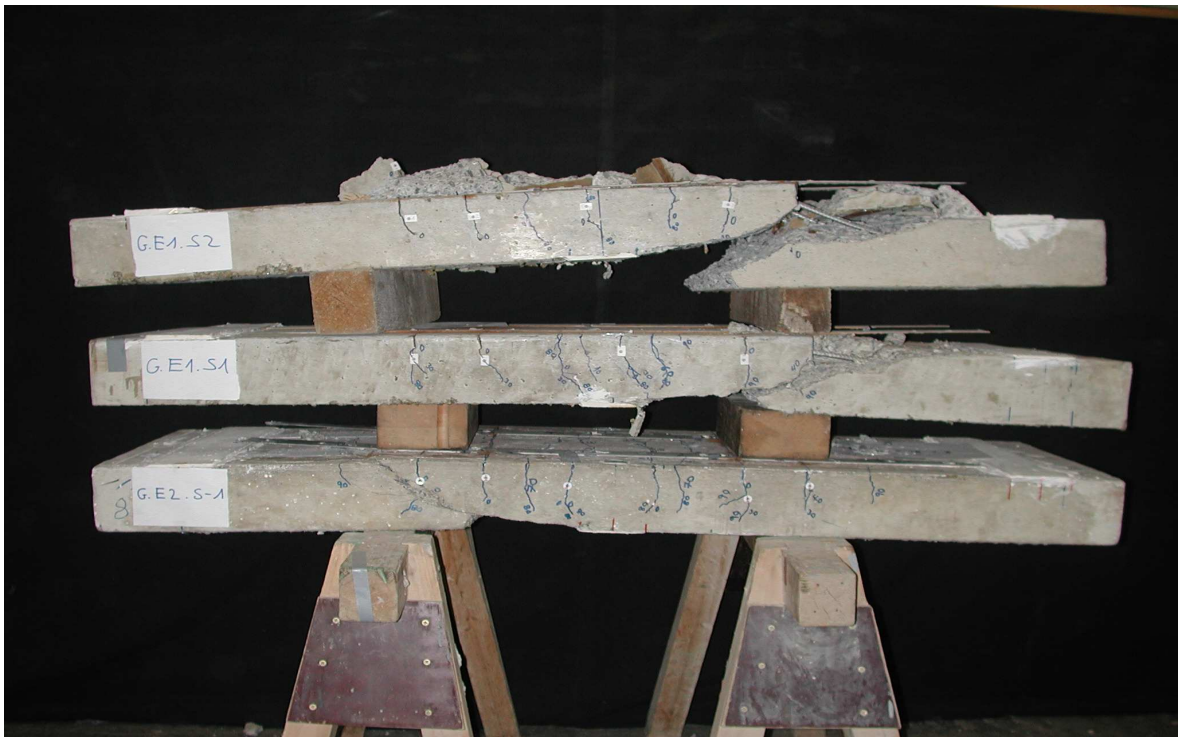

Figure B.3: Failure modes of specimens exposed to salt solution and normal laboratory conditions at iBMB laboratory-Germany

Figure B.4: Failure modes of specimens exposed to real-life environment at Amman-Jordan

Figure B.5: Failure modes of specimens exposed to real environment at Aqaba region-Jordan

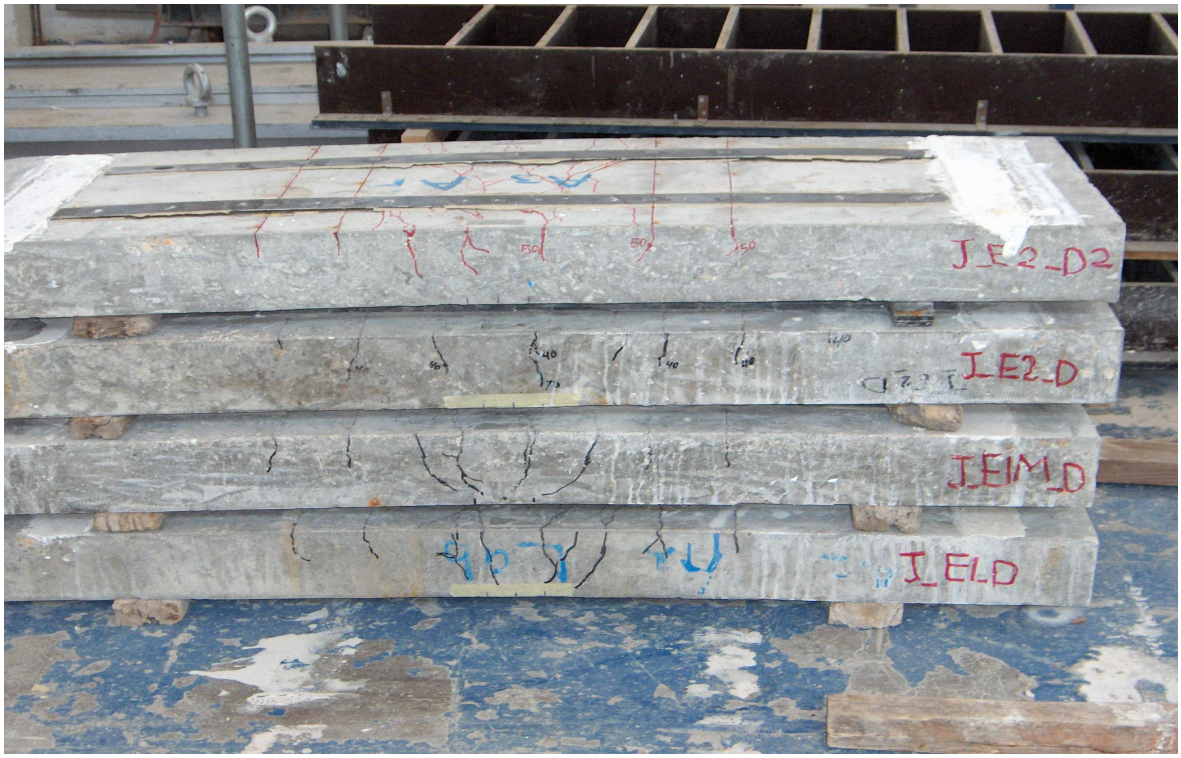

Figure B.6: Failure modes of specimens exposed to real environment at Dead Sea region-Jordan

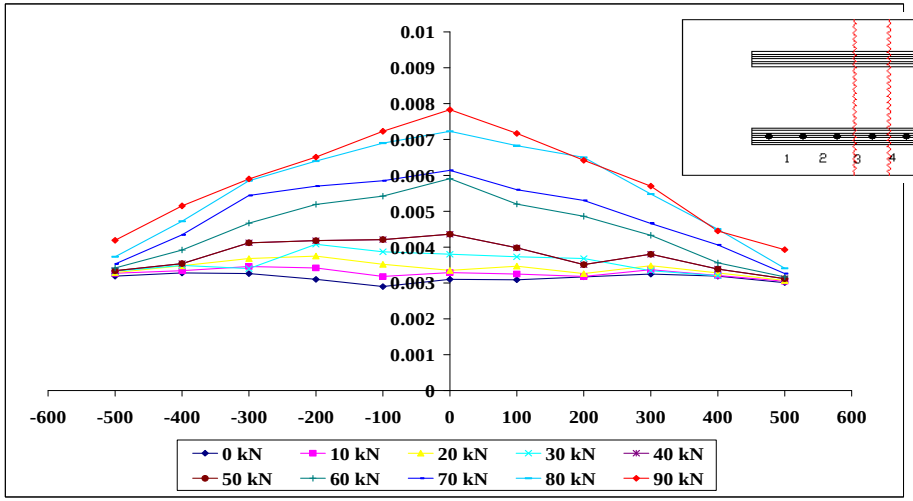

Figure B.7: Strains along CFRP plate for specimen G_E1_N

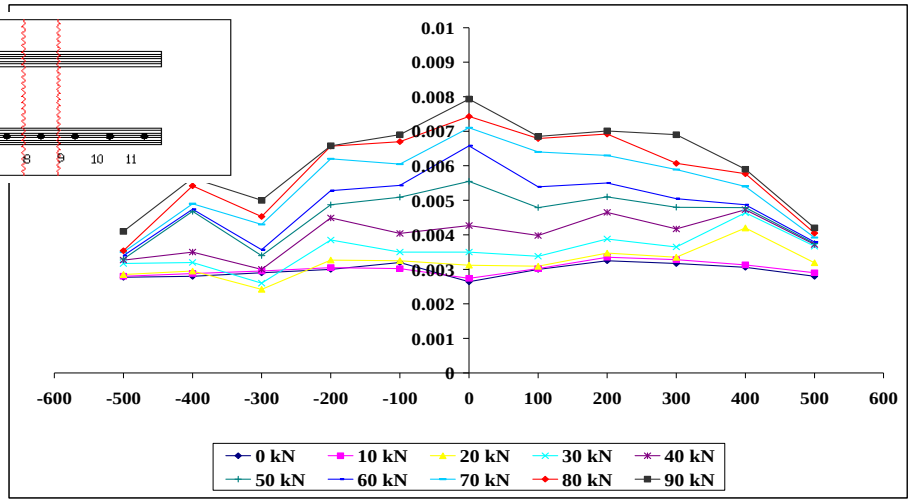

Figure B.8: Strains along CFRP plate for specimen G_E1M_N

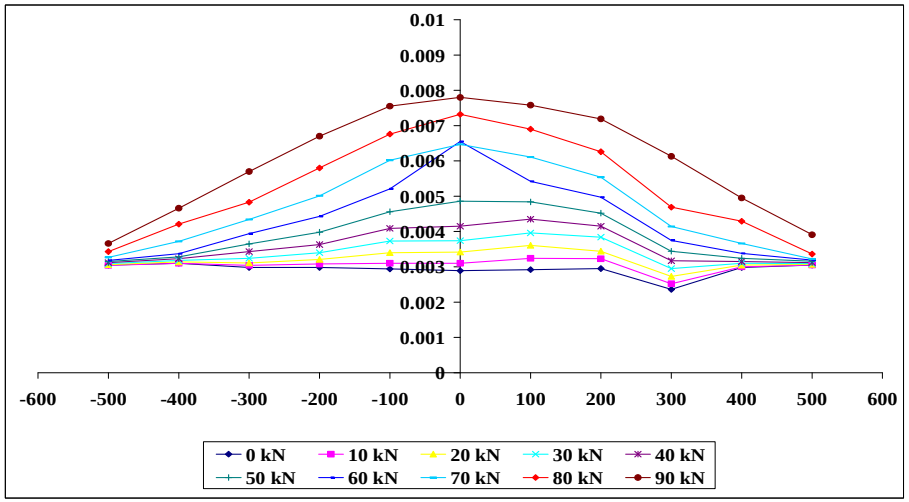

Figure B.9: Strains along CFRP plate for specimen G_E2_N

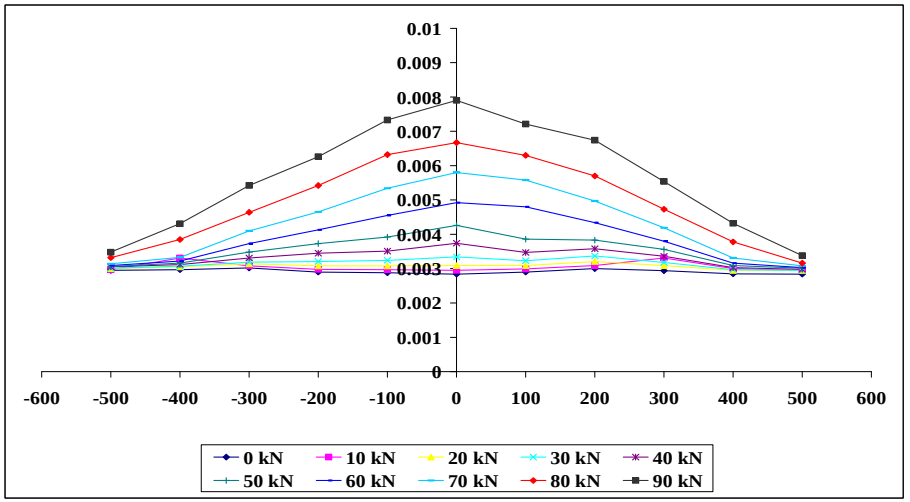

Figure B.10: Strains along CFRP plate for specimen G_E1_S

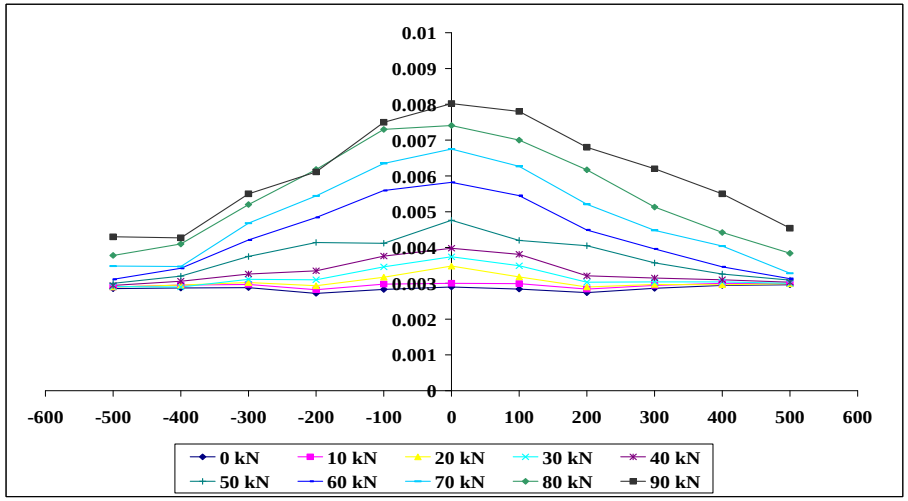

Figure B.11: Strains along CFRP plate for specimen G_E1M_S

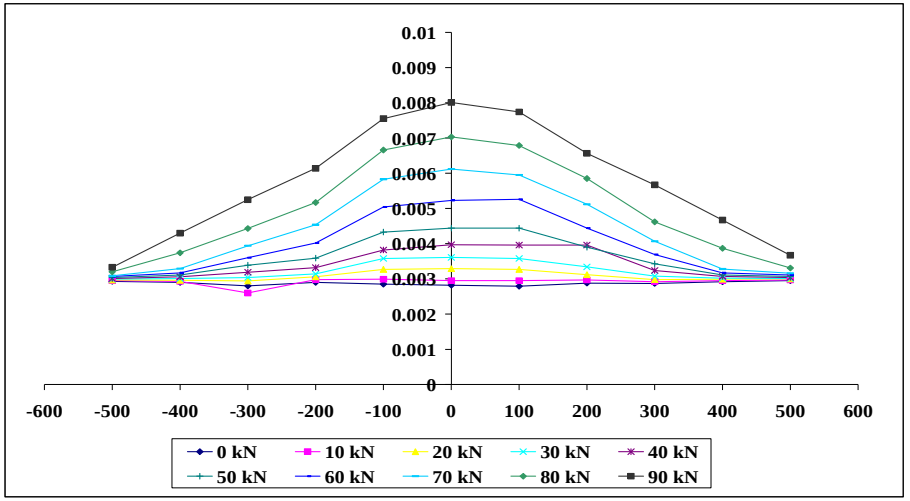

Figure B.12: Strains along CFRP plate for specimen G_E2_S

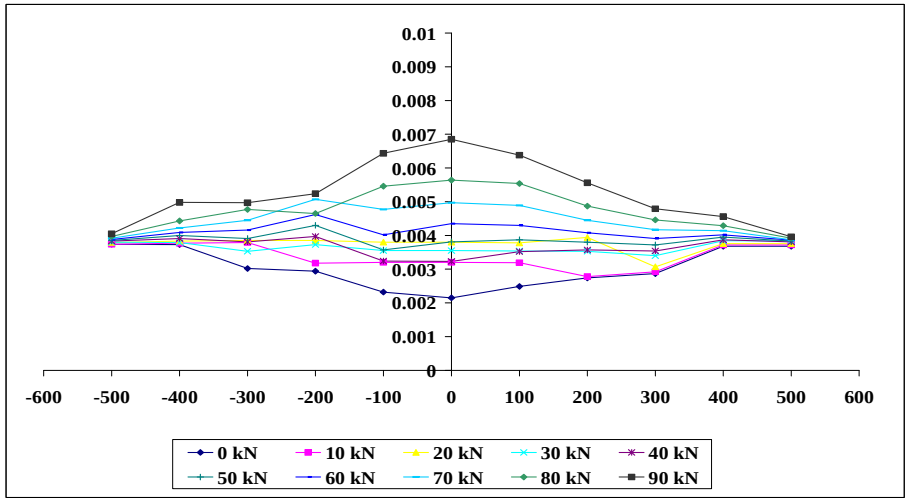

Figure B.13: Strains along CFRP plate for specimen J_E1_A

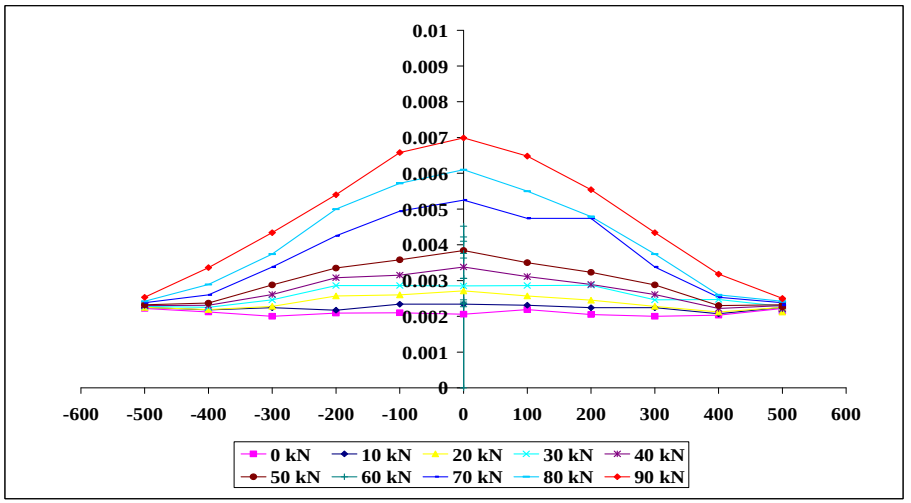

Figure B.14: Strains along CFRP plate for specimen J_E1M_A

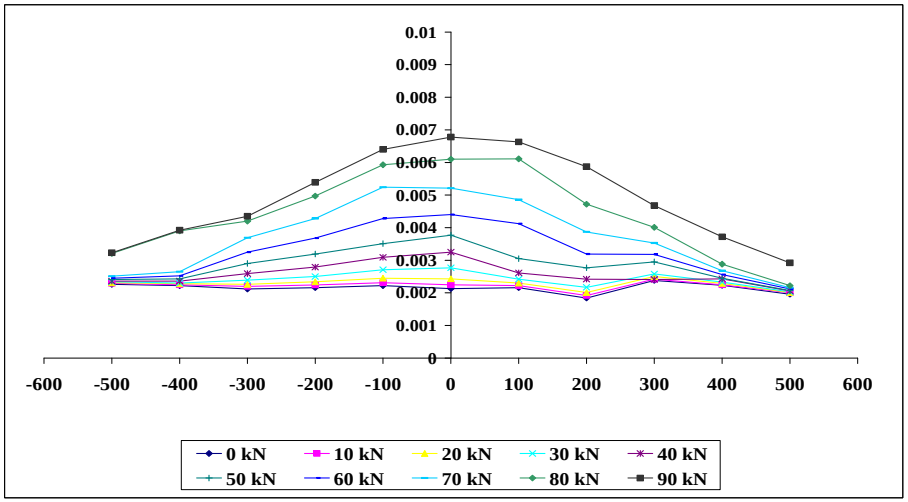

Figure B.15: Strains along CFRP plate for specimen J_E2_A

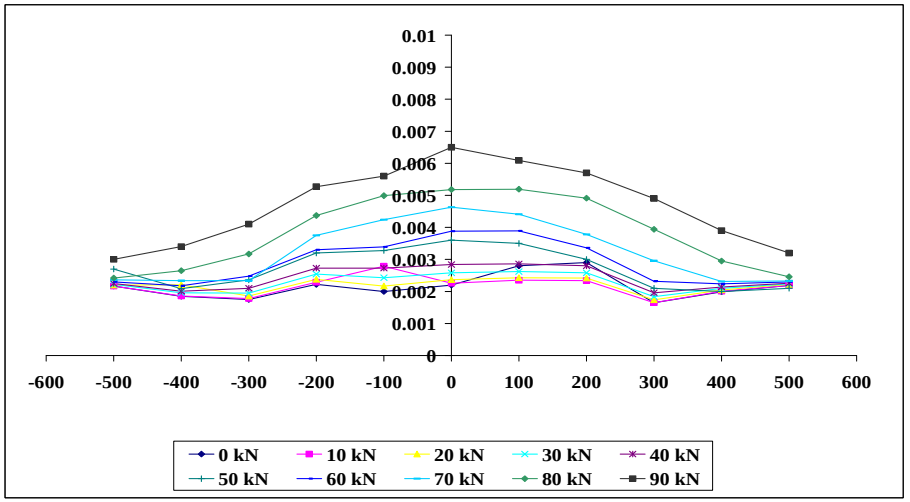

Figure B.16: Strains along CFRP plate for specimen J_E1_Q

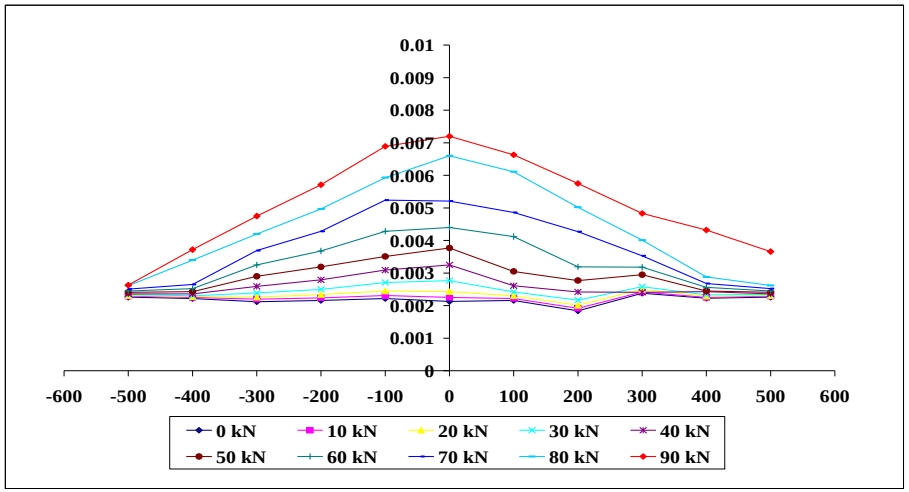

Figure B.17: Strains along CFRP plate for specimen J_E1M_Q

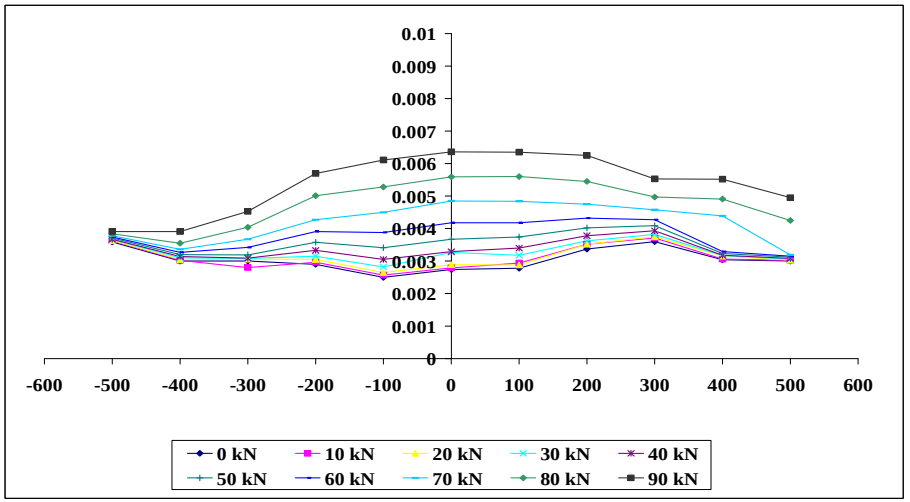

Figure B.18: Strains along CFRP plate for specimen J_E2_Q

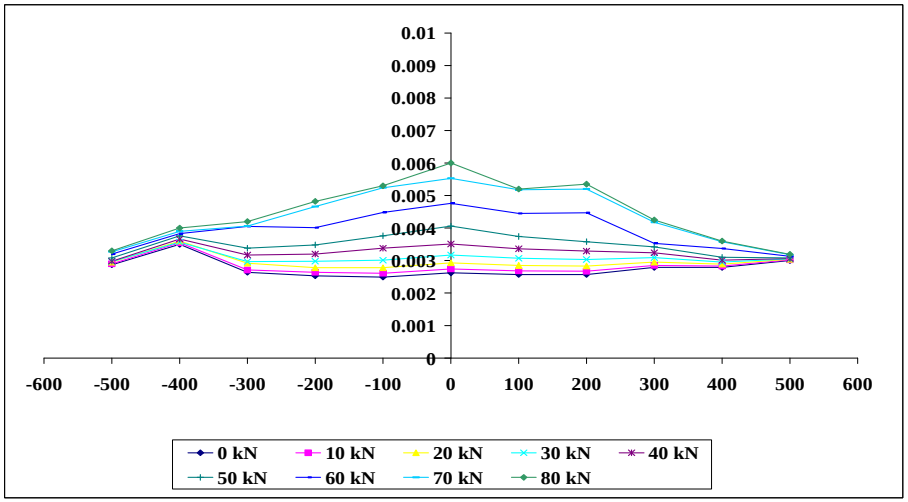

Figure B.19: Strains along CFRP plate for specimen J_E1_D

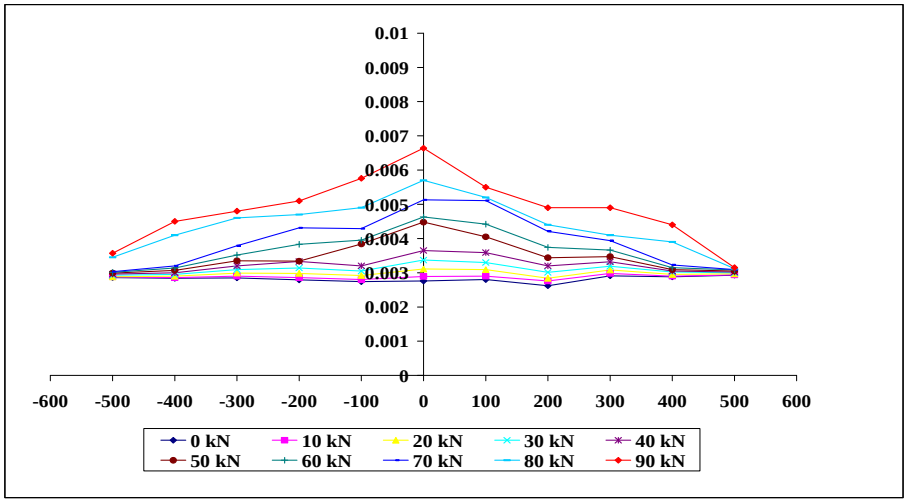

Figure B.20: Strains along CFRP plate for specimen J_E1M_D

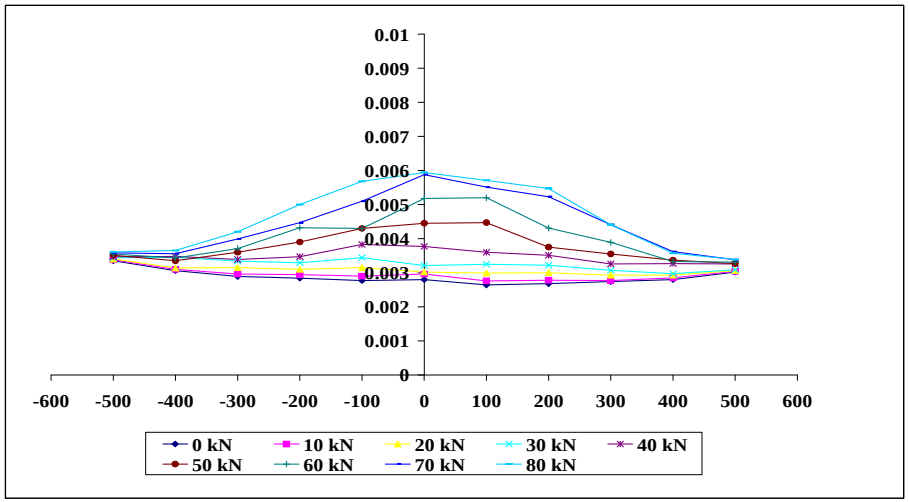

Figure B.21: Strains along CFRP plate for specimen J_E2_D

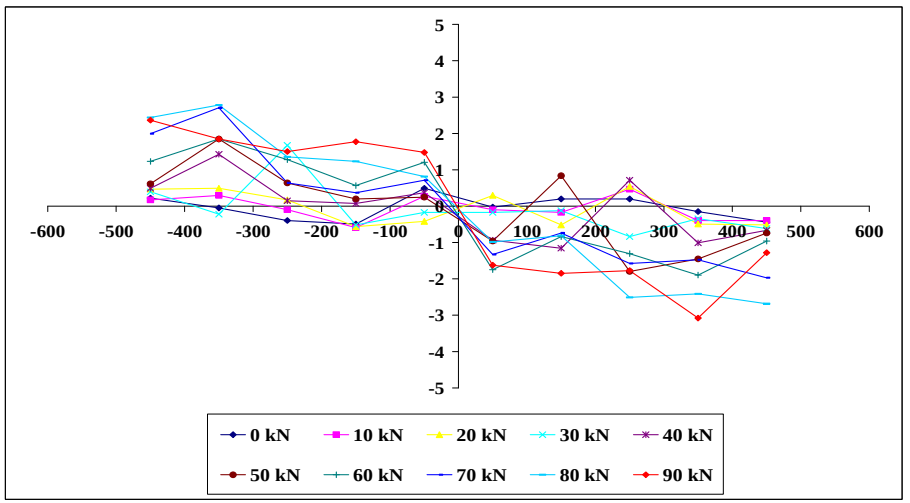

Figure B.22: Shear stresses along CFRP plate for specimen G_E1_N

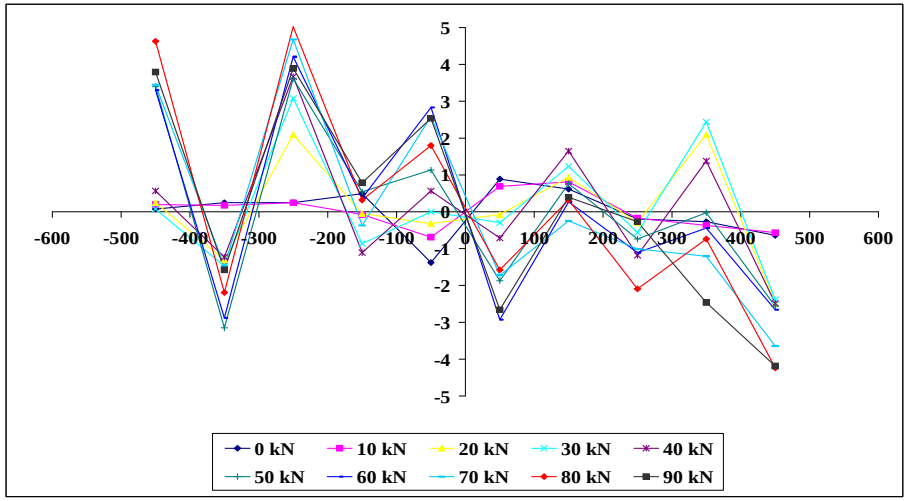

Figure B.23: Shear stresses along CFRP plate for specimen G_E1M_N

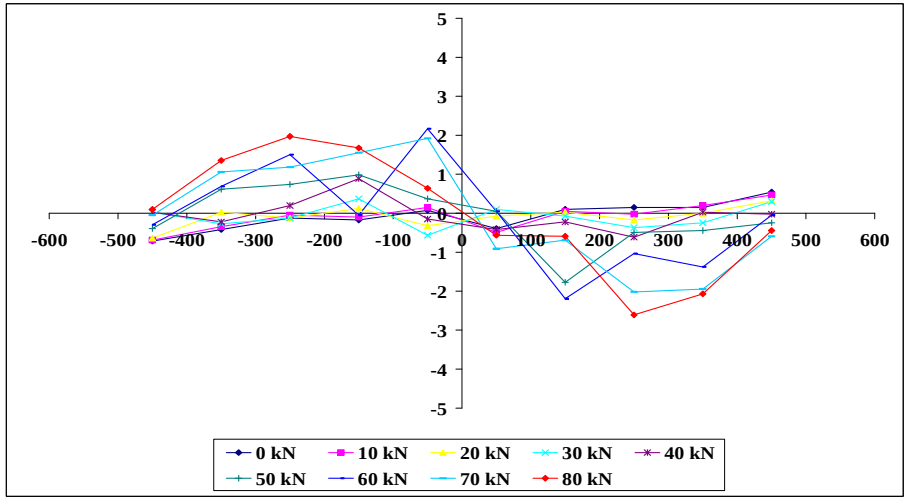

Figure B.24: Shear stresses along CFRP plate for specimen J_E2_D

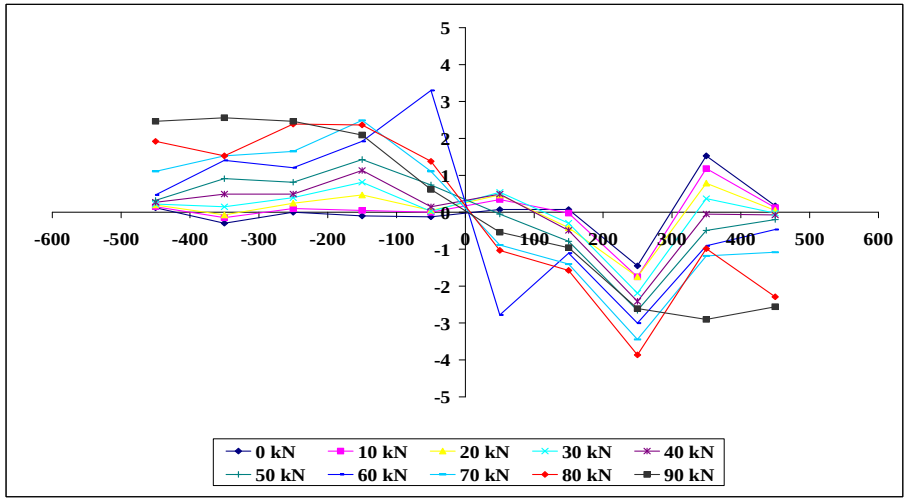

Figure B.25: Shear stresses along CFRP plate for specimen G_E2_N

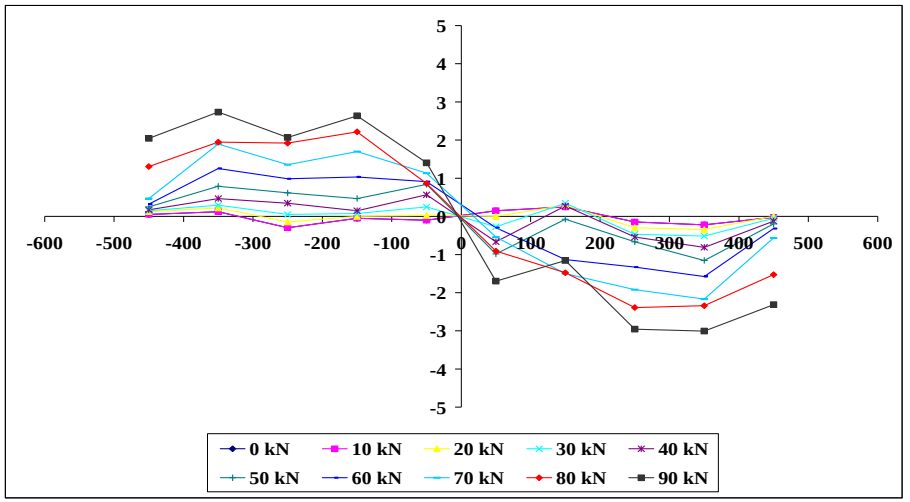

Figure B.26: Shear stresses along CFRP plate for specimen G_E1_S

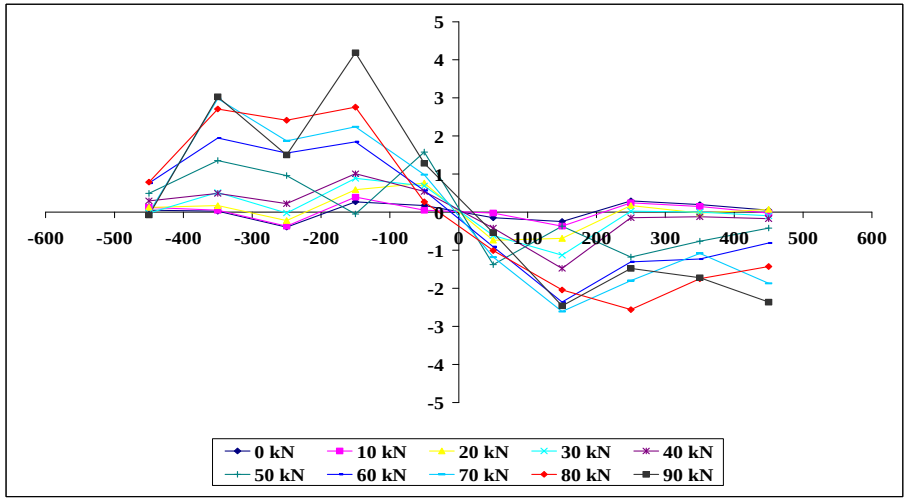

Figure B.27: Shear stresses along CFRP plate for specimen G_E1M_S

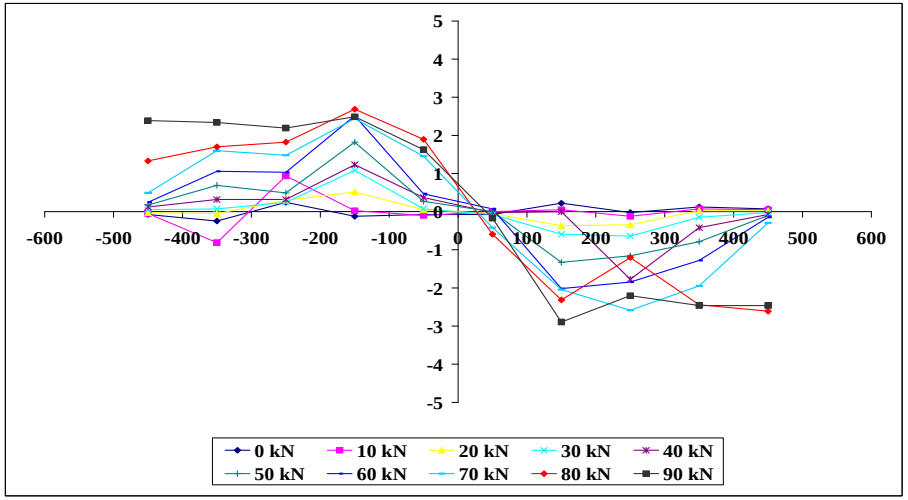

Figure B.28: Shear stresses along CFRP plate for specimen G_E2_S

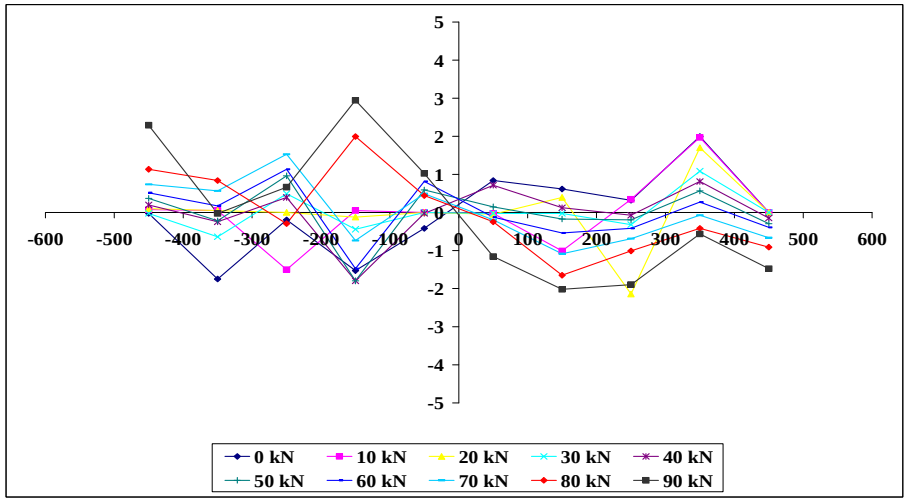

Figure B.29: Shear stresses along CFRP plate for specimen J_E1_A

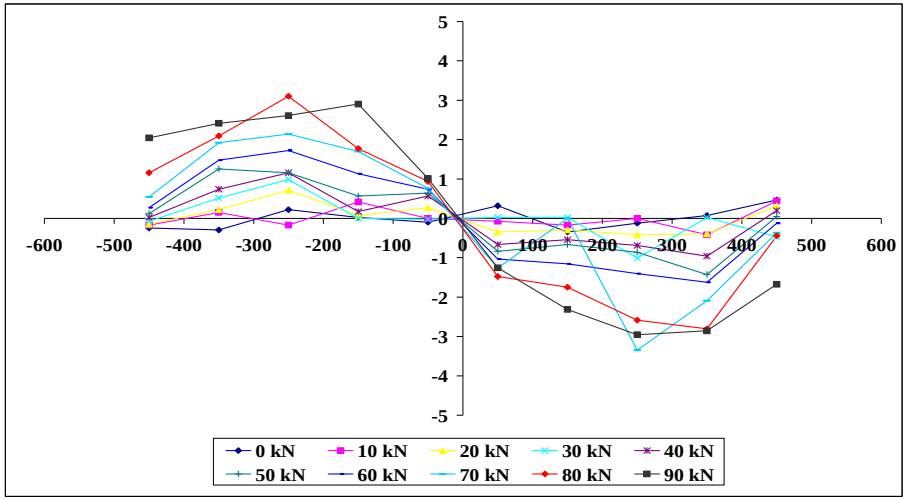

Figure B.30: Shear stresses along CFRP plate for specimen J_E1M_A

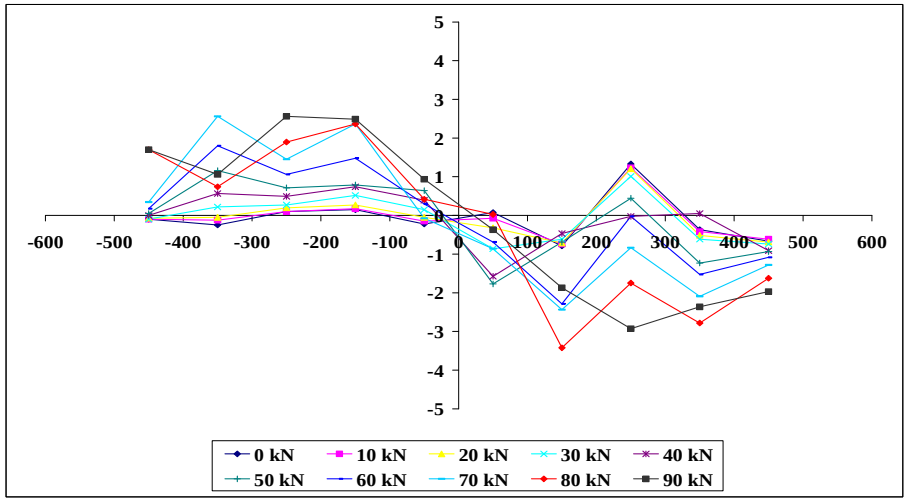

Figure B.31: Shear stresses along CFRP plate for specimen J_E2_A

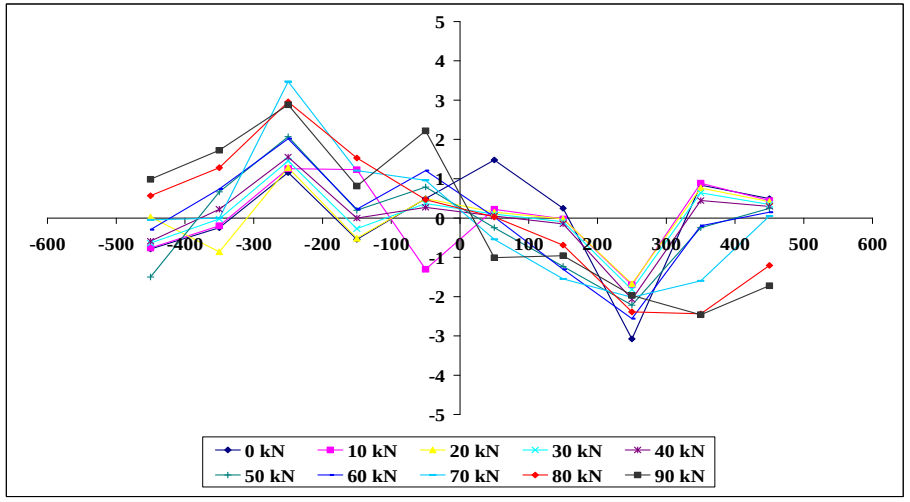

Figure B.32: Shear stresses along CFRP plate for specimen J_E1_Q

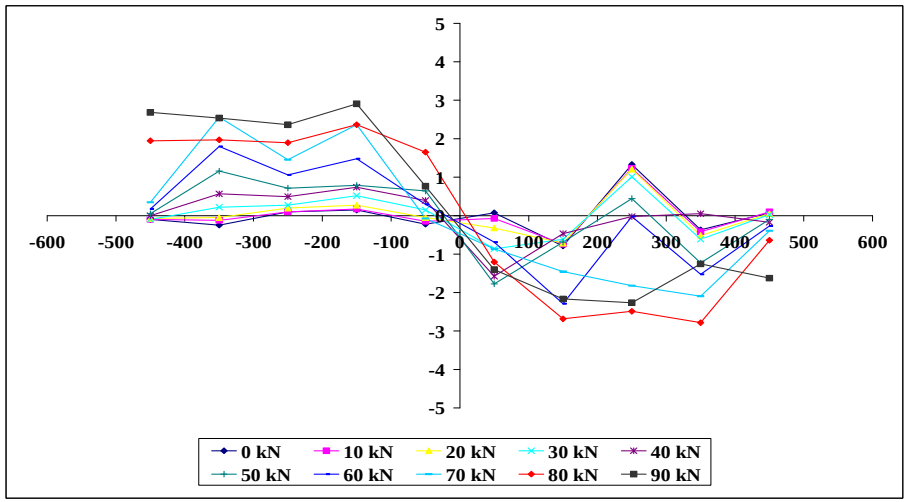

Figure B.33: Shear stresses along CFRP plate for specimen J_E1M_Q

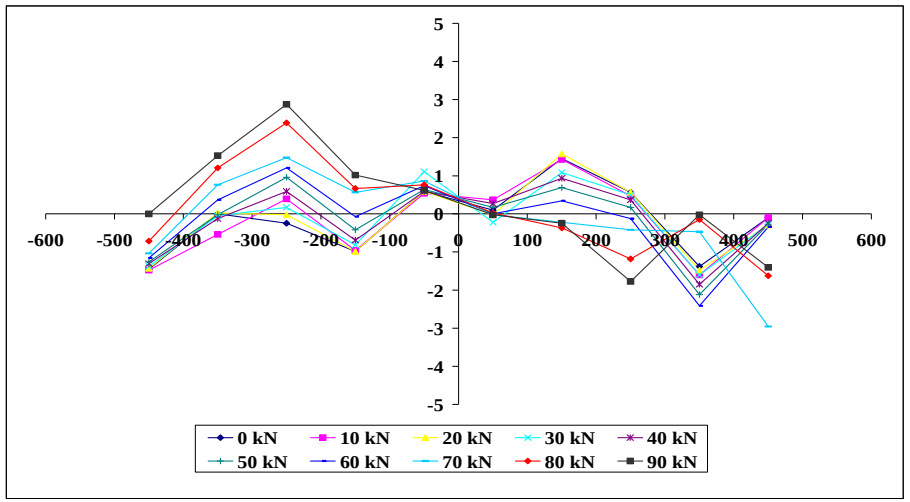

Figure B.34: Shear stresses along CFRP plate for specimen J_E2_Q

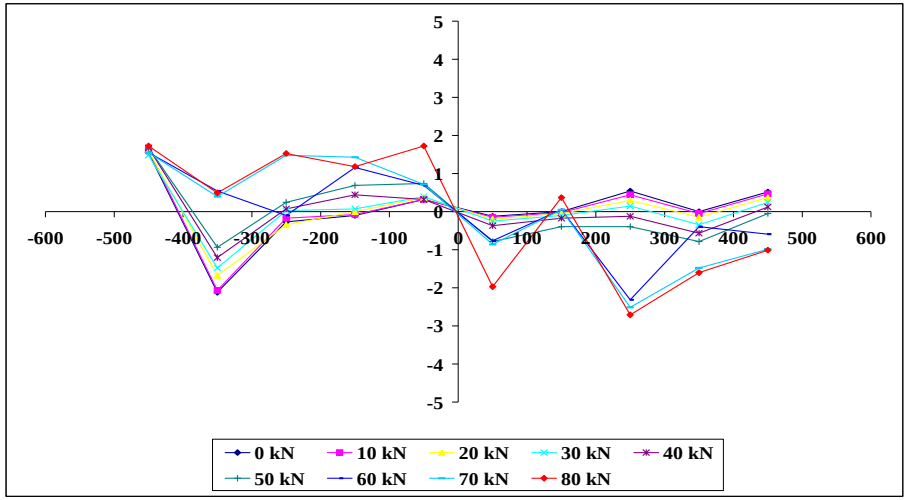

Figure B.35: Shear stresses along CFRP plate for specimen J_E1_D

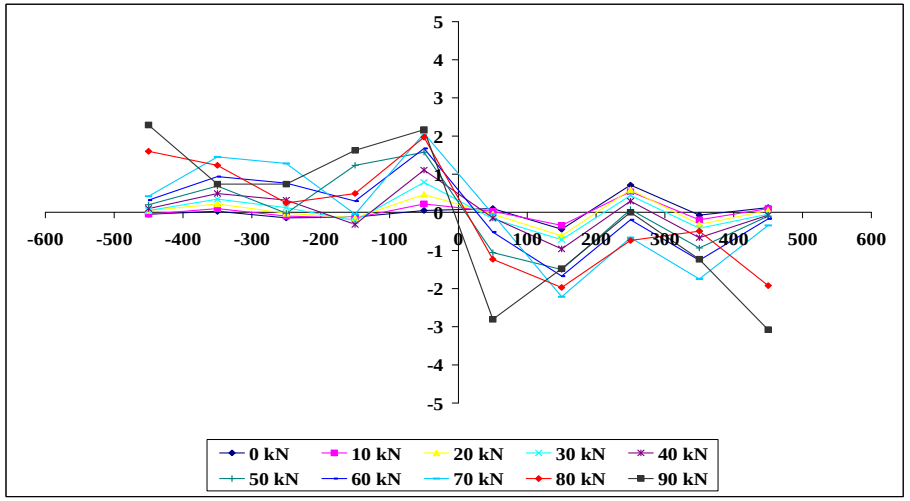

Figure B.36: Shear stresses along CFRP plate for specimen J_E1M_D

Appendix C

Approximate Analysis of Stress Concentrations in the Adhesive Layer of Plated RC Slab

The solution presented herein is for determining the maximum stresses in the adhesive layer is based on the following assumptions, (1) linear elastic behaviour in the FRP, adhesive, concrete and reinforcing steel; (2) linear strain distribution over the full depth of the section; and (3) the thickness of the adhesive layer is assumed to be thin so that the stresses can be considered as constant through the layers thickness.

The analysis outlined hereunder is made for specimens that were exposed to normal laboratory conditions, considering material properties, material dimensions and crack location as shown in Table C.1 and Figure C.1, in addition to the loading conditions of moments and shears at the considered crack.

Calculations are made for finding peeling stresses at crack No.3 of specimen G_E2_N to the right of midspan.

Table C.1: Dimensions and material properties

Material	Width (mm)	Thickness (mm)	Height (mm)	Elastic Modulus (N/mm^2)	Shear Modulus (N/mm^2)	Area (mm^2)
Concrete	b_c: 500	t_c: 120	-	27000		
CFRP	b_f: 50	t_f: 1.47	h_f: 121	167500		147
Epoxy Type 1	b_a: 50	t_a: 3	-	7905	2927.8	
Epoxy Type1 Modified	**ba: 50**	t_a: 3	-	5716	2117	
Epoxy Type2	b_a: 50	t_a: 3	-	8995	3331.5	
Steel	-		h_s: 90	210000		393

Epoxy poisonous ratio, $\nu = 0.35$

Shear modulus, $G = \dfrac{1}{2(1+\nu)}$

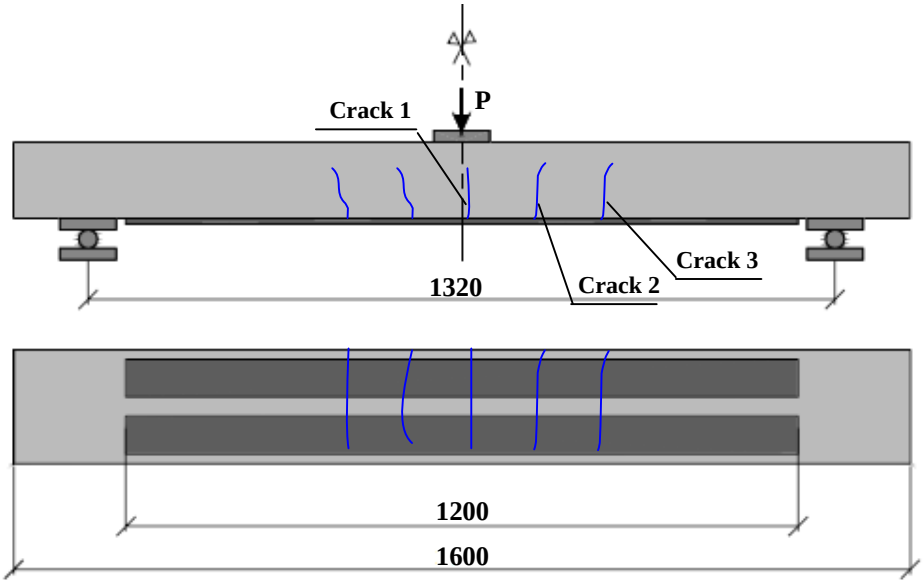

Figure C.1: Crack pattern for slab specimens

Assume linear material behaviour and that the concrete cannot sustain tension, the depth of the neutral axis, h, is given by:

The modular ratio is:

$n_s=E_s/E_c$, $n_s= 7.78$; $n_f=E_f/E_c$, $n_s= 6.2$

- The transformed area of the steal and CFRP plate are:

$A_{sc}= (n_s - 1).A_s$, $A_{sc}= 2664.54\ mm^2$

$A_{fc}= (n_f).A_f$, $A_{fc}= 911.4\ mm^2$

- The second moment of area of the equivalent section is given by

$$h = \frac{E_c b_c \frac{h_c^2}{2} + E_f b_f t_f (h_c + \frac{t_f}{2})}{E_c b_c h_c + E_f b_f t_f}\ , \qquad h= 60.9\ mm$$

$$I = \frac{E_c}{E_f}\left[\frac{b_c h_c^3}{12} + A_c (h - 0.5h_c)^2 + A_{sc}(h - h_s)^2 + A_{fc}(h - h_f)^2\right]\ , \qquad I = 12.51\times10^6 \quad mm^4$$

- The second moment of inertia of the concrete slab and CFRP plate alone given by:

$$I_c = \frac{b_c h_c^{\ 3}}{12} \qquad I_c = 72\times10^6 \quad mm^4 \qquad E_c I_c = 1.944\times10^{12} \quad mm^4$$

$$I_f = \frac{b_f t_f^{\ 3}}{12} \qquad I_f = 26.47 \quad mm^4 \qquad E_f I_f = 4.275\times10^6 \quad mm^4$$

Stage 1: Stresses are determined assuming fully composite action between reinforced concrete slab and externally bonded plate. Owing to applied loading, an element of the plate, length δ_x, is subjected to resultant axial forces, t_1 and shear force/unit length τ_1 in the adhesive layer.

$L_0 = 360\ mm$, distance between the right support and the center of crack

$x := 0\ mm$ from crack location

$P = 100000\ N$

$V = 50000\ N$

$m(x) := V.x$

$$\tau_1 = \frac{V.b_f.t_f}{I.b_a}(h_f - h)$$

$$t_1(x) = \frac{m(x).b_f.t_f}{I}(h_f - h)$$

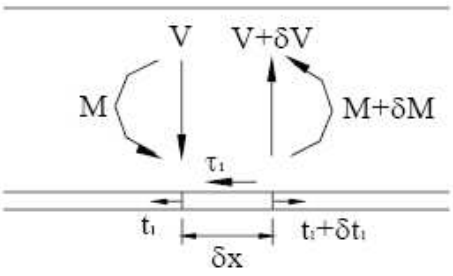

Values of $t1$ and τ_1 are evaluated at the crack location, t_{10} and τ_{10}, respectively.

$M_0 = V * 360$ $\qquad$ $M_0 = 18.0\times10^6 \quad N.mm$

$\tau_{10} = \frac{V.b_f.t_f}{I.b_a}.(h_f - h)$ $\qquad$ $\tau_{10} = 0.353 \quad \frac{N}{mm^2}$

$t_{10} = \frac{M_0.b_f.t_f}{I}.(h_f - h)$ $\qquad$ $t_{10} = 12740 \quad N$

State 2: Since the assumed axial forces t_1 do not exist in practice due to equilibrium, the next stage of the solution is to apply opposite forces $-t_1$ at infinitesimal element. An approximation of this problem can be obtained by assuming the plate to be bonded to an assumed rigid concrete slab by an adhesive layer having a shear stiffness/unit length, K_s : is given by:

$K_s := G_a \frac{b_a}{t_a}$

For epoxy Type 1

$K_s = 9.76\times10^4 \quad N/mm^2$

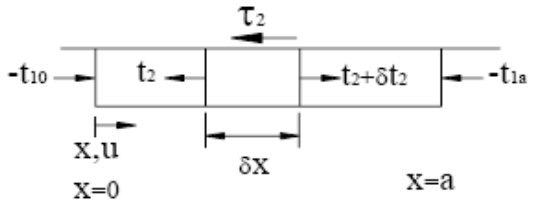

Considering the equilibrium of an element of the CFRP plate, length = δ_x, gives:

$t_2 = K_s.u$

Where u is the displacement of the plate in the x-direction leading to the differential equation,

$\frac{d^2u}{dx} - \alpha^2 = 0$,

The solution of the equation is,

$\alpha = \sqrt{\frac{K_s}{E_f.b_f.t_f}}$ $\qquad$ $\alpha = 0.063 \quad \frac{1}{mm}$

$\tau_2(x) = \frac{1}{b_a}\left(\frac{K_s}{E_f.b_f.t_f}\right)^{0.5}.\left(t_{10}.\cosh(\alpha.x) - t_{10}.\sinh(\alpha.x)\right)$

Forces at the crack location, i.e. $x = 0$

$$\tau_{20} = \frac{1}{b_a}\left(\frac{K_s}{E_f.b_f.t_f}\right)^{0.5}.\left(t_{10}.\cosh(\alpha.0 \quad mm) - t_{10}.\sinh(\alpha.0 \quad mm)\right) \quad , \qquad \tau_{20} = 8.02 \quad \frac{N}{mm^2}$$

The resultant forces in the CFRP plate at the end of stage 2 are as shown in the figure below in which m denotes moment and *f* denotes shear forces.

$$\tau(x) = \tau_1 + \tau_2(x)$$

at x: 0 mm from crack location

$$\tau(x) = \frac{V.b_f t_f}{I.b_a}.(h_f - h) + \frac{1}{b_a}\left(\frac{K_s}{E_f b_f t_f}\right)^{0.5}.(t_{10}.\cosh(\alpha.x) - t_{10}.\sinh(\alpha.x))$$

$$\tau(x) = 0.353 + 1.44\cosh(0.0672.x) - 1.44\sinh(0.0672.x)$$

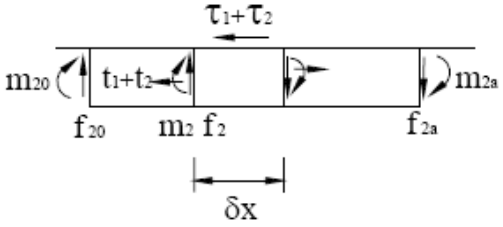

Maximum normal stress at the crack, $x = 0$.

$$\tau(x) = 8.3 \quad N/mm^2$$

The curvature of the concrete slab and the CFRP plate are approximately equal and hence m_{20} related to the global bending moment M_0 by the following equation:

$$m_{20} := M_0.\left(\frac{E_f.I_f}{E_f.I_f + E_c.I_c}\right) \qquad m_{20} := 12.4 \quad N.mm$$

$$f_{20} := V.\left(\frac{E_f.I_f}{E_f.I_f + E_c.I_c}\right) + b_a.(\tau_{10} + \tau_{20}).\frac{t_f}{2} \qquad f_{20} := 615.459 \quad N$$

Stage 3: Since the moment m_{20} and M_{2a} and shear forces f_{20} and f_{2a} do not exist in practice, the next stage of solution is to apply opposite moments and shear at x=0 and x=a, as shown in figure below. An approximate solution of this problem can be obtained by assuming the CFPP plate to be bonded to an assumed rigid concrete slab by an adhesive layer having a normal stiffness/unit length K_n given by

$$K_n := E_a \frac{b_a}{t_a}$$

$$K_n := 2.998 \times 10^5 \quad N/mm^2$$

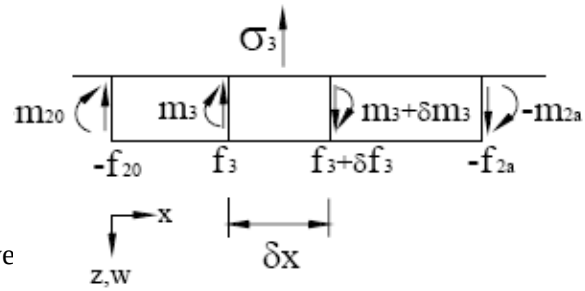

Noting that the normal force in the adhesive σ_3 is give

$$\sigma_3 = \frac{K_n.w}{b_a}$$

Where *w* is the relative displacement of the plate in the Z direction, the governing differential equation can be obtained as

$$\frac{d^4 w}{dx^4} + 4\gamma^4 w = 0 \ , \qquad \gamma = \sqrt[4]{\frac{K_n}{4.E_f.I_f}} \qquad \gamma = 0.36$$

Assuming that *w* tends to zero with increasing *x*,

At *x*= 0 mm

$$\sigma(x) = \frac{2}{b_a}.e^{-\gamma.x}.\left[(f_{20}\gamma + m_{20}\gamma^2).\cos(\gamma.x) - m_{20}\gamma^2 \sin(\gamma.x)\right]$$

$$\sigma(x) = \frac{2}{b_a}.e^{-0.36x}.(223.17.\cos(0.36.x) - 1.6\sin(0.36.x))$$

The maximum shear stress at the crack location, *x*= 0.mm, is

$$\sigma(x) = 4.46 \quad N/mm^2$$

The concrete delamination is assume to start if the maximum principal stress σ_p = at the crack is larger than the strength of the concrete, σ_2

Measured concrete strength for specimen G_E2_N,

$$f_t = 2.99 \quad MPa$$

$$\sigma_y = \sigma(x) = 4.46 \quad N/mm^2$$

$$\sigma_x = \frac{M_0.(h_c - h)}{I_c} \ \Rightarrow \ \sigma_x = 15 \quad N/mm^2$$

$$\tau = \tau(x) = 8.3 \quad N/mm^2$$

$$\sigma_p = \frac{\sigma_x + \sigma_y}{2} + \sqrt{\left(\frac{\sigma_x - \sigma_y}{2}\right)^2 + \tau^2} \quad \Rightarrow \quad \sigma_p = 19.56 \quad N/mm^2$$

Delamination will surely occur since $\sigma_p > f_t$

CURRICULUM VITAE

1. Family Name: Alfar

2. First Name: Amal

3. Nationality: Jordanian

4. Education:

Institution:	University of Jordan
Date:	1988
Degree or Diploma obtained:	Master of Civil Engineering / Structures

5. Professional Experience Record:

Company	Institute for Building Materials, Concrete Structures & Fire protection
Location:	Braunschweig, Germany
Date:	2005 - 2006
Position	Researcher
Company	Royal Scientific Society
Location:	Amman, Jordan
Date:	1999 – 2005
Position	Researcher
Company	Abdoun Consulting Engineering Office /Jordan
Location:	Amman, Jordan
Date:	1998 - 1999
Position	Head of Structural Division
Company	Al-Qaser Consulting Engineering Office / Jordan
Location:	Amman, Jordan
Date:	1994 - 1998
Position	Head of Structural Division
Company	Amal Alfar Engineering Office /Jordan
Location:	Amman, Jordan
Date:	1991 - 1994
Position	Head of Structural Division
Company	Arab Community College/ Jordan
Location:	Amman, Jordan
Date:	1988 - 1989
Position	Head of Structural Division